

CMOS Biochips for Rapid Assessment of New Chemicals

Subtask C-4-3; SRC 425.012

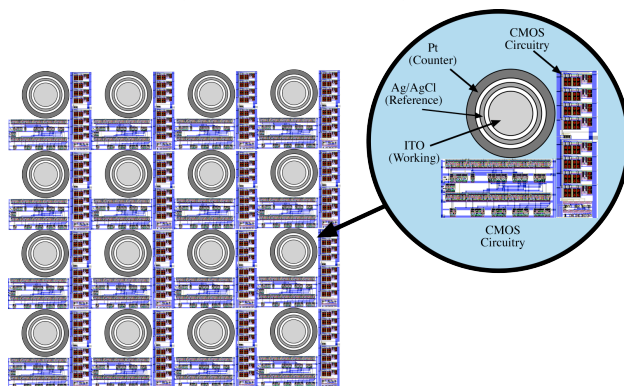
David Mathine^{1,2}, Joseph J. Bahl³, and Raymond B. Runyan⁴

¹Optical Sciences, ²Electrical Engineering, ³Sarver Heart Center, and

⁴Cell Biology and Anatomy, University of Arizona, Tucson

SRC/Sematech Engineering Research Center for Environmentally Benign Semiconductor Manufacturing

Project Objectives

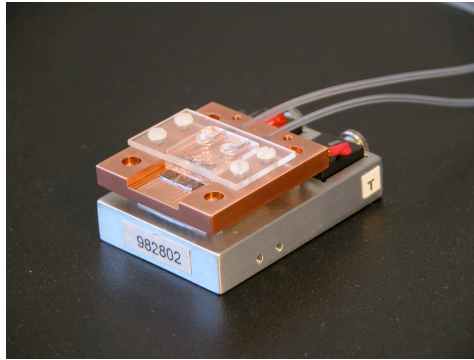


Traditional means of determining chemical toxicity, which typically involve expensive and laborious animal studies, cannot keep pace with the demand for new chemicals by industry. The advent of biochip technology promises to yield a high-throughput means of screening even complex mixtures of chemicals for toxicity. By monitoring the exposure response of reporter cells/tissues, investigators can identify signature reactions that indicate toxic insult.

Cell health will be monitored in real time using a CMOS based sensor where each pixel is capable of optical, chemical, and electrical measurements.

SRC/Sematech Engineering Research Center for Environmentally Benign Semiconductor Manufacturing

Environmental Control

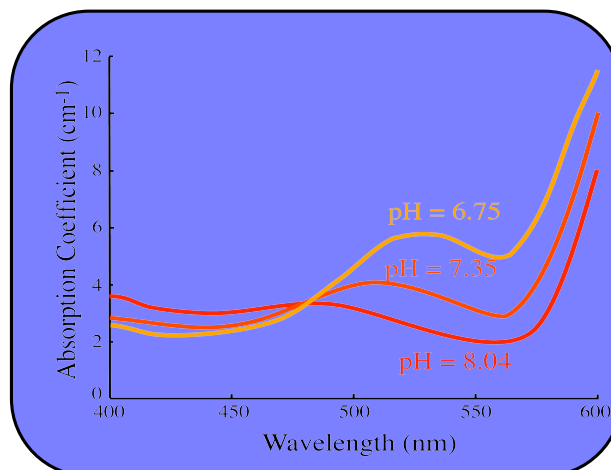


The overall biochamber design is based on controlling the environment for cell growth while providing the means to stimulate the cells chemically, thermally, optically and electrically.

Temperature in the chamber is controlled with a TEC module while a syringe infusion pump is used to control fluid flow through the chamber.

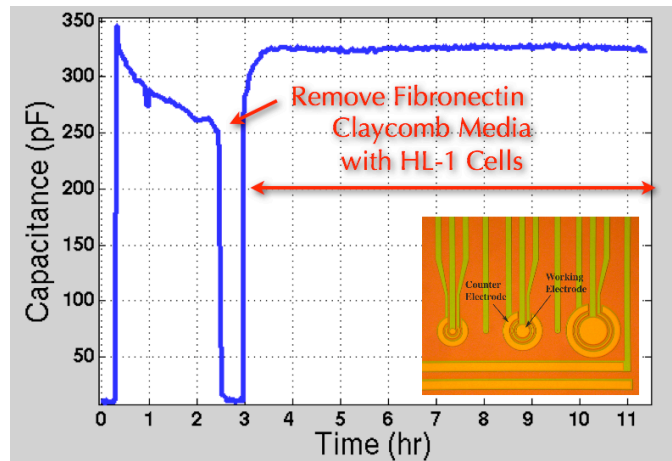
SRC/Sematech Engineering Research Center for Environmentally Benign Semiconductor Manufacturing

Spectroscopic CMOS Photodetectors



SRC/Sematech Engineering Research Center for Environmentally Benign Semiconductor Manufacturing

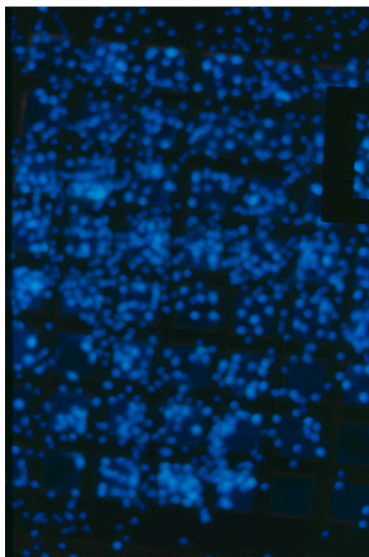
Monitoring Pad Capacitance



The capacitance from ITO electrodes is monitored in real time to detect protein coating of the electrodes and the induction of HL-1 cells. The HL-1 cells are cardiomyocytes and provide spontaneous beating which can be monitored during chemical exposure.

SRC/Sematech Engineering Research Center for Environmentally Benign Semiconductor Manufacturing

Cell Attachment Studies



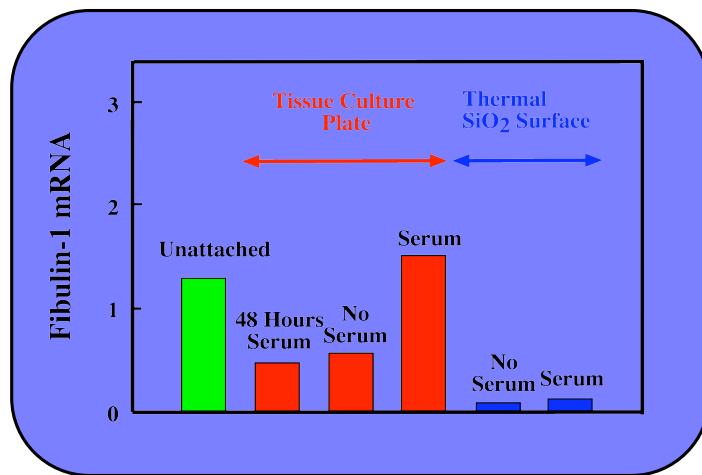
The biosensor surface is foreign to cells. Therefore, the attachment to the SiO_2 and ITO surfaces was studied. We found that COS-7 cells derived from monkey kidney cells, attached and grew well on ITO and SiO_2 coated silicon substrates without patterned biomolecules. COS-7 cells attached better to ITO coated substrates and we were able to obtain confluent cell layers.

The above figure shows DAPI stained COS-7 cells attached to a CMOS chip. An electrode grid pattern can be seen in the image.

SRC/Sematech Engineering Research Center for Environmentally Benign Semiconductor Manufacturing

Fibulin-1 Expression

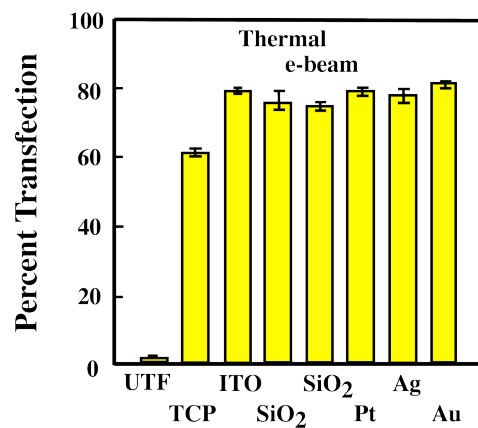
- Fibulin-1 is an extracellular matrix produced by COS-7 cells.
- Provides a measure of the cellular response to the substrate.
- SiO₂ provides a smaller stimulus than tissue culture plate!



SRC/Sematech Engineering Research Center for Environmentally Benign Semiconductor Manufacturing

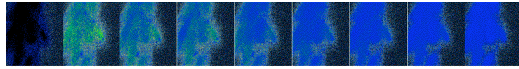
Percent Transfection

- Transfection is the introduction of DNA into animal cells.
- Changes in gene expression can be readily evaluated.
- Designed for real time monitoring with the biochip.

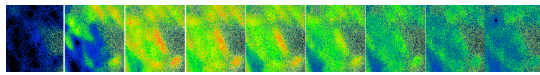


SRC/Sematech Engineering Research Center for Environmentally Benign Semiconductor Manufacturing

Chemical Toxicity Measurement



Control for 10ppb/100ppb TCE cells @ 10nM VP



Treated: 10ppb TCE cells @ 10nM VP



Low Calcium flow High Calcium flow

- Developed novel technique based on calcium handling in cells.
- P19 cells were exposed to low levels of TCE for 24 hours and then treated with vassopression to measure intracellular flux of calcium.
- Measured calcium flux by changes in fluorescence.

[SRC/Sematech Engineering Research Center for Environmentally Benign Semiconductor Manufacturing](#)

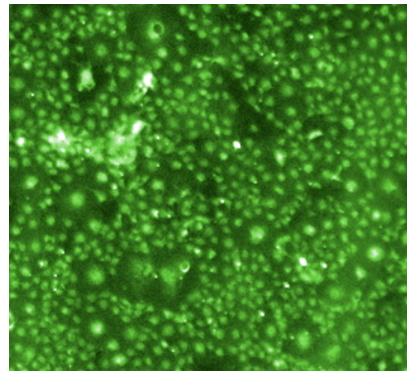
EHS Metrics

I) Basis of Comparison - Current best technology involves animal studies to determine toxicity of new chemicals. Approaches to solve this problem center around reduced usage of toxic materials.

II) Manufacturing Metrics - The new approach aims to increase the through put of chemical toxicity testing so that new chemicals will not be introduced into the manufacturing line before the toxicity effects of these chemicals is known.

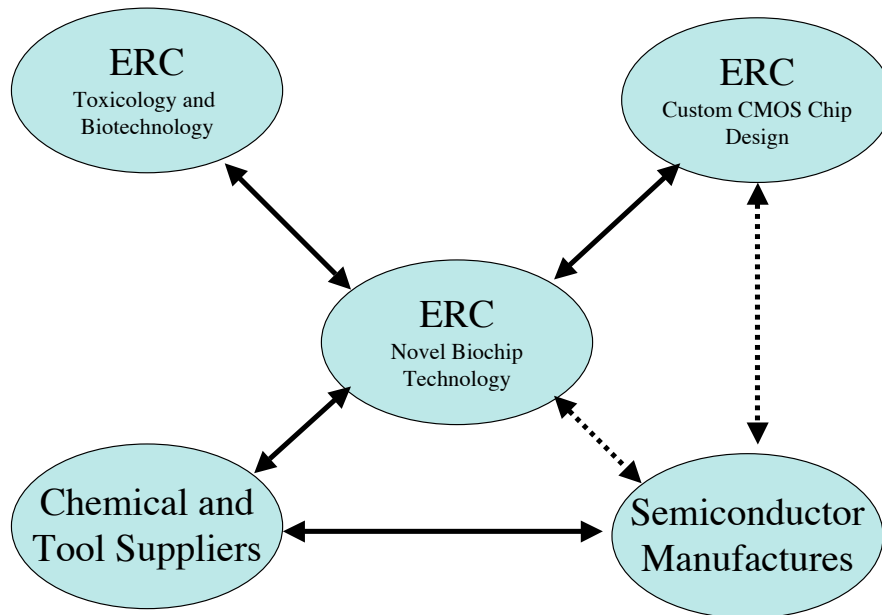
III) ESH Metrics

The goals of this work are to determine the toxicity of new chemicals. This work hopes to define the standards for toxicity.



[SRC/Sematech Engineering Research Center for Environmentally Benign Semiconductor Manufacturing](#)

Technology Development and Application



SRC/Sematech Engineering Research Center for Environmentally Benign Semiconductor Manufacturing

Future Plans

Next year plan:

- Determine toxicity of new chemicals
- Integrate multiple sensors on CMOS chip
- Monitor cellular responses to chemicals in real time

Future Plans:

The CMOS biochip promises to deliver a new generation of highly selective and inexpensive sensors for real-time and online monitoring at the manufacturing site. Future plans include building low-cost sensors for use by chemical suppliers (responsible for starting feed materials) and process engineers and ESH professionals (responsible for evaluation of new chemistries during and after the processing cycle).

SRC/Sematech Engineering Research Center for Environmentally Benign Semiconductor Manufacturing



Thrust D; SRC: 425.013

Non-PFOS/non-PFAS Photoacid Generators: Environmentally Friendly Candidates for Next Generation Lithography

Victor M Gamez¹, Ramakrishan Ayothi², Yi Yi², James A Field¹, Chris K Ober², Reyes Sierra¹

¹ Department of Chemical & Environmental Engineering, University of Arizona

² Department of Materials Science and Engineering, Cornell University



SRC/Sematech Engineering Research Center for Environmentally Benign Semiconductor Manufacturing





Project Background & Objectives



- This project aims to develop novel PFOS-free PAGs that meet the stringent performance demands required by semiconductor manufacturing and do not pose a risk to public health or the environment.
- Work on the development of the novel non-PFOS/non-PFAS PAGS is conducted at Cornell University (Dr Ober's group).
- Environmental studies of these new materials are in progress at the University of Arizona (Dr Sierra's group). Studies undertaken to evaluate the inhibitory potential of the new chemistries are presented here.



SRC/Sematech Engineering Research Center for Environmentally Benign Semiconductor Manufacturing





ESH Benefits



These studies will be of critical importance in assessing synthetic strategies for environmental acceptability and will be used to guide the design of new PFOS-free photoacid generators.



SRC/Sematech Engineering Research Center for Environmentally Benign Semiconductor Manufacturing





Material and Methods



- The inhibitory potential of three non-PFOS PAGs (SF1, SF2 and PF1) and their counter ions, diphenyl iodonium (DPI) and triphenyl sulfonium (TPS), (Fig. 1) was evaluated using three different bioassays:
 - the Mitochondrial Toxicity Test (MTT);
 - Microtox[®] (a widely-used, commercial assay utilizing a marine bacterium that emits fluorescence), and
 - the methanogenic inhibition test.

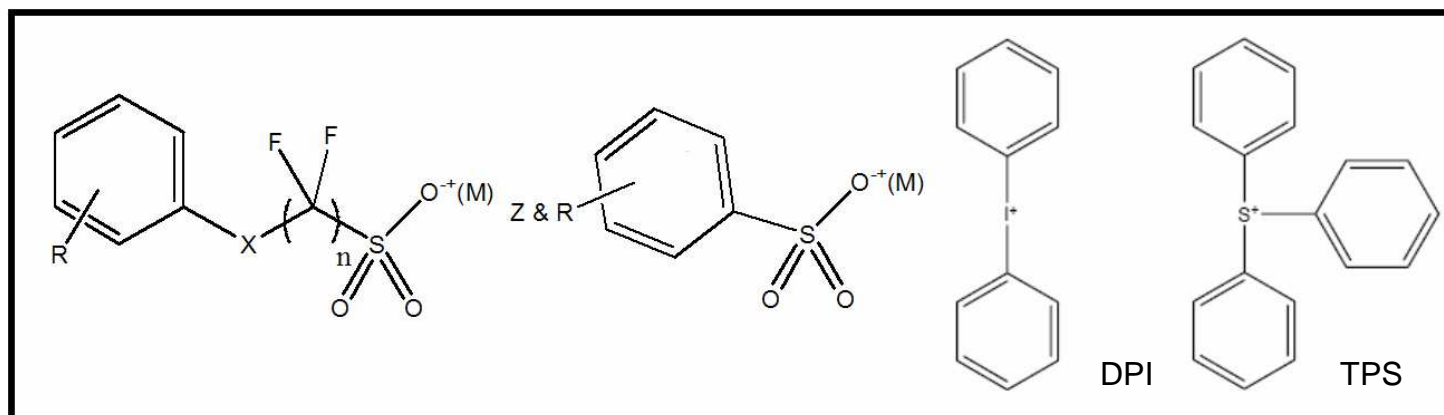


Fig. 1- Non-PFOS PAGs that will be synthesized and studied. Counter ions studied.





Results: MTT Assay



- The PAG counter ions, DPI and TPS, showed the highest toxic effects in the MTT assay (Fig. 2). PF1 was the only PAG displaying toxicity in this bioassay.

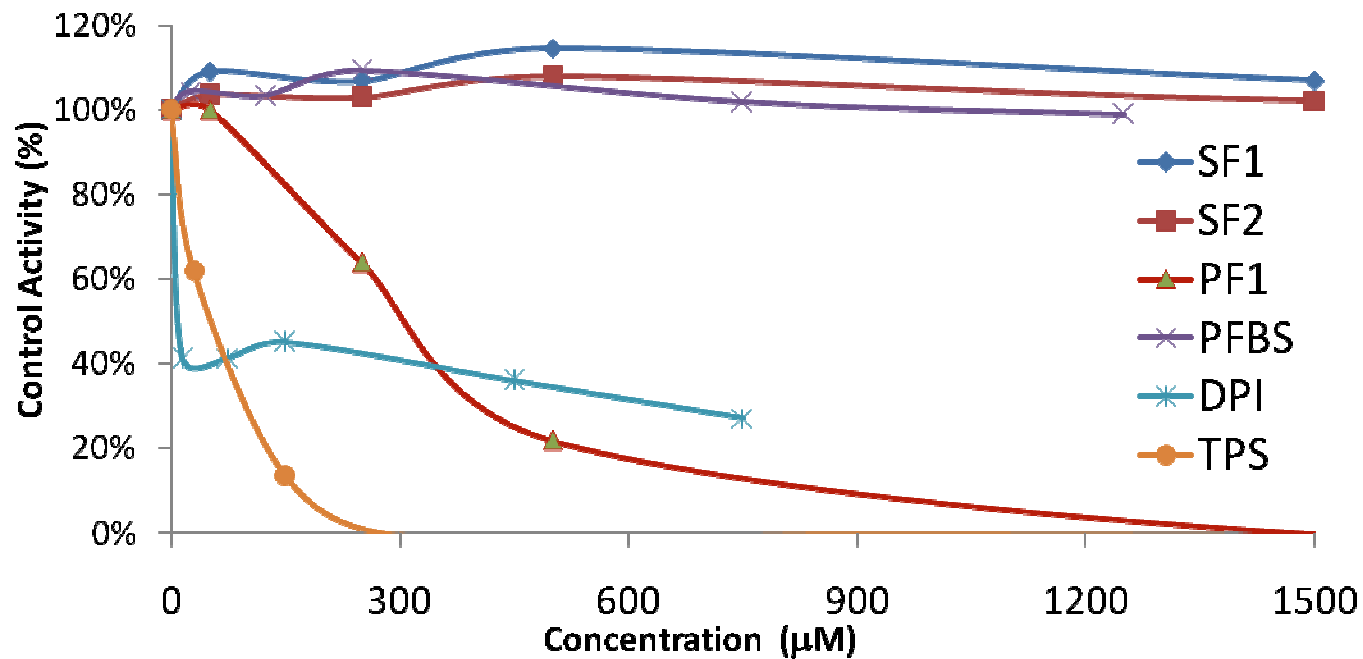


Fig. 2- Inhibitory effect of the new non-PFOS PAGs and the PAG counter ions in the MTT bioassay.





Results: Microtox Assay



- In agreement with the findings of the MTT assay, the PAG counter ions were also the most inhibitory compounds in the Microtox assay (Table 1). PF1 also displayed microbial inhibition, albeit at relatively high concentrations (50% inhibitory concn. (IC₅₀)= 1.6-2.2 mM).

Table 1. Inhibitory effect of the new PAGs and their counter ions in the Microtox bioassay. IC₅₀ and IC₈₀ are the concentrations of the compounds causing 50 and 80% inhibition in the assay.

Compound	IC ₅₀ (μM)			IC ₈₀ (μM)		
	5 min	15 min	30 min	5 min	15 min	30 min
SF1	NT*	NT	NT	NT	NT	NT
SF2	NT	NT	NT	NT	NT	NT
PF1	2,195	1,705	1,614	9,698	5,467	4,371
PFBS	NT	NT	NT	NT	NT	NT
DPI	40	10	5	179	48	22
TPS	40	29	38	145	78	76

*NT= Not toxic at the highest concn. tested for SF1, SF2 and PFBS (11,250 μM).





Results: Methanogenic Inhibition



- The counter ions displayed inhibition towards H_2 and acetate-utilizing methanogens (Fig. 3). In contrast, the PAGs were generally not toxic. SF2 was an exception, with an IC_{50} value of $1,470 \mu M$. Methanogens constitute an important microbial population in anaerobic sludge digestors. Severe methanogenic inhibition can result in process failure.

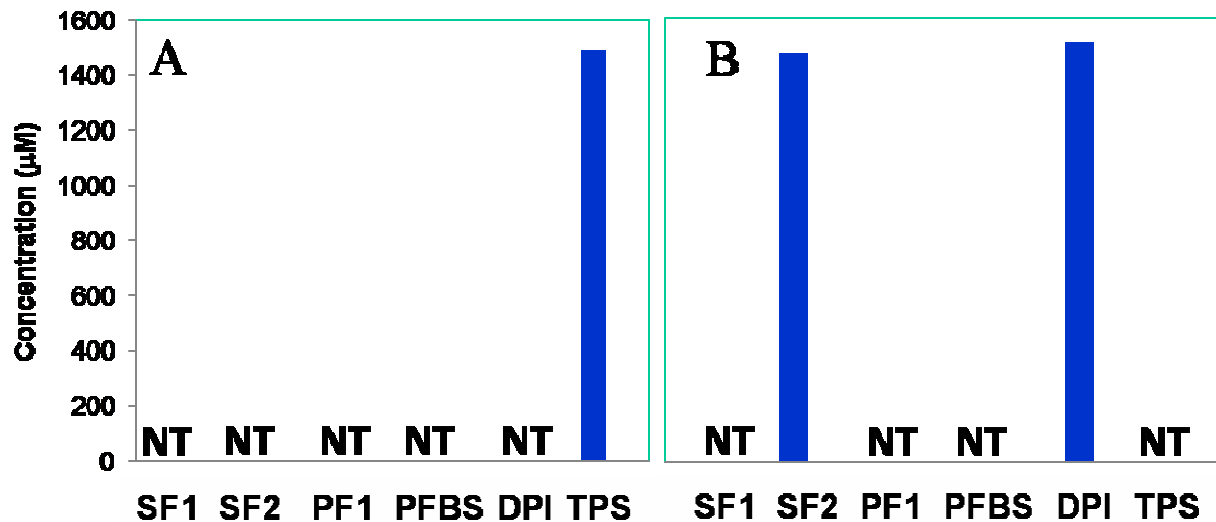


Fig. 3- Inhibitory effect (IC_{50}) of the new PAGs and counter ions in (A) autotrophic methanogens and (B) acetoclastic methanogens in anaerobic sludge. *NT= Not toxic at the highest concn. tested (in μM): SF1 (2,560); SF2 (1,850), PF1 (1,830), PFBS (1,670).





Conclusions



- The counter ions, diphenyl iodonium (DPI) and triphenyl sulfonium (TPS), showed the highest toxic effects in all three tests.
- The new PAGs, SF1 and SF2, were not inhibitory, or only at very high concentrations.
- PF1 displayed inhibition in the MTT and Microtox assays but the IC50 levels were 1-2 orders of magnitude higher compared to those determined for the counter ions.





Future Work



- Complete ongoing studies of the toxicity of PAGs and counter ions under aerobic and nitrifying conditions.
- Investigate the susceptibility of the novel PAGs to biodegradation by microorganisms commonly found in wastewater treatment systems.
- Investigate the treatability of the most promising PAG(s) by conventional biological and/pr physio-chemical methods.



SRC/Sematech Engineering Research Center for Environmentally Benign Semiconductor Manufacturing





Industrial Collaboration / Technology Transfer



Industrial Collaboration:

Jim Jewett, Intel Corporation

Ralph Dammel, AZ-Microelectronic Materials, Inc.

George Barclay, Rohm and Haas Microelectronics

Disclosures and Patents:

A patent application has been filed on ionic non-PFOS/non-PFAS PAGs following the general design strategy described in the proposal.

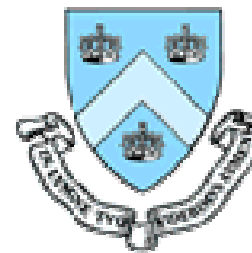


SRC/Sematech Engineering Research Center for Environmentally Benign Semiconductor Manufacturing



Planarization Long Range Plan

February 2007



SRC/Sematech Engineering Research Center for Environmentally Benign Semiconductor Manufacturing

Team

- PIs:

- Ara Philipossian (UA)
- Duane Boning (MIT)
- Srini Raghavan (UA)
- Vincent Manno (Tufts)
- Chris Rogers (Tufts)
- Robert White (Tufts)
- Stephen Beaudoin (Purdue)
- Alan West (Columbia)

- Other Researchers:

- Ed Paul (MIT)
- Len Borucki (Araca)
- Yun Zhuang (UA)
- Fransisca Sudargho (UA)
- Yoshi Nishimura (Inoac)

- Advisory Committee

- Paul Fischer (Intel)
- Laertis Economikos (IBM)
- Cliff Spiro (Cabot)
- Chris Borst (University at Albany)

Team

- Graduate (PhD) Students:

- Ashok Muthukumaran (UA)
- Yasa Sampurno (UA)
- Ting Sun (UA)
- Daniel Rosales-Yeomans (UA)
- Hyosang Lee (UA)
- Xiaomin Wei (UA)
- Rumin Zhuang (UA)
- Nicole Braun (Tufts)
- Caprice Gray (Tufts)
- Andrew Mueller (Tufts)
- James Vlahakis (Tufts)
- Hong Cai (MIT)

- Graduate (PhD) Students (continued):

- Daniel Truque (MIT)
- Xiaolin Xie (MIT)
- Kristin Shattuck (Columbia)
- Bum Soo Kim (Purdue)
- Caitlin Kilroy (Purdue)
- Gautam Kumar (Purdue)

- Undergraduate Students:

- Anita Lee (UA)
- Geoff Steward (UA)
- Jessica Torres (Purdue)

Next Five Years

- Landscape:

- Research, fundamental in nature yet industrially relevant, addressing the technological, economic and environmental challenges of planarizing:

- Copper
- Tantalum and Ruthenium
- Dielectrics (STI, and ILD relating to barrier polish)
- New materials (relating to new memory devices)

- Gaps to be Filled:

- Processes & consumables for:

- Advanced processes and consumables for planarization
- Electrochemically assisted planarization
- Post-planarization cleaning and surface preparation

Advanced Processes & Consumables for Planarization

Philipossian
Boning
Manno
Rogers
White
Beaudoin



Advanced Processes & Consumables for Planarization

- Focus:

- Basic scientific investigations of the controlling processes in planarization of advanced materials over several length scales and levels of complexity
- Development of validated, science-based descriptions that relate specific planarization process and material attributes (including material micro-structure) to measurable process outcomes

- **Specification and testing of environmentally-conscious process and material alternatives for rapid feedback into the planarization design process**

Advanced Processes & Consumables for Planarization

- Objectives

- Real-time detection and modeling of pattern evolution

- Develop novel force-spectra endpoint detection methods by determining how various wafer and pad surface states during polish affect the frictional energy in particular frequency bands
- Relate these signals to details of the wafer topography evolution by integrating pattern evolution models with the above endpoint or diagnostic signal analysis

- Effect of pad grooving on process performance

- Empirical and numerical investigation of the effect of various pad designs (materials, groove shapes and dimensions) as well as different types of slurries on RR, COF and pad temperature for copper and tantalum CMP
- Identification and verification of optimal pad designs for technology transfer to 300-mm platforms

Advanced Processes & Consumables for Planarization

- Objectives (continued)

- Wear phenomena and their effect on process performance
 - Isolate, quantify and model the hydrodynamic, van der Waals, hydrophobic and electrostatic processes that determine how nanoparticles (both silica and ceria), pads, diamonds and wafers interact with one another in representative systems and how these interactions evolve with extended use.
 - Develop methods to visualize and measure local wafer-pad mechanical interactions using laser-induced fluorescence and micro-machined shear stress sensors

Once fundamentals of pad asperity evolution & the effect of the multitude of contacting bodies on pad asperities are understood, their impact on planarization capability can be modeled.

This will lead to the design of new polishing protocols & consumables that will deliver superior performance with reduced environmental consequences.

Advanced Processes & Consumables for Electrochemically Assisted Planarization

Raghavan
Boning
West
Philipossian



Advanced Processes & Consumables for Electrochemically Assisted Planarization

- Focus and Objectives:

- Development and implementation of a ‘full’ process that includes clearing of copper AND planarization of the barrier (i.e. tantalum) layer

- **Novel chemistries** to enhance and control electrochemical removal and passivation of copper, tantalum and ruthenium
- **Novel pads** to ensure electrical contact with isolated copper islands during clearing (requires development of conducting pad technology, with appropriate mechanical, electrochemical & environmental properties)
- **Modeling and characterization** of tool, pad and wafer interactions for design and control (particularly endpoint detection) are needed to minimize process cost and environmental impact

Advanced Post-Planarization Cleaning Processes and Consumables

Philipossian



SRC/Sematech Engineering Research Center for Environmentally Benign Semiconductor Manufacturing

Advanced Post-Planarization Cleaning Processes & Consumables

- Focus and Objectives:

- Fundamental study of the effects of brush (new and used) material and design on shear force, creep, rebound and cleaning efficiency of insulator and metal films

- **Novel surface mechanical testing methodologies** to perform cyclic and incremental brush deformation measurements before and after extended wear to understand failure mechanisms
- **Design and use of novel tribometers** to study the frictional forces in post-planarization scrubbing
- **Modeling and characterization** of brush, cleaning fluid and wafer interactions within the realm of nano-lubrication theories

**Environmentally Benign
Electrochemically-Assisted Chemical-
Mechanical Planarization (E-CMP)
Task ID : 425.014**

Srini Raghavan (PI)

Graduate student:

Ashok Muthukumaran

*Department of Materials Science and Engineering
The University of Arizona*

ESH Metrics for Task 425.014

➤ **Basis of comparison:**

- Conventional slurry based Copper CMP
 - Requires slurries with higher solid content
 - Higher polishing pressure
 - Higher polish time during bulk copper removal

➤ **Manufacturing Metrics:**

- The use of ECMP will reduce the polish time, polishing pressure and the amount of waste generated by a typical slurry based CMP

➤ **ESH Impact:**

	Usage Reduction		Waste Reduction	
Goals	Chemicals	Abrasives	Solid	Liquid
Using ECMP	N/A	80% reduction	<0.01%	N/A

Ta CMP

➤ Conventional Ta CMP

- Silica particles in slurry ~ 5-10 weight %
- Alkaline pH ; H₂O₂ as oxidant
- Mostly *mechanical* in nature

➤ Literature information

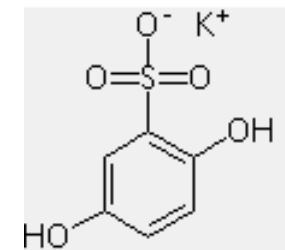
➤ Benzene sulfonic acid

- Recent patent applications mention derivatives of benzene sulfonic acid as oxidant under acidic condition

- United States Patent Application 20060030158, Cabot Microelectronics (2006)

- United States Patent Application 2005090109, EKC Technology (2005)

- Etching and polishing of Ta
- pKa of dihydroxy benzene sulfonic acid ~12.2



Potassium salt of dihydroxy benzene sulfonic acid

➤ Aryl disulfonic acid (e.g: dihydroxy benzene disulfonic acid or Tiron)

- Complexes with refractory metals

Objective

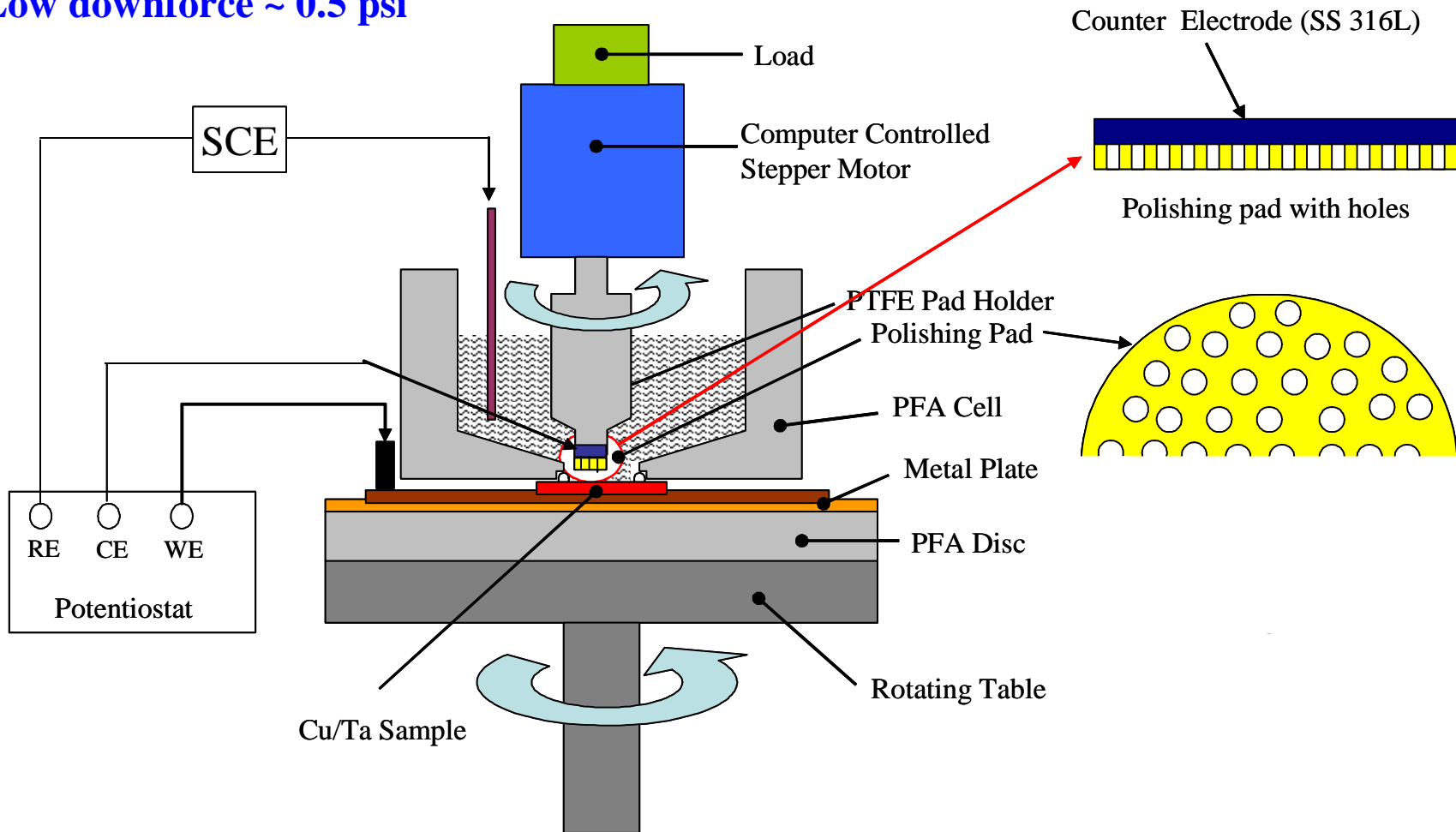
- To develop chemical system suitable for electrochemical mechanical removal of tantalum films with a 1:1 selectivity with respect to copper under ECMP conditions.

Accomplishments During the Current Contract Year

- Developed sulfonic acid based chemical system suitable for electrochemical mechanical removal of tantalum films.

Modified ECMP Tool

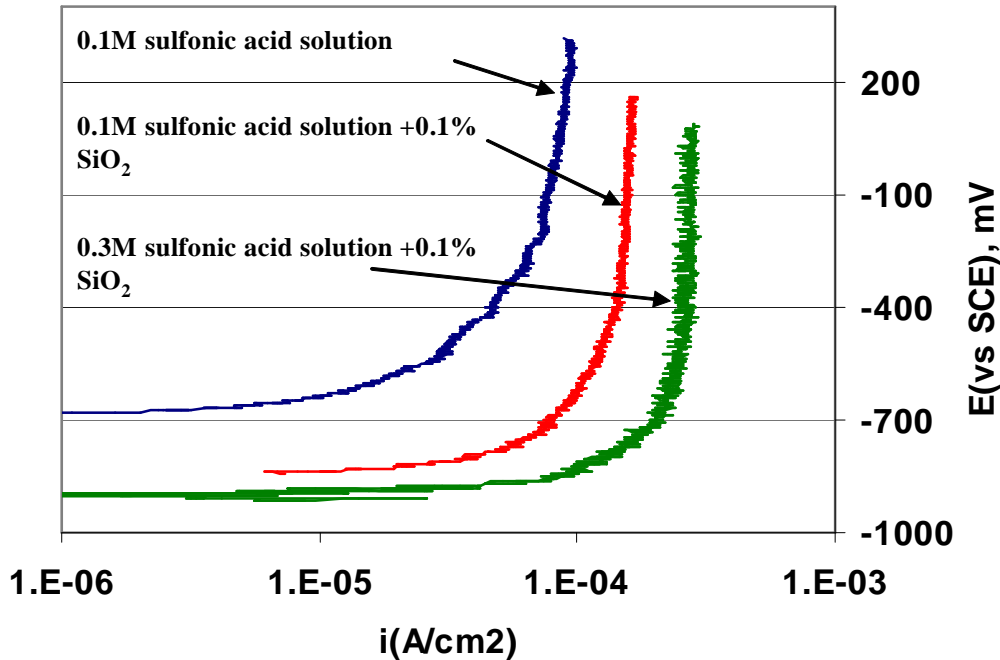
Polishing area = 22 cm²
Low downforce ~ 0.5 psi



Note: Picture drawn not to scale

Anodic Polarization of Tantalum (under abrasion)

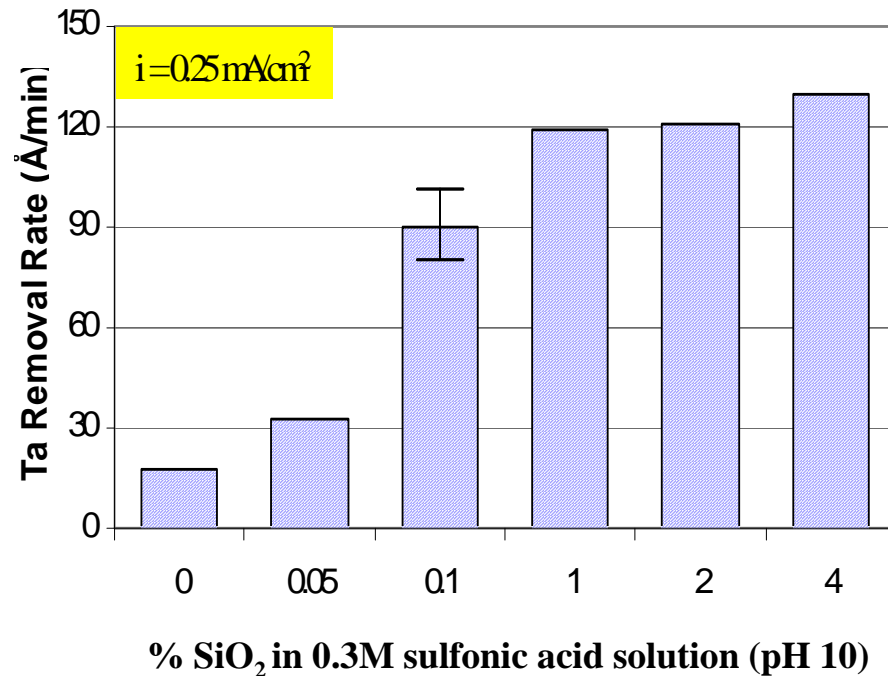
Load ~ 0.5 psi



Note: Maximum solubility of 2, 5 dihydroxybenzene sulfonic acid ~ 0.3M

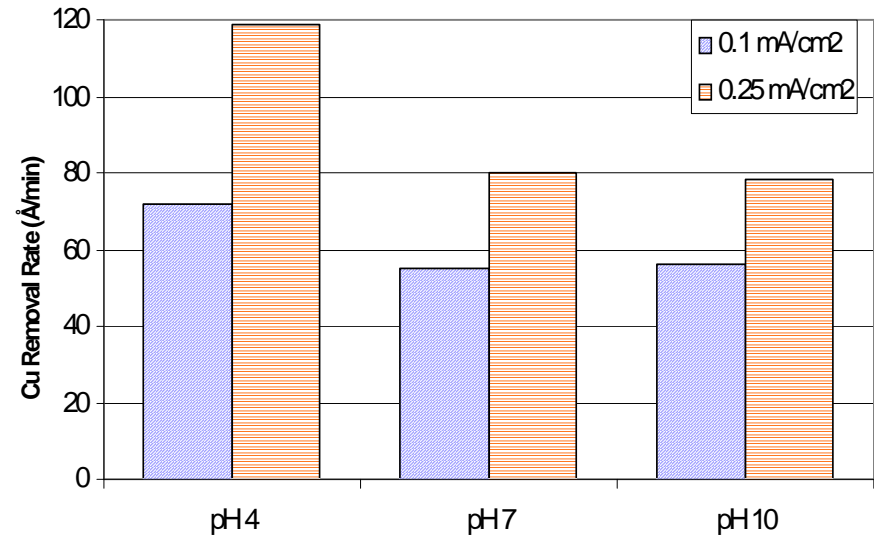
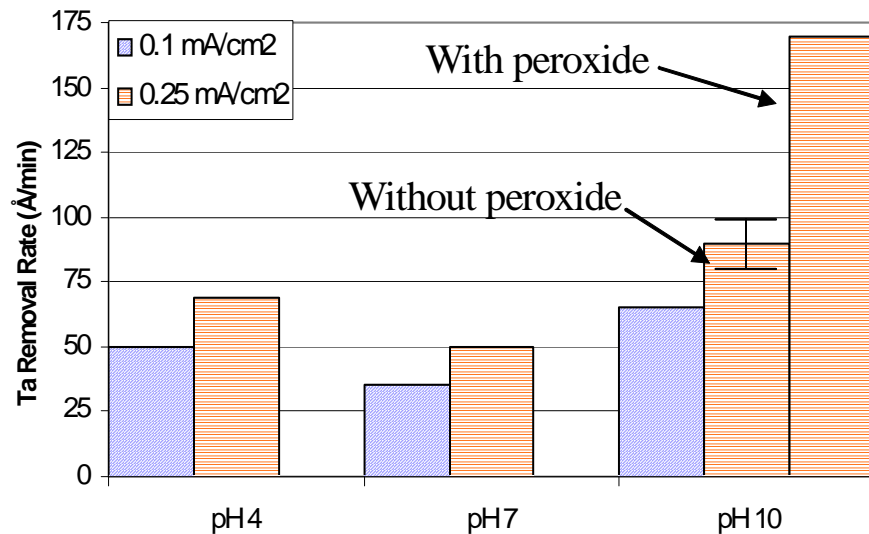
- 2,5 Dihydroxybenzene sulfonic acid solutions, in the presence and absence of silica at pH 10
- Potential sweep = OCP to 1V vs. OCP ; Scan rate = 5 mV/s
- Low current density in 0.1M sulfonic acid solution in the absence of silica particles
- Addition of silica (0.1%) to 0.1M sulfonic acid solution slightly increases the current density
- Higher current density of 0.3 mA/cm² was observed in solution containing 0.3 M sulfonic acid and 0.1% SiO₂

Effect of Silica Concentration



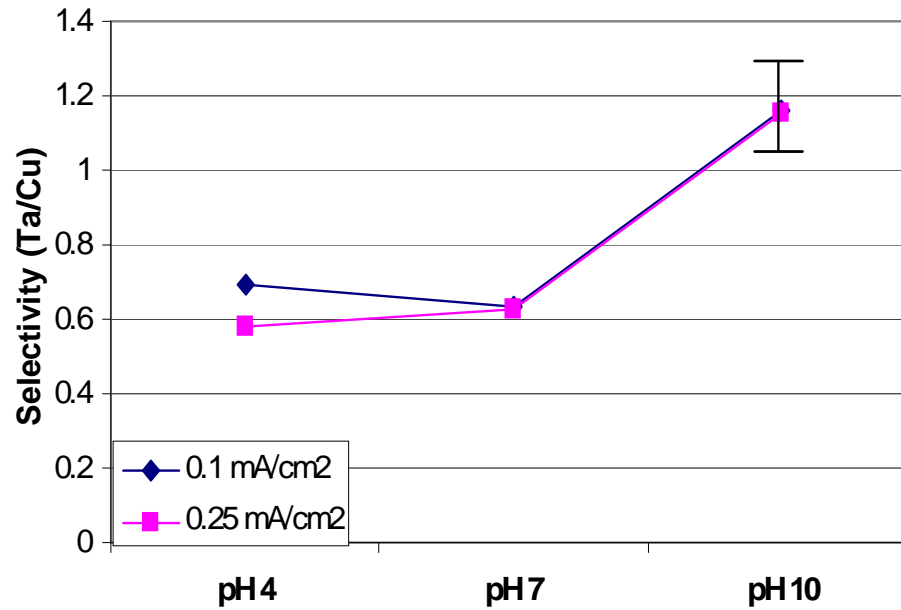
- 0.3 M sulfonic acid solution (pH 10), at a current density of 0.25 mA/cm²
- Very low Ta removal rate in the absence of SiO₂ ~ 20 Å/min
- Addition of 0.05% SiO₂ slightly increases the removal rate to 35 Å/min
- At 0.1% SiO₂ removal rate nearly doubles ~ **90 ± 10 Å/min**
- Above 0.1% SiO₂ removal rate does not significantly increase

Electrochemical Mechanical Removal of Tantalum and Copper



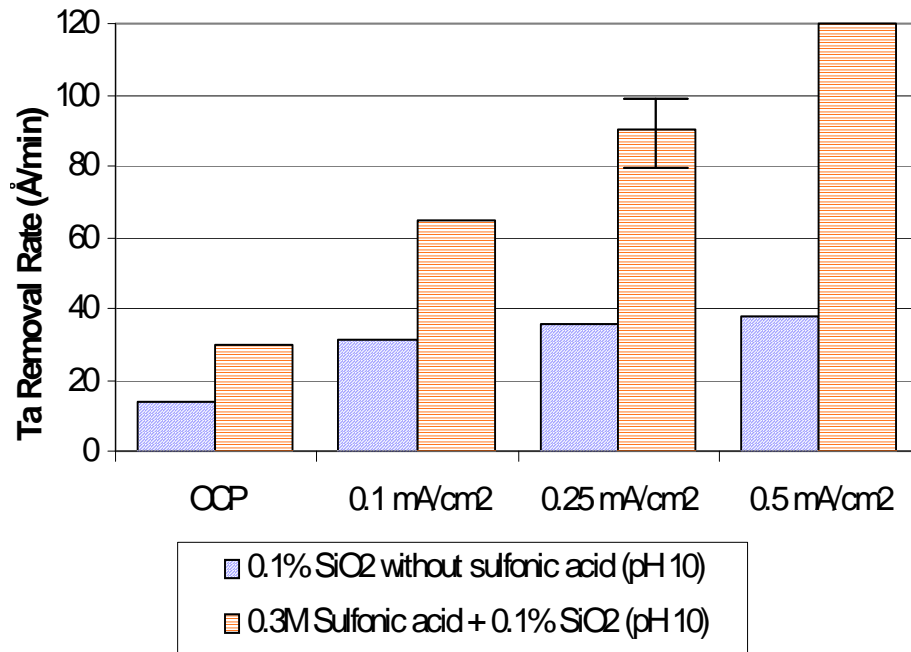
- 0.3 M Sulfonic acid solution + 0.1% SiO₂
- At pH 10, removal rate of Ta is higher $\sim 90 \pm 10$ Å/min for $i = 0.25$ mA/cm²
- Addition of 1.2M H₂O₂, removal rate of Ta increases to ~ 170 Å/min for the same current density
- At pH 10, Cu removal rate is 80 Å/min for a current density of 0.25 mA/cm²

Selectivity



- 0.3 M sulfonic acid solution + 0.1 % SiO₂ at pH 10
- At pH 4 and 7, selectivity is ~ 0.6
- At pH 10, ideal selectivity of **1.1 ± 0.1** was obtained

Effect of Applied Current Density on Tantalum Removal



➤ Absence of sulfonic acid solution

➤ Removal rate of Ta *plateaus* above 0.25mA/cm²

➤ Higher removal rate of Ta
~ 36 Å/min

➤ Presence of sulfonic acid solution

➤ Removal rate of Ta increases *linearly* with increasing applied current densities

➤ Highest removal rate ~ 120 Å/min, observed in 0.3 M Sulfonic acid + 0.1% SiO₂ (pH 10) at current density of 0.5 mA/cm²

Current Efficiency

Applied current density (mA/cm ²)	Estimated Removal Rate of Ta (Å/min)	Actual Removal Rate of Ta (Å/min)			Current efficiency (%) after correcting for OCP removal rate		
		pH4	pH7	pH10	pH4	pH7	pH10
OCP	-	23	12	30	-	-	-
0.1	23	52	35	65	120*	102*	142*
0.25	56	71	52	100	84	69	119*
0.5	112	-	-	119	-	-	77

* Current efficiency greater than 100% indicates some *mechanical removal of metallic Ta*

➤ Current efficiency calculated after correcting for OCP removal rate and based on *three electron transfer*

Future Directions

- Possibility of increasing removal rate by peroxide addition
- Develop chemical systems for the removal of other barrier layers (TaN, Ru)
- Electrochemical endpoint detection

Industrial Interactions and Technology Transfer

- Had many telephone discussions with Dr. Renhe Jia of Applied Materials on tantalum removal under ECMP conditions

Summary

- Ta removal rate of $\sim 100\text{\AA}/\text{min}$ obtained in 0.3 M Sulfonic acid solution containing 0.1% SiO_2 (pH 10) at a current density of $0.25\text{ mA}/\text{cm}^2$
- Ta/Cu selectivity of $\sim 1:1$ observed at pH 10
- Small amount ($\sim 0.1\%$) of silica is required for good removal rates of Ta
- 2,5 dihydroxy benzene sulfonic acid is a promising chemical for electrochemical mechanical removal of Ta barrier layer under ECMP conditions

Effect of Conditioning Force on Pad Topography and Removal Rate during Copper CMP

Task A; SRC 425.014

R. Zhuang ¹, L. Borucki ², Y. Zhuang ^{1,2}, M. Lacy ³, C. Spiro ³ and A. Philipossian ^{1,2}

¹ The University of Arizona, Tucson, AZ USA

² Araca Incorporated, Tucson, AZ USA

³ Cabot Microelectronics Corporation, Aurora, IL USA

Project Objectives

Determine how **conditioning force** affects pad topography, coefficient of friction (COF), pad temperature and RR

Use a previously developed **two-step Langmuir-Hinshelwood RR model** to explore RR data in greater detail

Perform **pad surface profilometry** to analyze mean peak spacing, mean peak curvature and surface roughness

Use **pad surface** data to **independently** calculate Langmuir-Hinshelwood model parameters and understand their physical meaning

Demonstrate, for the first time, that a strong correlation exists between pad surface profile and kinetic rate constants

ESH Impact & ESH Metrics

- Possible prolonged pad life and reduced pad consumption.
- Potential reduction in slurry use.

Goals/ Possibilities	Usage Reduction			Emission Reduction			
	Energy	Water	Chemicals	PFCs	VOCs	HAPs	Other Hazardous Wastes
Optimum polishing performance	N/A	N/A	Slurry, Polyurethane	N/A	N/A	N/A	N/A

Experimental Conditions

– Wafer

- 200-mm blanket copper wafers

– Pad

- 20-inch Cabot Microelectronics Corporation D100 pad (concentric grooves)

– Slurry

- Cabot Microelectronics Corporation iCue 600Y75 slurry
- Flow rate: 200 ml/min

– Platen Temperature

- 25 °C

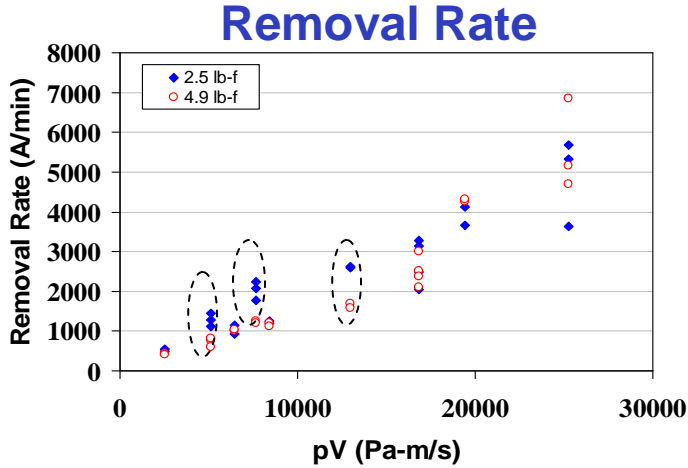
– Pad conditioning

- In-situ conditioning
- 4-inch Mitsubishi Materials Corporation 200-grit disc rotating at 30 RPM and sweeping at 20 times/min
- Conditioning force: 2.5 and 4.9 lb-f

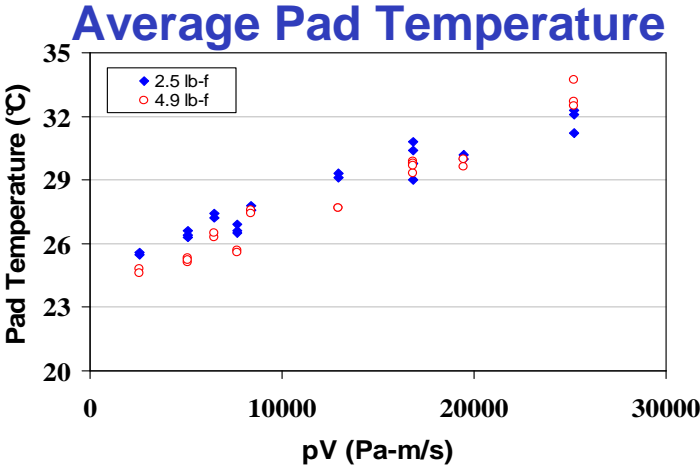
– Wafer Polishing

- Polishing pressure: 1, 2 & 3 PSI
- Sliding velocity: 0.37, 0.94 & 1.22 m/s
- Polishing time: 1 min

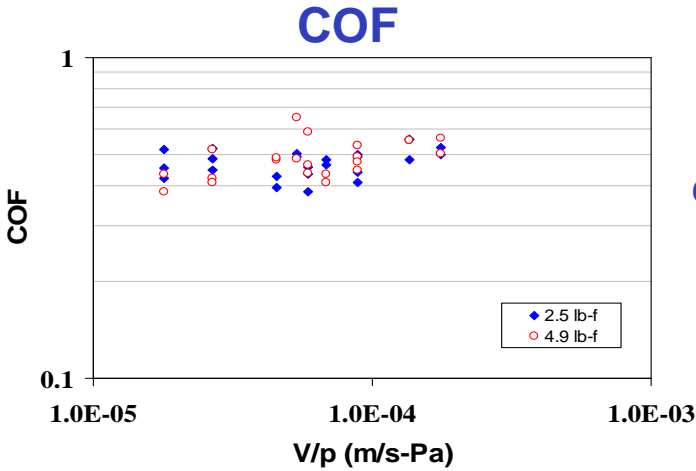
Experimental Results



At moderate values of pV,
RR (2.5 lb-f) > RR (4.9 lb-f)



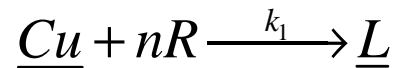
In general, $T_{\text{pad}} (2.5 \text{ lb-f}) > T_{\text{pad}} (4.9 \text{ lb-f})$



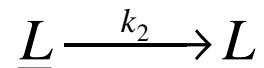
COF (2.5 lb-f) \approx COF (4.9 lb-f)

Chemical-Mechanical Rate Model

Two-step Langmuir-Hinshelwood model:



$$k_1 = Ae^{-E/kT} \quad \text{Chemical Rate}$$



$$k_2 = c_p \mu_k pV \quad \text{Mechanical Rate}$$

$$RR = \frac{M_w}{\rho} \frac{k_2 k_1}{k_2 + k_1}$$

Mean reaction temperature model:

$$\bar{T} \approx \bar{T}_p + \frac{\beta}{V^{1/2+e}} \mu_k pV$$

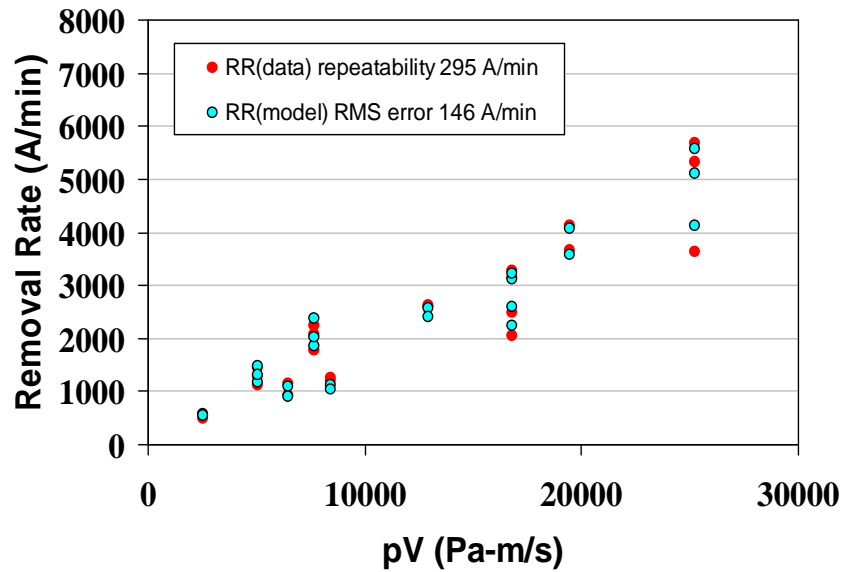
A , c_p , β and e are fitting parameters

A depends on slurry chemistry

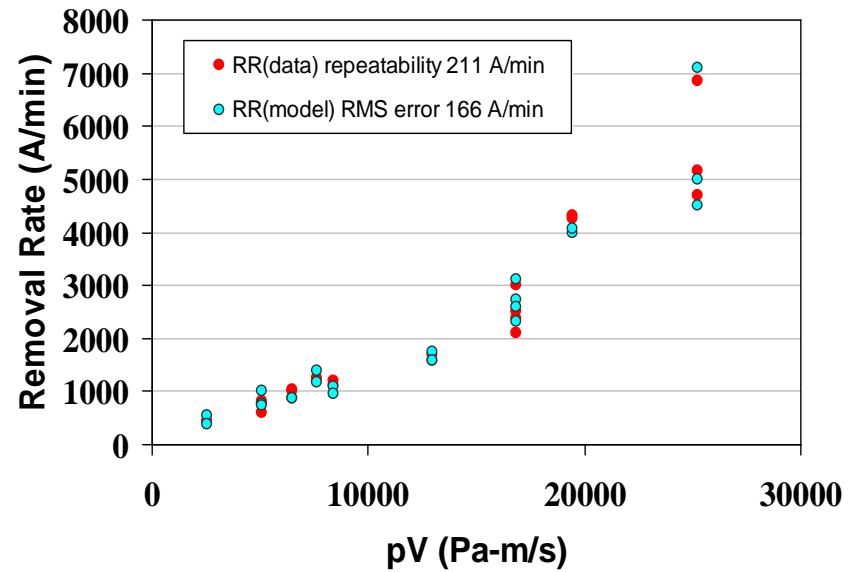
c_p , β and e depend on pad thermal & mechanical properties & on conditioning

Removal Rate Simulation

Conditioning Force: 2.5 lb-f



Conditioning Force: 4.9 lb-f

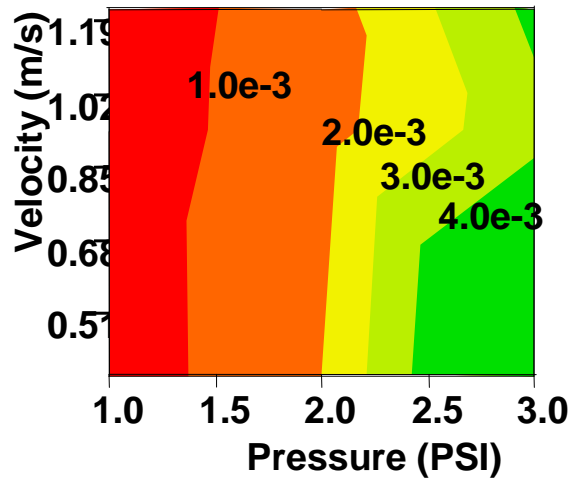


Simulated RR values agree well with experimental data

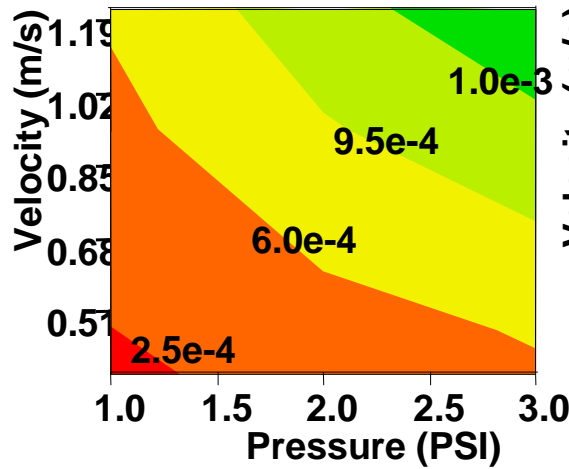
Chemical/Mechanical Rate Constants

2.5
lb-f

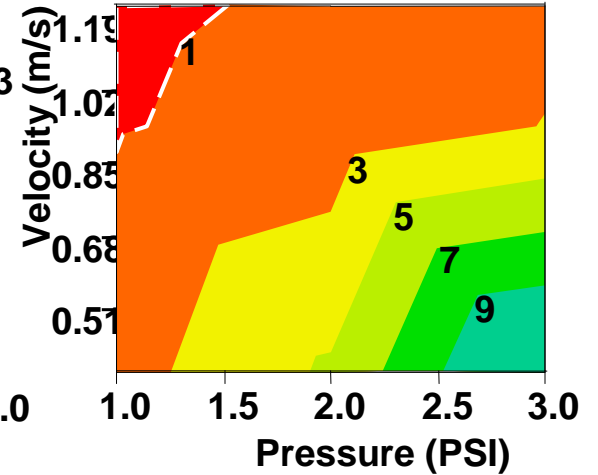
Chemical Rate Constant k_1



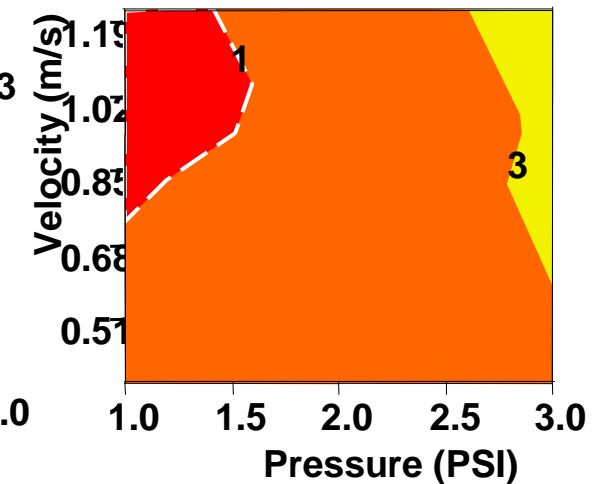
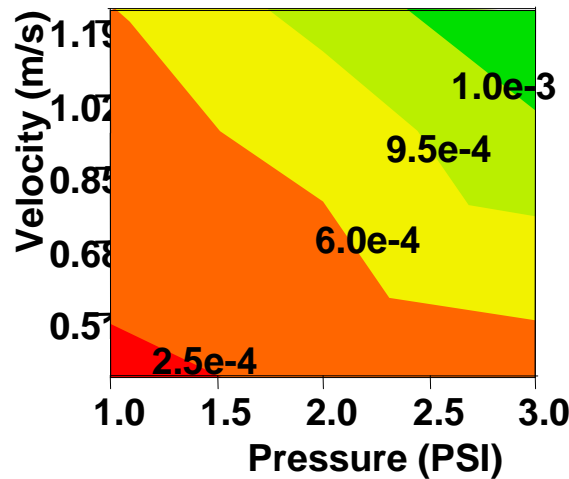
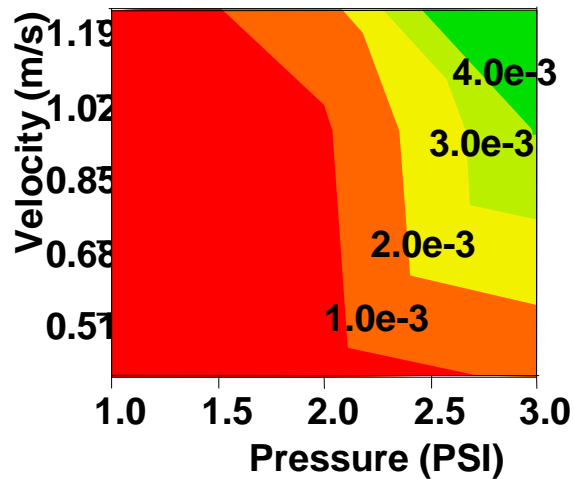
Mechanical Rate Constant k_2



k_1/k_2

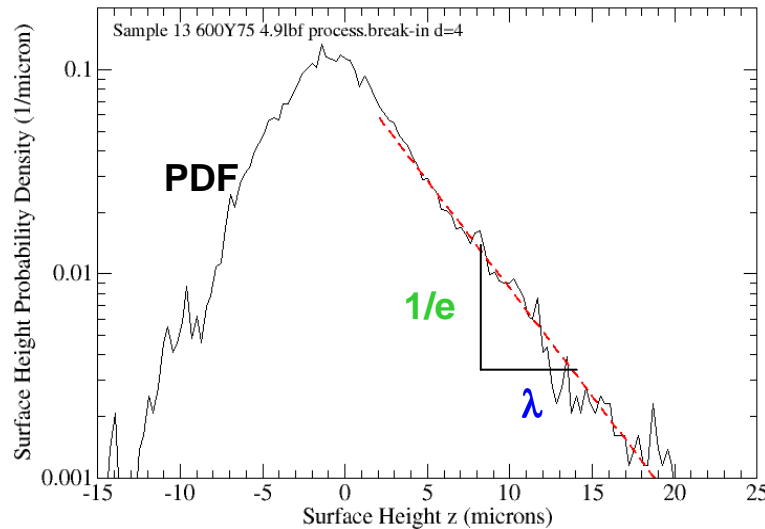


4.9
lb-f



Pad Surface Profilometry Analysis

---Terminology and Extracted Data

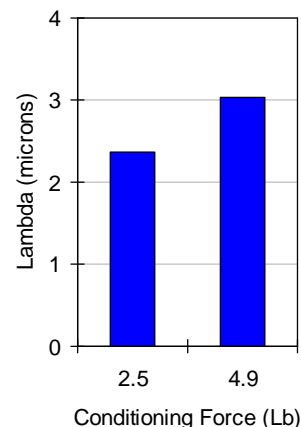
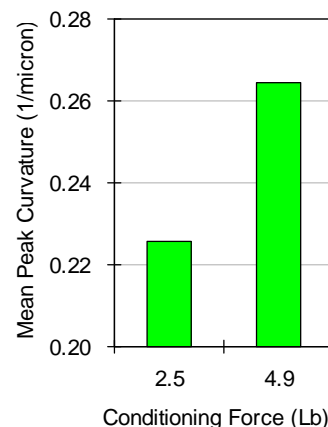
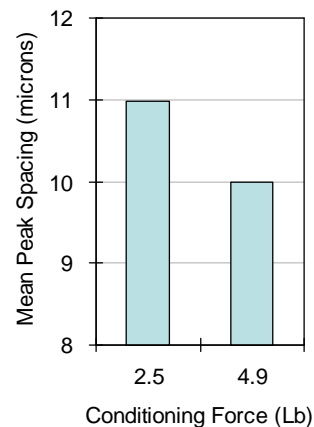


Density of Peaks η – the number of peaks per unit length of scan

Mean Peak Curvature κ – a measure of peak sharpness. Higher curvature means sharper peaks.

PDF – Probability density function, a histogram of surface heights whose area is normalized to 1.

λ - For PDFs with an exponential tail, λ is the distance over which the tail drops by a factor of 1/e. A larger λ corresponds to a rougher surface.



As conditioning force **increased**, mean peak spacing **decreased**, mean peak curvature **increased**, and the surface became **rougher**

Parameter Comparison

$$\beta = \beta_1 \kappa^{3/4} \lambda^{-1/4} \eta^{-1}$$

L. Borucki et al.
 Trans. ASME J. Tribology,
 127(3), pp. 639-651 (2005).

$$c_p = c_{p1} \lambda^{-1/2} \kappa^{-1/2} \propto \text{Contact Area}$$

		2.5 lb-f	4.9 lb-f
c_p	Pad surface analysis and conditioning theory	1.60E-07	1.24E-07
	Langmuir-Hinshelwood model	1.50E-07	1.31E-07
β	Pad surface analysis and conditioning theory	5.84E-03	5.46E-03
	Langmuir-Hinshelwood model	5.95E-03	5.36E-03

The differences between the two methods are 2-7 percent

Industrial Collaboration

**Cliff Spiro, Mike Lacy – Cabot Microelectronics Corporation–
CMP Pads and Slurries**

Future Plans

- **Investigating conditioners and conditioning recipes' effect on polishing performance stability.**
- **Determining the mechanism of pad hardness and pad porosity's impact on polishing performance.**

Conclusions

- The effect of conditioning force on pad topography and RR during copper CMP was investigated
- **COF (2.5 lb-f) \approx COF (4.9 lb-f)**
- **T_{pad} (2.5 lb-f) > T_{pad} (4.9 lb-f)**
- **RR (2.5 lb-f) > RR (4.9 lb-f) at moderate values of pV**
- Simulated RR from the L-H model agreed well with experimental data
 - **k_1 (2.5 lb-f) is considerably larger than k_1 (4.9 lb-f)**
 - **k_2 (2.5 lb-f) is slightly larger than k_2 (4.9 lb-f)**
 - **k_1/k_2 (2.5 lb-f) is significantly larger than k_1/k_2 (4.9 lb-f)**
 - **$k_1/k_2 > 1$ (in most cases) ... 'mechanically-controlled' polishing**
- **Pad surface profilometry results indicated that when conditioning force increased, mean peak spacing decreased, mean peak curvature increased, and pad surface became rougher**
- Parameters independently calculated from pad surface profilometry data were consistent with extracted values from the L-H model
- **For the first time, we have experimentally and theoretically demonstrated a strong correlation between pad surface profile and kinetic rate constants**

Modeling and Physical Understanding of CMP Process

Hong Cai – Ph.D. Candidate, Material Science

Xiaolin Xie – Ph.D. Candidate, Physics

Professor Duane Boning, EECS

Microsystems Technology Laboratories

Massachusetts Institute of Technology

Task 425.020

An Integrated, Multi-Scale Framework for Designing Environmentally-
Benign Copper, Tantalum and Ruthenium Planarization Processes

ERC Annual Review, February 2007

ESH Metrics

- Yield improvements of several % by identification of problem topography on chip
- Circuit performance of ~5-10% through model-based dummy fill may be possible

	Usage Reduction			Emission Reduction			
Goals/Possibilities	Energy	Water	Chemicals	PFCs	VOCs	HAPs	Other Hazardous Wastes
Real-time Sensing and Control	10%	10%	10%	N/A	N/A	N/A	10% reduction
Integrated plating/polishing optimum	35%	35%	35%	N/A	N/A	N/A	35% reduction
Replace abrasive-slurries with AFP	comparable	50% reduction in rinse & clean	comparable	N/A	N/A	N/A	No solid particles in polishing effluent stream

Relating Pad Properties to Feature/Chip-Scale Topography Evolution

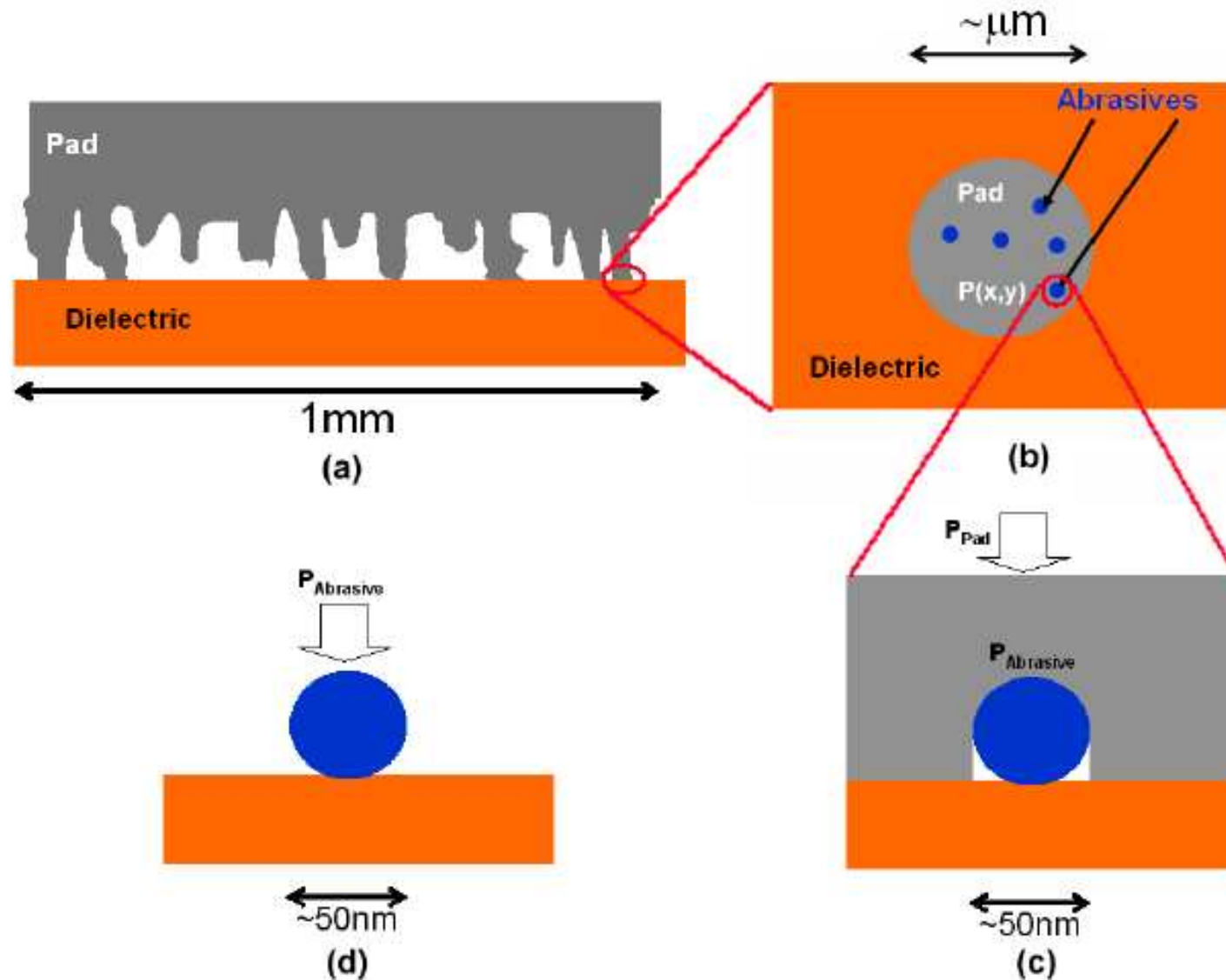
Subtask 1: Wear phenomena and their effect on process performance

- Key issue: how can we relate pad structure and parameters to the efficiency of planarization?
- Approach:
 - Develop a physical understanding of CMP process, and the roles of consumables
 - Extend previous *empirical* CMP model, specifically to...
 - Address the role of surface asperities in planarization, dishing, and erosion
 - Enable integration with detailed experiments and models of larger ERC team (UA, Tufts, Purdue) in pad/slurry effects
- Results:
 - Model extensions which improve physical basis for chip-scale CMP model, and explicitly account for pad surface properties

Physical Understanding of CMP

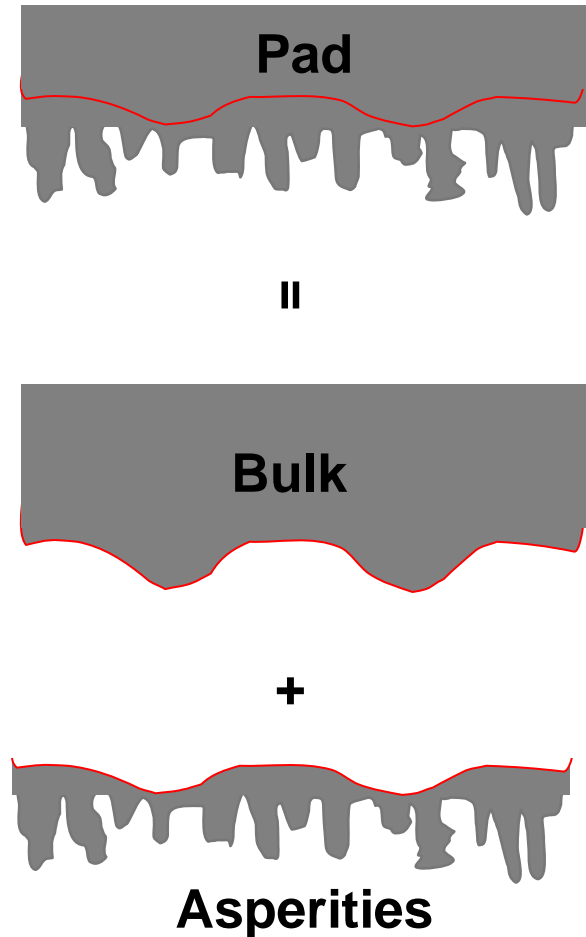
- CMP is due to a “3-body” contact mechanism
 - Polishing pad, abrasive, and wafer surface
- “3-body” contact can be broken down in the following interactions
 - Abrasive-wafer interaction: *removal rate of a single abrasive*
 $RR0(\phi, L)$
 - Pad-abrasive interaction: *load applied on a single abrasive*
 $L(\phi, P_{Pad})$
 - Abrasive occupation rate: *surface abrasive density*
 $q(\phi, n(\phi), P_{Pad})$
 - Pad-wafer interaction: *distribution $S(P_{Pad})$ of contact pressure P_{Pad}*
 - *Where ϕ is the abrasive diameter, $n(\phi)$ is the distribution of abrasive size.*

Top-Down Breakdown of CMP



Basis for Extended Model

- Pad is assumed to consist of a “bulk” material with surface asperities
- Bulk material obeys
 - contact wear model
- Asperities are assumed to
 - have negligible width
 - observe Hook’s law, i.e. the force it exerts is proportional to its compression



Opportunities: Pad Properties Integrated with Chip-Scale Model

- Physical-based model
 - Uses reasonable assumptions
 - Computationally feasible
 - Verifies and extends previous CMP models
 - Link empirical model parameters with physical pad property parameters (bulk modulus; pad surface asperity height distributions)
- Next steps
 - Implement time-step CMP model
 - Verify with experimental data
 - Empirical pad asperity height info (UA, Tufts interaction)

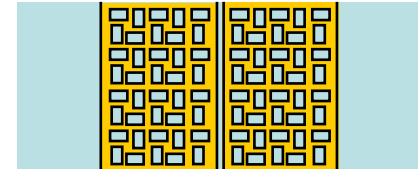
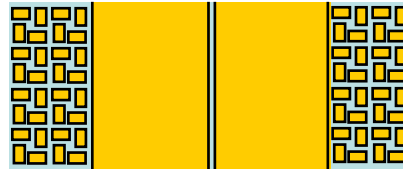
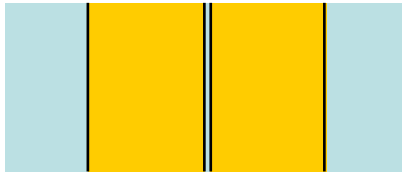
Control of Dishing/Erosion in Copper Interconnect

Subtask 2: Real-time detection and modeling of pattern evolution

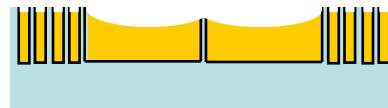
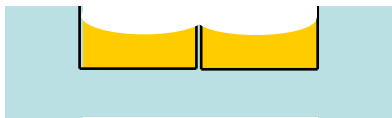
- **Problems in Conventional Copper CMP**
 - Low copper removal rate at low pressure compatible to low-K materials
 - Dishing and erosion problems
 - Competition from other planarization techniques, eg. ECMP
- **Strategy to Extend Conventional CMP**
 - Reduce the electroplated copper film thickness (1 times of trench depth)
 - Improve the slurry and polishing pad to increase the removal rate at low down force
 - High linear relative polishing velocity
 - Dummy fills!

Alternative Dummy Fill Strategies

Top view



Side view



(a) Without dummy fills

(b) With between-pattern
dummy fills



**Conventional
Approach**

(c) With in-pattern
dummy fills



**Alternative
Approach**

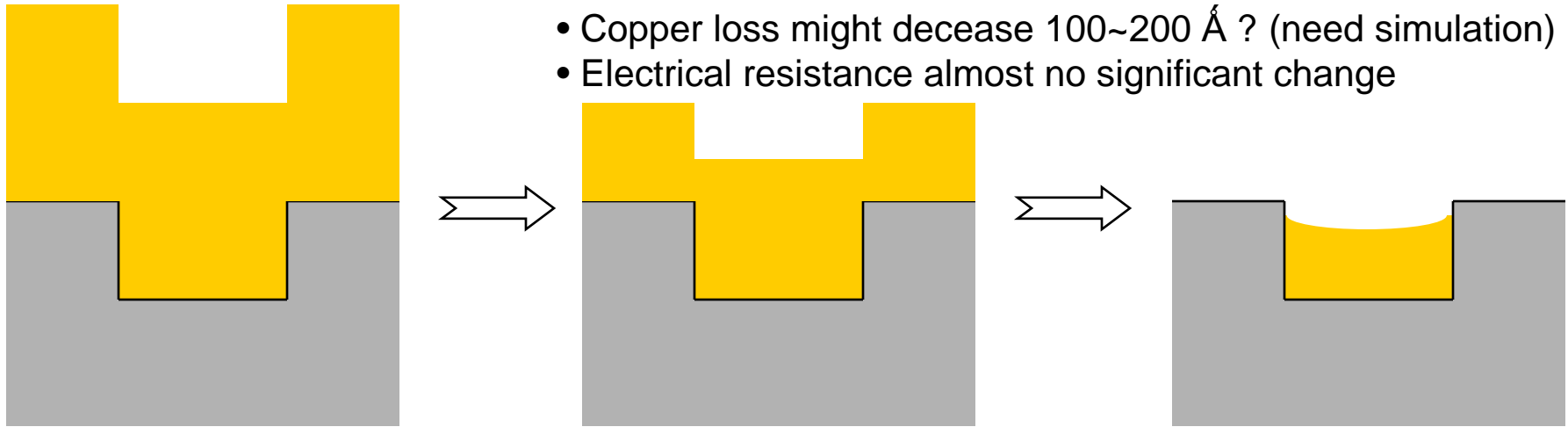
Between-Pattern Dummy Fills

- Sacrifice the inserted copper to even the topography after polishing
- Relative ineffective to even the topography due to the low dishing for the dummy fills in the advanced CMP process

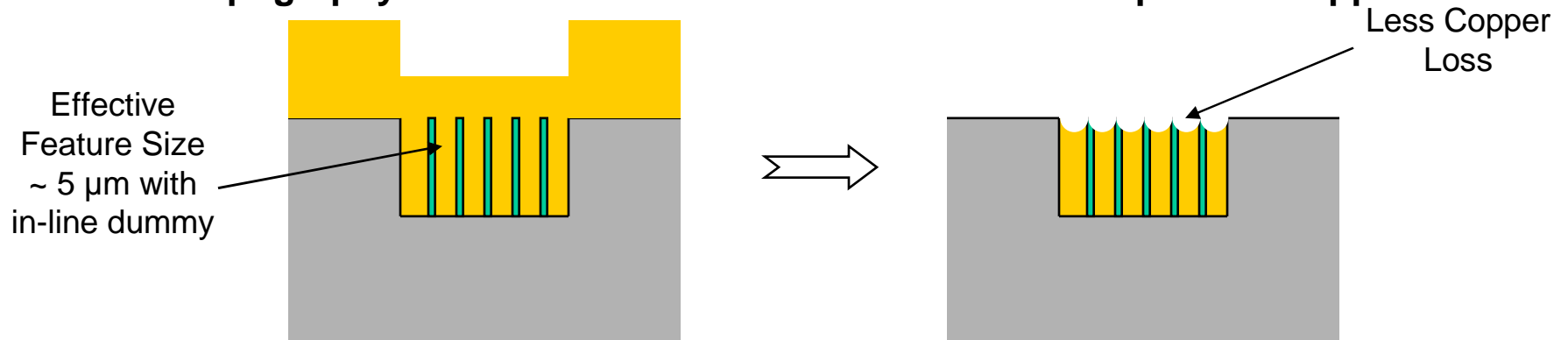
In-Pattern Dummy Fill

In-Line Dummy

- Total effective line width decreases 5 ~10%
- Copper loss might decrease 100~200 Å ? (need simulation)
- Electrical resistance almost no significant change

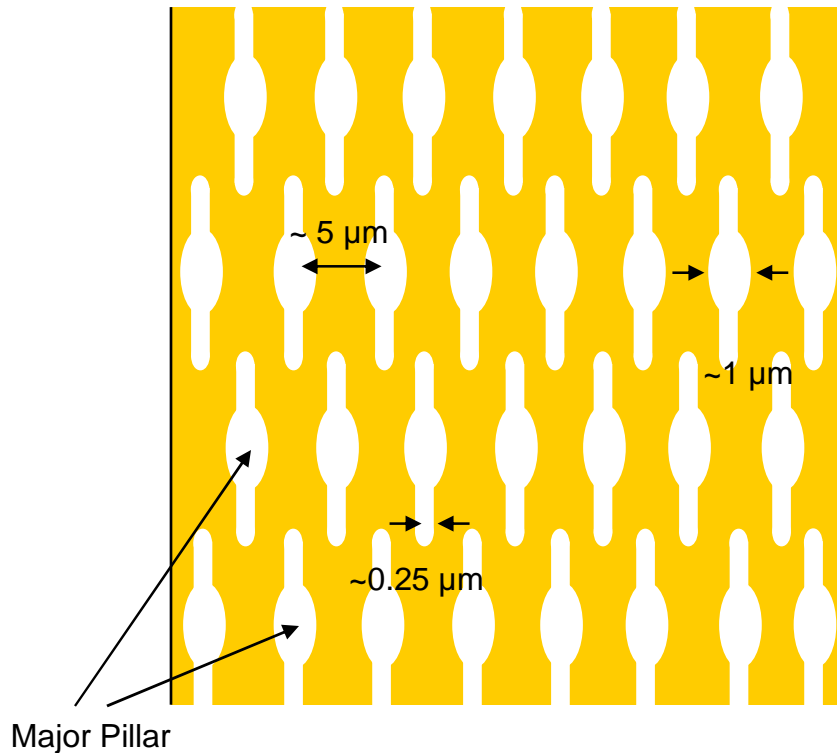


CMP Topography Evolution for Wide Feature with Thick Deposited Copper Film



CMP Topography Evolution for Wide Feature with Thin Deposited Copper Film and In-Line Dummy

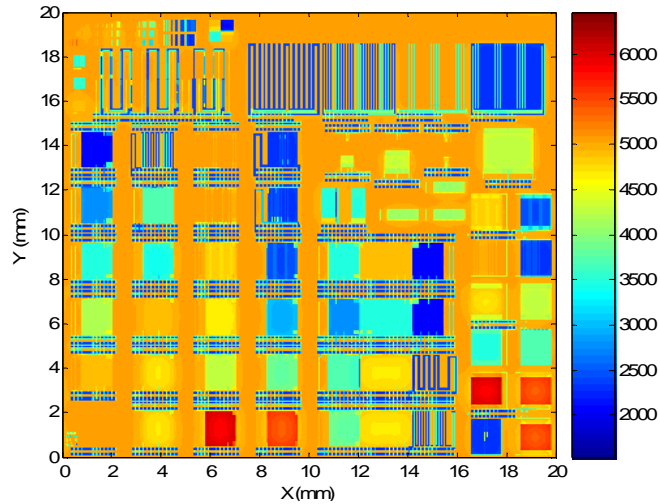
In-Pattern Dummy Design



- Goals:
 - Optimize dummy design to improve *both* plating and post-CMP topography
- Approach:
 - Add “slot” to increase trench wall surface areas, thus increasing plated copper thicknesses
 - Add “pillar” oxide structures to support the pressure of the pad, and restrict ability of asperities to reach copper between fill structures

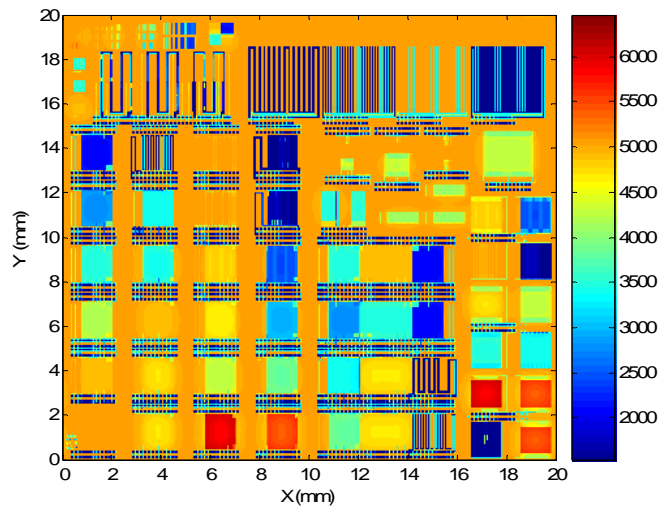
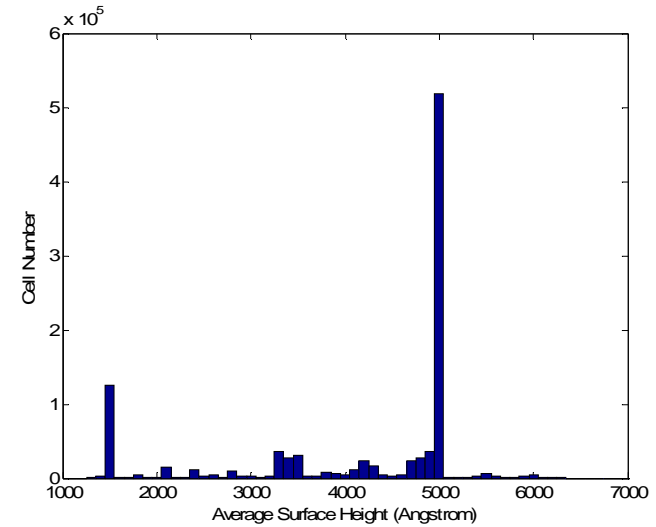
ECD Chip-Scale Simulation at 100 sec

Average surface height map (\AA)

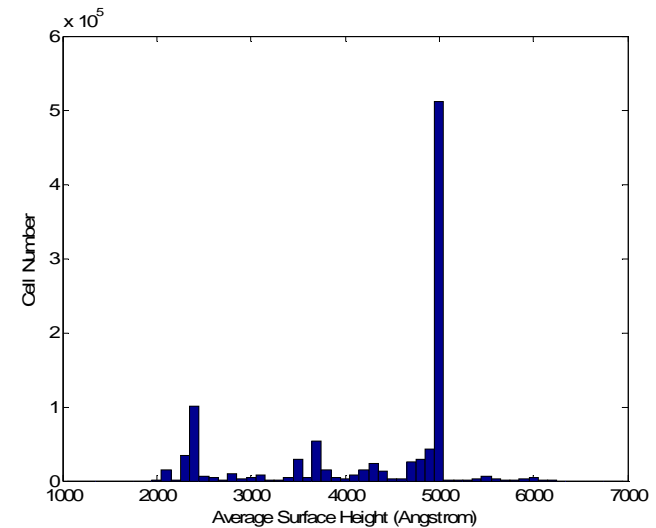


w/o dummy fills

Histogram of average surface height



w/ dummy fills

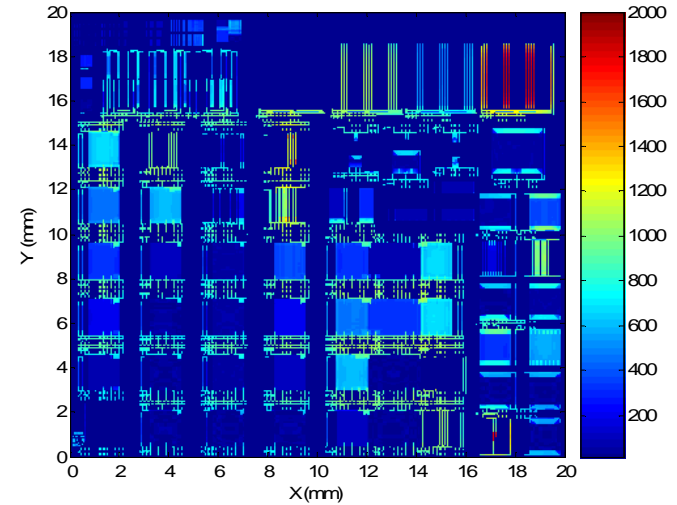
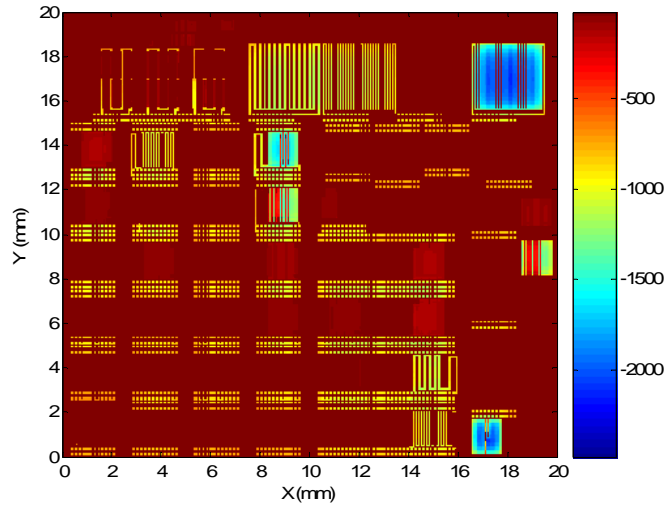


CMP Chip-Scale Simulation at 120 sec

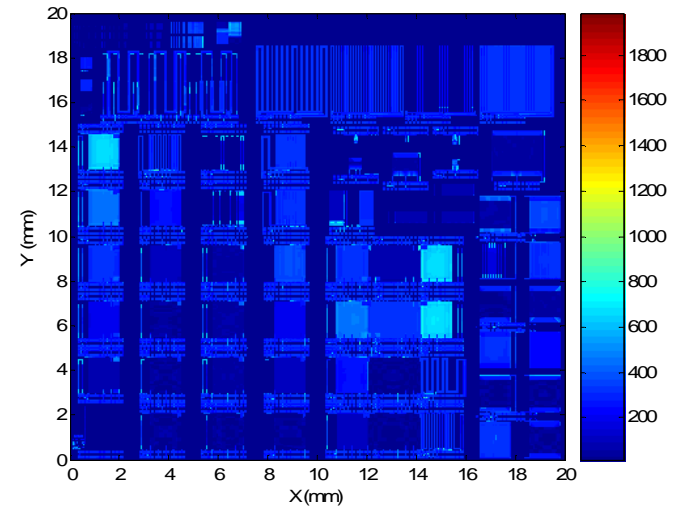
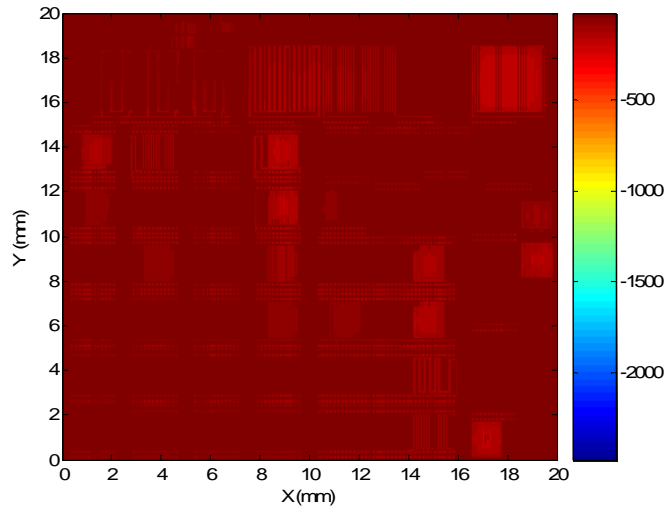
Envelope map (\AA)

Step height map (\AA)

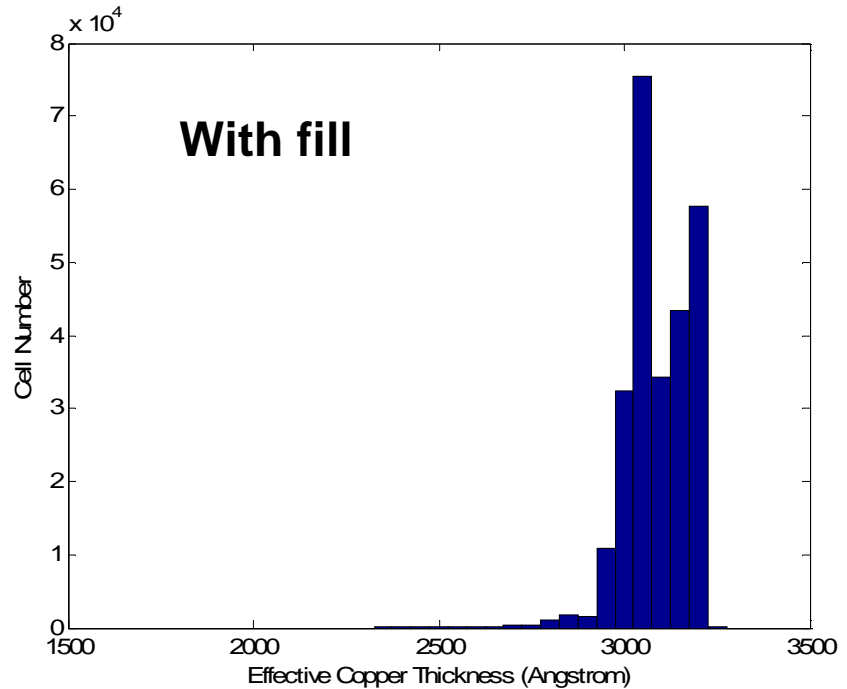
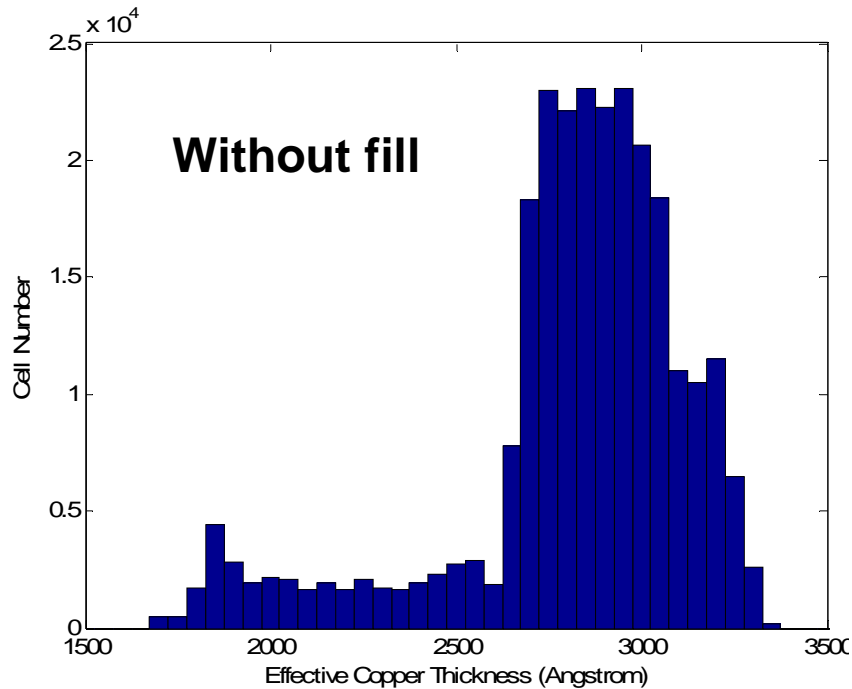
w/o dummy fills



w/ dummy fills



Comparison: Effective Copper Thickness w/o and w/ In-Pattern Dummy Fills



- **Key results**

- Dramatically improved topography based on fills designed with *both* ECD and CMP in mind
- Reduction of copper thickness required, from 8500 Å to 5000 Å, results in >40% reduction in plating and polishing

Summary and Next Steps

- Results

- Developed a physical understanding of dielectric CMP
- Extended our previous *empirical* chip-scale CMP model to include pad surface asperity effects and statistics
- Completed an integrated ECD/CMP chip-scale model
- Developed an “in-pattern” dummy fill strategy to control and reduce dishing/erosion loss

- Next Steps

- Relate additional pad/slurry properties to planarization performance
- Explore real-time endpoint signal relationships with pattern evolution model

Subtask C; SRC 425.015

**Reductive Dehalogenation of Perfluorooctane
Sulfonate (PFOS) and Related Compounds in
Semiconductor Effluents**

Valeria Ochoa, Jim A Field and Reyes Sierra

***Chemical and Environmental Engineering
University of Arizona***

SRC / Sematech Engineering Research Center for Environmentally Benign Semiconductor Manufacturing

Introduction



- Perfluorooctane sulfonate (PFOS) and other perfluoroalkyl surfactants (PFAS) are key components in a variety of IC manufacture process steps, including photolithography, wet etch and wafer cleaning.
- Perfluorinated surfactants are emerging environmental pollutants which have been detected in human blood and in wildlife tissues throughout the world.
- US-EPA and other environmental agencies are considering regulations restricting or banning the use of PFOS and related compounds.
- The application of conventional treatments for the removal of is restricted by technical and/ or economical considerations.

Introduction



Reductive dehalogenation \longrightarrow potentially promising

- A) Anaerobic microbial dehalogenation
- B) Chemical biomimetic dehalogenation

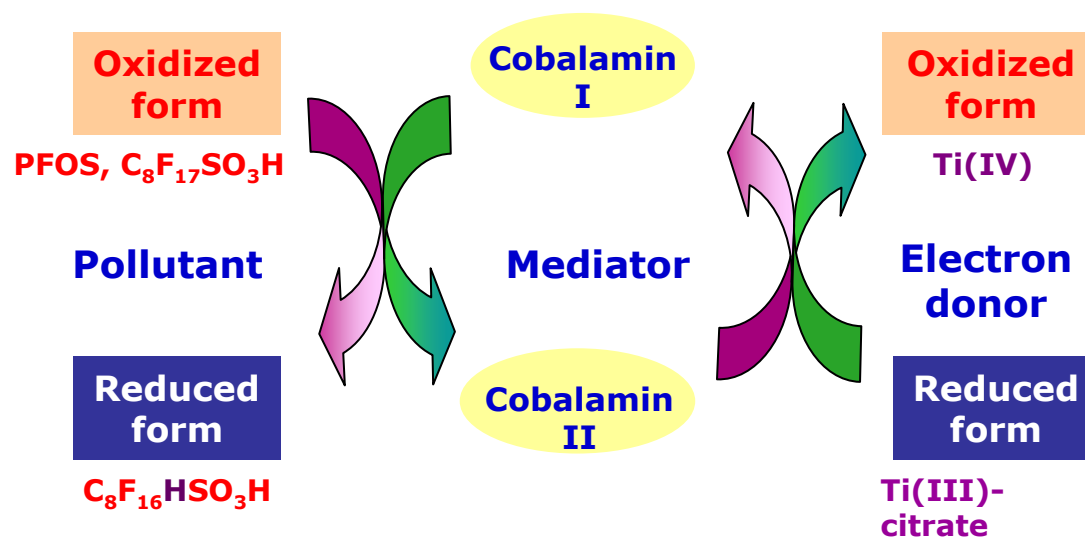


Fig 1. Proposed mechanism of the biomimetic reductive dehalogenation of PFOS with Ti(III) citrate and vitamin B₁₂.

Objective



Evaluate the feasibility of reductive dehalogenation of PFOS and other PFAS compounds using two different approaches:

- ❖ Microbial reductive dehalogenation
- ❖ Chemical biomimetic dehalogenation

ESH Impact



The replacement of fluorine with hydrogen atoms achieved by reductive dehalogenation is expected to improve the biodegradability of perfluorinated compounds in conventional biological wastewater treatment systems.

Materials and Methods



Biomimetic dehalogenation:

The susceptibility of PFOS to chemical dehalogenation catalyzed by vitamin B₁₂ and Ti(III)-citrate was evaluated at different pH and temperature levels in batch assays. Dosage of vitamin B₁₂ and Ti(III)-citrate were also optimized.

Monitoring dehalogenation:

Fluoride released was monitored using an ion selective electrode. PFOS and its degradation products were determined by a newly developed method using an HPLC system fitted with an Acclaim Polar Advantage II, C18 column and a suppressed conductivity detector. HPLC tandem mass spectroscopy (LC-MS/MS), GC-MS/MS and ¹⁹F-NMR were also utilized to aid in the identification and quantification of degradation products.

Analytical Methods

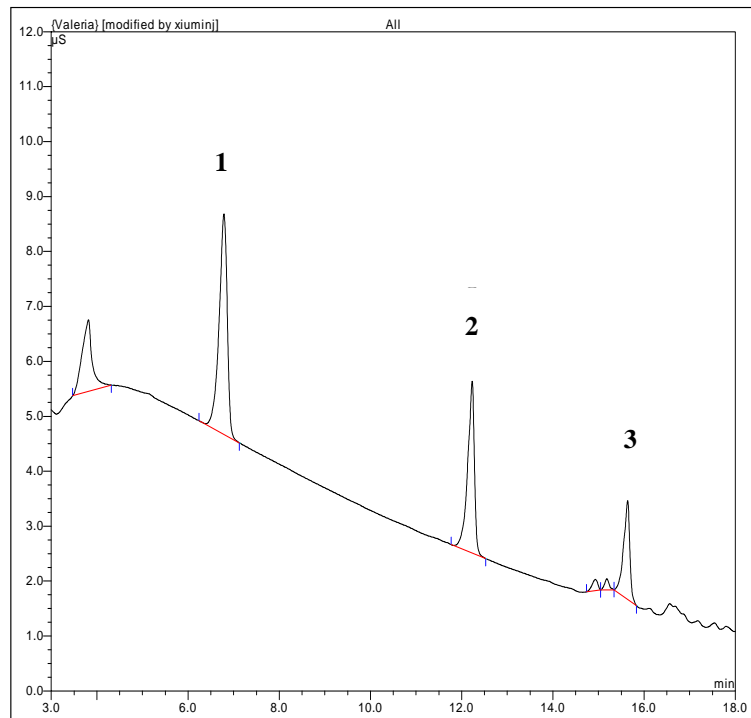


Fig. 2. HPLC-suppressed conductivity ion chromatograph of a solution containing PFBS (1), PFOA (2) and PFOS (3).

- ❖ ^{19}F -NMR Spectroscopy
- ❖ ESI/MS
- ❖ LC/MS/MS
- ❖ HPLC-suppressed conductivity detection

- a) Simple, rapid and efficient
- b) Short analysis times
- c) Low ppm-PFOS

Results



First report of reductive dehalogenation of PFOS catalyzed by vitamin B₁₂/Ti(III)

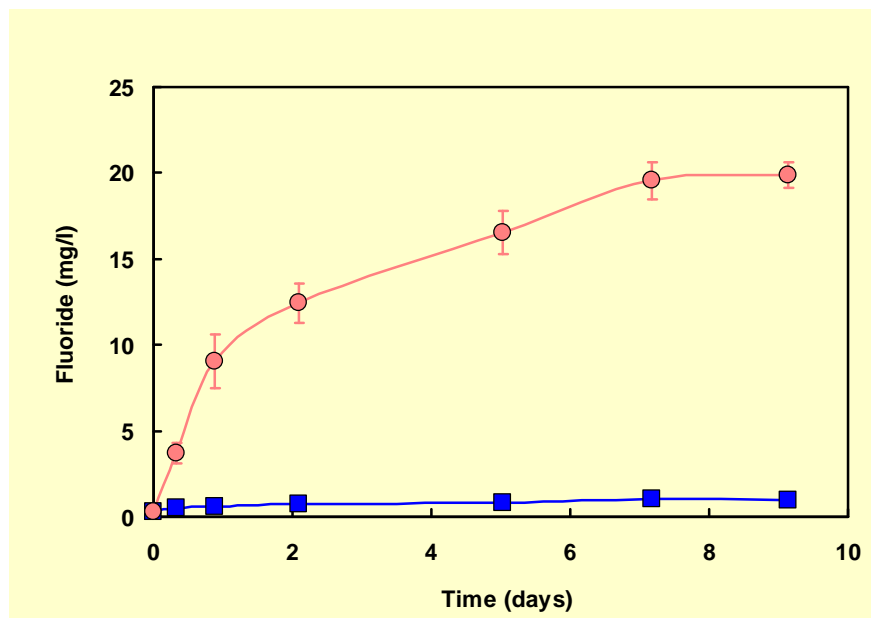


Fig 3. Time course of fluoride release at 70°C and pH 9.0

18% defluorination



3 mol F⁻/mol PFOS

Dehalogenation not observed when only Ti(III)-citrate of cobalt(II) were present

Results

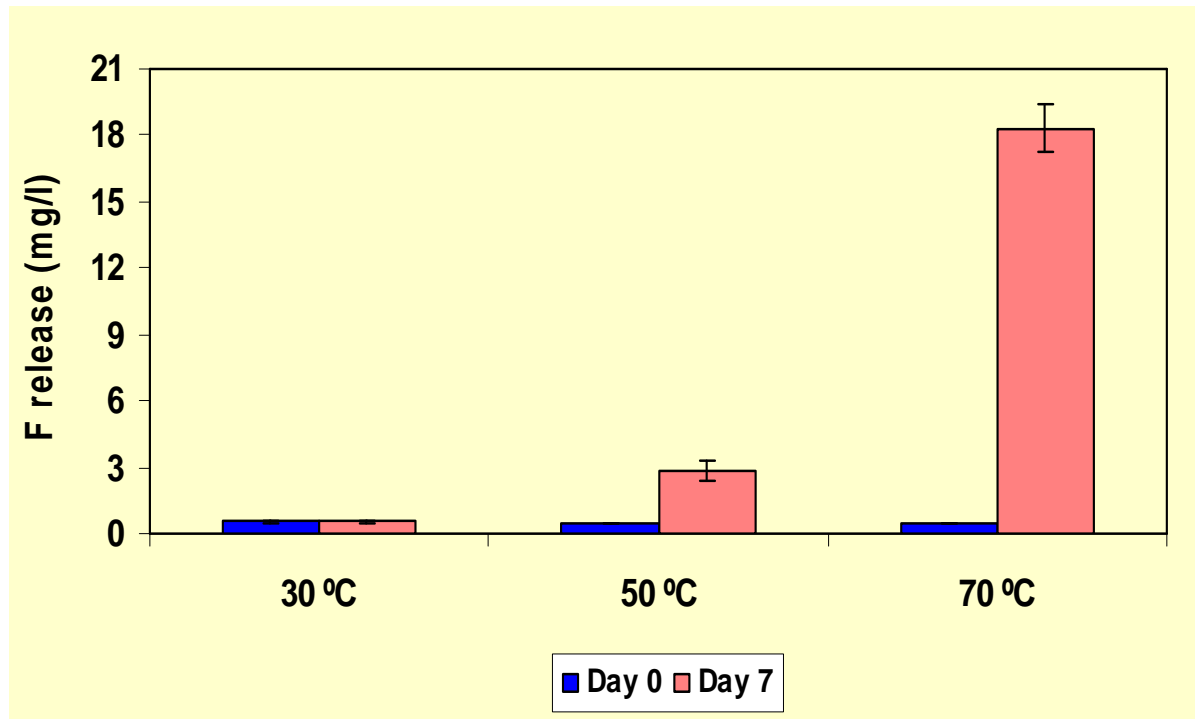


Fig 4. Effect of temperature on the reaction of PFOS and Ti(III)/vitamin B₁₂

Results

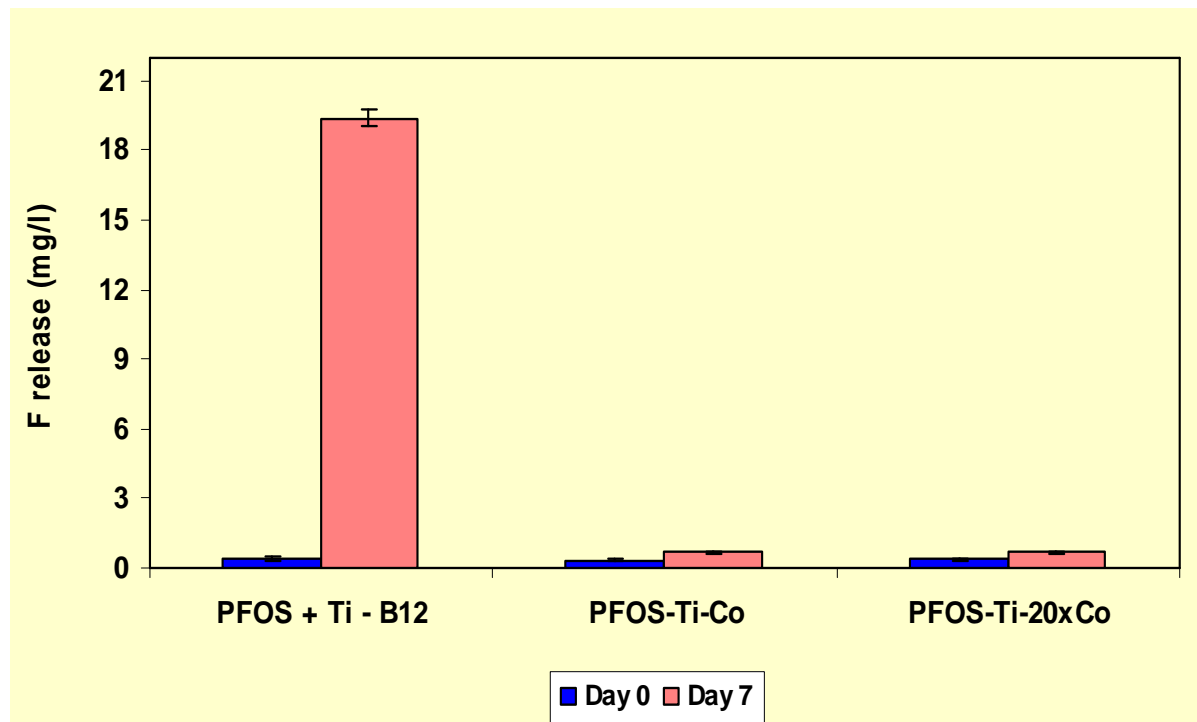


Fig 5. Effect of catalyst on the reaction of PFOS and Ti(III)/vitamin B12.

Conclusions



- PFOS was shown to be susceptible to biomimetic reductive dehalogenation by vitamin B₁₂/Ti(III) citrate.
- Considerable enhancement in the rate of reductive defluorination was attained by increasing the reaction temperature from 30°C to 70°C.
- Microbial degradation of PFOS might be possible.
- Analytical method to quantify PFOS in environmental samples by HPLC-suppressed conductivity detection was developed.

Industrial Collaboration/Technology Transfer



Industrial Liaisons:

Walter Worth - Sematech

Tim Yeakley – TI

Disclosures:

UA07-037 (active) - Biomimetic degradation of perfluorinated and highly-fluorinated organic compounds. R. Sierra-Alvarez.

SRC / Sematech Engineering Research Center for Environmentally Benign Semiconductor Manufacturing

Future Plans



- ❖ Identification of degradation products from the biomimetic reductive dehalogenation of PFOS.
- ❖ Complete the optimization of the biomimetic reductive dehalogenation of PFOS and related perfluorinated compounds.
- ❖ Evaluation of the susceptibility of PFOS and related PFAS to microbial reductive dehalogenation using inoculum sources exposed to long chain perfluoroalkyl compounds for extended periods of time.
- ❖ Assessment of the susceptibility of partially dehalogenated perfluoroalkyl surfactants to biodegradation by aerobic microorganisms in municipal wastewater treatment systems, including co-oxidation by ammonia monooxygenase-producing nitrifying bacteria.

Environmental Health and Safety (EHS) Impact of Electrochemical Planarization Technologies

Kristin G. Shattuck

February 22, 2007

Task Number

425.016

Faculty Research Advisor

Alan West

Project Commenced

May 2006

Affiliation

Columbia University

Project Objectives

- **Develop and characterize novel chemistries to control Cu/barrier selectivity**
 - Ru and Ta-based liners
 - Investigate eCMP barrier-removal rates
 - Determine Cu/liner selectivity
 - Influence of inhibitors and pH on selectivity
 - Consider electrolyte/dielectric compatibility
- **Determination of planarization mechanisms for Cu e-CMP (Electro-Chemical Mechanical Planarization)**
 - Influence of various complexing agents
 - Role of additives
 - BTA (Benzotriazole), PTA (Phenyl-1H-Tetrazole)
 - Pad/Additive Interactions
- **Current Focus**
 - Effect of BTA/PTA concentration & pH in H_3PO_4 -based electrolyte
 - Previous work indicates this a promising electrolyte when combined with the correct pad
 - e-CMP Tool
 - Design Completed
 - Preliminary Polishing results

EHS Impact/ Metrics

- Environmental Health and Safety (EHS) impact of Electrochemical Planarization Technologies
 - Eliminating need for abrasive particles in electrolyte
 - Particles make waste difficult to treat
 - Possibly eliminating the use of strong oxidizing agents in electrolytes
 - Electrolytes without these oxidizing are less toxic and easier to treat
 - Potential reduction in electrolyte volume
 - Reduce waste generation

BACKGROUND: Previous Results

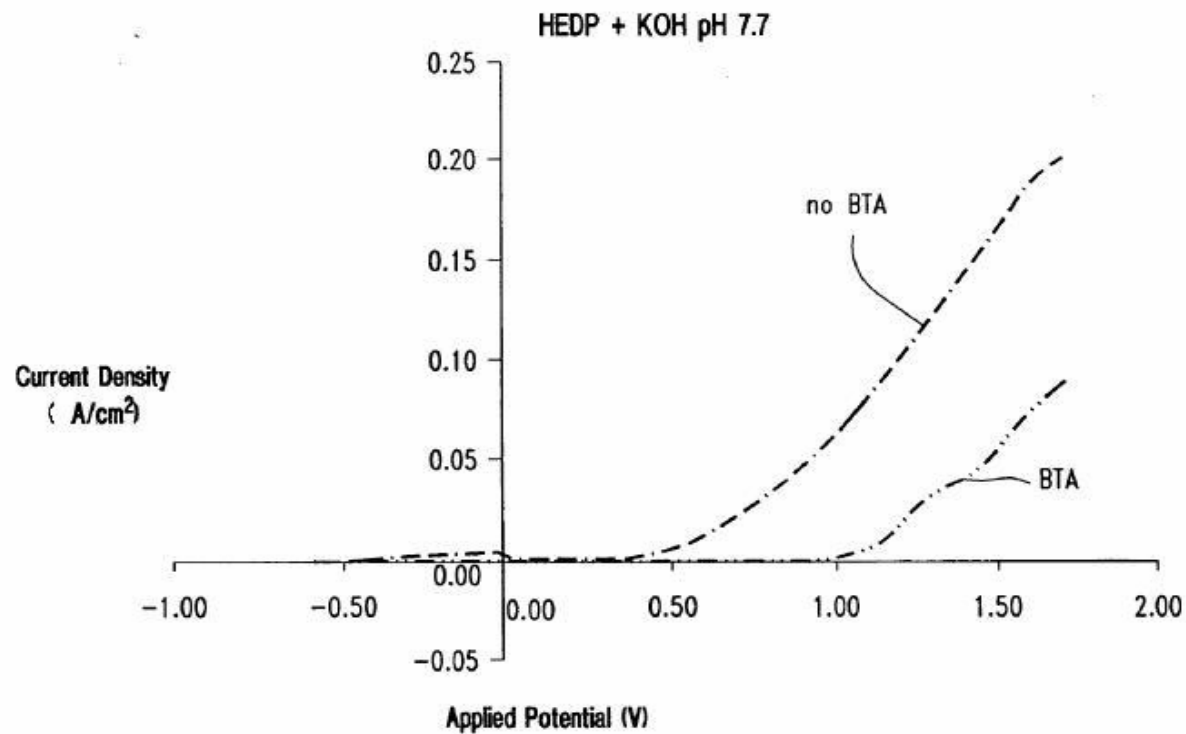


Figure 1: Potentiodynamic curve for Cu dissolution in 60% HEDP titrated with concentrated KOH with and without BTA present*

*US Patent Application 20060163083A1 – Andricacos et al., IBM Yorktown. July 27, 2006

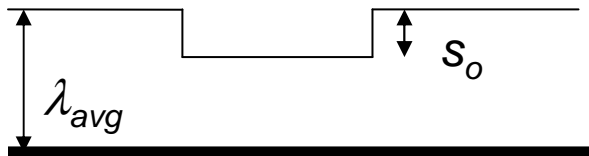
SRC/Sematech Engineering Research Center for Environmentally Benign Semiconductor Manufacturing

PF of BTA/HEDP System

- Define Planarization Factor: PF

- $PF = s / \lambda$

- S = decrease in average step height
 - λ = the decrease in the average metal layer thickness



- Planarization results using eCMP test structure

- Utilizing electrolyte with pH = 7.7

- **Figure 2** - PF ~ 0.65
 - 18 mA/cm¹

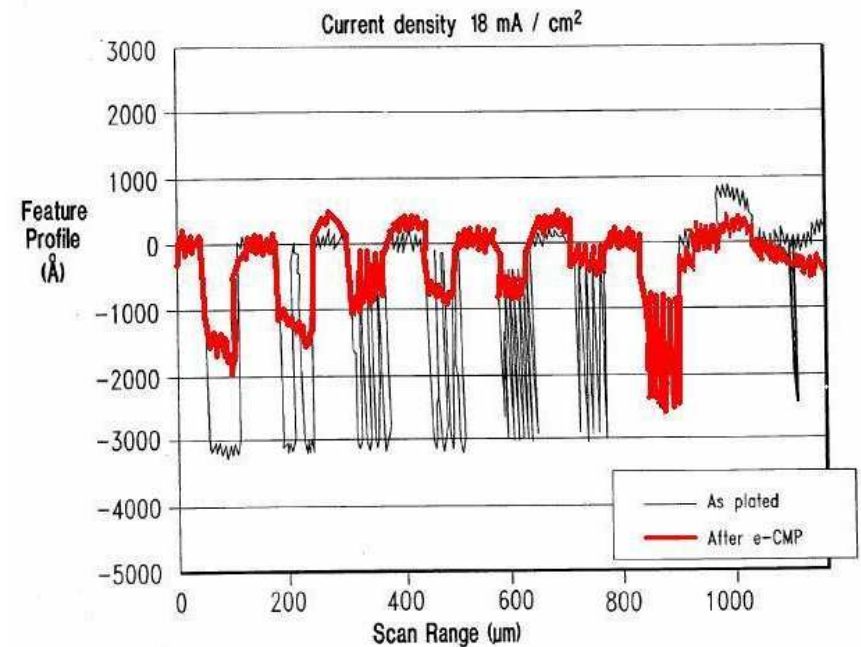


Figure 2: Profiles of Cu features before and after eCMP (pH 7.7) ¹ 18 mA/cm²

*US Patent 20060163083A1 – Andricacos et al., IBM Yorktown. July 27, 2006

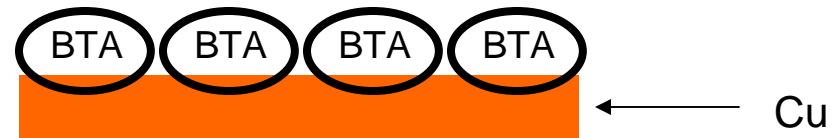
Electrolyte Characterization

- **Phosphoric acid based systems similar to HEDP**
- **Current Studies Focus on:**
 - $\text{KPO}_3 - \text{H}_3\text{PO}_4$ / BTA
 - H_3PO_4 /PTA
- **Experimental Parameters**
 - pH
 - Range 0 – 10.3
 - BTA/PTA Concentration
 - Range 0- 0.01 M
 - Mass Transfer
- **Characterization**
 - Electrochemical Impedance Spectroscopy (EIS)
 - Linear Sweep Voltametry (LSV)
 - Cyclic Voltametry (CV)

Proposed eCMP Mechanism Utilizing BTA

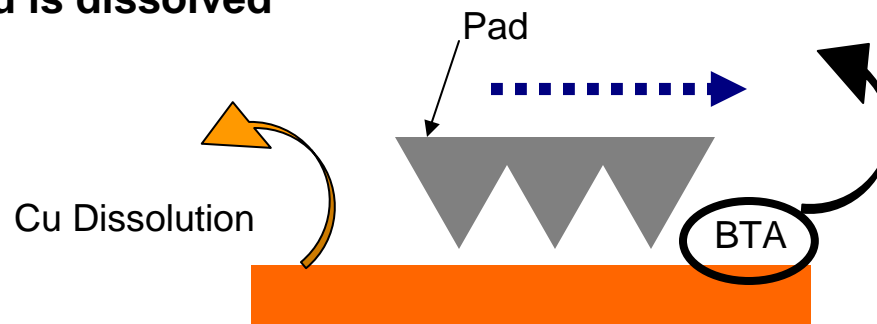
1. BTA adheres to surface

- Forms BTA-Cu complex

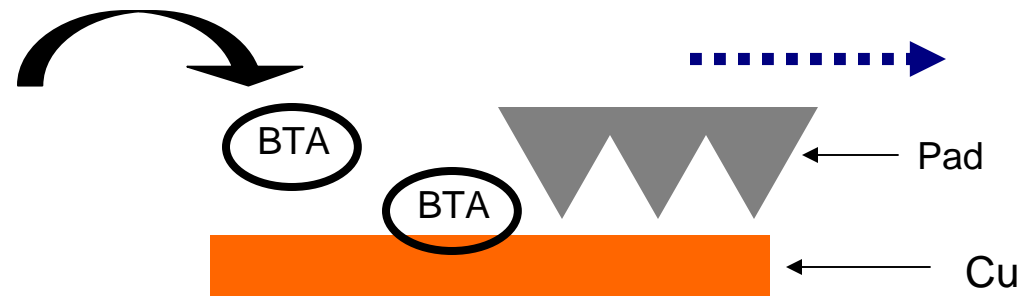


2. Pad mechanically removes Protective BTA layer

- Exposed Cu is dissolved



3. BTA re-attaches to protect new CU surface



Results of BTA Inhibitor Study

- **Effect of pH and Concentration**
 - Scan rate 5 mV/s – RT – 100 RPM
 - pH 2.3 (Fig 3)
 - pH 4.3 (Fig 4)
 - pH 7.3 (Fig 5)

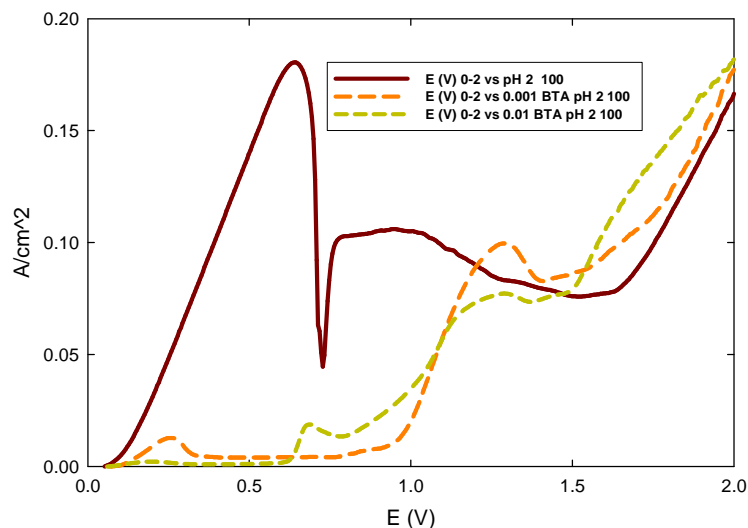


Figure 3: Anodic polarization curves of pH 2.3 using various BTA Conc

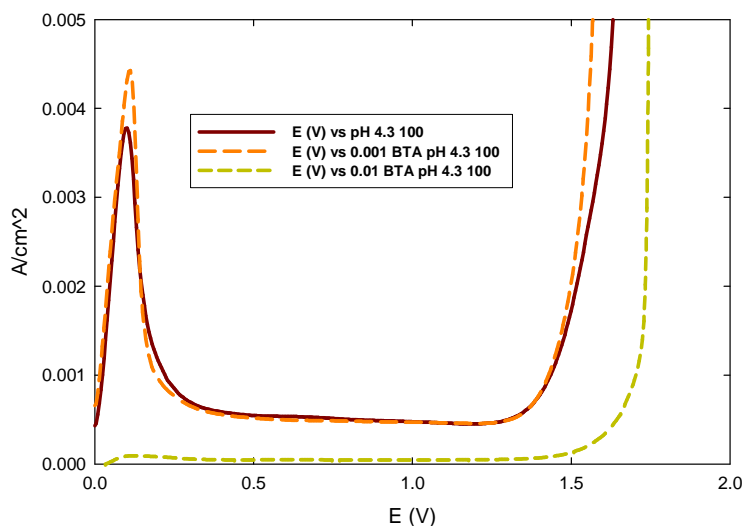


Figure 4: Anodic polarization curves of pH 4.3 using various BTA Conc

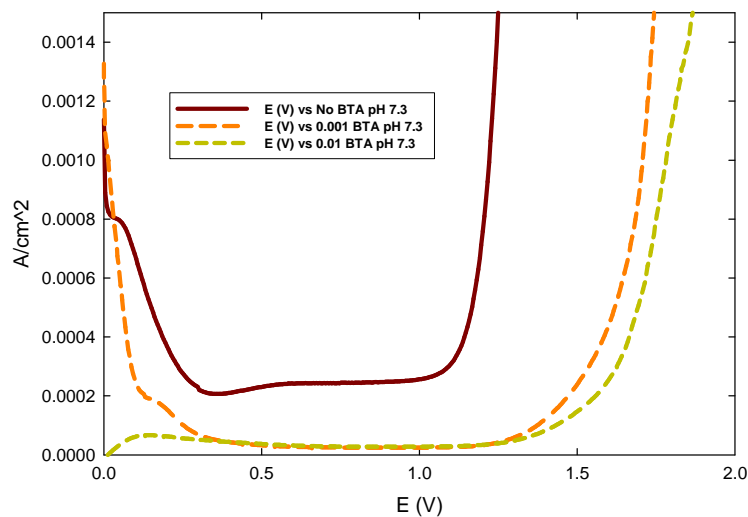


Figure 5: Anodic polarization curves of pH 7.3 using various BTA Conc

Planarization Capability

•Where:

- I = current with 0.001 M BTA
- I_{No} = current with No BTA

•Related to dissolution rate with and without a polishing pad

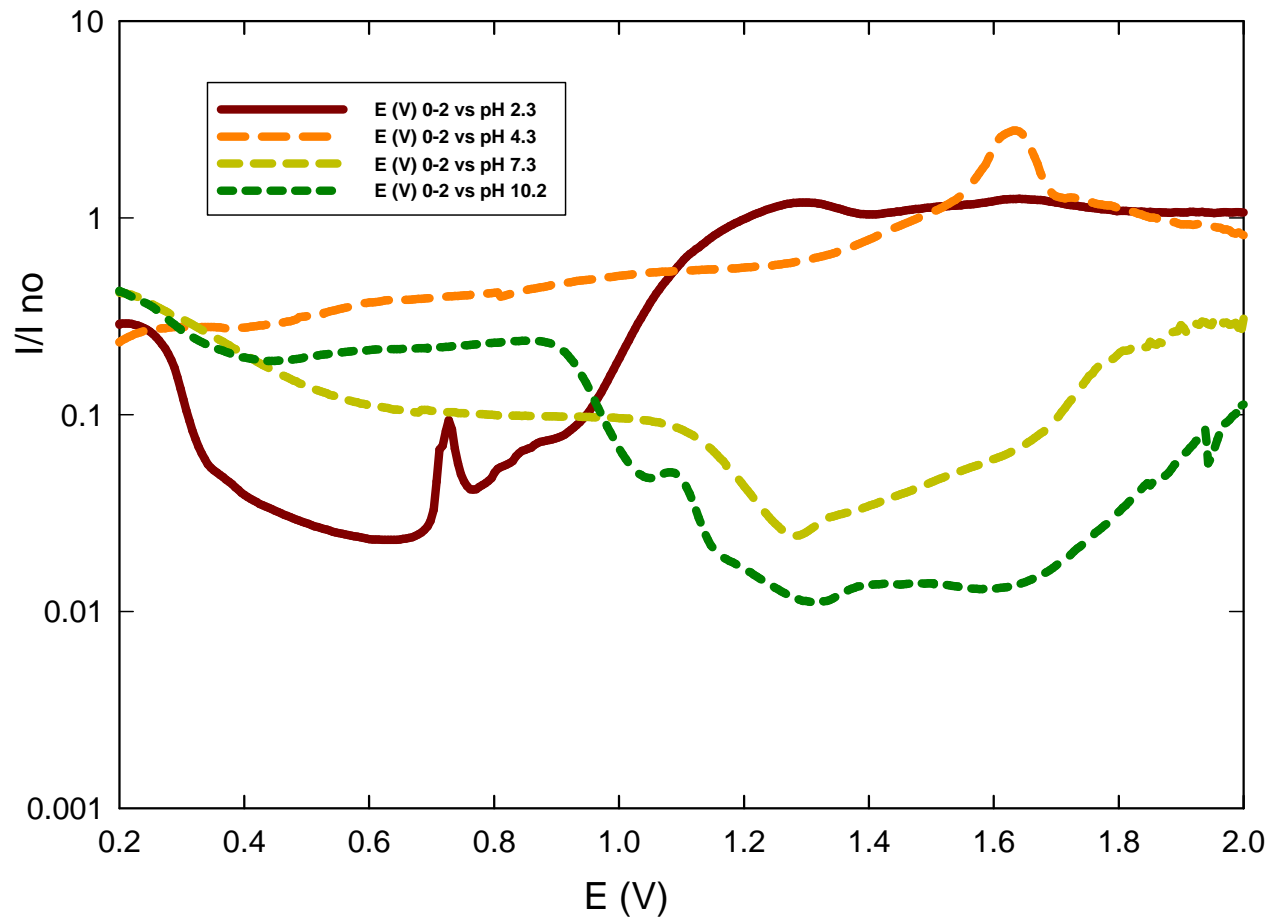
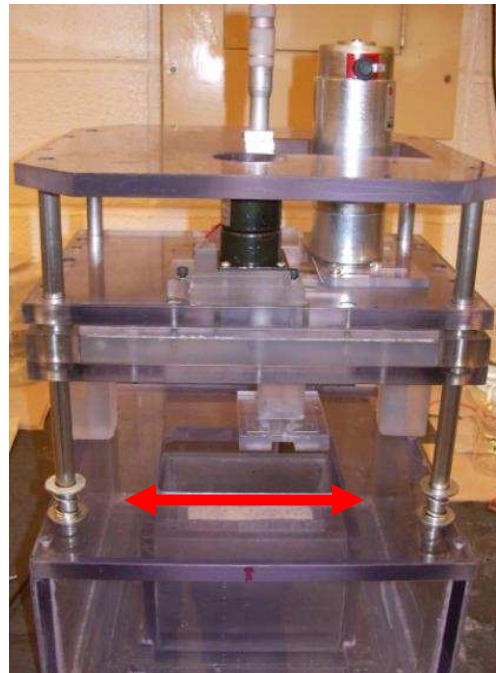
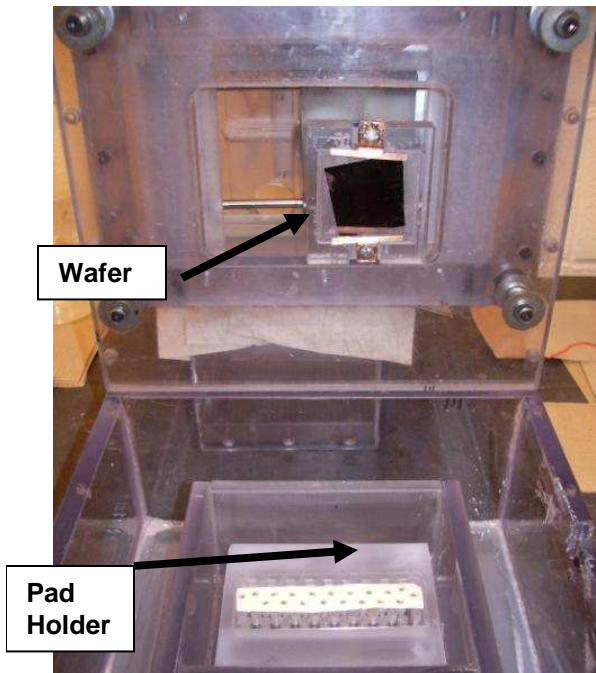


Figure 6: Planarization Capabilities of eCMP electrolytes containing 0.001 M BTA concentration varying from pH 2.3 – pH 10.2

eCMP Tool



- **Design features:**
 - 2D linear motion
 - Apply and control low downforces (<0.3 PSI)
 - Ease of changing between various electrolytes and pads
 - Operate in contact and non-contact modes
- **Major Characterization**
 - Metal-removal rates
 - Selectivity
 - Planarization efficiency

- **Good Agreement with RDE polarization curves**

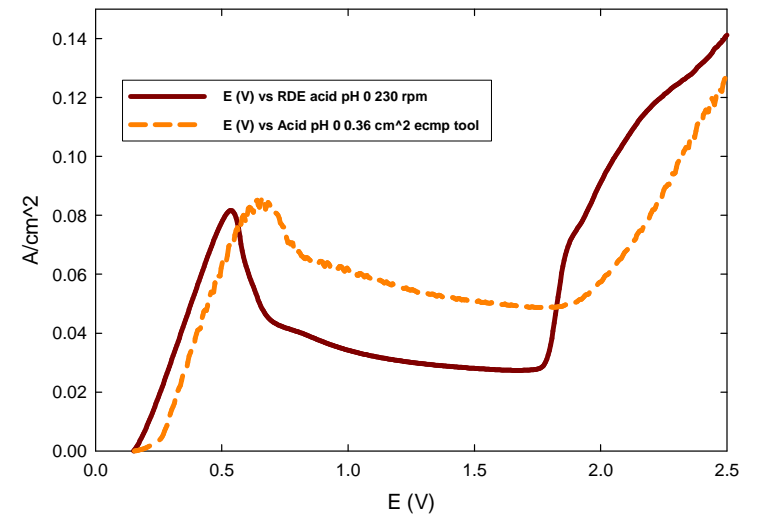


Figure 7: Anodic polarization curves of H_3PO_4 using e-CMP tool and RDE

Preliminary Polishing Results

- pH 2.3 - no pad contact

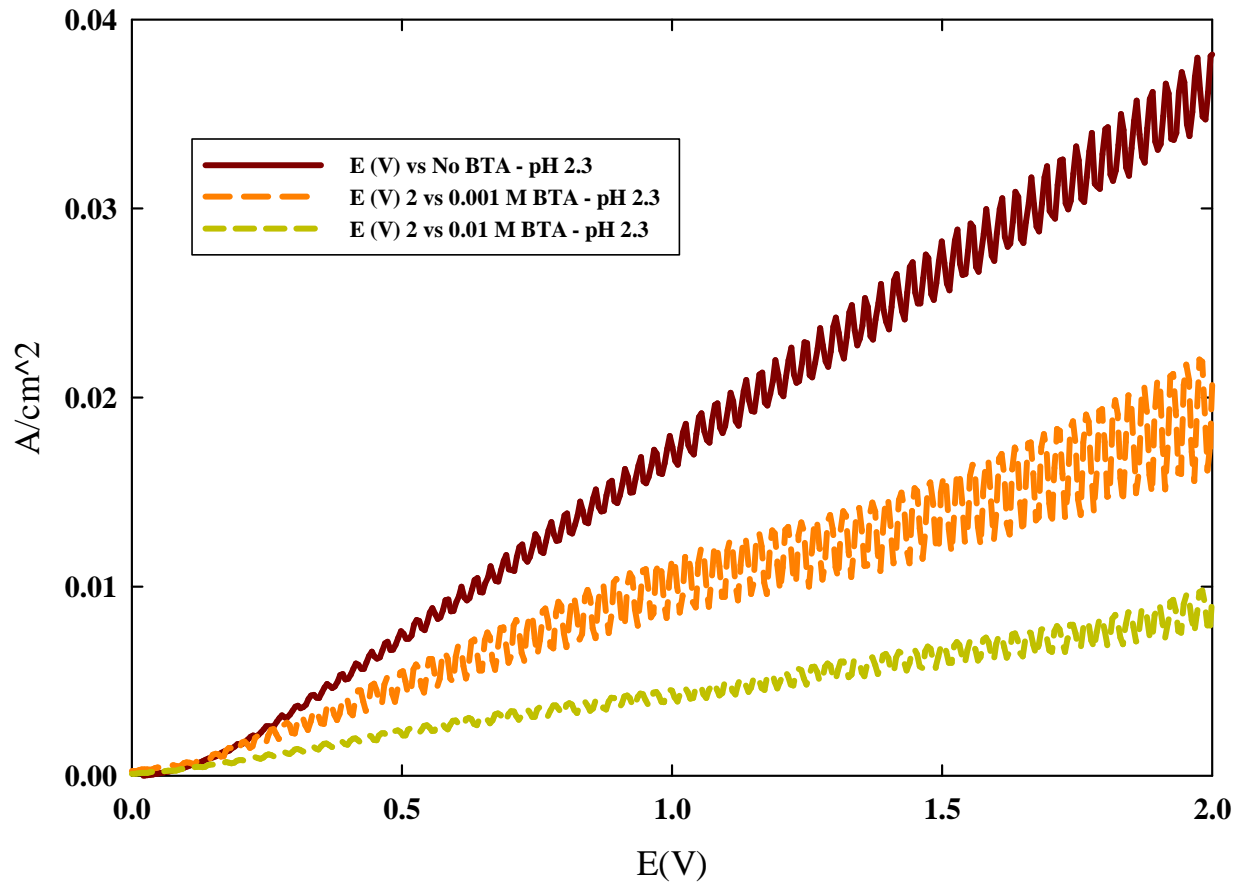


Figure 8: Anodic polarization curves of pH 2.3 varying BTA concentration (no BTA, 0.001 M BTA, 0.01 M BTA)

Summary

- **H₃PO₄/BTA Electrolytes**
 - **pH lower than 4**
 - BTA had little passivation effect
 - **pH above 4**
 - Change in RPM did not effect current density
 - Inhibition of Cu dissolution increased with both 0.001 and 0.01 M BTA concentrations
 - For all pH's above 4.3
- **eCMP Tool successfully completed**
 - Device accuracy confirmed with RDE experiments
 - Initial wafer testing has begin
- **Future Work**
 - Perform eCMP experiments to determine optimal electrolyte polishing composition
 - Begin investigation on polishing liner materials

Acknowledgements

- **Columbia University**
 - Alan West
 - Paula Cojocararu – visiting scholar
- **CMP Pads**
 - Cabot
 - Rohm & Haas
- **Industry mentors/contacts**
 - Intel
 - Novellus
 - Texas Instruments
- **SRC/ Sematech**

Synthesis of Low-k Mesoporous Silica Films in Supercritical CO₂



Alvin H. Romang, Gaurav Bhatnagar, and James J. Watkins
Polymer Science and Engineering
University of Massachusetts-Amherst

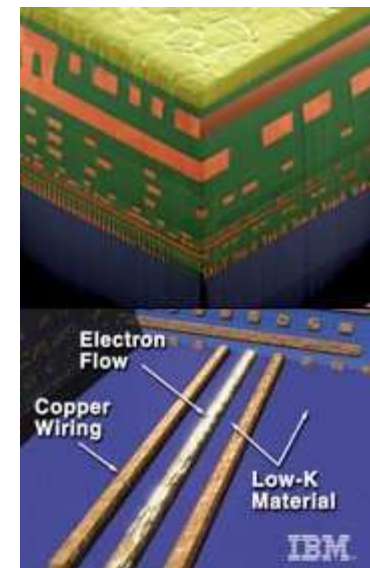
SRC: 425.017

SRC/Sematech Engineering Research Center for Environmentally Benign Semiconductor Manufacturing



Motivation

- Produce ultra low dielectric constant organosilicate thin films ($k < 2.0$) through infusion of silica precursors into a sacrificial polymer template in supercritical CO_2 .
- Prepared thin films provide balance between porosity and mechanical robustness in achieving low dielectric constant and surviving microelectronic processing.



Strategy

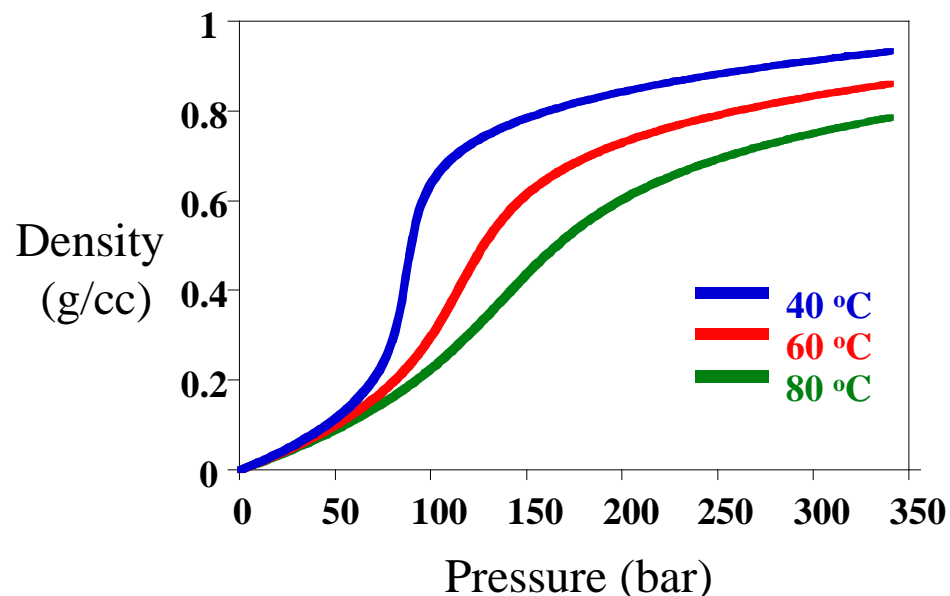
- Create ordered mesoporosity to reduce k while preserving mechanical robustness with different molecular weight polymers.
- Trap TSI POSS in the silica matrix to increase hardness.
- Use organosilicate precursors to reduce k and increase mechanical strength.



Supercritical CO₂ as Solvent

	Liquid	Gas	SCF
Density (g/cc)	1.0	0.001	0.1-1.0
Viscosity (Pa•s)	10 ⁻³	10 ⁻⁵	10 ⁻⁴ - 10 ⁻³
Diffusion (cm ² /s)	10 ⁻⁵	10 ⁻¹	10 ⁻³

$T_c = 31.06\text{ }^\circ\text{C}$ & $P_c = 73.83\text{ bar}$ for CO₂

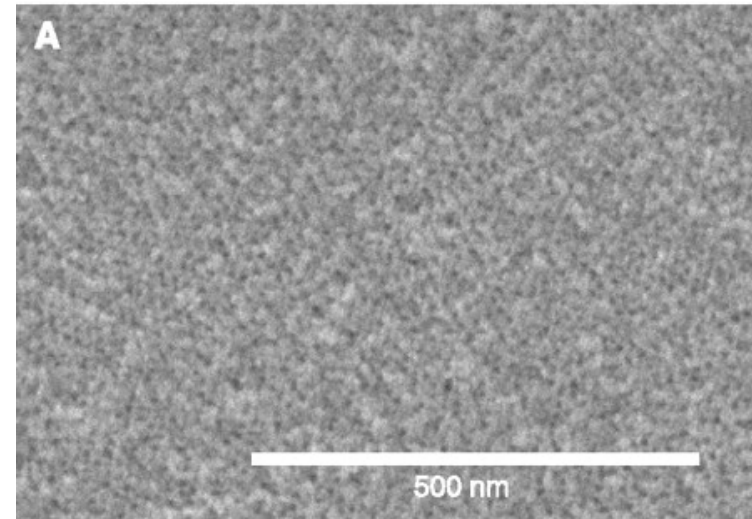
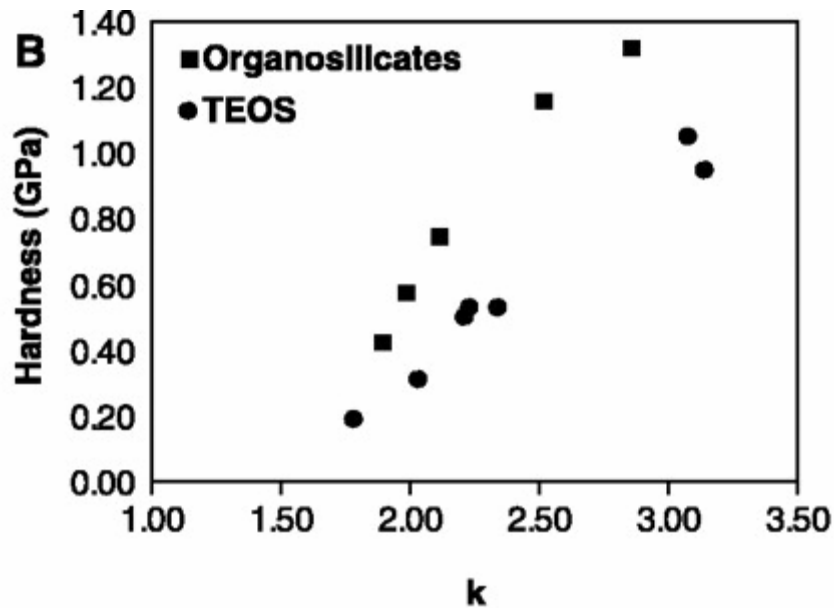


Supercritical CO₂ have:

- High diffusion rates and no surface tension
- Solvent properties that can be tuned using pressure and temperature to adjust fluid density
- Poor solvency for polymers but are able to dissolve small molecules
- Environmentally friendly solvent



Low-k films through scCO₂

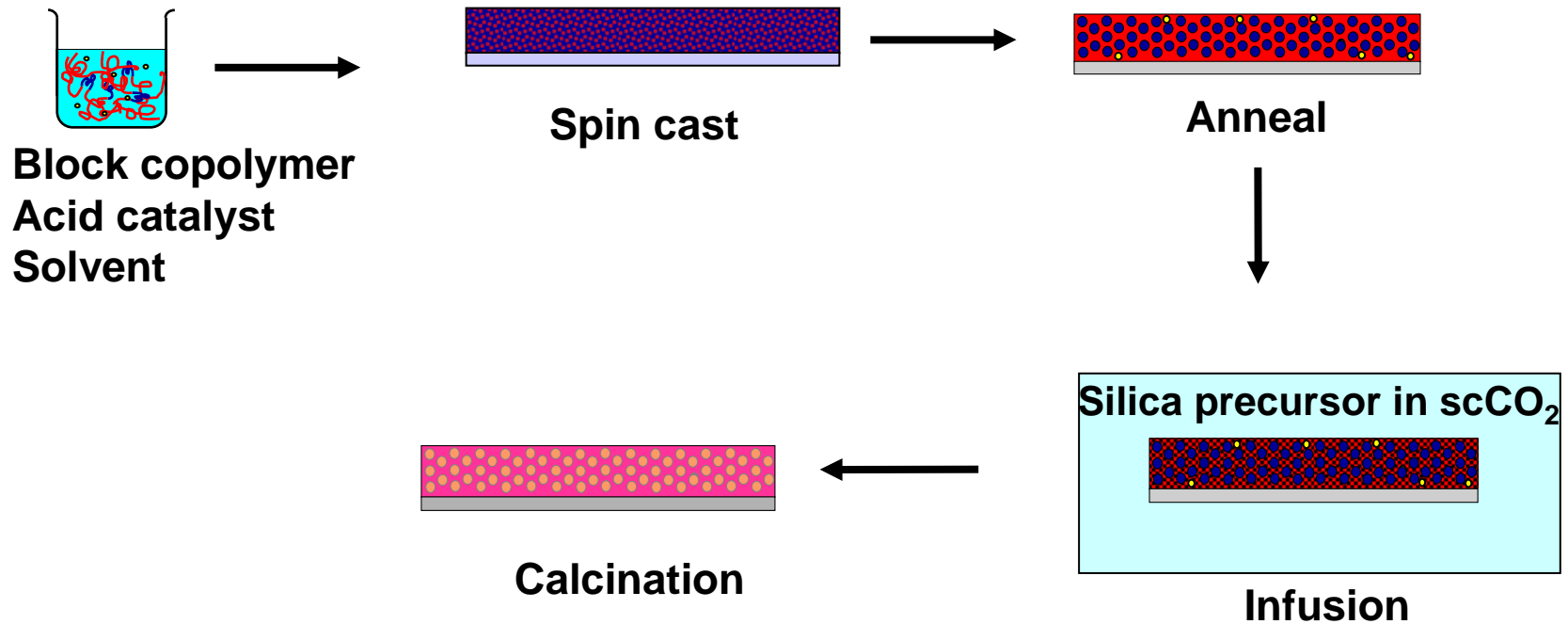


Tradeoff between mechanical strength and k

SEM image of a low- k porous silica film

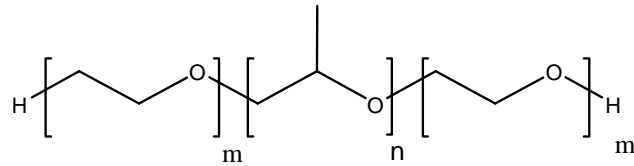
Previous work shows that low- k thin films can be fabricated through the infusion of silica precursors in ScCO₂.

Supercritical CO₂ Synthesis Process

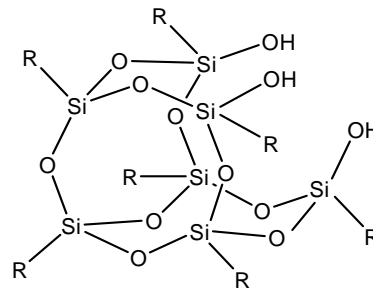


Materials

- Pluronic (PEO-b-PPO-b-PEO)

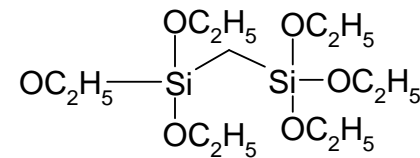


- TSI-POSS

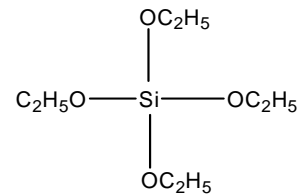


R = Isobutyl

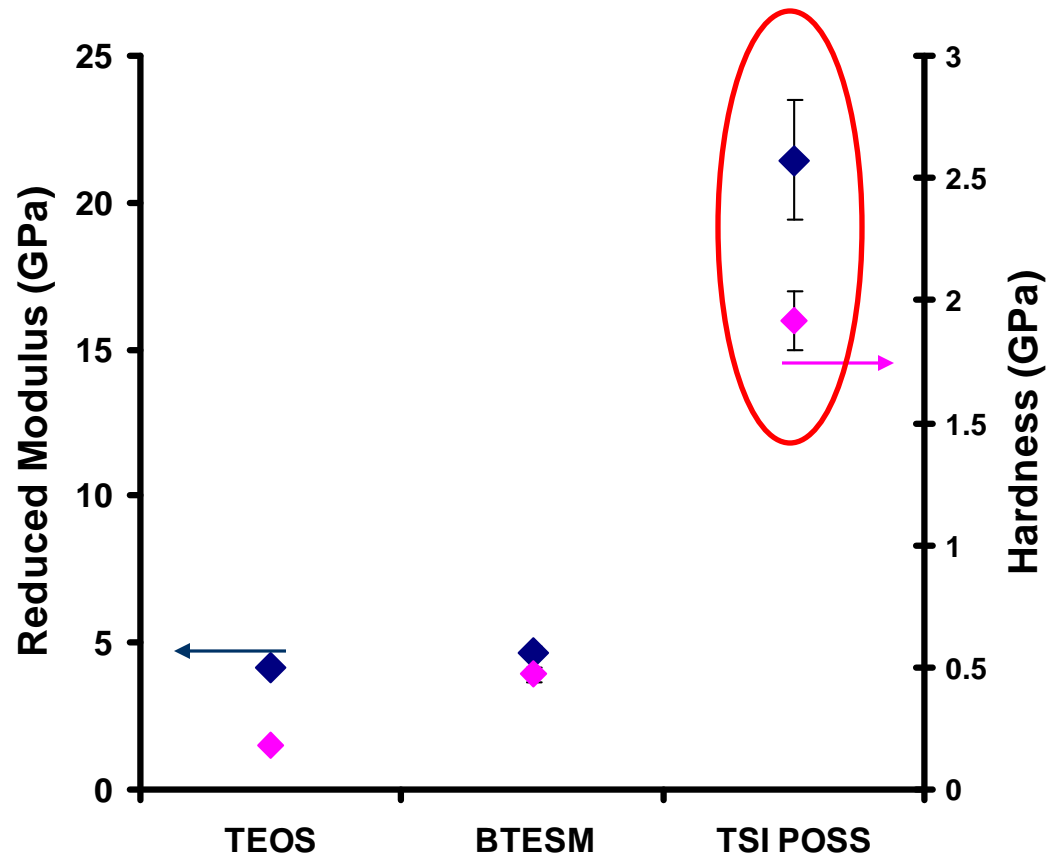
- Bis(triethoxysilyl)methane



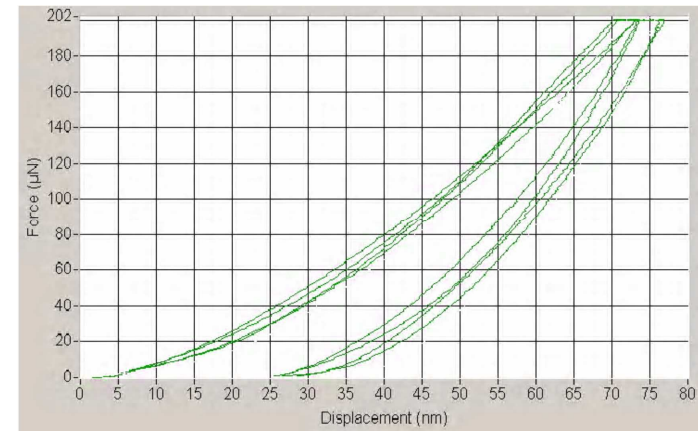
- TEOS



Film Hardness of 2 GPa



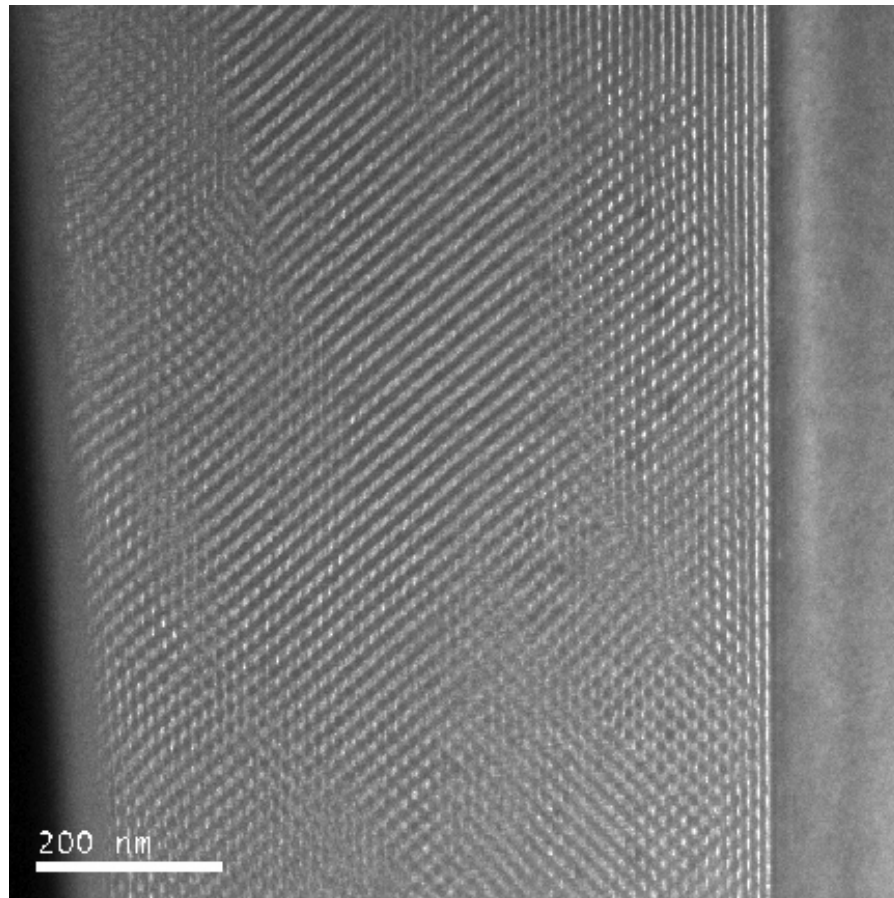
Addition of TSI POSS increases film hardness to 2 GPa and modulus to 20 GPa.



- TEOS: Mesoporous silica from F108 template infused with TEOS at 124 Bar and 60°C
- BTESM: Mesoporous silica from F108 template infused with BTESM at 124 Bar and 60°C
- TSI POSS: Mesoporous silica from F108 template and 10% TSI POSS infused with BTESM at 124 Bar and 65°C (Insert: AFM image of TSI POSS surface)



TEM of Silica/TSI POSS Film

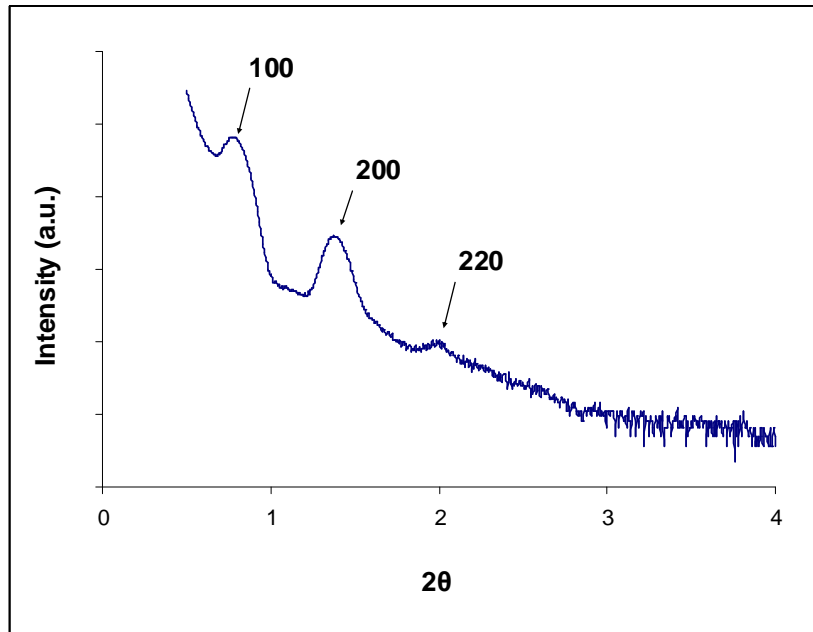


20% TSI POSS in Pluronic F127

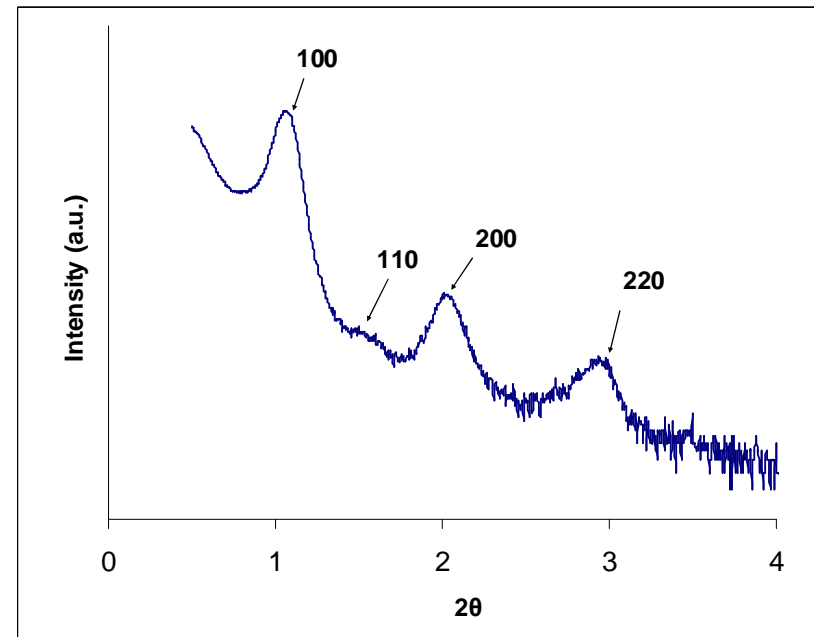
Image: Brian Gorman, UNT



POSS in Silica Structure



10% TSI POSS in Pluronic F127

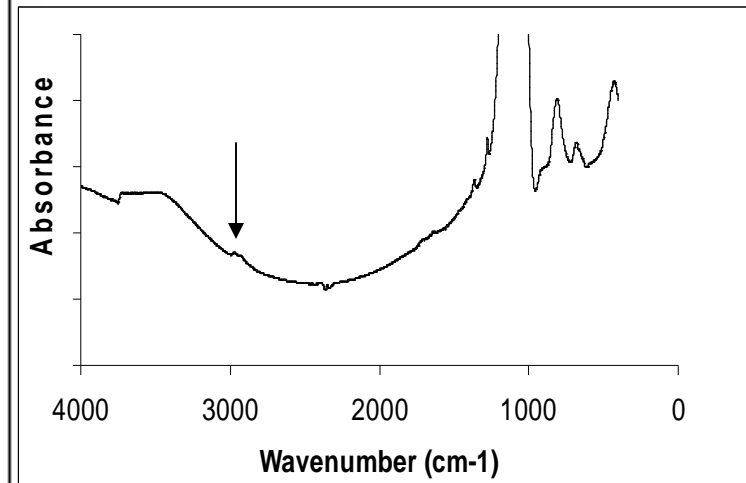
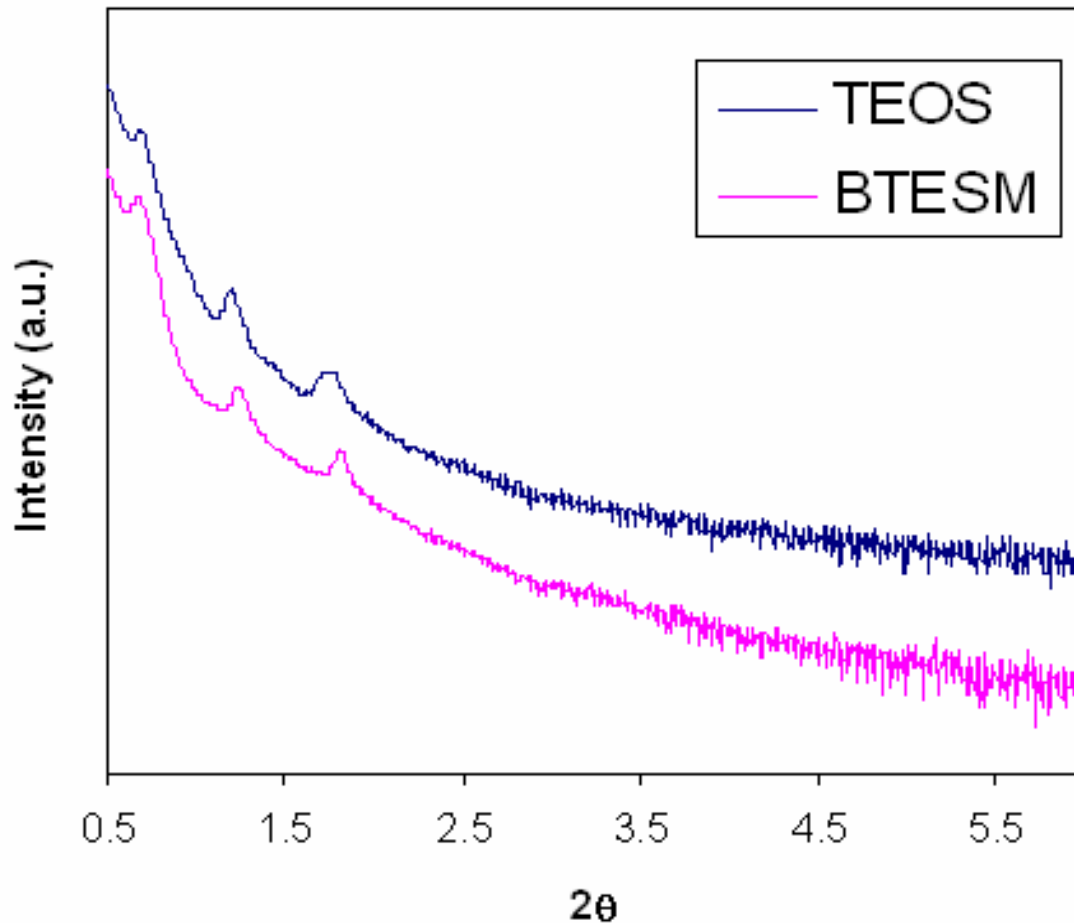


20% TSI POSS in Pluronic F127

Addition of POSS decreases the d-spacing of silica, which is partially responsible for the noted increase in mechanical strength.



Comparison of BTESM and TEOS



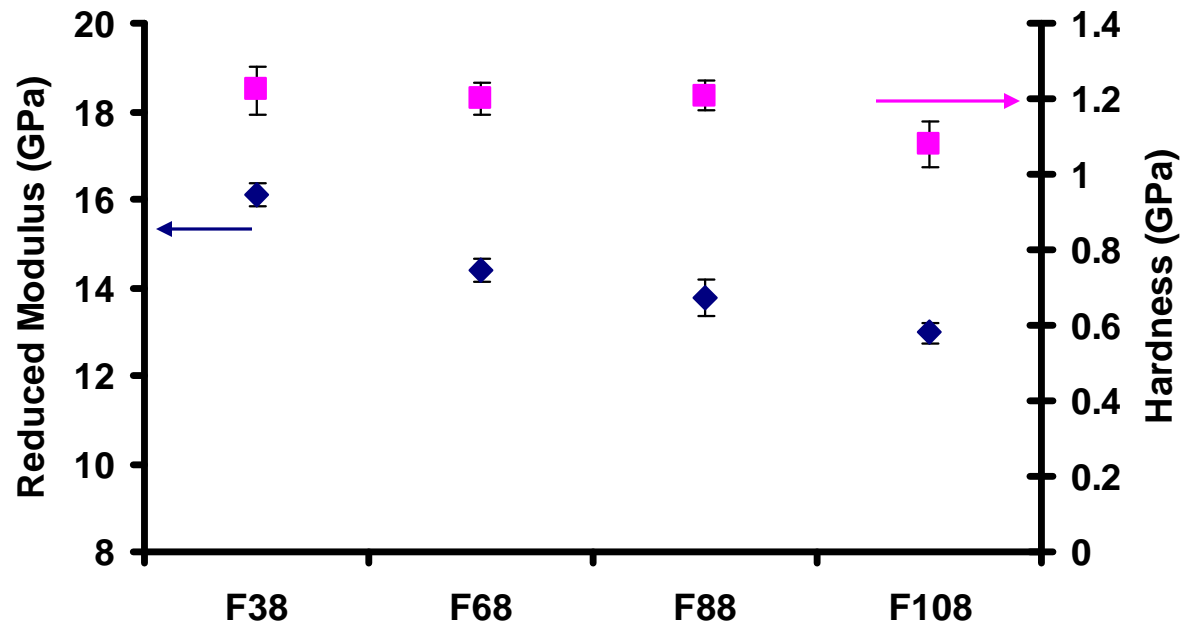
Calcined BTESM on F127 film. Methylene peak is at 2950 cm-1.

The methylene moiety increases hydrophobicity of films, which decreases k

XRD plot showing comparison between silica films infused into a Pluronic F108 with TEOS and BTESM as precursors. Similar structure was observed, suggesting infusion with BTESM did not significantly alter silica morphology.



Effect of Pore Size



- F38 Mn = 4700 g/mol, F68 Mn = 8400 g/mol
F88 Mn = 11400 g/mol, F108 Mn = 14600 g/mol
Polymers are 80% PEO
- The films were infused simultaneously at 124 Bar, 60°C



Conclusions

- Thin film hardness increases significantly with the addition of TSI POSS.
- Organosilicate precursors increase the mechanical strength and reduce the dielectric constant of silica thin films.
- The increase in d-spacing reduces the mechanical strength of as-calcined silica thin films.

Additional support provided by CHM and NSF





Cornell University



Processing of Molecular Glass Resist Components Using Vapor Deposition and Supercritical CO₂

Thrust D, Subtask D-1
SRC: 425.017

Nelson Felix, Jin Kyun Lee and
Christopher K. Ober

Department of Materials Science, Cornell University

SRC/Sematech Engineering Research Center for Environmentally Benign Semiconductor Manufacturing

D-1 Project Objectives

Objectives:

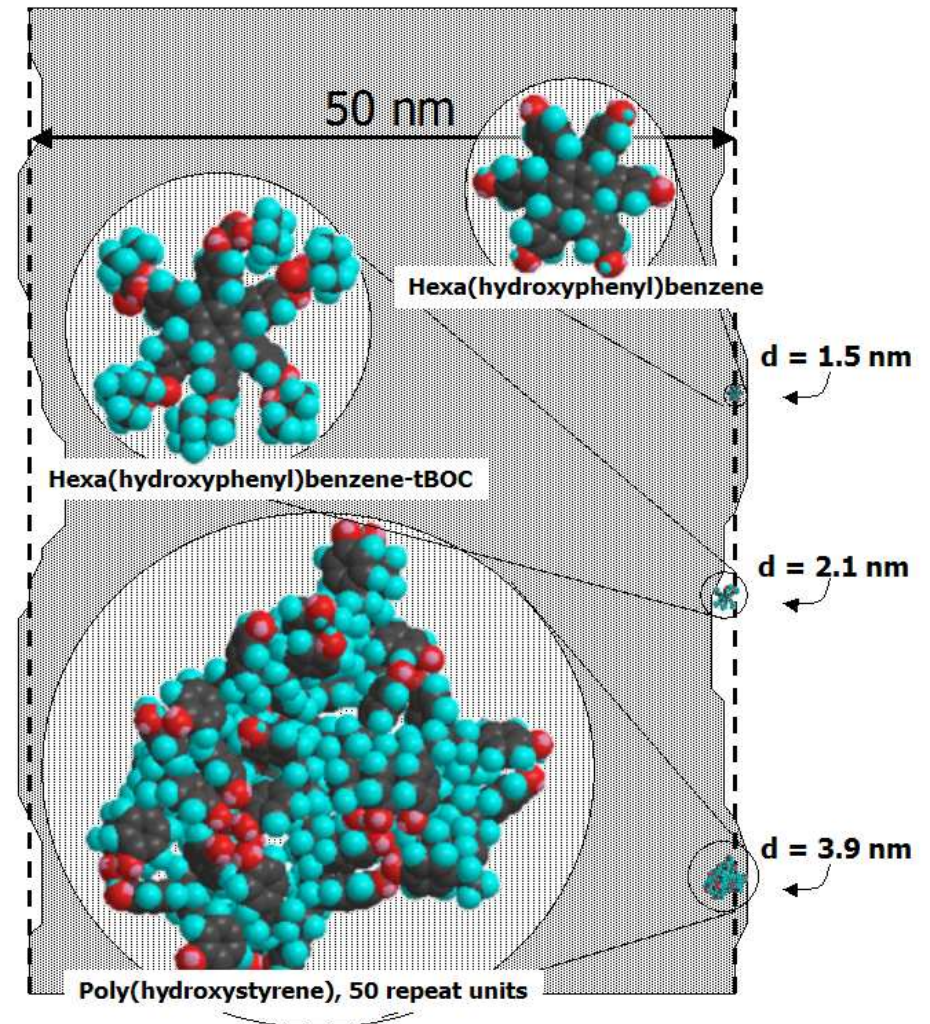
- Develop new methods to deposit, pattern and process low k materials to meet the roadmap goal of dielectric constants lower than 2.0
 - Demonstrate initiation and growth of patterned low-k structures
 - Show ability to deposit and pattern wide range of small molecules
 - Use supercritical CO₂ to drive low-k ordering, pore formation, and development

ESH Metrics

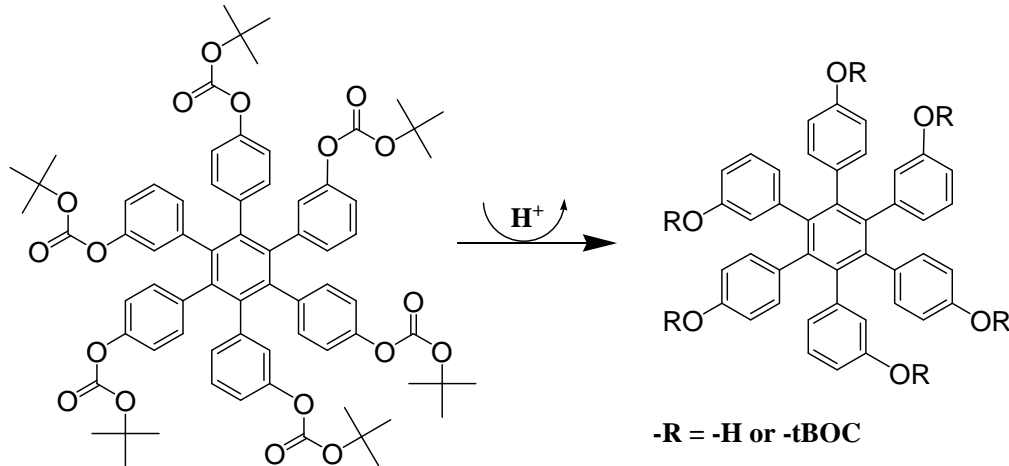
	Usage Reduction			Emmision Reduction			
Goals/Possibilities	Energy	Water	Chemicals	PFCs	VOCs	HAPs	Other
Reduce organic solvents used in processing materials	No energy used to purify and treat water	Eliminate need for water usage	Up to 100% reduction of organic solvents used	N/A	Minimal use of organic solvents	Up to 100% reduction of HAPs	N/A
Reduce processing time / temperature	Reduce anneal process costs	N/A	N/A	N/A	N/A	N/A	N/A
Additive processing	N/A	N/A	Eliminate waste of costly material	N/A	Minimal use of organic solvents	N/A	N/A

Molecular Glasses

- Small molecule size ~1-2nm
 - Potential for lower Line-Edge Roughness (LER)
- Well defined molecular structures
 - No distribution of mass
- Low tendency towards crystallization
 - bulky irregular shape or different conformation states
- Strong intermolecular attractive forces for high T_g
 - Specific interactions such as H-bonding
- Better miscibility with other small components

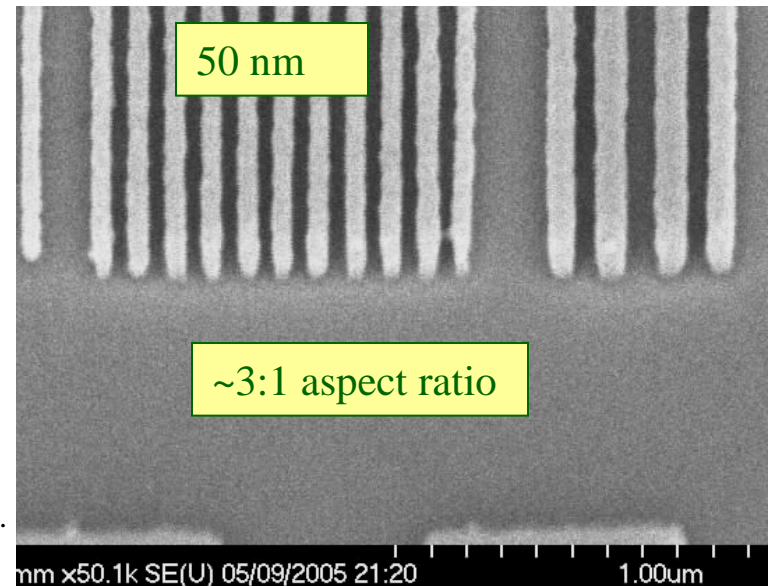
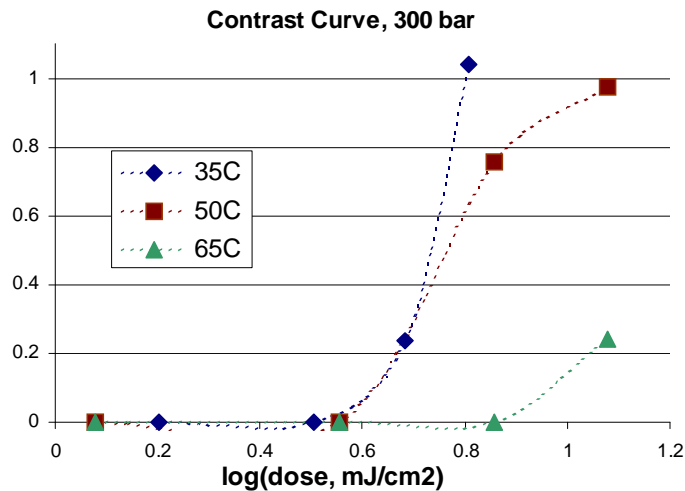


Supercritical CO₂ Solubility



Developed in scCO₂

LER ~ 7nm



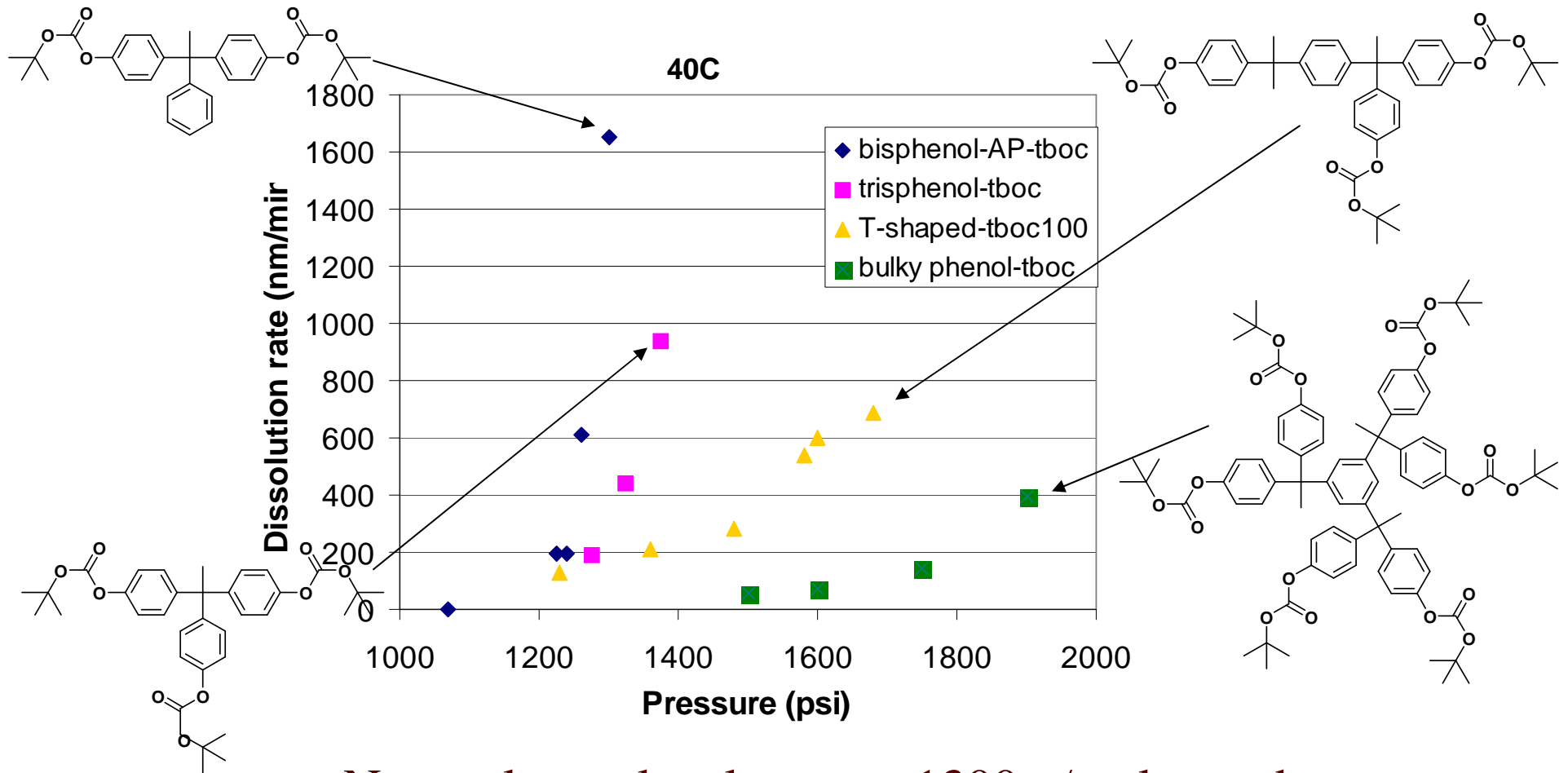
Felix, N. M, Tsuchiya, K., and C. K. Ober, *Adv. Mater.*, 18(4), 2006, p 442-446.



Cornell University

NSF/Sematech Engineering Research Center for Environmentally Benign Semiconductor Manufacturing

CO₂ Dissolution Rates of Small Molecule Films



- Non-polar molecules up to 1300 g/mol tested
- Solubility varies predictably with molecular wt.



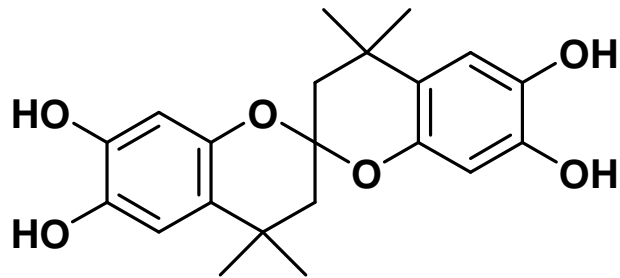
Cornell University

SRC/Sematech Engineering Research Center for Environmentally Benign Semiconductor Manufacturing

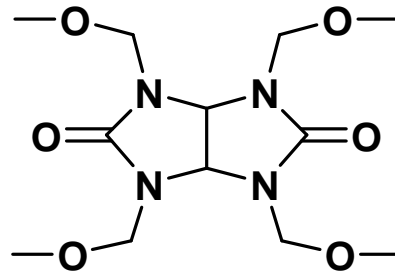
Vapor Deposition of Molecular Glasses

- Small molecules sufficiently volatile and stable to deposit by dry deposition technique without degradation
- Allows for precise control of resist components - deposition on curved surfaces

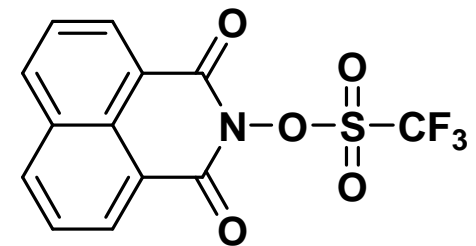
Sample System Used



Glass-former



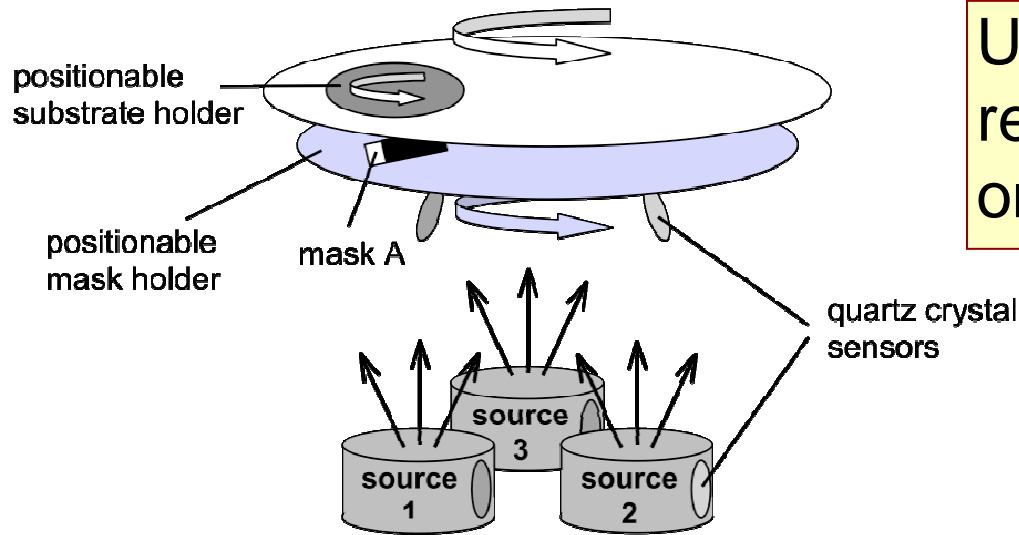
Crosslinker



Photoacid Generator

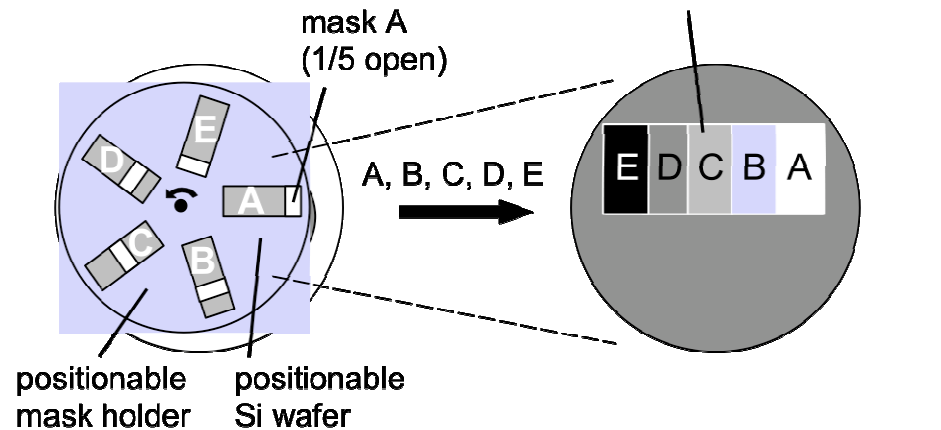


Deposition and Screening



Up to 10 different resist compositions on one wafer

Gradients, controlled mixtures, and rapid screening

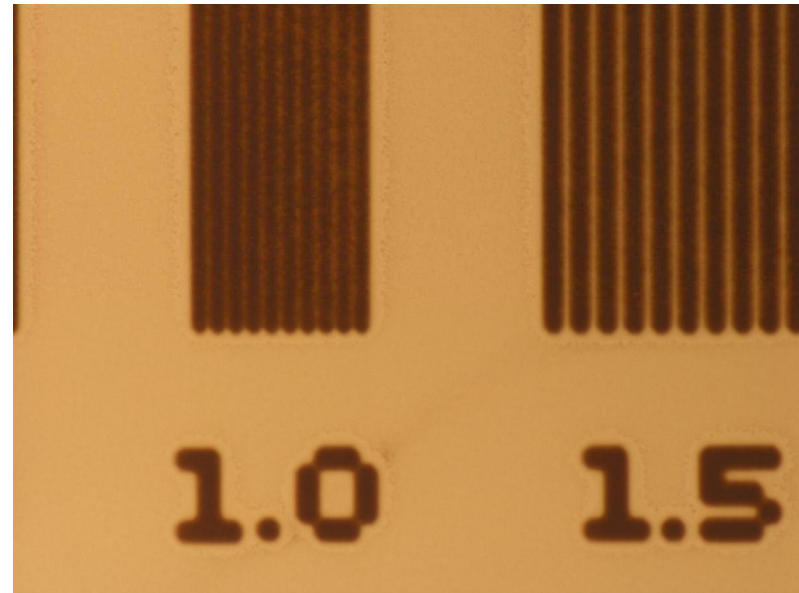


Cornell University

SRC/Sematech Engineering Research Center for Environmentally Benign Semiconductor Manufacturing

Results

- Test exposure using 365 nm Stepper
- Developable in water



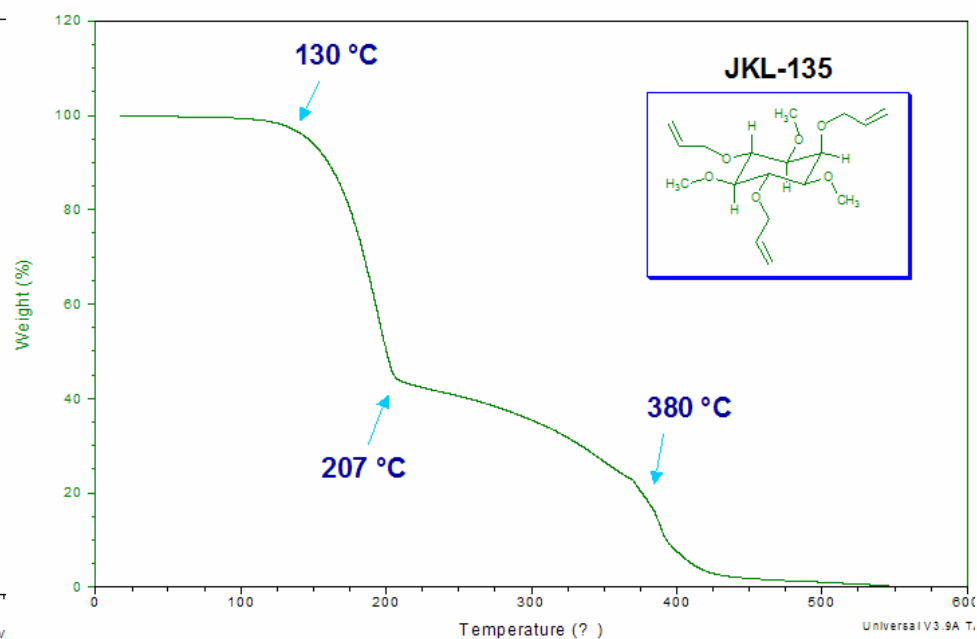
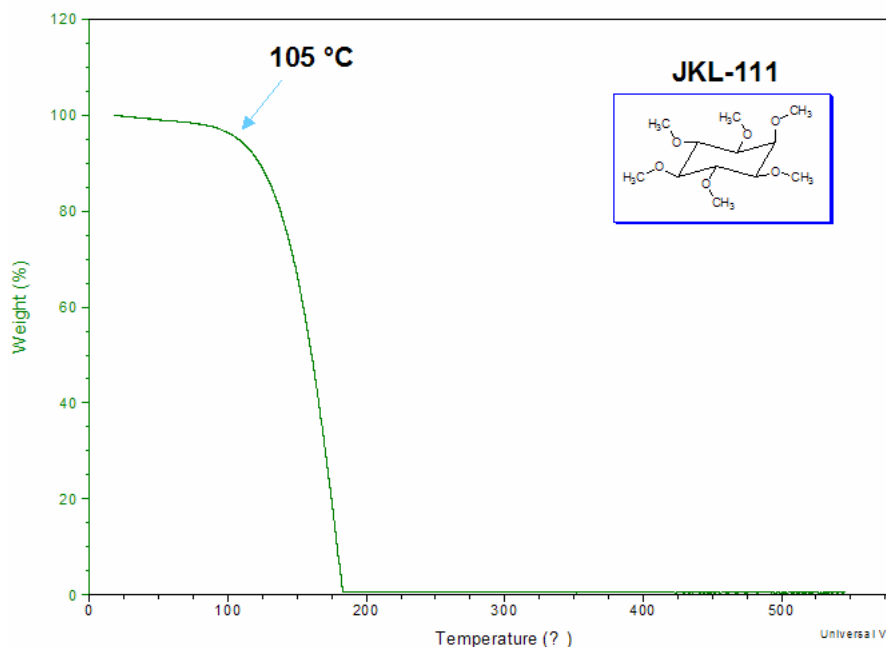
Cornell University



SRC/Sematech Engineering Research Center for Environmentally Benign Semiconductor Manufacturing

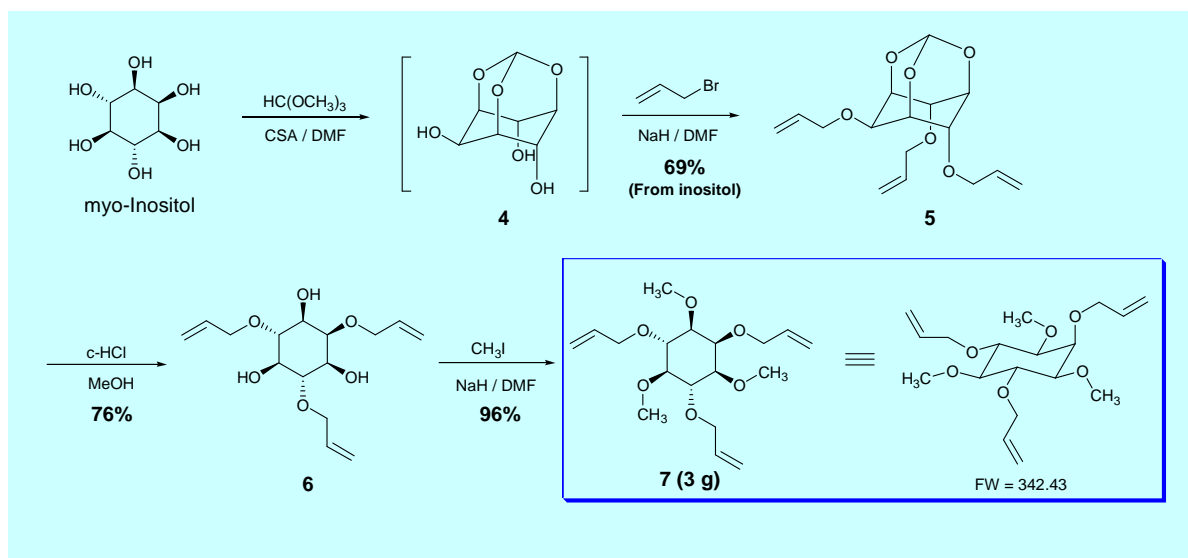
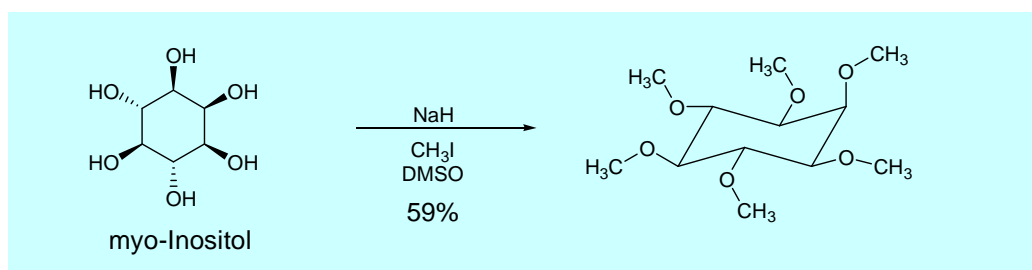
Inspiration: MG-type Porogens

- Small molecule porogens with low decomposition temperatures
- Simple, easily-synthesized structures
- Potential for lower annealing temperature, time.



Porogen Synthesis

- Ease of synthesis
- Cheap starting materials



Conclusions / Acknowledgements

- Molecular glass components have shown great synergy with environmentally-friendly processing
 - Demonstrated ability to process a variety of small molecules with scCO₂
 - Vapor Deposition possible
 - Deposition of blanket films of resist components
 - Compatibility with vapor-based low-k dielectric processes

-
- Cornell Nanofabrication Facility (CNF)
 - Cornell Center for Materials Research (CCMR)
 - Semiconductor Research Corporation (SRC)
 - IBM; Heidi Cao / Intel; Will Conley / Freescale
 - Ober Group members
 - Anuja De Silva, Camille Luk
 - Dr. Jin Kyun Lee, Dr. Xavier Andre

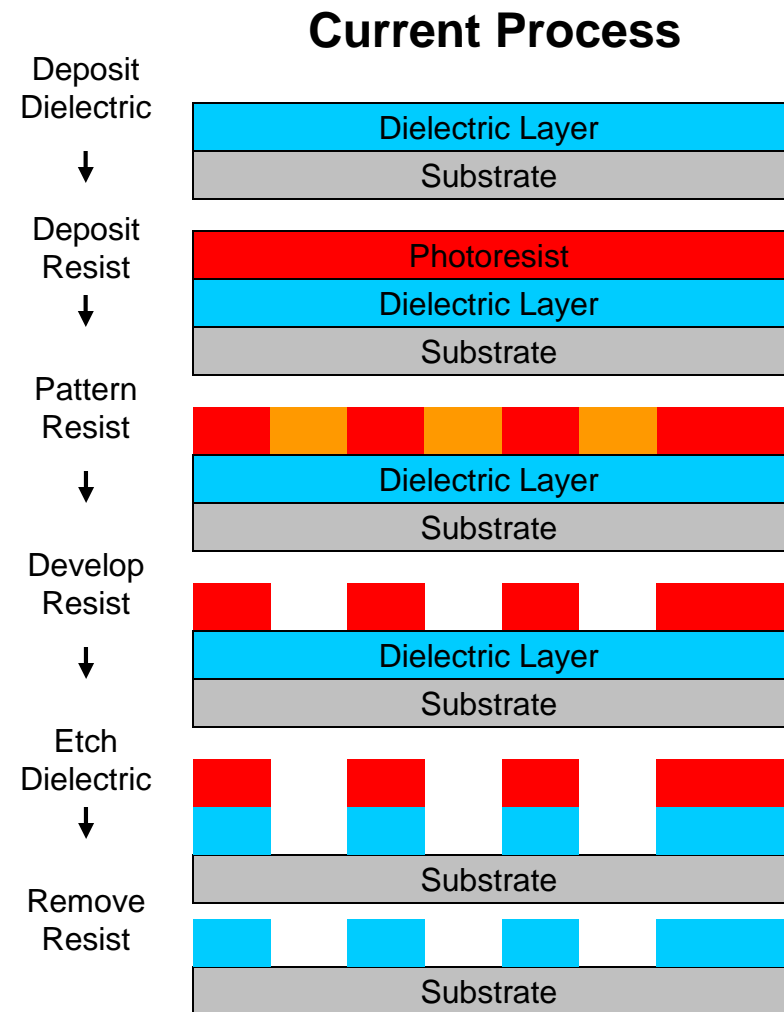
Environmentally Benign Vapor Phase and Supercritical CO₂ Processes for Patterned Low-k Dielectrics

W. Shannan O'Shaughnessy, Sal Baxamusa, and
Karen K. Gleason

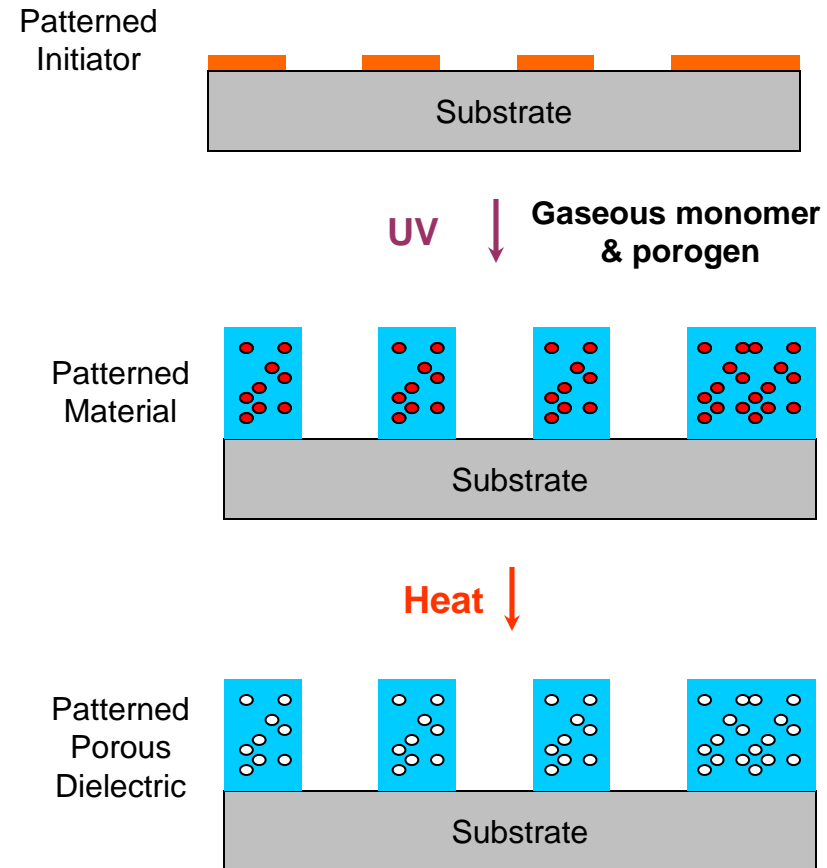
Department of Chemical Engineering
Massachusetts Institute of Technology

Selective deposition of patterned low k materials

- Current Process
 - Resist based lithography of blanket dielectric layer
 - Many steps
 - High solvent use
- Novel approach to reduce number of processing steps
 - Faster
 - Less Solvent
- Cost and ESH “Win-Win”

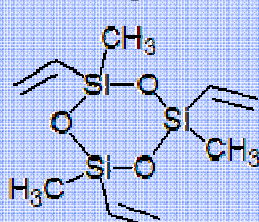


- In situ Patterned Growth
 - Apply Initiator
 - Lithographic Patterning
 - Microcontact Printing
 - E-beam lithography
 - Dip pen lithography
 - Photobleaching
 - Grow piCVD material
 - Gas phase monomer & porogen
 - Remove porogen
- Improves cost and ESH
 - Fewer steps
 - Less solvent
- Complementary to sacrificial materials patterning

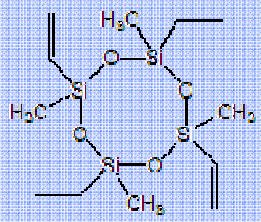


Goals/Possibilities	Usage Reduction			Emmision Reduction			
	Energy	Water	Chemicals	PFCs	VOCs	HAPs	Other
Reduce organic solvents used in processing materials	No energy used to purify and treat water	Eliminate need for water usage	Up to 100% reduction of organic solvents used	N/A	Minimal use of organic solvents	Up to 100% reduction of HAPs	N/A
Reduce processing time / temperature	Reduce anneal process costs	N/A	N/A	N/A	N/A	N/A	N/A
Additive processing	N/A	N/A	Eliminate waste of costly material	N/A	Minimal use of organic solvents	N/A	N/A

piCVD Monomers



Trivinyl-trimethyl-
cyclotrisiloxane
(V₃D₃)



Tetravinyl-Tetramethyl-
cyclotrisiloxane
(V₄D₄)

Dielectric Constant ≈ 2.5

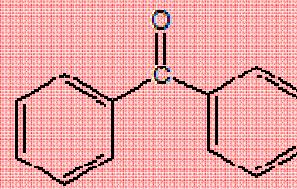
Model Systems:

Cyclohexyl Methacrylate

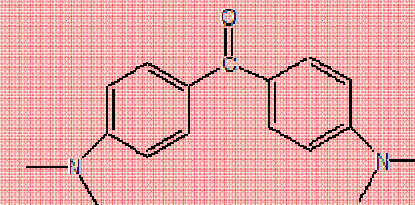
Hydroxyethyl Methacrylate

Plasma Organosilicate Glass

piCVD Initiators



Benzophenone

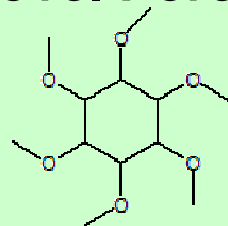


Michler's Ketone

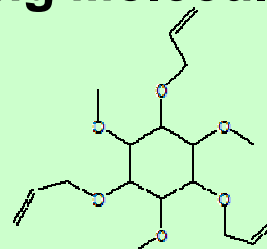
Surface tethered Benzophenone
derivatives (Cornell)

Active @ 254nm & 365nm

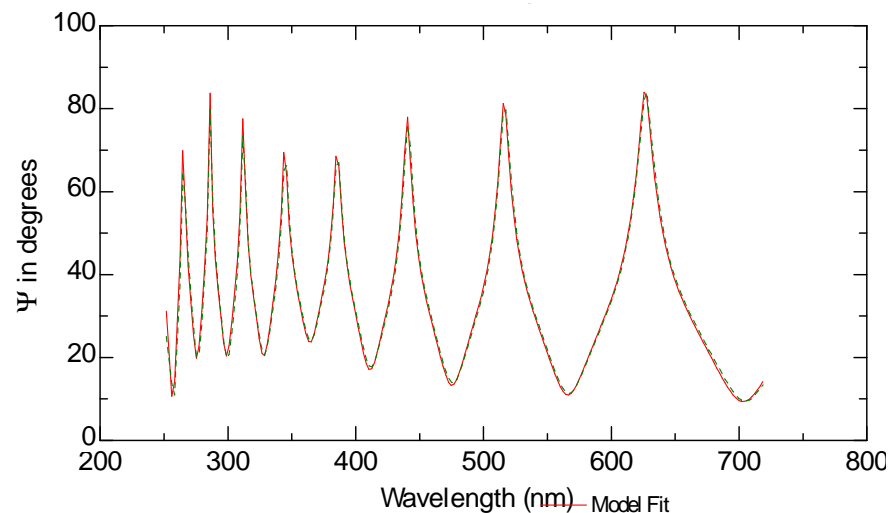
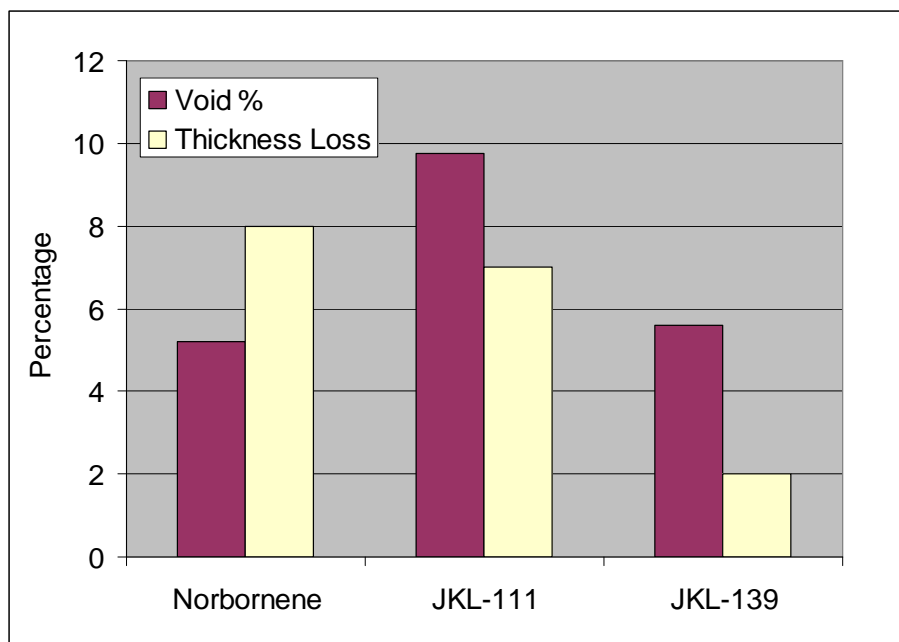
Novel Pore Generating Molecules



Hexamethyl ether of *myo*-inositol
JKL-111

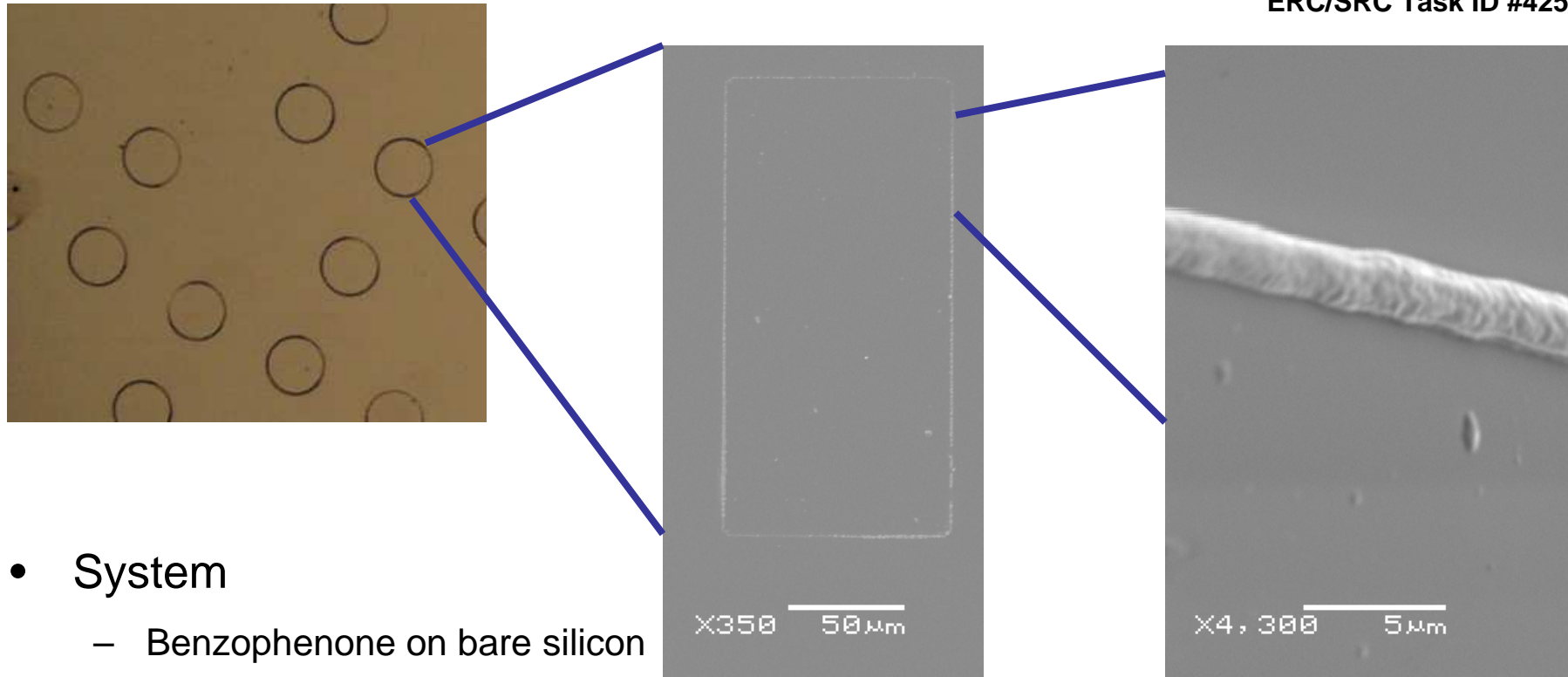


JKL-139



Ellipsometry data plus model fit for porous film

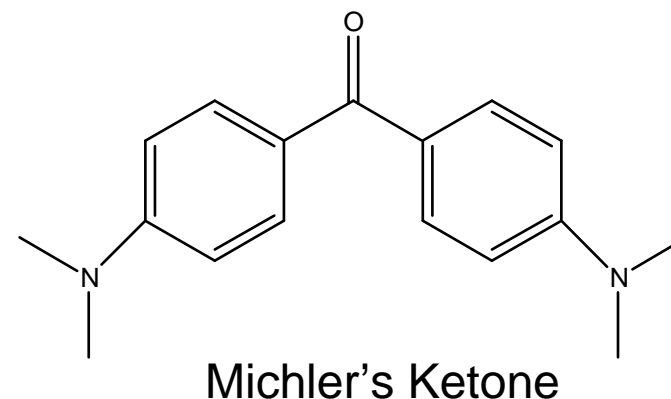
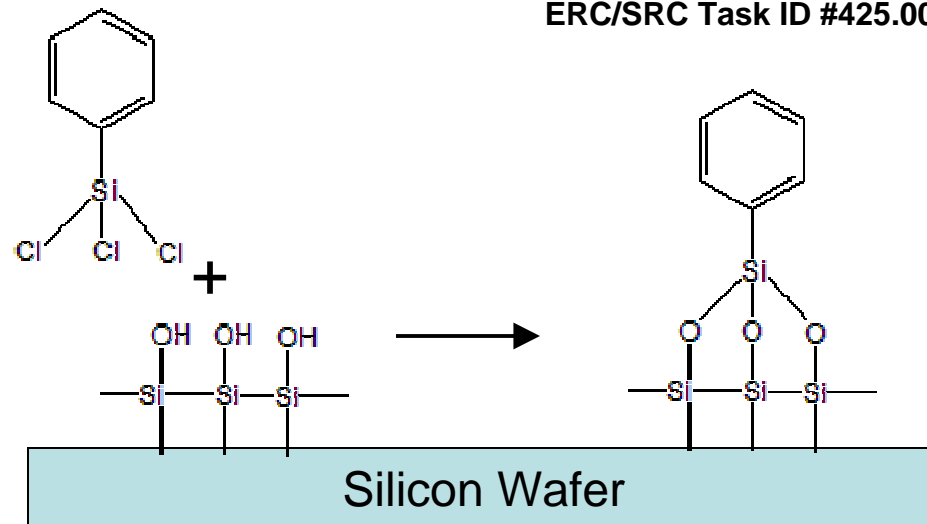
- Test properties of novel molecules as porogens
 - Ensure incorporation and thermal removal
 - Compare to Norbornene
 - Commercially available porogen
 - Void percentage modeled using spectroscopic ellipsometry
 - Effective medium approximation

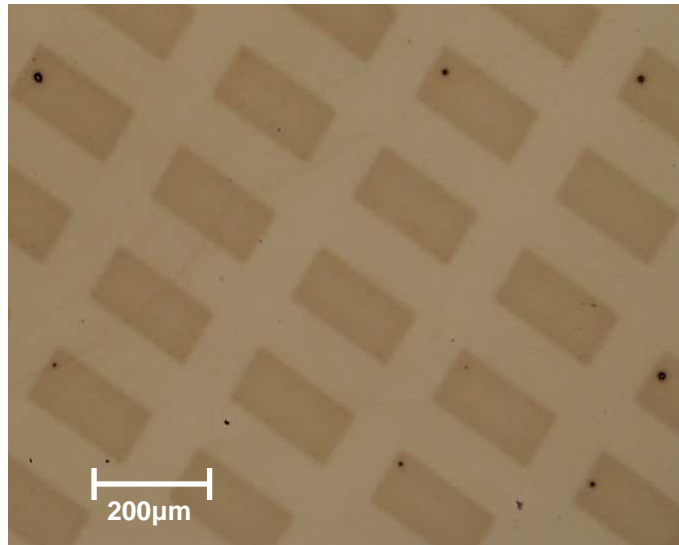


- System
 - Benzophenone on bare silicon
 - 100 μ m circles and rectangles
- See patterned growth but no fill in

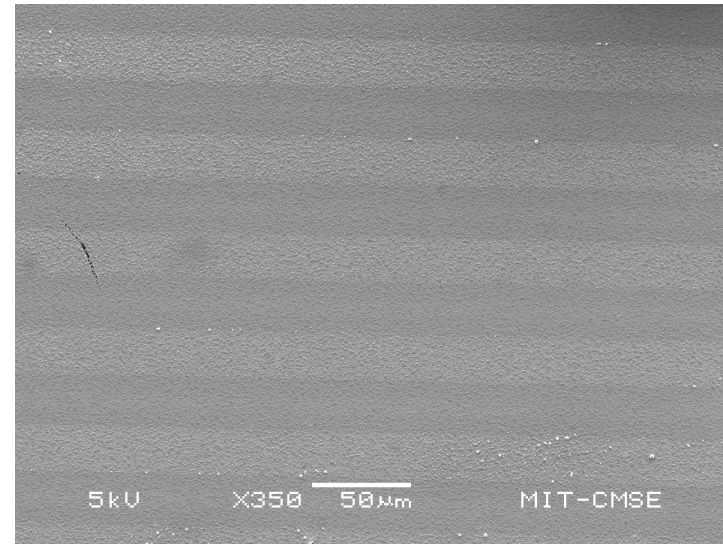
- Issues
 - Limited initiator surface affinity
 - Poor coverage
 - Max initiator concentration limited by onset of crystallization
 - Results in thin structures

- Solutions
 - Modify substrate surface
 - Create more favorable interactions
 - Switch Initiators
 - Same mode of action
 - Less solvent affinity & crystallization





Optical micrograph of 100µm X 200µm rectangles created through piCVD on pre-patterned initiator



SEM image of 25µm lines created through piCVD on pre-patterned initiator

- Full coverage of patterned area achieved
- Feature thickness increased
 - 25µm features at >200nm thickness

- George Barclay, Rohm & Haas Microelectronics
- Heidi Cao, Intel
- Dr. Kelvin Chan, AMAT
- Ralf Dammel, AZ-Microelectronics
- Dr. Thomas Diamond, IBM
- Li Jia, Rohm & Haas Microelectronics
- Mingqi Li, Rohm & Haas Microelectronics
- Dr. Todd Ryan, AMD
- Richard Schenker, Intel
- Dr. Dorel Toma, TEL
- Dr. Qingguo Wu, Novellus

- Conclusions
 - Patterned dielectric growth
 - Proof of concept achieved
 - 25 μ m features with >200nm thickness
 - Novel Porogen materials validated
 - 9.7% porosity achieved with novel porogen KLM-111
 - >93% thickness retention
- Future Plans
 - Optimize initiator lithography
 - Smaller Features
 - Tethered initiators
 - Optimize porogen incorporation and chemistry
 - Integrate pattern film growth with porogen addition



Directly Patterned Mesoporous Silicate Films Templated From Chemically Amplified Block Copolymers

SRC: 425.017

**Sivakumar Nagarajan¹, Joan K. Bosworth², Christopher K. Ober²,
Thomas P. Russell¹ and James J. Watkins¹**

- 1. University of Massachusetts, Amherst**
- 2. Cornell University**

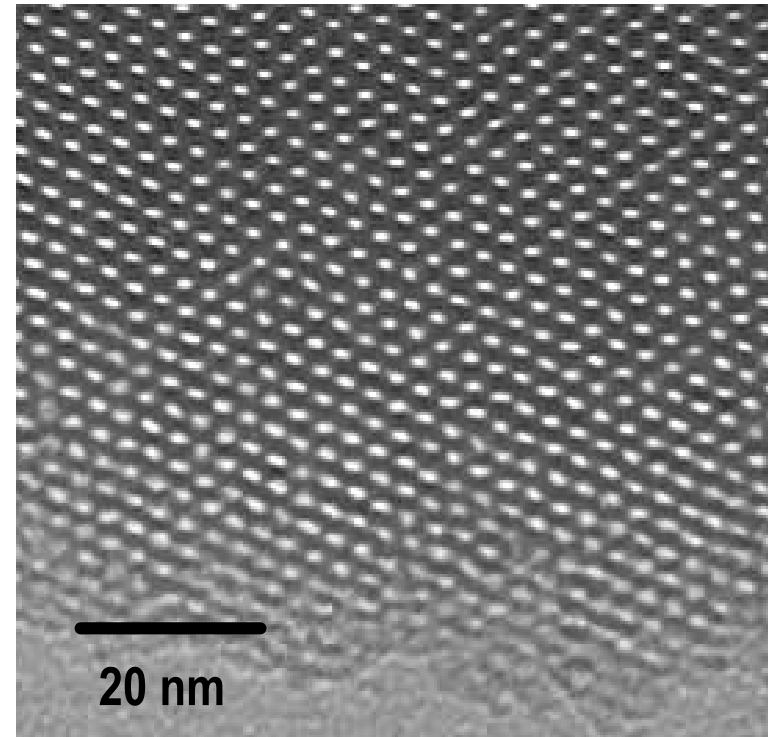


SCF Infusion of Templates is Rapid and Yields Extremely Well-Ordered Films

- $k < 2.2$ demonstrated
- Rapid process times, 1st generation survives CMP
- Low stress, high crack threshold
- Mechanical properties can be optimized
 - inclusion of POSS (see A. Romang poster)
 - use of bridged silsesquioxanes
 - fully condensed networks
- Small pores are accessible via template blends

Direct patterning provides process differentiation

- directly patterned fat lines for BEOL process compression
- subsequent market entry for ULK < 2.2

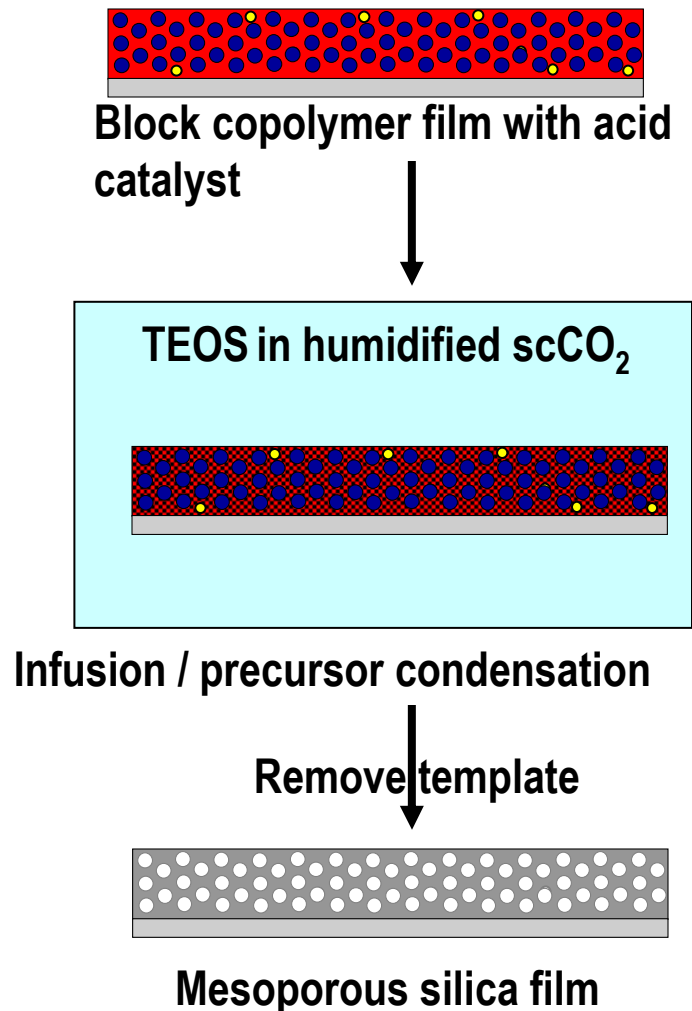


Supercritical fluids provide a unique, environmentally friendly, reaction environment that is ideally suited for materials chemistry for semiconductor and nanostructured devices

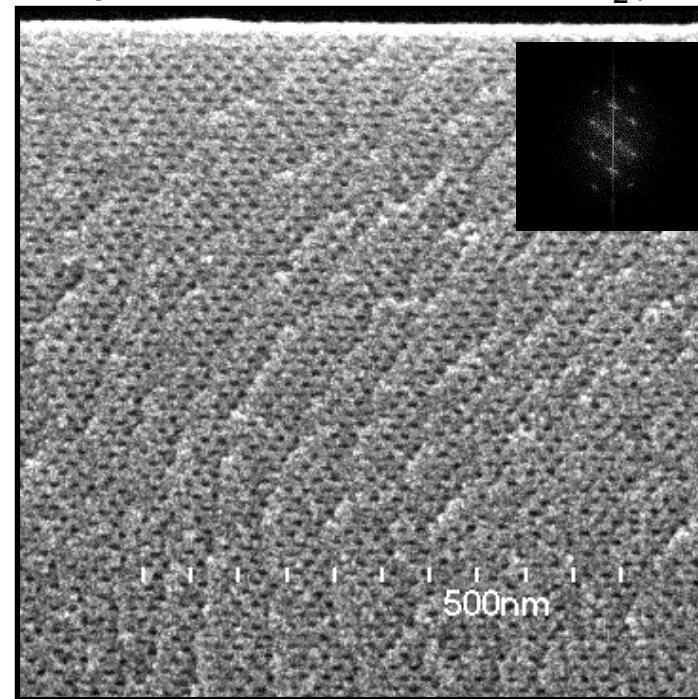
Our Approach to Mesoporous Silica Films¹



3-D replication in supercritical carbon dioxide



Template: Pluronic F108; PEO-b-PPO-b-PEO[80:20]
 Acid Catalyst: p-Toluene sulfonic acid(pTSA)
 Silica precursor: Tetra ethyl ortho silicate(TEOS)
 Processing Solvent: Supercritical CO₂(sc CO₂)



Cross-sectional SEM of mesoporous silica film with spherical pores

1. Pai et al., *Science*, 303, 507, 2004



Key Advantages:

- ❖ Silica precursor (alkoxide) condensation can be decoupled from template Self-assembly.
- ❖ Segregation of acid catalyst into one domain of the block copolymer ensures domain-selective silica infusion.

These features enable:

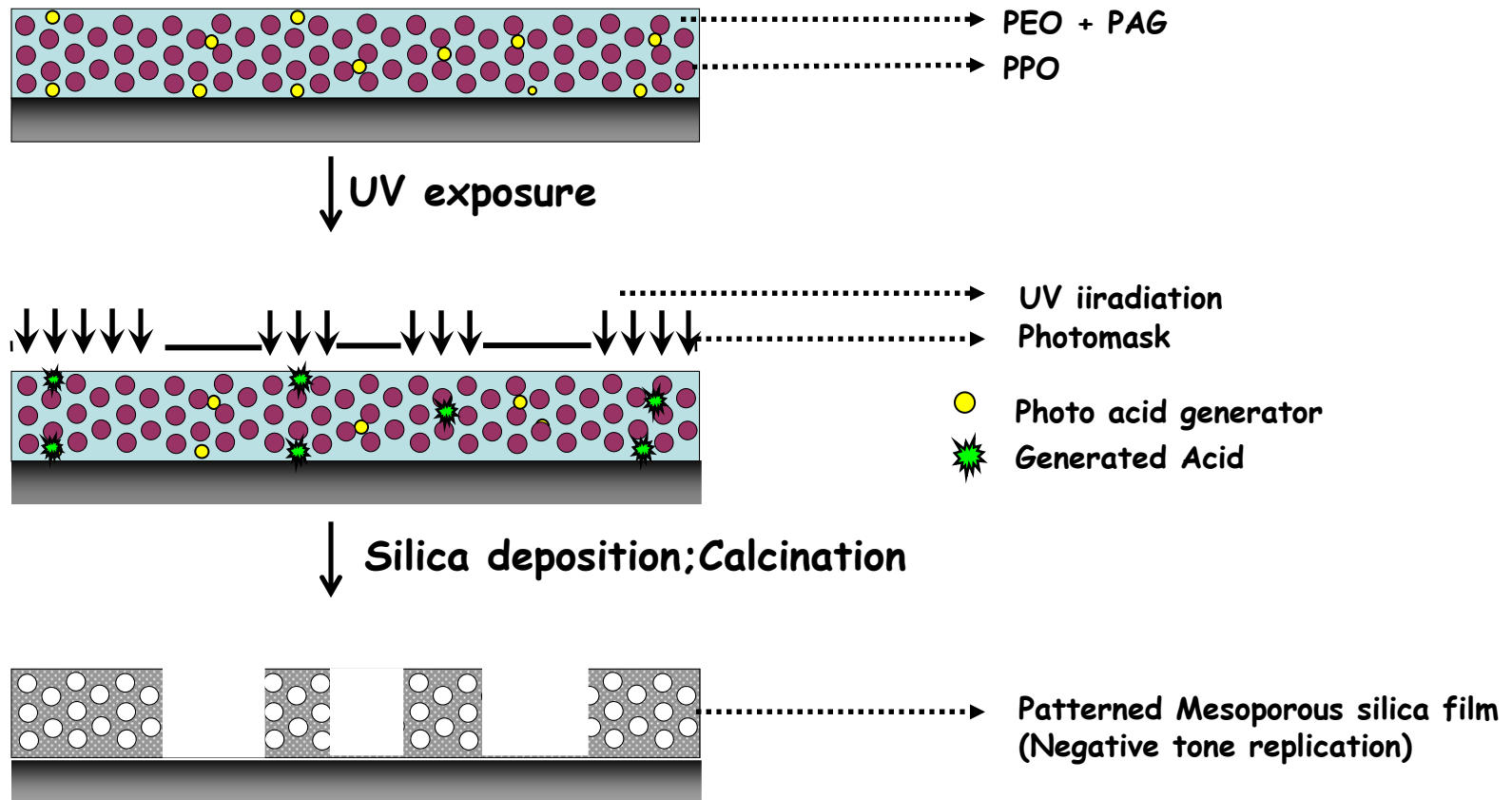
- (i) Direct replication of highly ordered block copolymer templates.
- (ii) Fabrication of Patterned mesoporous silica films with domain and device level definitions.**

Patterned Mesoporous Silica Films



Mesoporous films with Domain (nanoscopic) and Device (microscopic) level definitions:

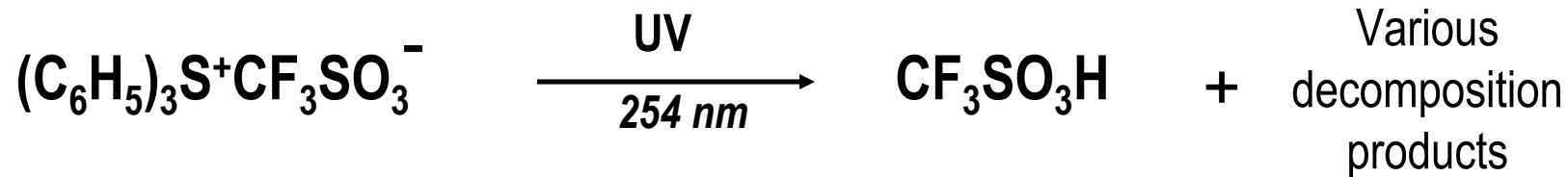
-Controlling the presence of acid in two different length scales by using a photo acid generator (PAG) instead of straight acid (pTSA).



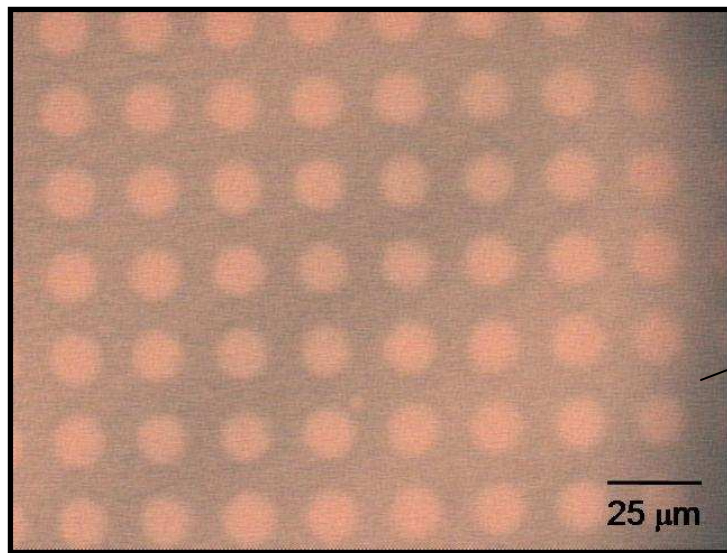
Patterned Mesoporous Silica Films from Pluronics(F108)



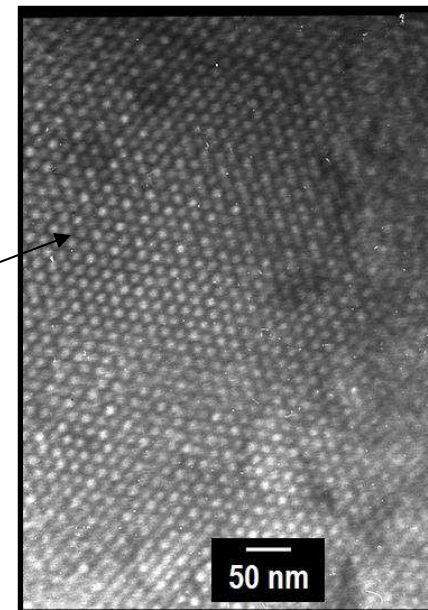
Photo acid generator: Tri phenyl sulfonium triflate – generates Triflic acid.



Device Level Replication:
Microscopic structures.



Domain level Replication:
Nanosopic structures



- OM Images lack sharp boundaries – Possibility of PAG diffusion to unexposed area.

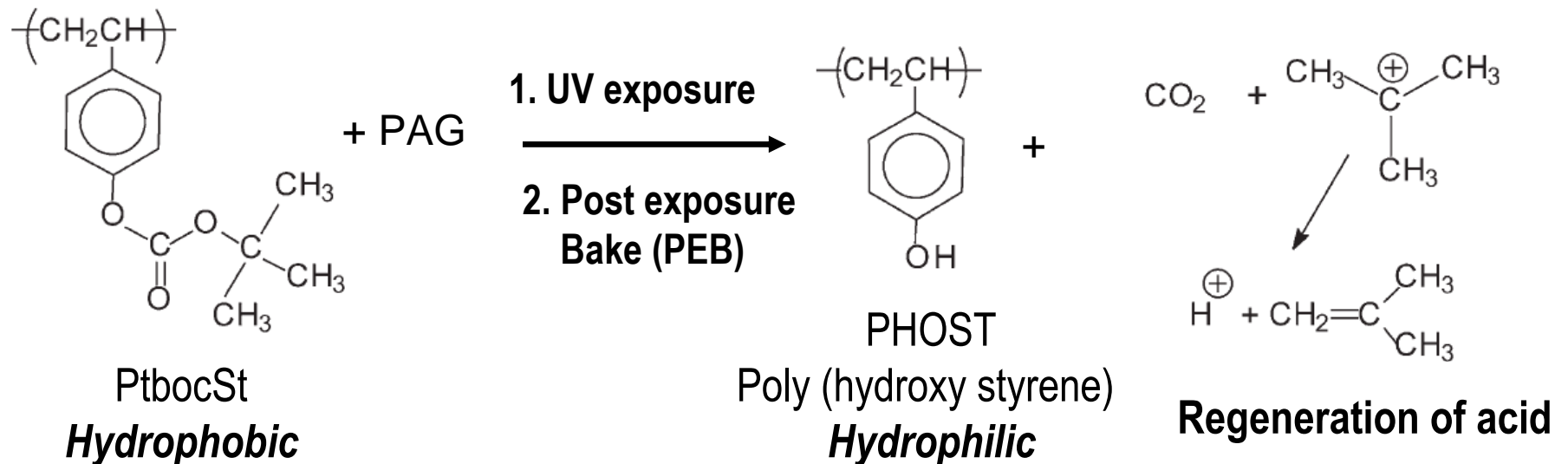
SRC/Sematech Engineering Research Center for Environmentally Benign Semiconductor Manufacturing

Patterned Mesoporous Silica Films



Alternative system to restrict PAG diffusion: Poly(tertiary-butoxy carbonyl oxy styrene) based films. (PtbcSt)

Chemical Amplification process involved in PtbcSt systems²:



- Diffusion of generated acid (H^+) into hydrophobic PtbcSt is highly limited.
- Regenerated acid should be good enough to do silica condensation too.

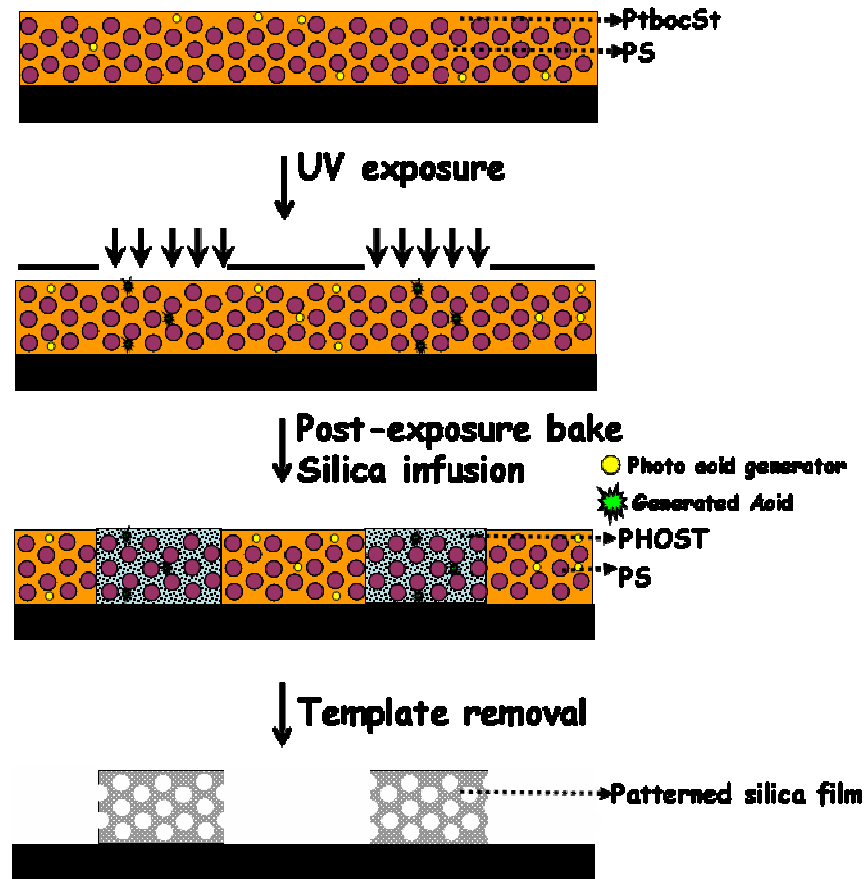
2. Ito H, Willson CG, Fréchet JM (1982) *Digest of Technical Papers of 1982 Symposium on VLSI Technology*, p 86

[SRC/Sematech Engineering Research Center for Environmentally Benign Semiconductor Manufacturing](#)

Patterned Mesoporous Silica Films from PtbcSt Films



Simultaneous Chemical amplification and Silica Condensation in PS-b-PtbcSt films:

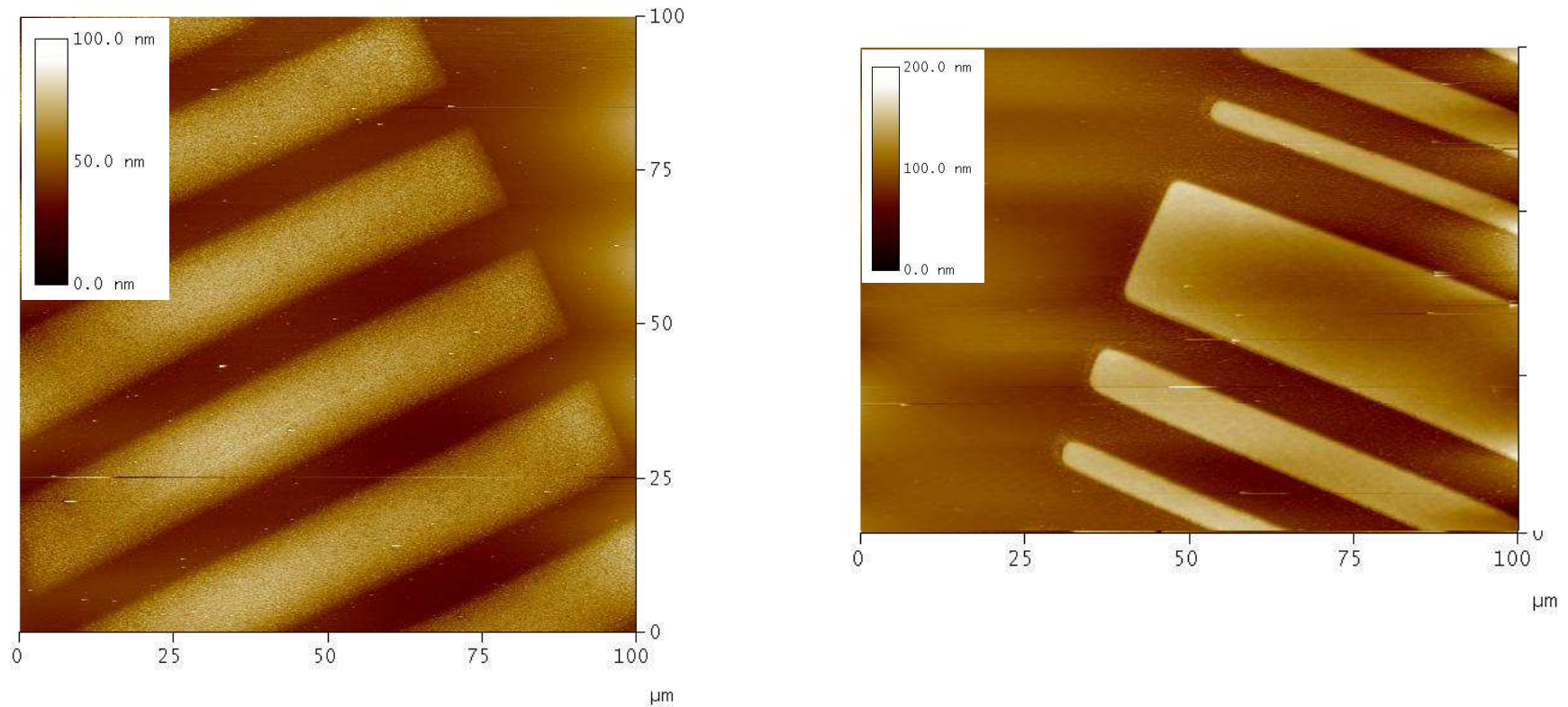


Modified Scheme

Feasibility: Patterned Mesoporous Silica Films from PtboCSt Films



AFM images of the Patterned silica film templated from PtboCSt films:

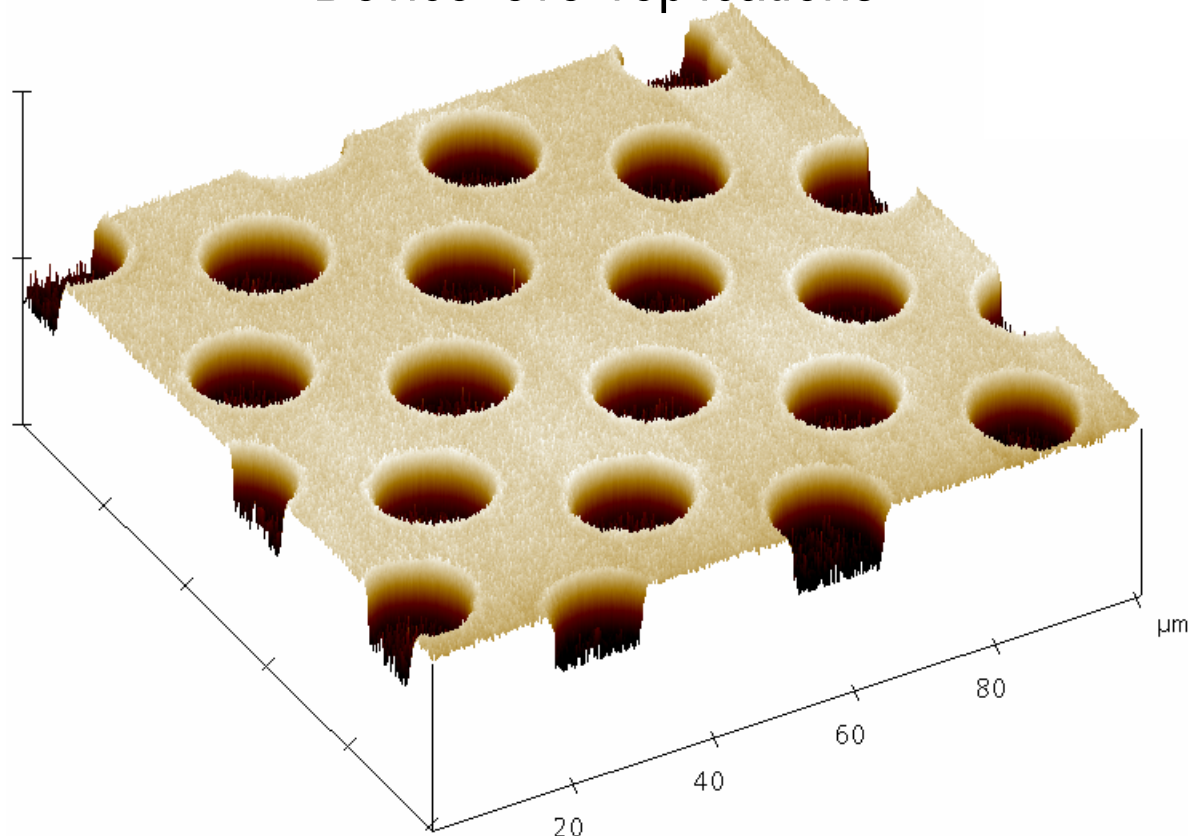


- Good pattern replication with sharp boundaries.
- Device level replications of features down to few microns in size have been done.



- Both Device (Microscopic) level & domain (nanoscopic) level replications are expected:

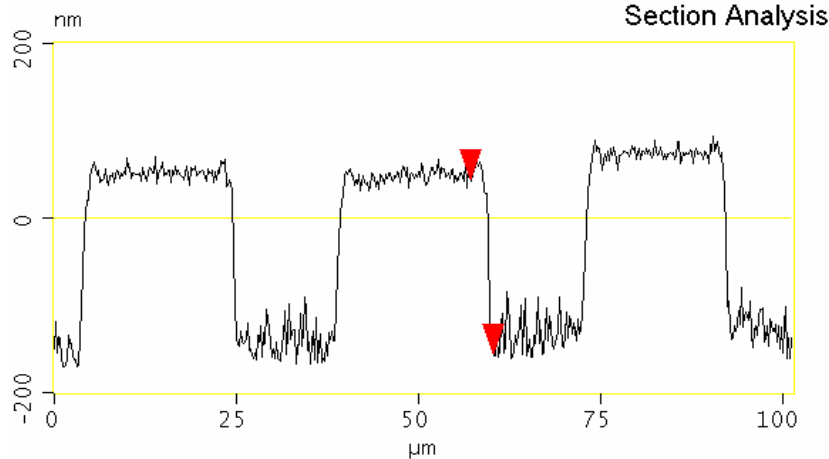
Device level replications



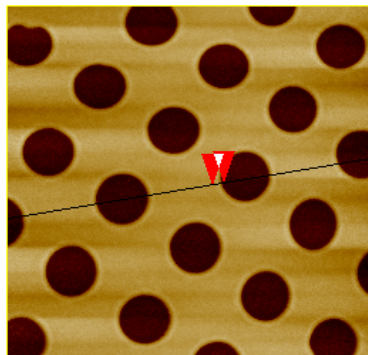
AFM 3D image of the mesoporous silica film templated from P(S-b-tbocSt) film



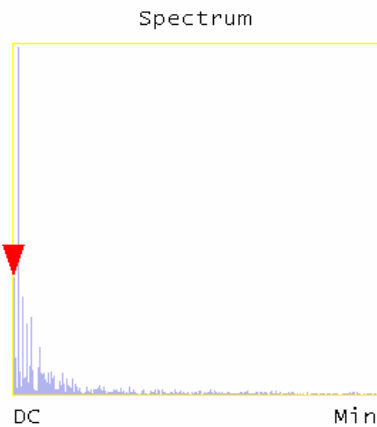
Device level replications



L	3.125 μm
RMS	79.598 nm
lc	DC
Ra(lc)	38.627 nm
Rmax	134.61 nm
Rz	134.61 nm
Rz Cnt	2
Radius	8.241 μm
Sigma	22.697 nm



s053106_m_ht2.001



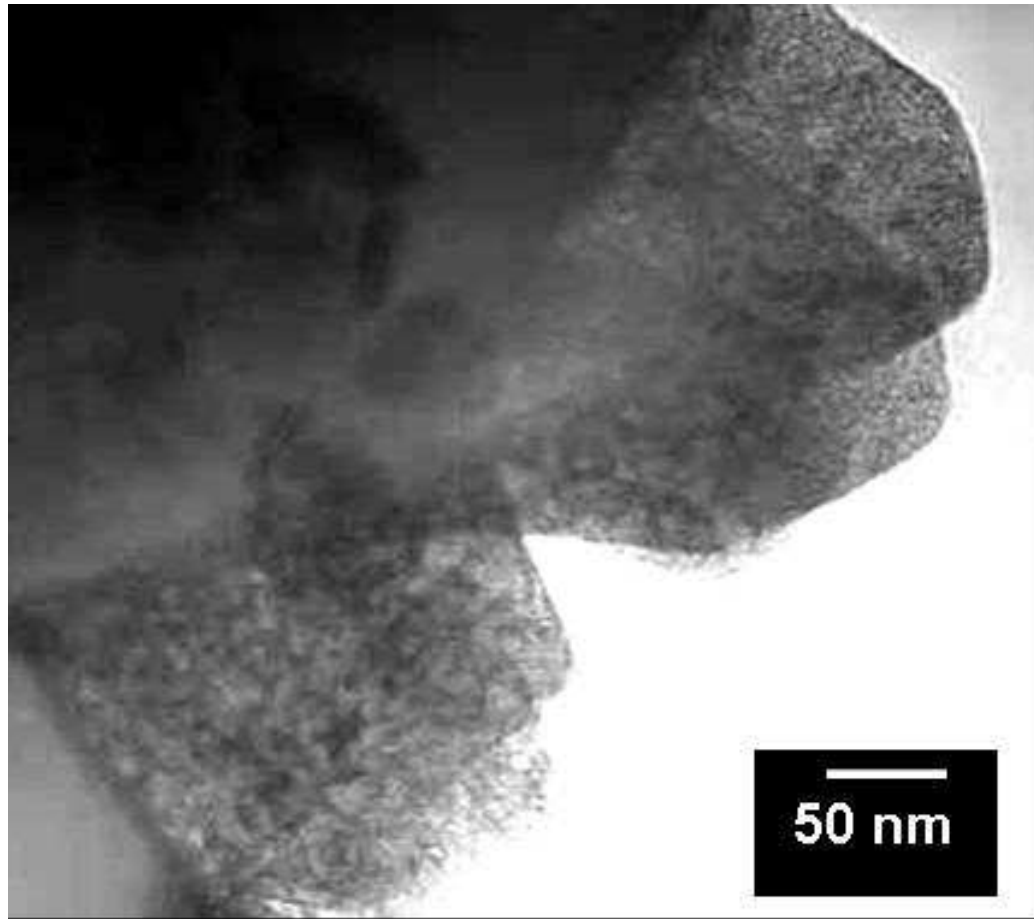
Surface distance	3.160 μm
Horiz distance(L)	3.125 μm
Vert distance	200.40 nm
Angle	3.669 °

Surface distance	
Horiz distance	
Vert distance	
Angle	
Surface distance	
Horiz distance	
Vert distance	
Angle	
Spectral period	DC
Spectral freq	0 Hz
Spectral RMS amp	0.027 nm

➤ AFM section analysis showing the sharp sidewalls



Domain level replications



- Shows mesoporosity
- ✓ PAG segregates to one domain (PtbocSt)
- No order; Randomly oriented pores.

- TEM image of the mesoporous silica film templated from P(S-b-tbocSt) films.

Conclusions & Future Work



- Substitution of pTSA with PAG enables patterning of mesoporous silica films with domain and device level architecture.
- Although domain level replication is perfect in mesoporous silica films templated from Pluronics, device level replication is not perfect -- PAG diffusion.
- PAG diffusion is restricted to minimum in PtbcSt systems. PAG diffusion can further be suppressed by anchoring the PAG to polymer.
- By using PS-b-PtbcSt block copolymer as template, both domain and device level replications with high fidelity can be obtained.
- High Resolution pattern replication is under study
- Additional support from NSF-NIRT, NSF-CHM & MRSEC is acknowledged

Destruction of Perfluoroalkyl Surfactants (PFAS) in Semiconductor Process Waters using Boron Doped Diamond Film Electrodes

Task # 425.018 / Thrust C

Kimberly Carter, James Farrell, Valeria Ochoa, Reyes Sierra
Department of Chemical and Environmental Engineering
The University of Arizona

Research Objectives

- Determine the feasibility of electrochemical destruction of PFAS in dilute aqueous waste streams.
- Determine the degree of electrolysis required to generate products that are readily biodegraded in municipal wastewater treatment plants.
- Develop an adsorptive method using hydrophobic zeolites or anion exchange resins for concentrating PFAS compounds from dilute aqueous solutions.

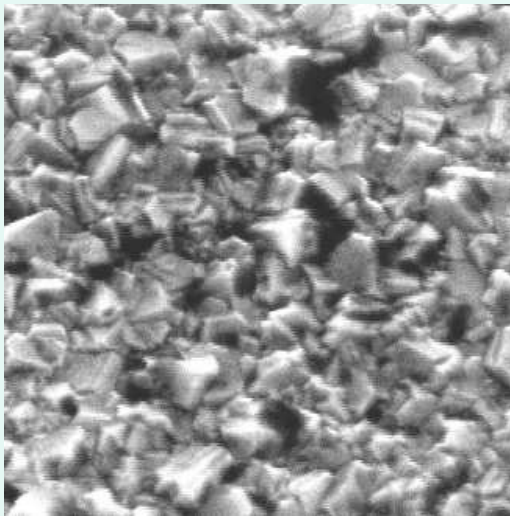
ESH Impact / ESH Metrics

- PFAS are used in photoresist developers and antireflective coatings.
- Most PFAS waste is contained in organic solvents and destroyed by incineration.
- There is a need to treat dilute aqueous streams containing PFAS.
- Ion exchange, carbon adsorption, UV/peroxide, sonolysis & biodegradation treatments are impractical or ineffective.
- An effective method for removing PFAS from aqueous waste streams is needed in order to secure a limited use exemption from the U.S. Environmental Protection Agency.

Goal/Possibilities	Energy	PFCs
Remove PFAS from aqueous waste streams	Elimination of costly reverse osmosis treatments	99% removal from disposed wastewaters

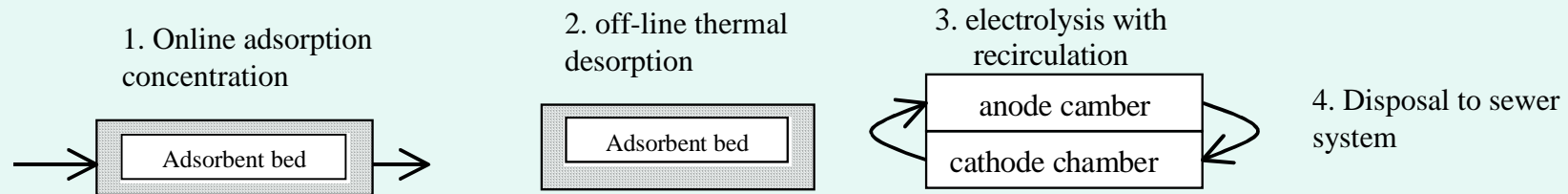
Boron-Doped Diamond Film (BDD) Electrodes

- Diamond film grown on p-silicon substrate using CVD
- Boron doping provides electrical conductivity
- Highly stable under anodic polarization
- No catalyst to foul or leach from electrode
- Emerging technology being adopted for water disinfection



Scanning electron micrograph of BDD electrode. The individual diamond crystals are $\sim 0.5 \mu\text{m}$ in size.

Proposed Treatment Scheme



Multi-step treatment scheme:

1. Concentrate PFAS from dilute aqueous solutions on an adsorbent.
2. Thermally desorb PFAS into a concentrated solution.
3. Recirculate concentrated PFAS solution through a BDD electrode reactor for electrolytic destruction.
4. Dispose of biodegradable electrolysis products to the sanitary sewer system.

Experimental Systems



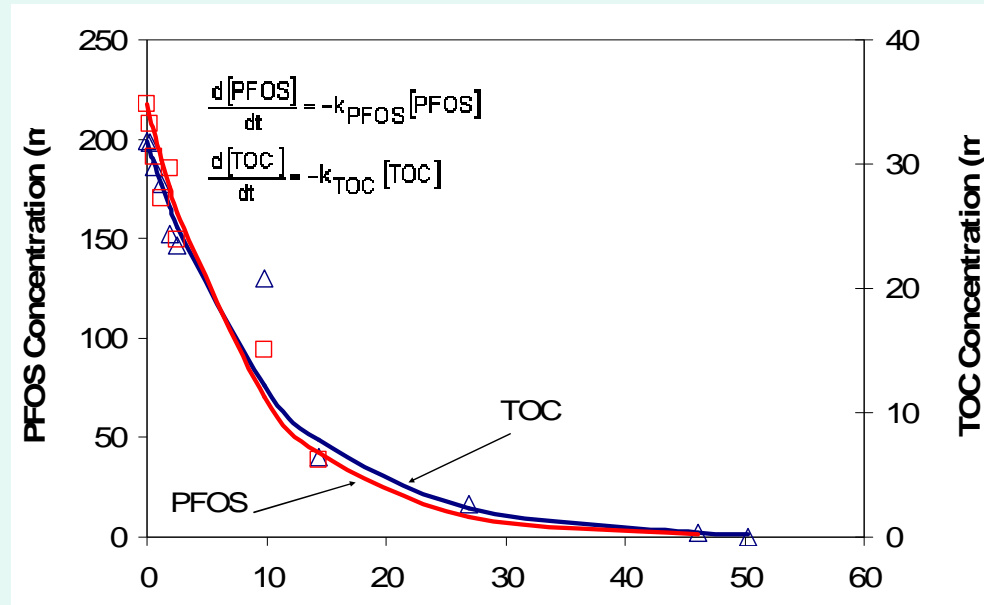
Rotating disk electrode (RDE) in batch reactor.

- no mass transfer limitations
- electrode surface area = 1 cm²
- solution volume = 350 mL
- $a_s = 0.00286$ cm²/mL

Parallel plate flow-cell.

- rates similar to real treatment process
- electrode surface area = 25 cm²
- solution volume = 15 mL
- $a_s = 1.67$ cm²/mL

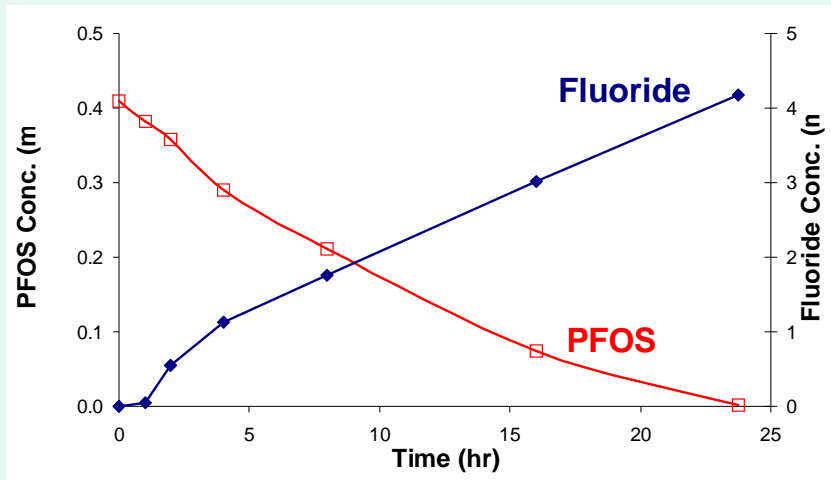
Experimental Results



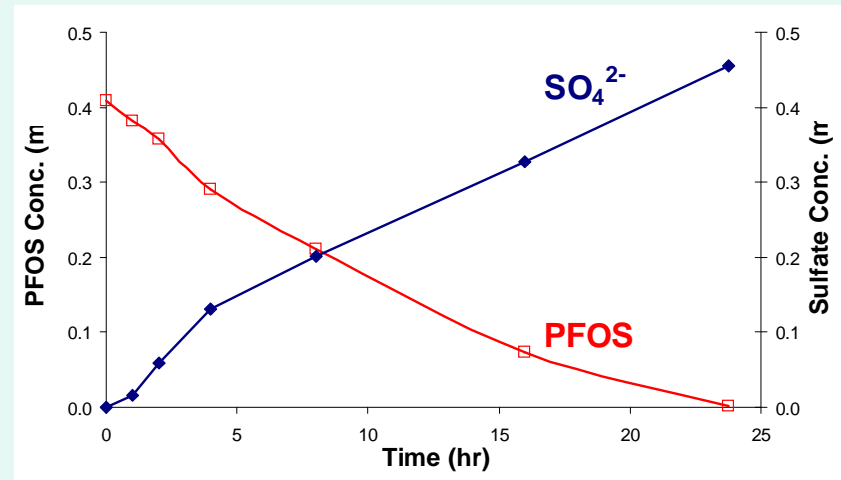
PFOS and total organic carbon concentration (TOC) in flow-cell operated at a current density of 15 mA/cm².

- PFOS can be rapidly removed from water
- Reaction rates are first order in concentration
- Treatment half-life of less than 10 minutes
- No build-up of reaction products

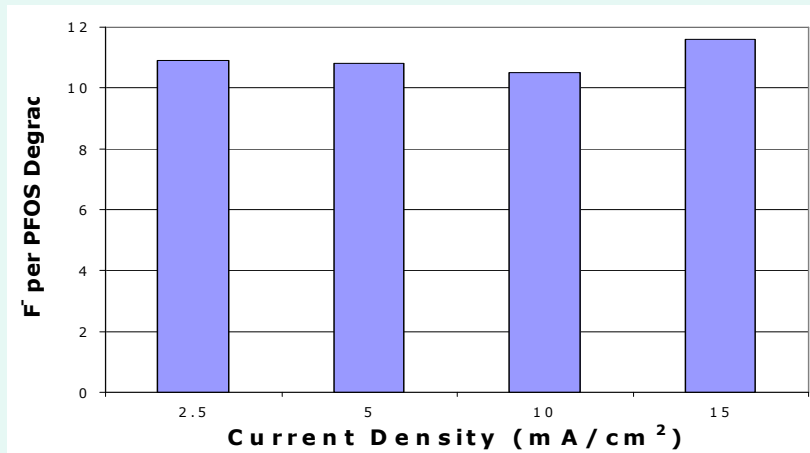
Reaction Products



Comparison of Fluoride evolution to PFOS degradation



Comparison of Sulfate evolution to PFOS degradation

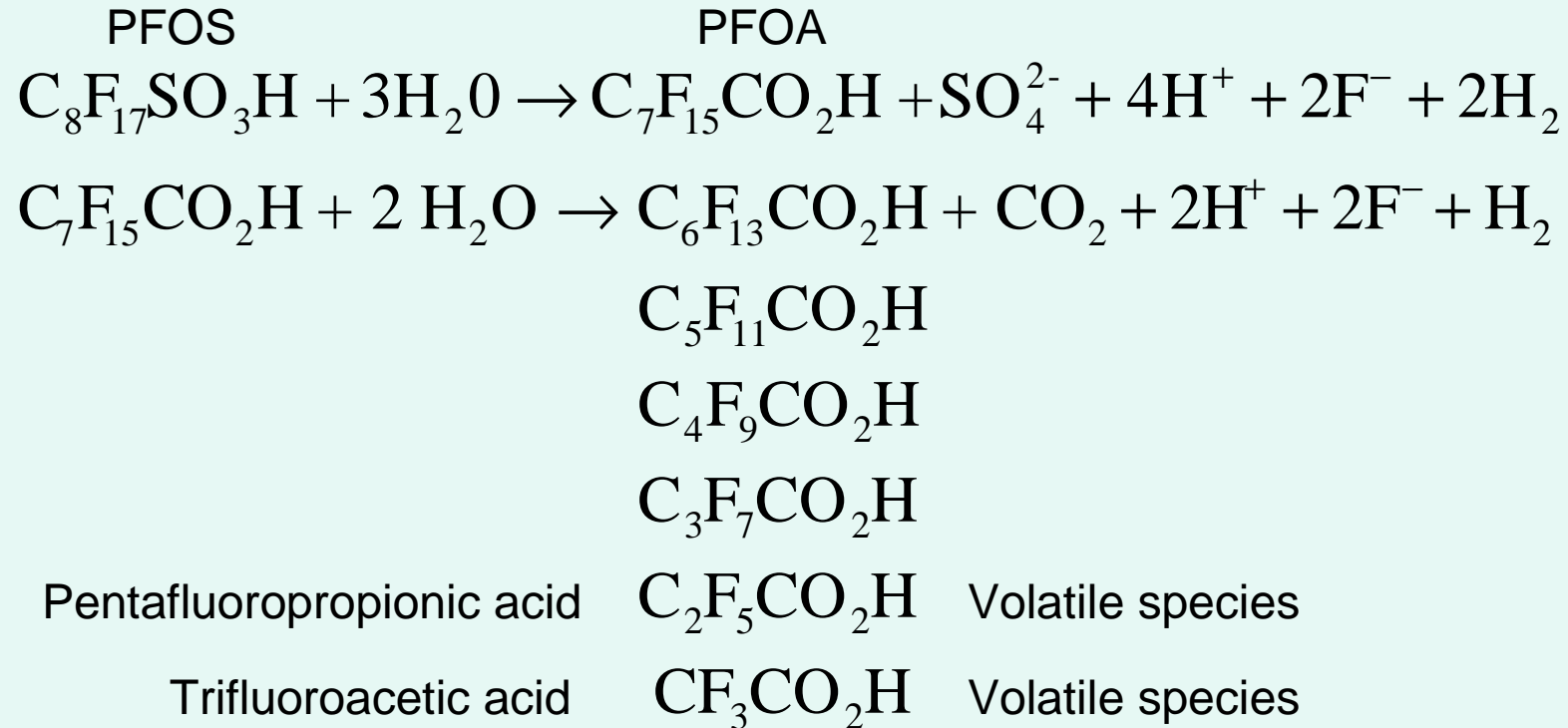


Fluoride per PFOS degradation for different current densities

Only trace quantities of:

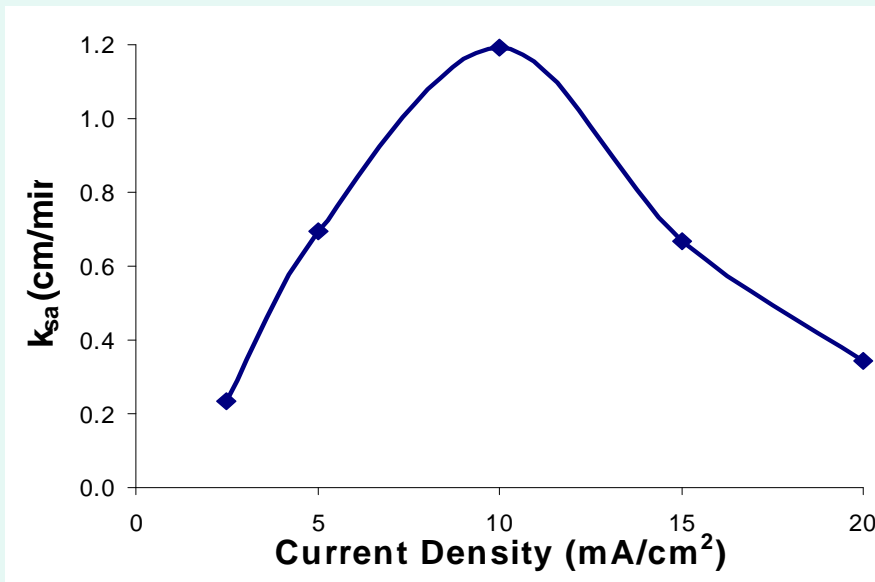
1. Perfluorooctanoic acid
2. Perfluoroheptanoic acid
3. Perfluorohexanoic acid

Proposed Reaction Sequence

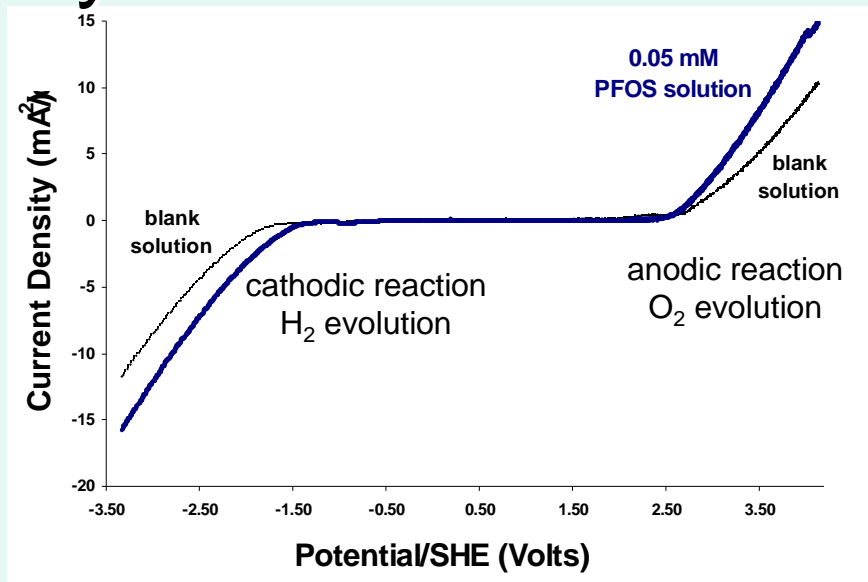


- Fluoride mass balance of 11 F⁻ released per PFOS degraded suggests that volatile species are lost from solution.
- No observation of intermediate products suggests near complete degradation in a single interaction with the electrode surface.

Effect of Current Density on Reaction Rates



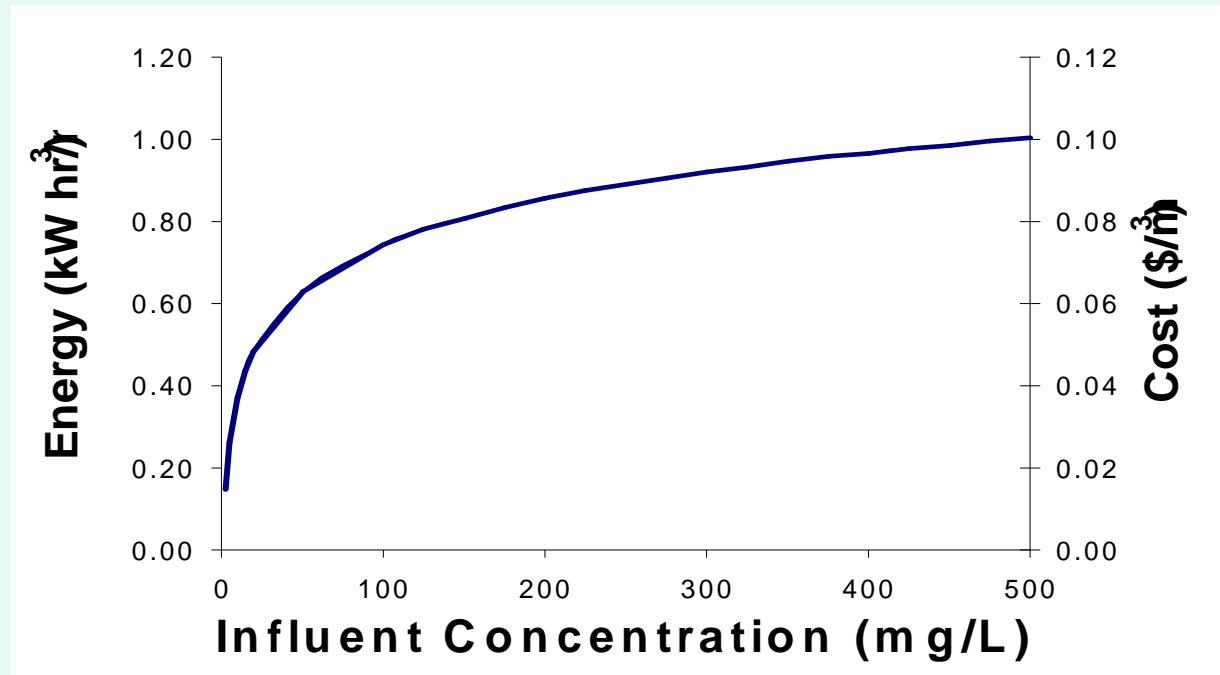
The effect of current density on the RDE surface area normalized rate constants (k_{sa}) for PFOS oxidation.



Linear sweep voltammograms from RDE in blank electrolyte and PFOS solutions.

- Oxygen gas bubbles at high current densities reduce the wetted surface area of the electrode and interfere with PFOS oxidation.
- Maximum practical reaction rates are limited by the competing reaction of oxygen evolution.

Treatment Costs



Electrical power requirements and costs required to reach a final PFOS concentration of 1 mg/L (2.5 μ M) as a function of the influent concentration. Costs based on flow-cell operated at a current density of 20 mA/cm².

- Electrical power costs are small compared to other treatment methods.
- Capital costs for a 10 liter per minute flow-cell are ~\$5000.

Conclusions

- Developed analytical methods for measuring PFAS compounds.
- Demonstrated that PFOS can be rapidly oxidized at BDD electrodes.
- Determined the products of PFOS oxidation.

Future Plans

- Determine the optimal operating conditions for oxidation of other PFAS compounds.
- Determine the most effective adsorbents for PFAS concentration.
- Determine the biodegradability of PFAS oxidation products
- Pilot test treatment scheme on real process wastewaters.

Acknowledgements

- Lily Liao and Arpad Somogyi
- NSF/SRC ERC 2001MC425
- NSF Chemical and Transport Systems CTS-0522790
- Petroleum Research Fund 43535-AC5

Industrial Collaboration

- Tim Yeakley Texas Instruments
- Thomas P. Diamond IBM
- Jim Jewett Intel
- Laura Mendicino Freescale Semiconductor



***Low Environmental Impact
Processing of Sub-50 nm
Interconnect Structures***

(Task ID: 425.019)

***Chia-Hua Lee and Karen Gleason
Department of Chemical Engineering
Department of Materials Science and Engineering
Massachusetts Institute of Technology***

Project Objective

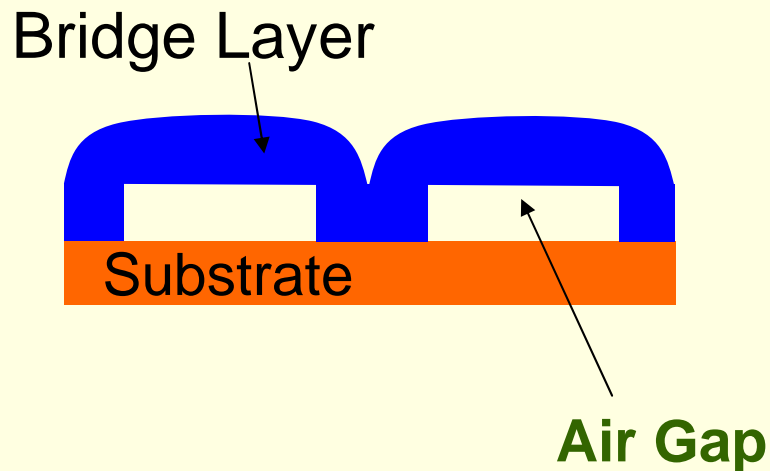
- Direct deposition patterned sacrificial layers rather than blanket
- Use of Dip-Pen Nanolithography (DPN) to create surface patterns (expected resolution sub 50nm) (collaboration with Prof. Angela Belcher's (MIT) group)
- Use Supercritical CO₂ to remove sacrificial materials (collaboration with Prof. Muscat (UA) group)

ESH Impact and ESH Metrics

- Using air ($k=1.0$) as a dielectric would allow the highest density of devices per layer and result in the fewest number of metal layers on the chip. This reduced number of steps results in lower materials and energy usage and in less waste production.
- Reductions in the volume of ESH relevant chemicals as well as minimization of photolithography and CMP steps can consequently make a significant impact on lowering the overall cost of device fabrication.

Sacrificial Materials for Air Gap

- Use of Sacrificial Materials (or Porogens) for Low-Dielectric-Constant Integration
 - Air has the lowest k of 1.0 (reduce RC delay, power, noise)



Direct Patterning Deposition

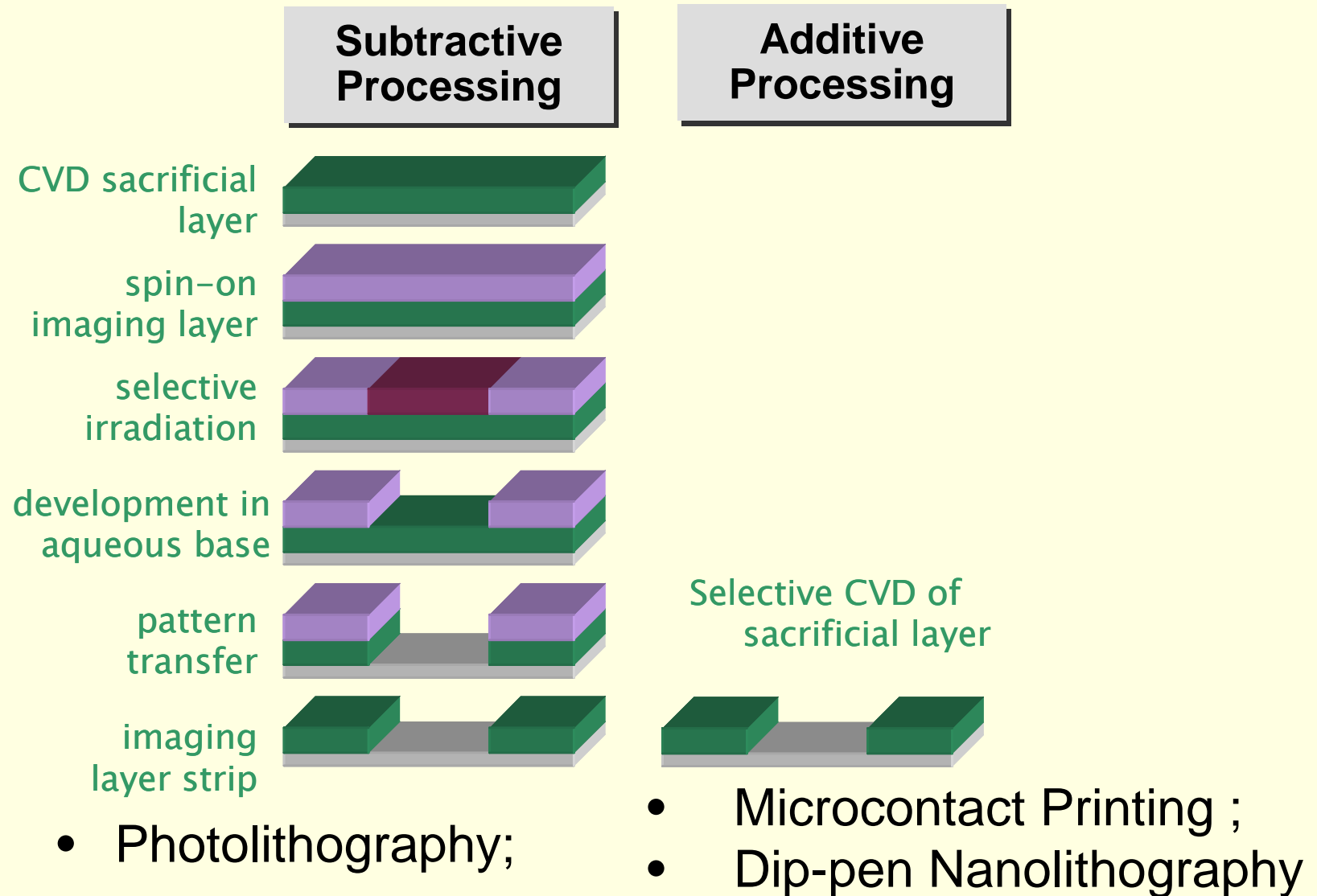


Deposition of Bridge Layer

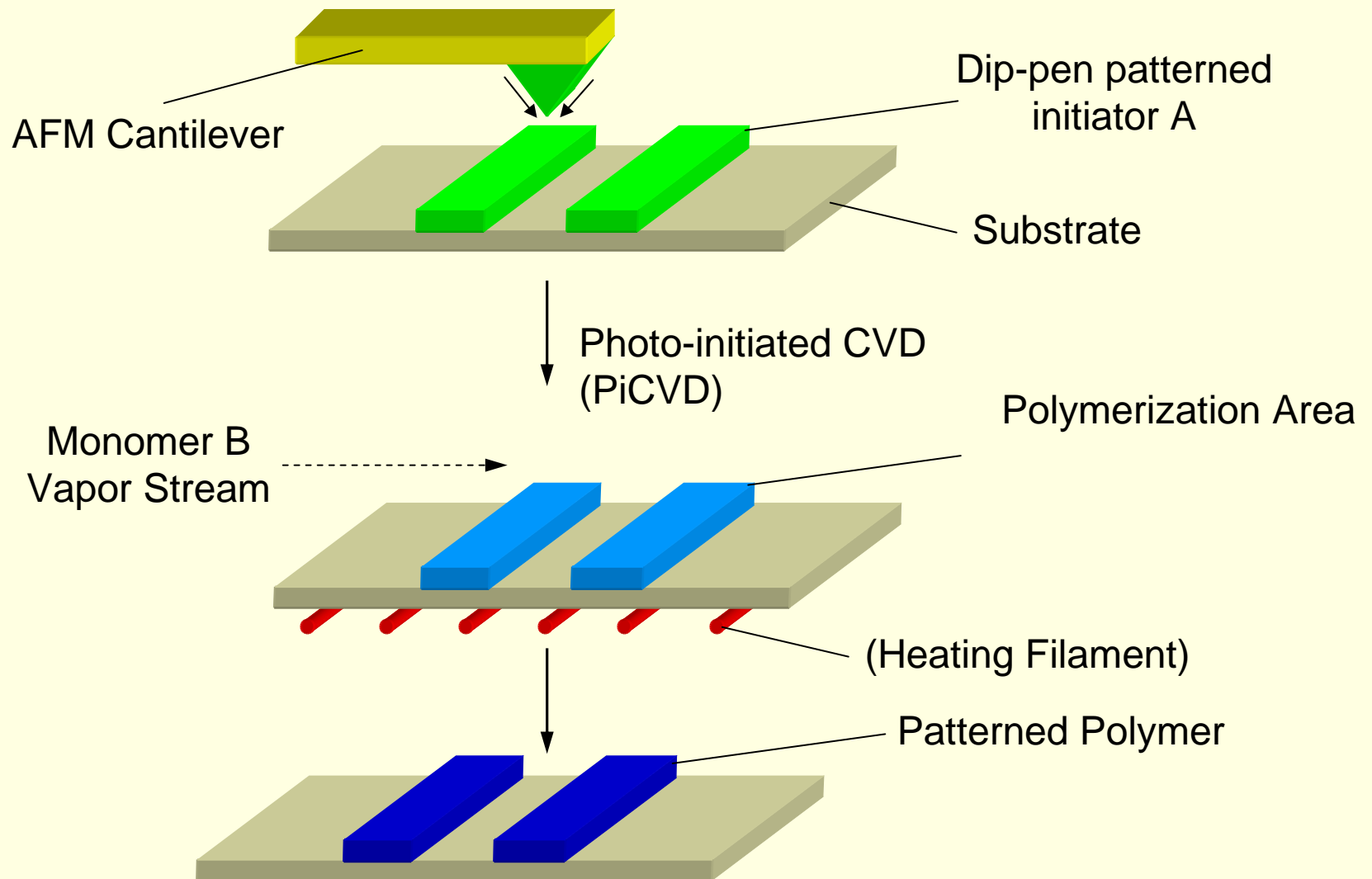


Decomposition

Patterning Approaches



Pattern Fabrication



Patterned Sacrificial Polymers

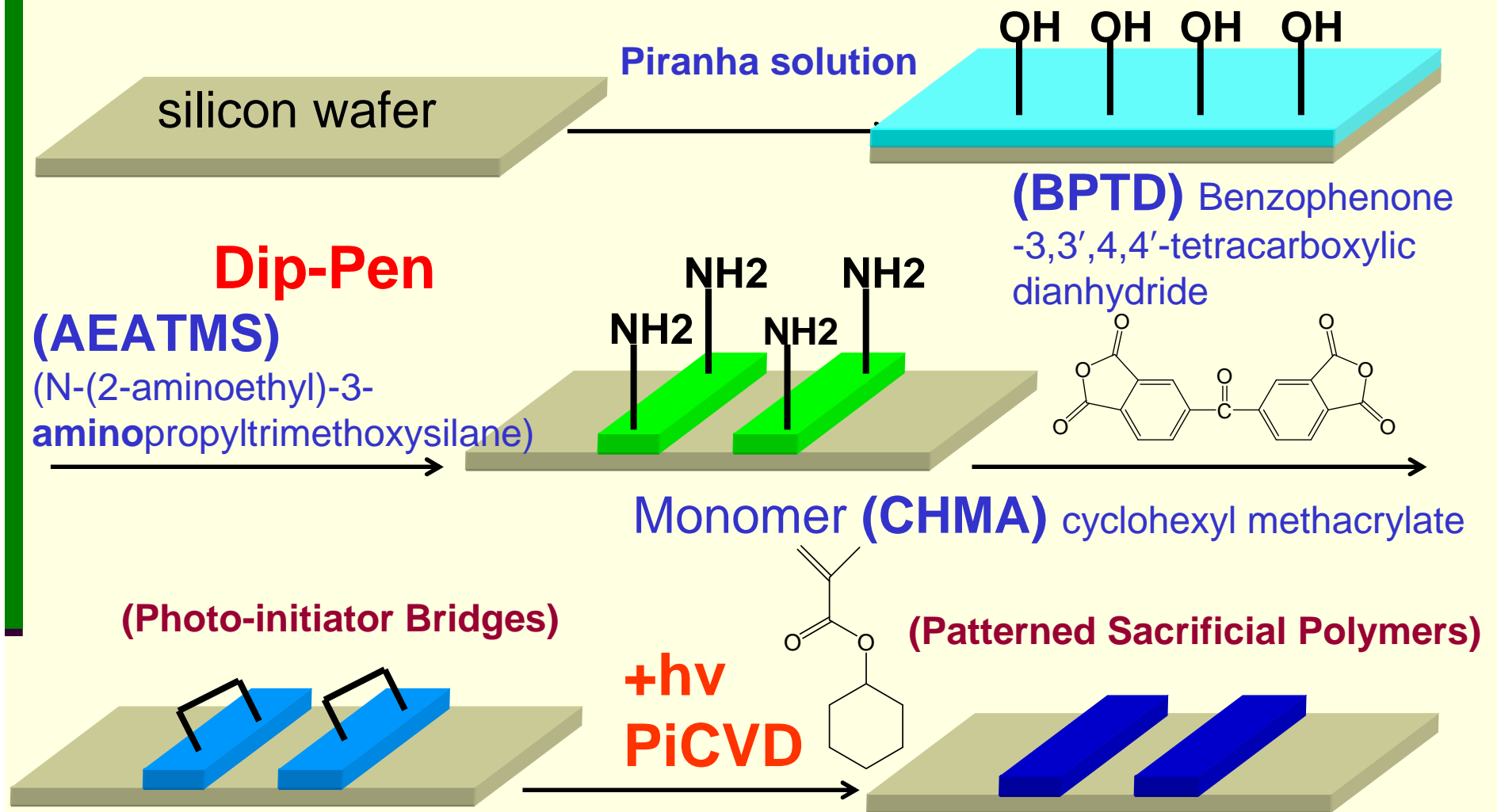
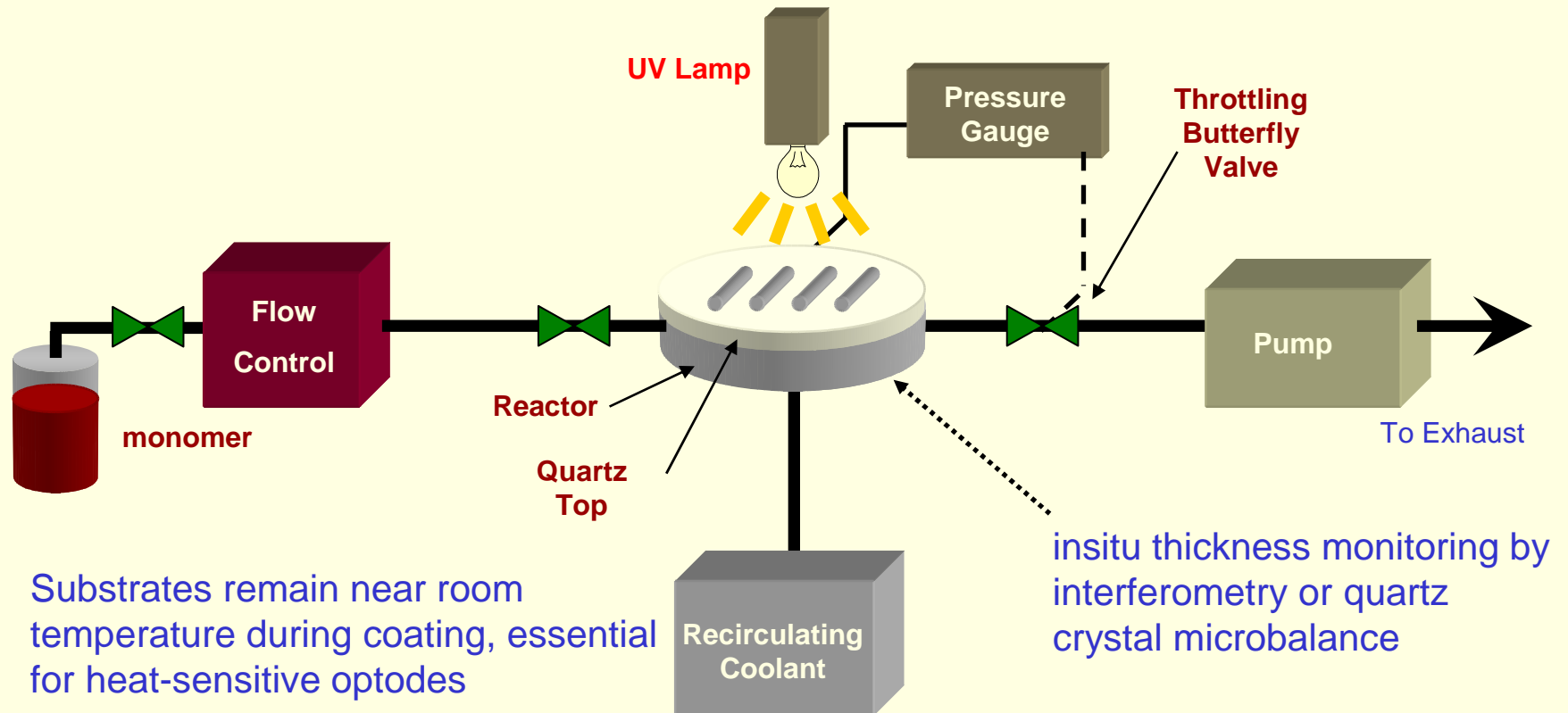


Photo-initiated CVD for sacrificial Polymers

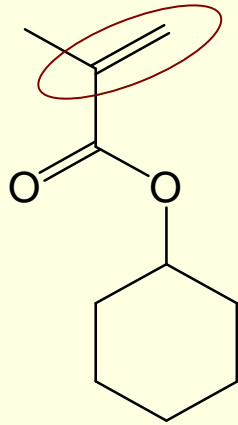


PiCVD process characteristics:

- All-dry process, no worker exposure to solvents
- low-temperature process
(substrate at ~ room temperature; no high-temperature filament)

PiCVD Sacrificial Layer Chemistry

Monomer Cyclohexyl Methacrylate (CHMA)



- selective bond scission
- systematic compositional variation using feed gas

- CHMA is not a photosensitive monomer
- Decomposition > 99.7% by thickness
- Onset temperature of decomp ~ 270 °C
- A environmental improvement over previously-reported spin-on sacrificial materials

Reference: [K. Chan](#) and [K. K. Gleason](#), J. Electrochem. Soc., 153, 4, C223-C228 (2006)

Lateral Force Microscope (LFM) Friction Images

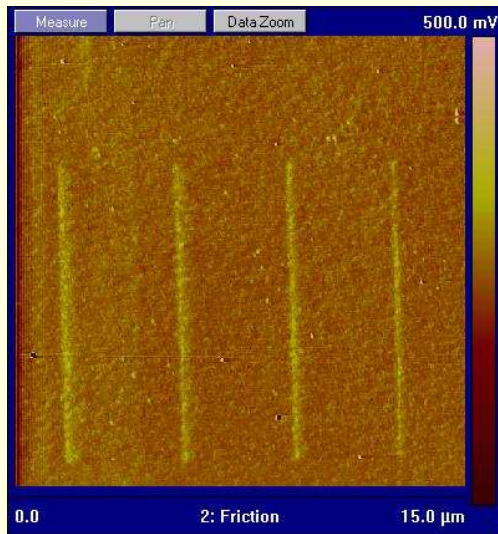
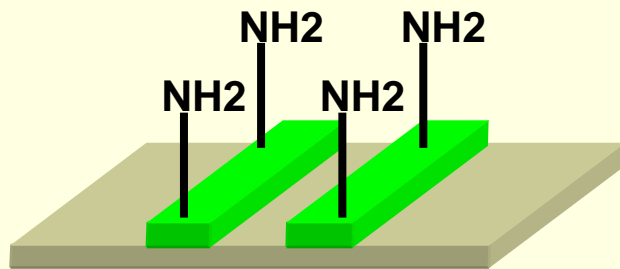
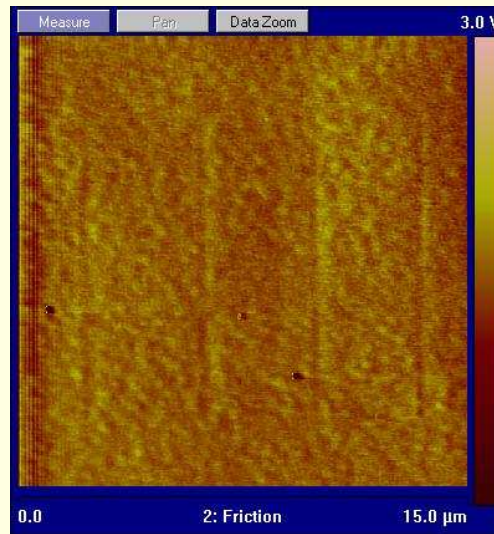
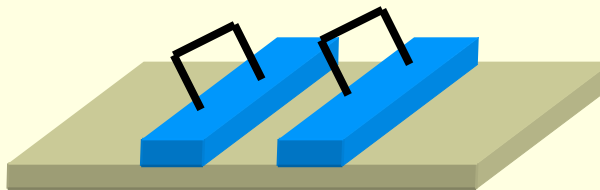
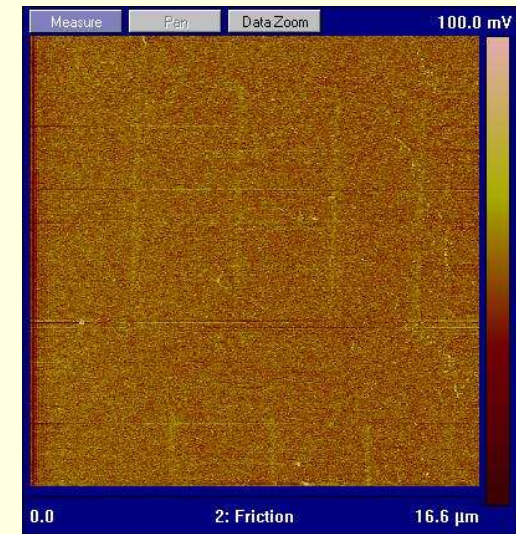
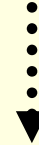
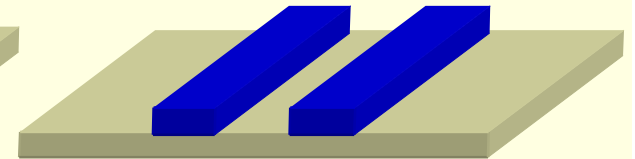


(Photo-initiator Bridges)



(Patterned polymers)



Acknowledgement: Chung-Yi Chiang and Prof. Angela Belcher

NSF/SRC Engineering Research Center for Environmentally Benign Semiconductor Manufacturing

Conclusion and Future Plans

- The direct patterning of sacrificial polymer has been demonstrated prepared by the combination of DPN and PiCVD technology. (collaboration with Belcher group)
- PiCVD processes for additive processing will be optimized for growth rate, uniformity, absence of surface defects, chemical structure, minimization of EHS impact, and compatibility with dry polymeric removal.
- Air gap structures will be tested to for removal of the sacrificial layer. (collaboration with Muscat group)

Industrial Collaboration/ Technology Transfer

- Dr. Kelvin Chan, AMAT
- Dr. Thomas Diamond, IBM
- Dr. Iacopi Francesca, IMEC
- Dr. Romano Hoofman, Phillips
- Dr. Dorel Toma, TEL

Low Environmental Impact Processing of Sub-50 nm Interconnect Structures

*Air gap fabrication through sacrificial polymer removal in
supercritical CO₂*

Rachel Morrish and Anthony Muscat

Department of Chemical and Environmental Engineering

University of Arizona, Tucson, AZ 85721

Task number 425.019



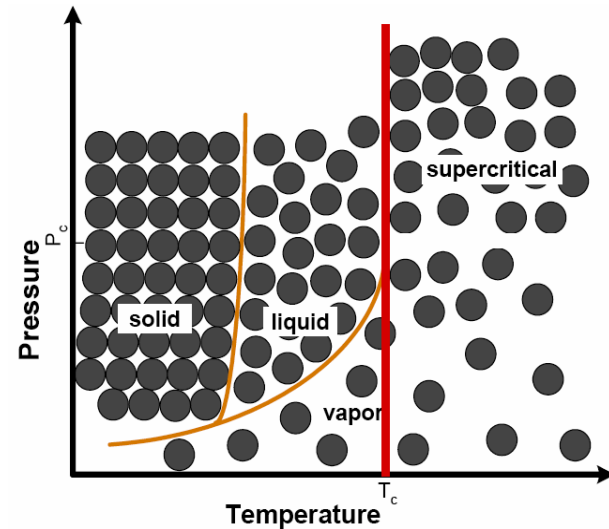
SRC/Sematech Engineering Research Center for Environmentally Benign Semiconductor Manufacturing

Objectives

- Develop a set of principles to guide the choice of materials and processing fluids to fabricate sub-50 nm structures with the lowest cost of ownership.
- Evaluate the performance of supercritical fluid processes to fabricate multilevel air gaps.
- Quantify the potential to reduce resource use and waste production by understanding process limitations in fabricating sub-50 nm structures.

Introduction - Supercritical fluid processing

- Supercritical CO₂ (scCO₂)
 - Liquid-like densities, gas-like mass transport properties
 - Moderate critical parameters (T_c = 31°C, P_c = 73 bar)
 - Environmentally benign solvent: chemically inert, recyclable
- EHS impact and matrix



Goals/ Possibilities	Usage Reduction			Emission Reduction			
	Energy	Water	Chemicals	PFCs	VOCs	HAPs	Other Hazardous Waste
Reduce organic solvent usage in processing	separations	up to 100%	up to 100% of org. sol.	N/A	capture cosolvents	CO ₂ is non-hazardous	dispose/recycle cosolvents
Eliminate plasma processing	lower T processing	N/A	unknown	up to 100%	up to 100%	CO ₂ is non-hazardous	dispose/recycle cosolvents
Reduce worker exposure to vapors	ventillation	N/A	up to 50% of vapors	N/A	volatiles during chemical input	N/A	N/A

Introduction – Experimental approach

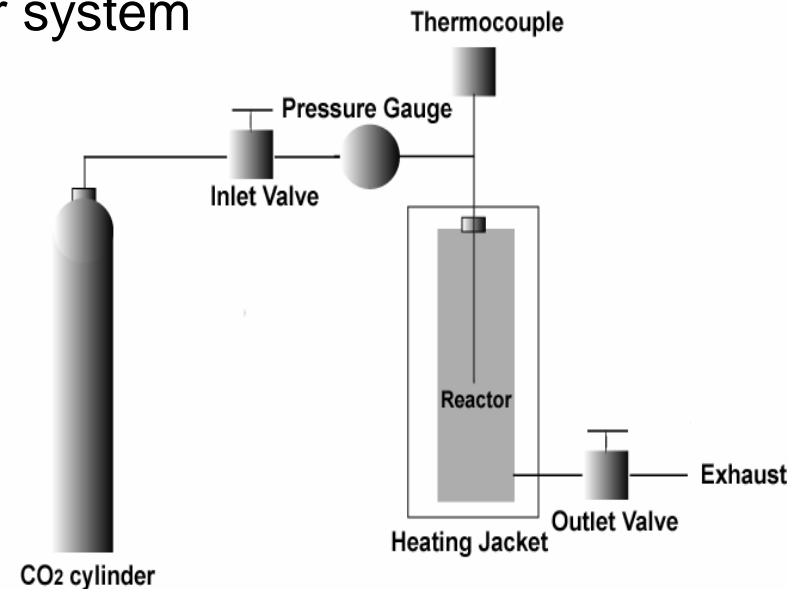
- Air gap structure fabrication by etching sacrificial polymer



- Remove sacrificial polymer in scCO_2
 - swell and plasticize polymer
 - add cosolvents to increase solubility
- Quantify removal
 - ellipsometry
 - Fourier transform infrared spectroscopy (FTIR)

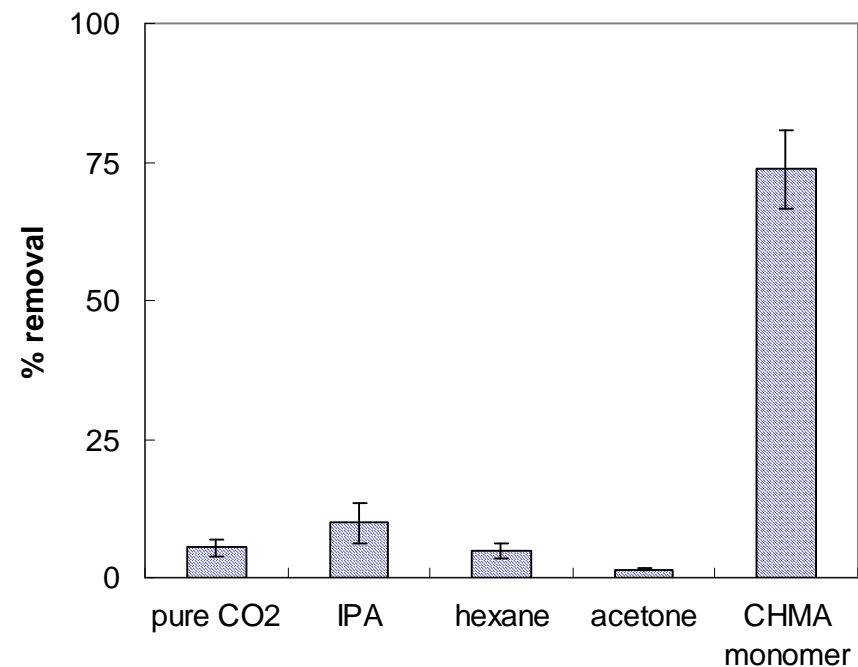
Experimental method

- Materials
 - Si wafer substrate with initiated CVD (i-CVD) deposited polycyclohexyl methacrylate sacrificial layer (100 – 250 nm)
 - Coleman grade CO₂, high purity cosolvents
- Reactor
 - batch style, stainless steel reactor system
- Processing
 - 60 – 75 ± 3°C, 170 ± 15 bar
 - cosolvent added to reactor
 - heated to desired conditions
 - react for 30 minutes
 - 13 min. clean in pure scCO₂



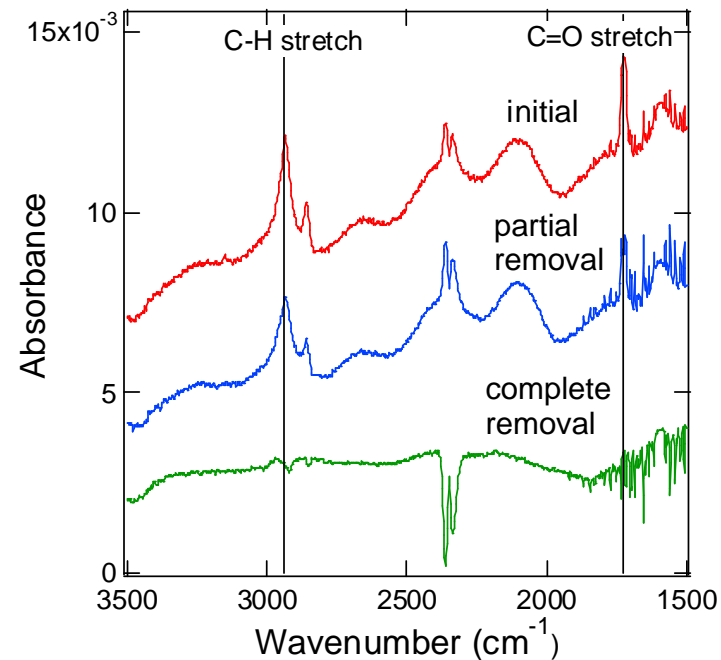
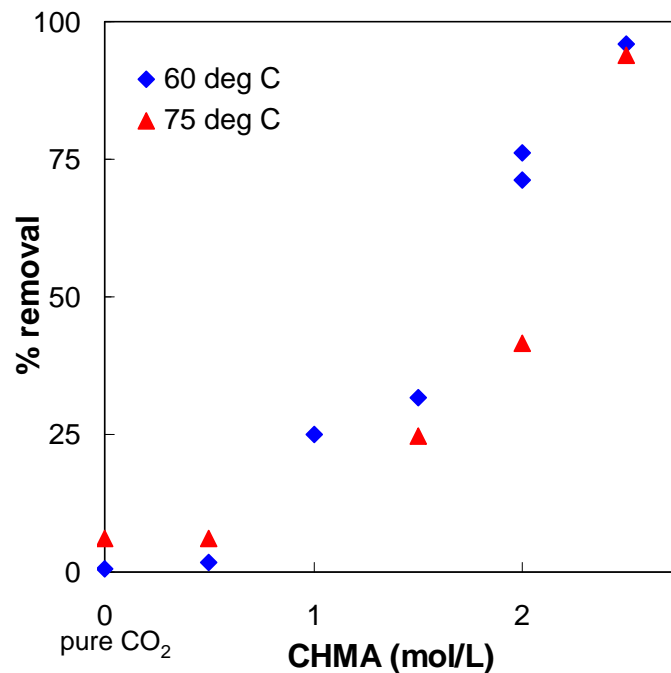
Results – CO₂/cosolvent mixture

- Polycyclohexyl methacrylate (CHMA) thin film removal in cosolvent/ CO₂ mixture
 - compared IPA, hexane, acetone, CHMA monomer cosolvents
- Initial study showed CHMA monomer exhibited highest removal
 - all other solvents removed remaining monomer or lower molecular weight portions of the film
 - CHMA increases solution density
 - CHMA provides favorable intermolecular interactions for dissolution



Results – CO₂/CHMA mixture

- Sacrificial polymer removed with CHMA monomer in scCO₂ at 170 bar
 - Solubility increased with increasing CHMA concentration
 - Verified removal using FTIR: decreased intensity of C-H and C=O vibrations



Conclusions and future work

- **Conclusions**

- Partially removed sacrificial polymer in pure CO₂ and cosolvents of IPA, hexane, and acetone
- Demonstrated complete polymer removal with CHMA monomer in scCO₂ solution

- **Future Work**

- Determine optimum processing conditions for etching
- Investigate dissolution kinetics using *in-situ* FTIR reactor
- Test sacrificial polymer removal on patterned substrates
- Explore viability of recycling CO₂ and monomer cosolvent

- **Acknowledgments**

- Gleason group (MIT)
- SRC/Sematech Engineering Research Center

Micromachined Shear Sensors for *in situ* Characterization of Surface Forces during CMP

ERC Task # 425.020

A. J. Mueller, R. D. White

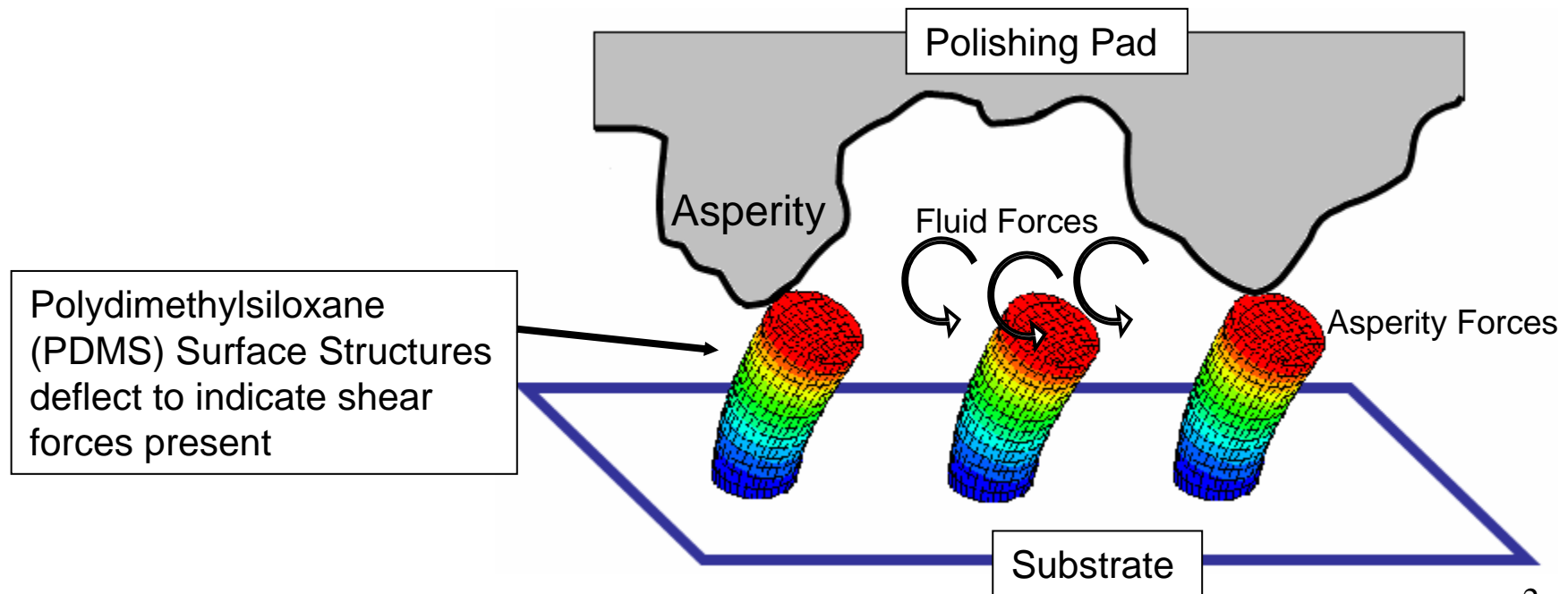
Dept. of Mechanical Engineering

Tufts University, Medford, MA

February 2007

Project Objectives

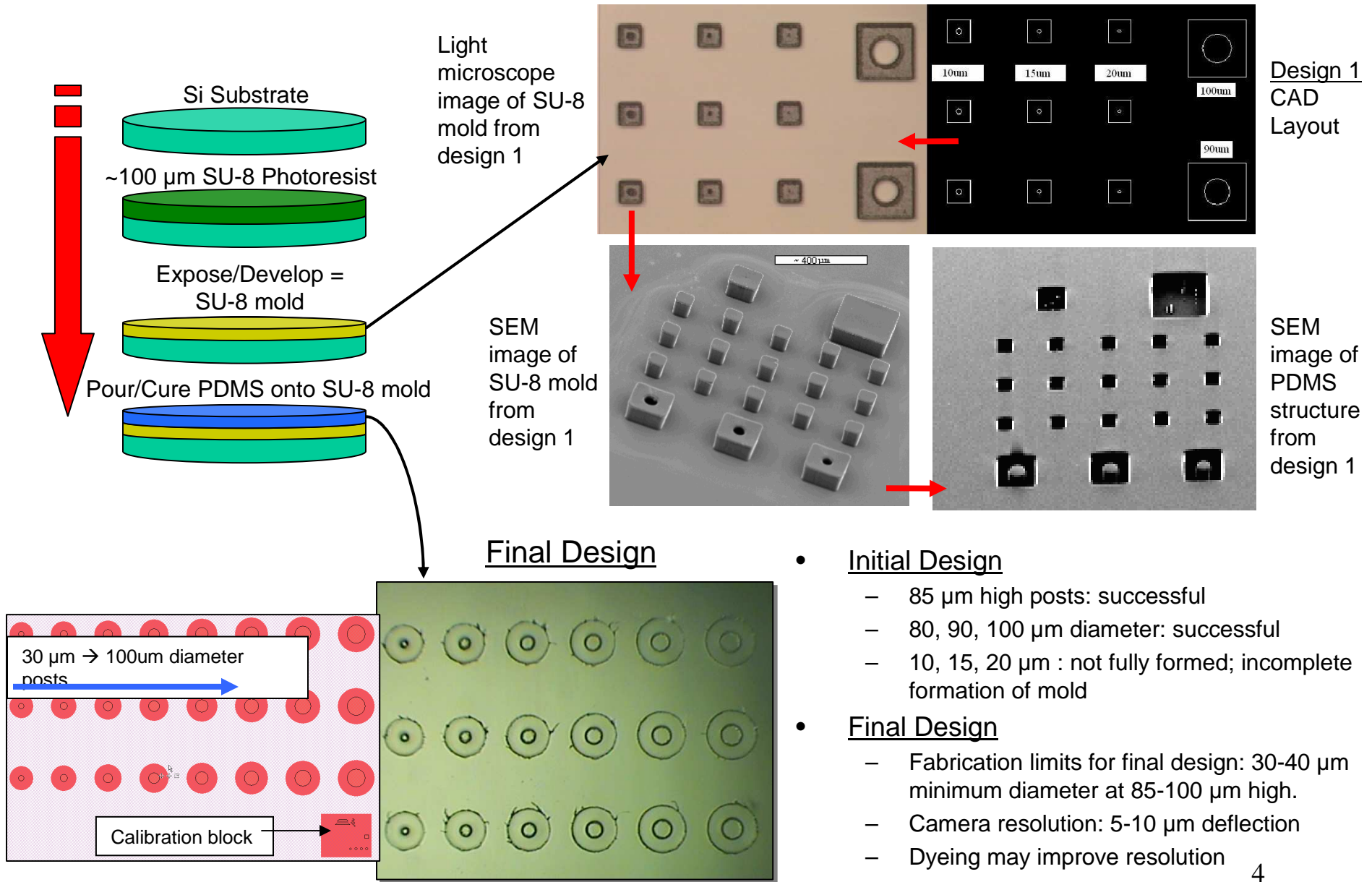
- Fabricate and implement micromachined shear stress sensors for characterization of surface forces during chemical-mechanical polishing (CMP).
- Measure local, real-time shear stress at the pad-wafer interface during CMP due to slurry and asperity interactions with the wafer.



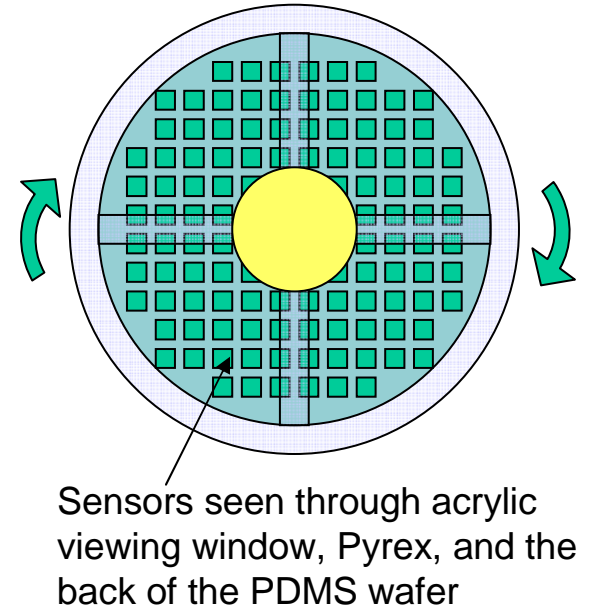
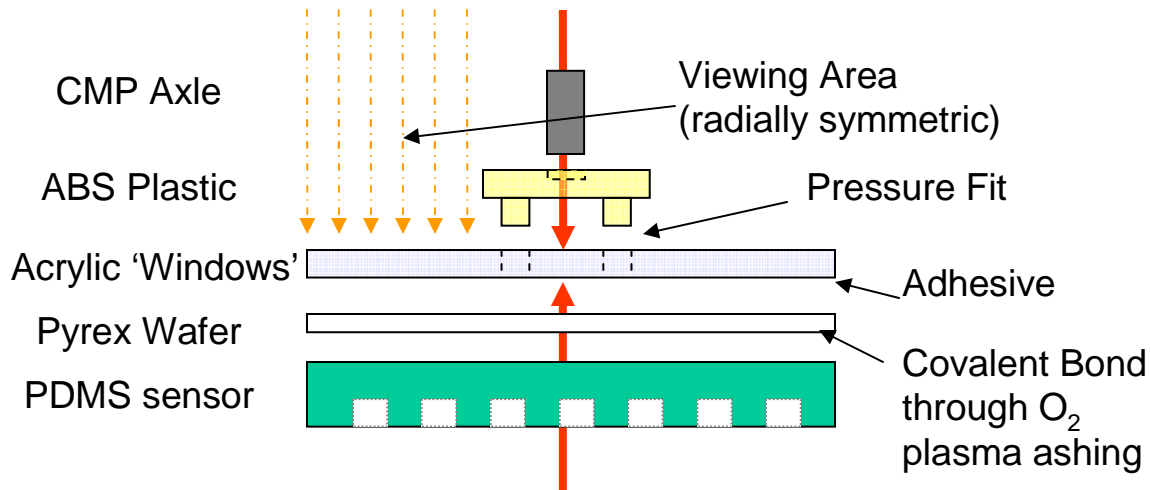
Environmental Safety and Health (ESH) Metrics and Impacts

<u>METRIC</u>	<u>IMPACT</u>
Energy Consumption During Process	Understanding wafer-pad interactions during polish leads to reduced time to polish and tool energy consumption
DI Water Consumption During Process	Optimized process parameters based on in-situ characterization of contact, and forces leads to reduced time to polish and slurry consumption
Process Chemical Consumption (Slurry Chemicals)	optimization

Sensor Process & Design Overview



Mounting

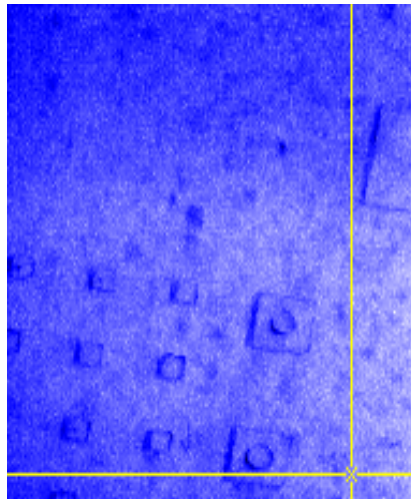


Imaging

Current Optics

Without dye: 80-100 μm structures visible.

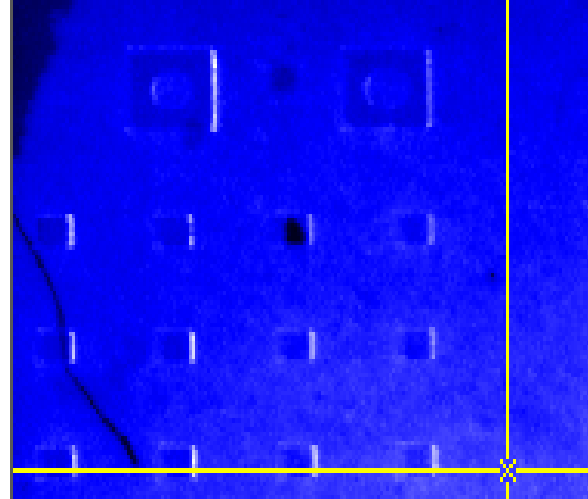
Expect to be able to resolve $\sim 5\text{-}10 \mu\text{m}$ displacement with existing optics.



Rhodamine B

With dye: some edges are very bright.

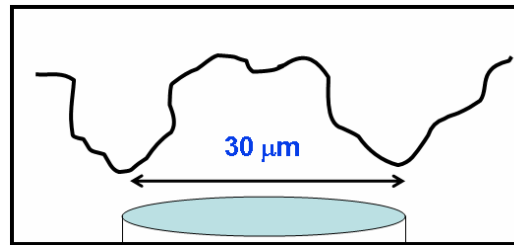
Additional experiments are planned to attempt to achieve uniform edge dyeing.



Asperity Force Estimations

Total shear force load is COF·Downforce·Wafer Area (for 4" wafer) $\approx 0.5 (1.8 \text{ psi}) (\pi (50 \text{ mm})^2) \approx 50 \text{ N}$

Option #1 : Assume 30 μm center to center spacing on asperity tips with a square grid.



Number of Asperities in Contact:
Wafer Area/Asperity Neighborhood Area (for 4" wafer)

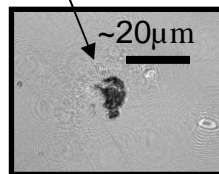
$$\approx (\pi (50 \text{ mm})^2) / ((30 \mu\text{m})^2)$$

$$\approx 8.7 \cdot 10^6 \text{ asperity contacts/wafer}$$

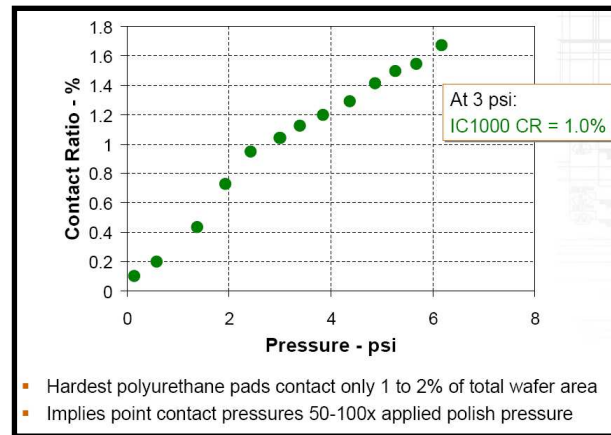
Force per asperity is total force over number of asperities $\approx 50 \text{ N} / (8.7 \cdot 10^6 \text{ asperities}) \approx 6 \mu\text{N}$

Option #2 : Determine number of contacts based on ratio of total contact area to individual asperity contact area.

$$\approx \pi(5 \mu\text{m})^2 \approx 80 \mu\text{m}^2$$



Carolina L. Elmufdi and Gregory P. Muldowney, "The Impact of Pad Microtexture The Impact of Pad Microtexture and Material Properties and Material Properties on Surface Contact and Defectivity in CMP on Surface Contact and Defectivity in CMP"



- Hardest polyurethane pads contact only 1 to 2% of total wafer area
- Implies point contact pressures 50-100x applied polish pressure

Estimate of static wafer contact % area for IC1000 pad at 1.8 psi downforce is **0.7%**.

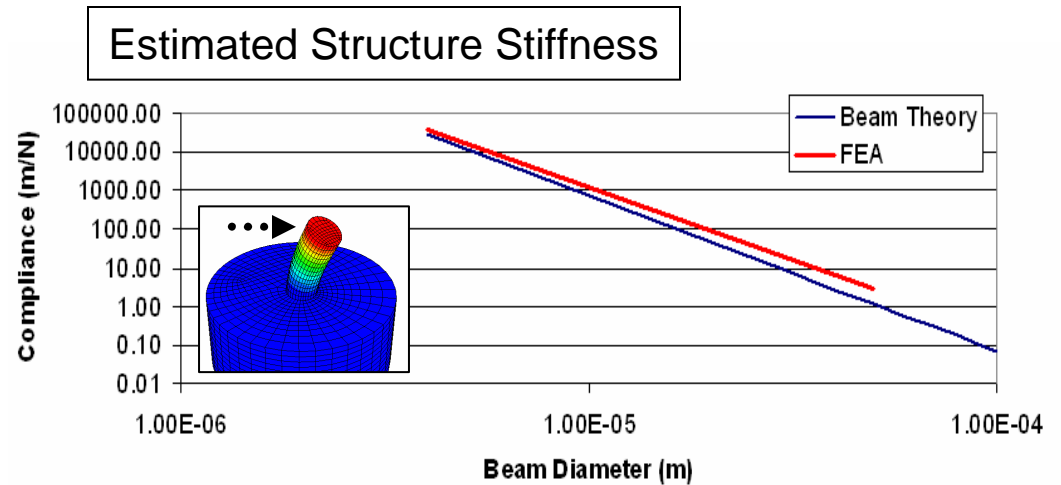
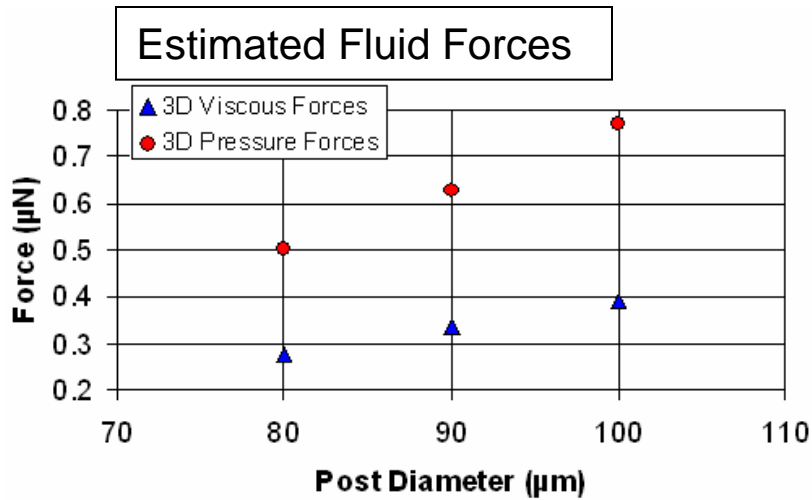
Number of Asperities in Contact:

$$\approx (0.007 \cdot \pi (50 \text{ mm})^2) / 80 \mu\text{m}^2$$

$$\approx 6.9 \cdot 10^5 \text{ asperity contacts/wafer}$$

Force per asperity is total force over number of asperities $\approx 50 \text{ N} / (6.9 \cdot 10^5 \text{ asperities}) \approx 70 \mu\text{N}$

Expected Sensitivities and Deflections



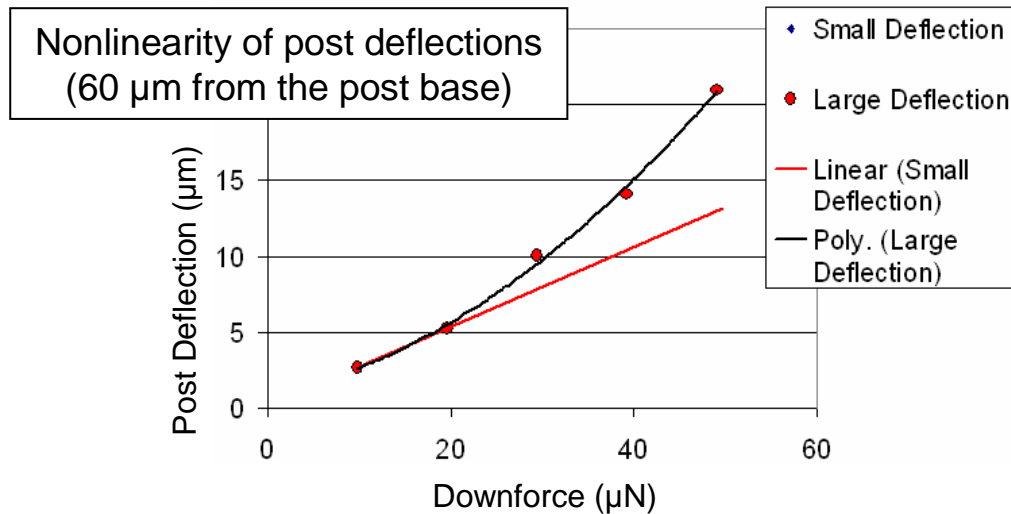
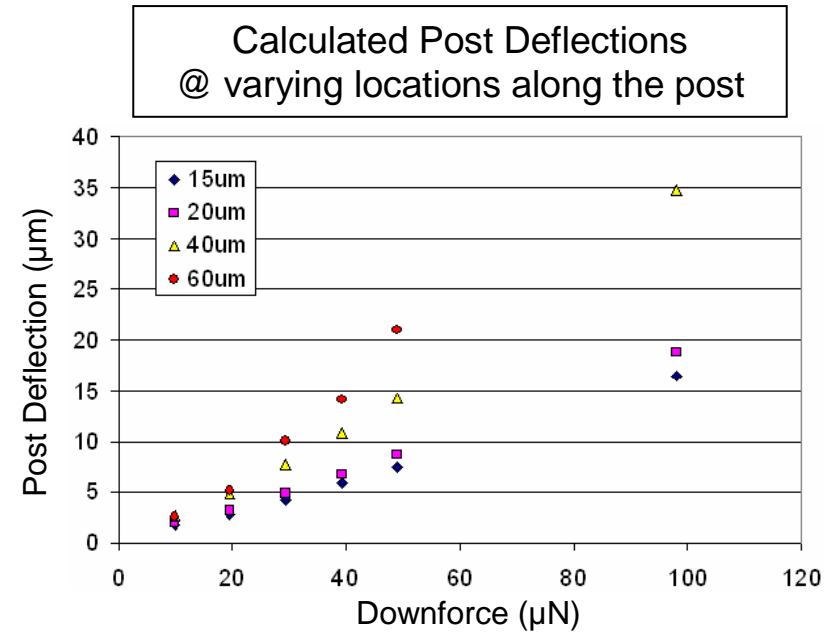
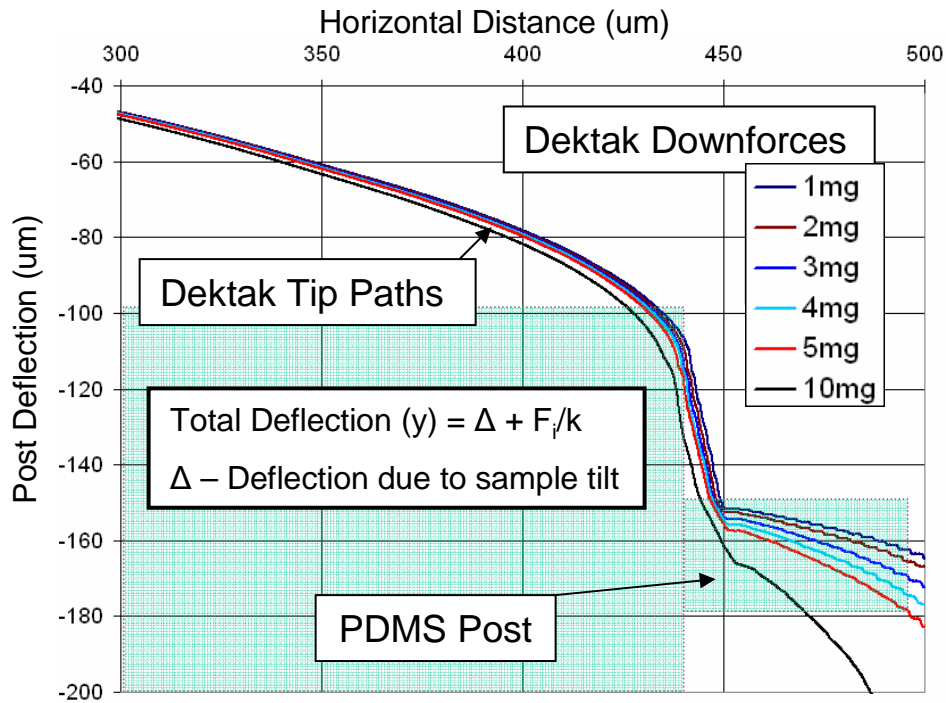
Estimated Sensitivities

$L=85 \mu\text{m}$
 $E_{\text{estimated}}=750 \text{ kPa}$

Diameter (µm)	30	40	50	60	70	80	90	100
Compliance (µm/µN)	8.75	2.77	1.13	0.55	0.30	0.17	0.11	0.07
Compliance (nm/Pa)	6.19	3.48	2.23	1.55	1.14	0.87	0.69	0.56
Deflection from Single Asperity Force (µm)	50-600	20-200	7-80	3-40	2-20	1-10	0.6-8	0.4-5
Deflection from Fluid Forces (µm)	2.8	1.4	0.75	0.47	0.31	0.22	0.16	0.12

Deflections due to asperity forces are expected to be at least 5x to 100x larger than deflections due to fluid forces. 7

Preliminary Sensor Calibrations



Calculated stiffness at 60 μm from the base = 3.1 N/m ($\sigma = 0.63$)
 ~10% of the value estimated from beam theory

Non-linearity at 60 μm from the post base with a downforce of 100 μN is around 5%

Future Plans

- Develop experimental apparatus for calibrating post deflection under known:
 - Fluid flow loads
 - Mechanical loads
- Improve dyeing ability to improve optical post resolution.
- Integrate with CMP rig for *in situ* surface force measurements.

Industrial Collaboration/Technology Transfer

- Close collaboration with industry partners – Cabot
Microelectronics and Intel
 - Monthly telecons – secure website for information exchange
 - Semi-annual face-to-face meetings
 - Thesis committees and joint publication authorship
 - Metrology and analysis methodology technology transfer
 - In-kind support – specialized supplies and equipment
 - Student internships (e.g. C. Gray at Intel during Summer 2005)
 - Close coordination with A. Philipossian research group at U of Arizona
- Information and results exchange with MIT (D. Boning)
ERC project
 - Monthly joint meetings of PIs and research students
 - Discussion of findings with other colleagues (e.g. E. Paul – Stockton College on leave at MIT)

Conclusions

- The sensors developed will allow measurement of shear forces during CMP at an estimated force resolution of 1-100 μN and spatial resolution of 300 μm .
- Sensor fabrication feasibility has been proven and diameter limitations have been established at 30 μm .
- Calibration and implementation of the shear sensors are ongoing.

An Integrated, Multi-Scale Framework for Designing Environmentally-Benign Copper, Tantalum and Ruthenium Planarization Processes

SRC ID #425.020 / ERC Thrust A / Subtask 1.2

Bum Soo Kim
Caiti Kilroy
Steve Beaudoin
School of Chemical Engineering
Purdue University

Project Objective

- ❖ Evaluate electrochemical processes occurring on Cu surfaces in slurry
 - ▶ CMP-relevant timeframes
 - ▶ Provides information on chemical state, mechanical properties of Cu surface
- ❖ Develop, validate models for Cu removal based on dissolution, abrasion
 - ▶ Including submodels for particle interactions with Cu surface

EHS Impact and Metrics

❖ Comparison

- ▶ Existing Cu CMP process

❖ Envisioned process

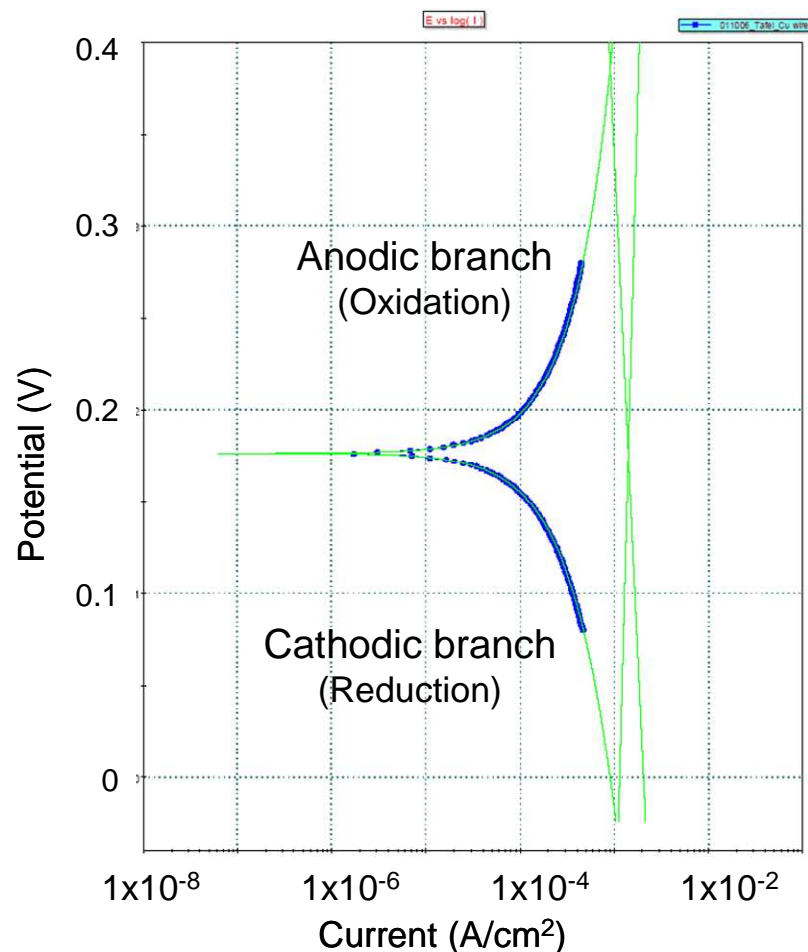
- ▶ Optimized slurry pH, ionic strength, additive composition
- ▶ Optimized abrasive size and composition

❖ Envisioned process

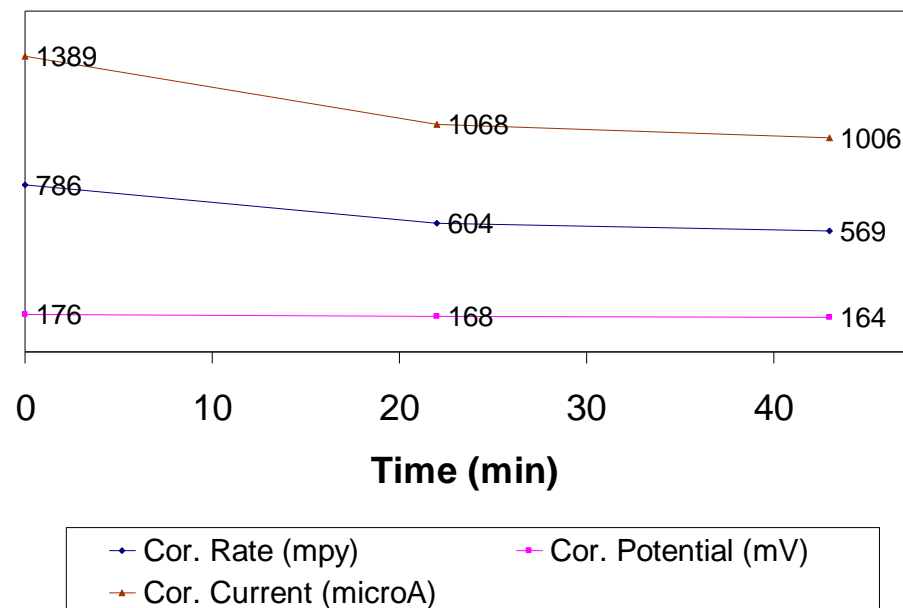
- ▶ Extend pad life by up to 15% by reducing aggressiveness of required conditioning
- ▶ Reduce slurry demand by 20% by enhancing interactions between abrasive particles and Cu surface

Corrosion Reaction on Cu

Tafel Analysis

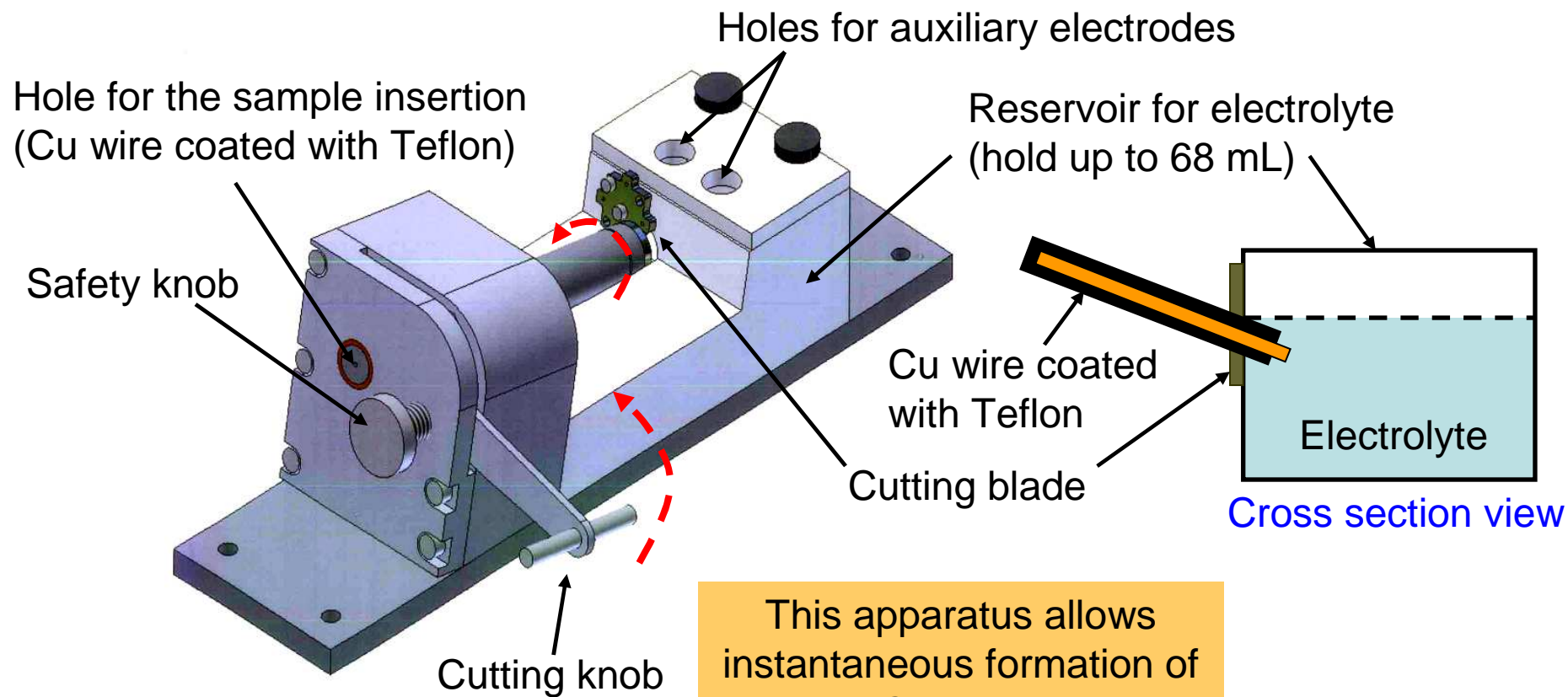


Obtained info from Tafel Plot



- ❖ Copper wire in pH=3 commercial CMP slurry with 5 wt% H₂O₂
- ❖ BTA does not completely quench reactions on Cu surface
- ❖ Dynamic system

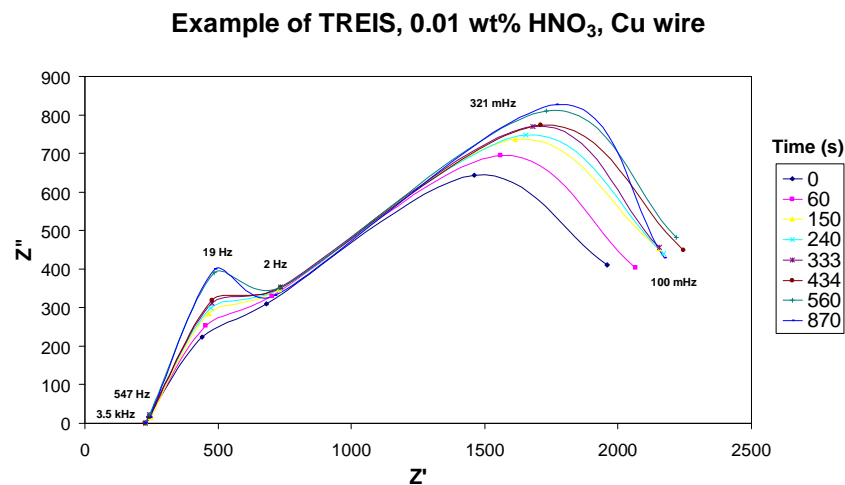
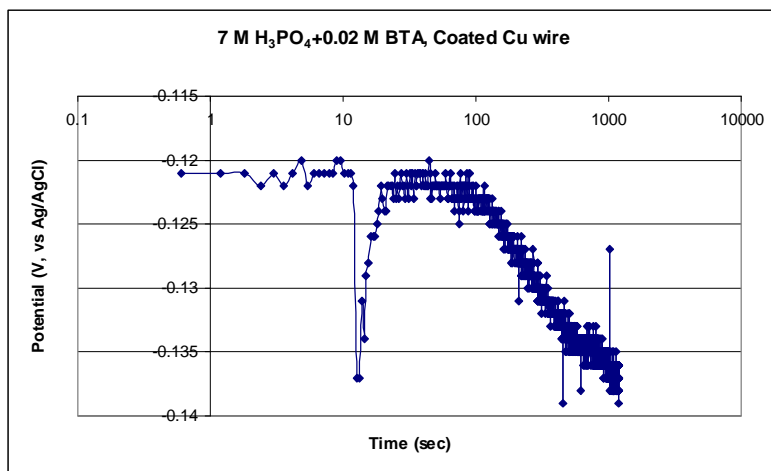
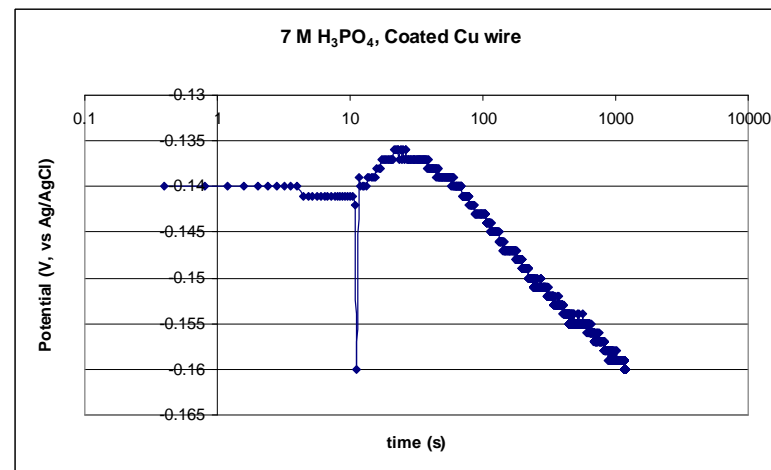
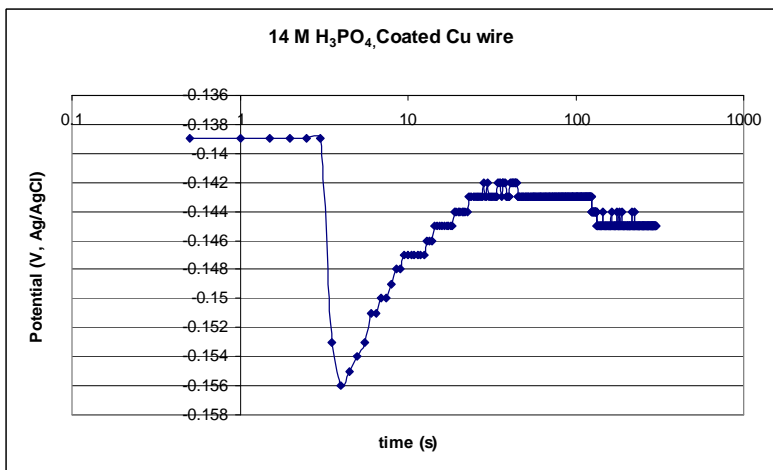
Guillotine Electrode: Reactions on CMP Timeframes



Advantages: Guillotine Electrode

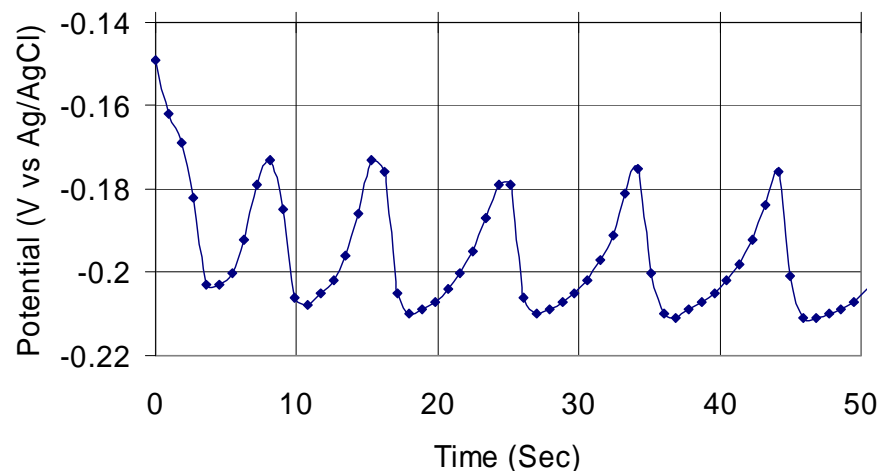
- ❖ Quantitative study of repassivation kinetics
 - ▶ Passivation layer growth
 - ▶ Competition between passivation and dissolution
- ❖ Time resolved electrochemical impedance spectroscopy (TREIS)
 - ▶ Track dynamics in impedance over time at different modulation frequencies
 - ▶ Allows reconstruction of electrical impedance spectra (Nyquist plots) as functions of time
 - Do not need special data processing/equipment
 - Allows reconstruction of surface reaction kinetics

Preliminary Results



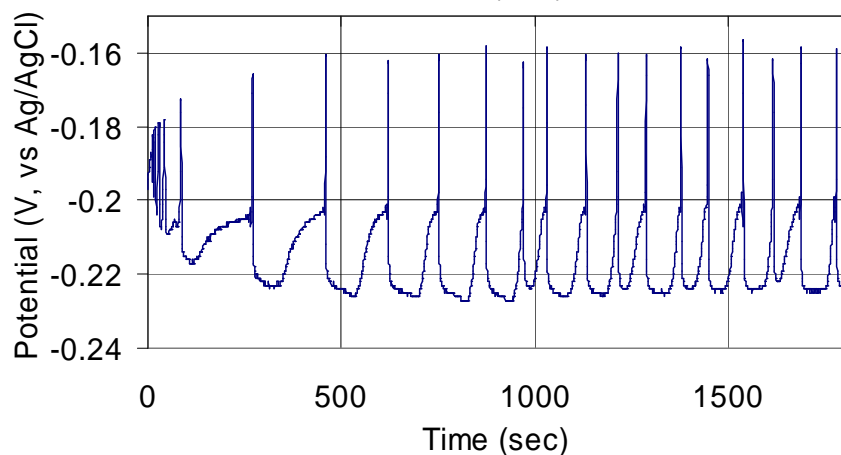
Reactions on Copper: E-Chem Oscillation

Observed electrochemical oscillation



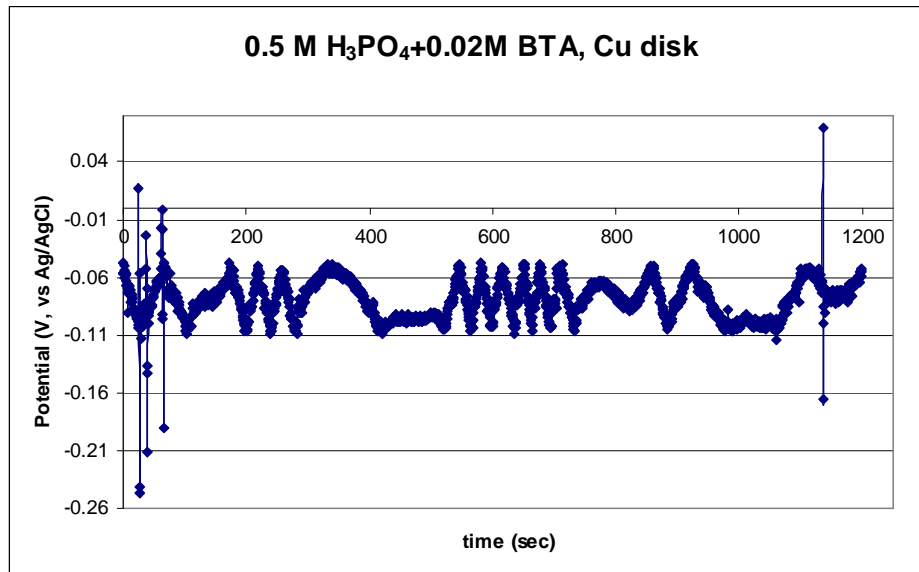
◀ Copper disk at 0 rpm

- Electrolyte
 - 2.25 M HCl
 - 0.43 M H₂O₂
- OCP (Open Circuit Potential) transient in time
- No applied potential



◀ Copper wire in stagnant slurry

Interpretation



- ❖ Rising potential
 - ▶ Net passivation
- ❖ Decreasing potential
 - ▶ Net dissolution
- ❖ Variables
 - ▶ Concentration
 - ▶ Temperature
 - ▶ System geometry
 - ▶ Mass transfer
 - ▶ Surface reaction rate

- ❖ OCP (Open Circuit Potential) oscillation due to
 - ▶ Balance of mass transfer to electrode surface, surface reaction
 - Geometry dependency
 - ▶ Local pH fluctuation due to surface reaction
 - ▶ Instability of the surface film
- ❖ Repetitive passivation and dissolution of Cu surface while the surface itself is being smoothed → possible **ECMP** application

Modeling E-Chem Oscillation

$$\frac{de}{dt} = \frac{v-e}{r} - m_1 k_1 u_1 - m_2 k_2 u_2$$

$$\frac{du_1}{dt} = -1.25d^{1/2} k_1 u_1 + 2d(w_1 - u_1)$$

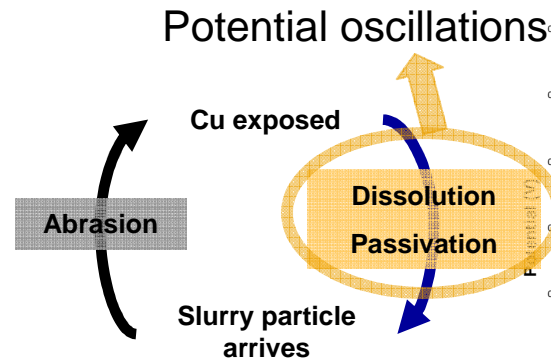
$$\frac{du_2}{dt} = 1.24d^{1/2} k_2 u_2 - 1.54d(w_2 - u_2)$$

$$\frac{dw_1}{dt} = 1.6d(2 - 3w_1 + u_1)$$

$$\frac{dw_2}{dt} = 0.386d(1 - 2w_2 + u_2)$$

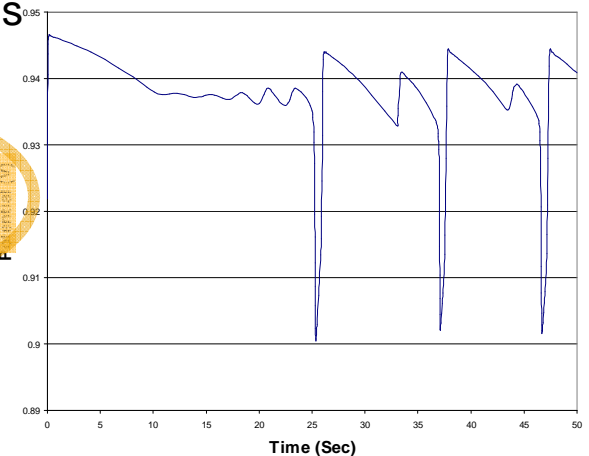
e: dimensionless electrode potential
 v: dimensionless applied potential
 u_i: dimensionless concentration in boundary layer 1 which contacts the electrode surface (H⁺(i=1), Cu²⁺(i=2))
 w_i: dimensionless concentration in layer 2 (H⁺(i=1), Cu²⁺(i=2))

k_i: dimensionless surface reaction constant (H⁺(i=1), Cu²⁺(i=2))
 r: dimensionless solution resistance
 d: dimensionless rotational speed
 m₁ and m₂: dimensionless numbers containing electrode surface area, Faraday number, capacitance, solution concentration, temperature

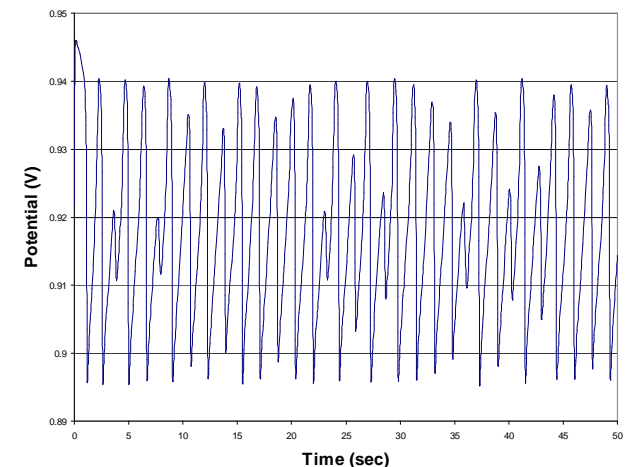


- Allows description of mass transfer and surface reaction effects in Cu CMP
- Following generalization and validation, may allow prediction of Cu reaction, dissolution, and passivation rates

Modified model proposed: Koper et al., *J. Chem. Phys.* **96(10)**, (1992)



Large (above) and small (below) diffusion coefficient



Conclusion

- ❖ Corrosion reaction on Cu surface
 - ▶ Corrosion rate dynamics obtained
 - ▶ BTA does not completely shut down the surface reaction
- ❖ Guillotine electrode: reaction on 'fresh' metal surface
 - ▶ Surface repassivation and dissolution can be monitored
 - Independent of any prior oxide film
 - ▶ TREIS can be achieved relatively easily compared to other methods
 - By equivalent circuit analysis, it is possible to describe the evolution of reactions in time
- ❖ Electrochemical oscillation
 - ▶ Continuous passivation and dissolution under various solution compositions observed
 - ▶ Can predict mass transfer and surface reaction effects in Cu CMP
 - ▶ Coupled with electrochemical polishing, has potential to be utilized in ECMP

Future Plans

- ❖ Further investigation of dissolution / repassivation kinetics
 - ▶ Surface film growth model
- ❖ TREIS
 - ▶ Full description of the dynamics in the surface reaction
- ❖ Refine electrochemical oscillation model
 - ▶ Complete study of mass transfer and reaction rates
- ❖ Industrial Collaboration and Technology Transfer
 - ▶ Multiple meetings with industry CMP council
 - Intel, Cabot, IBM

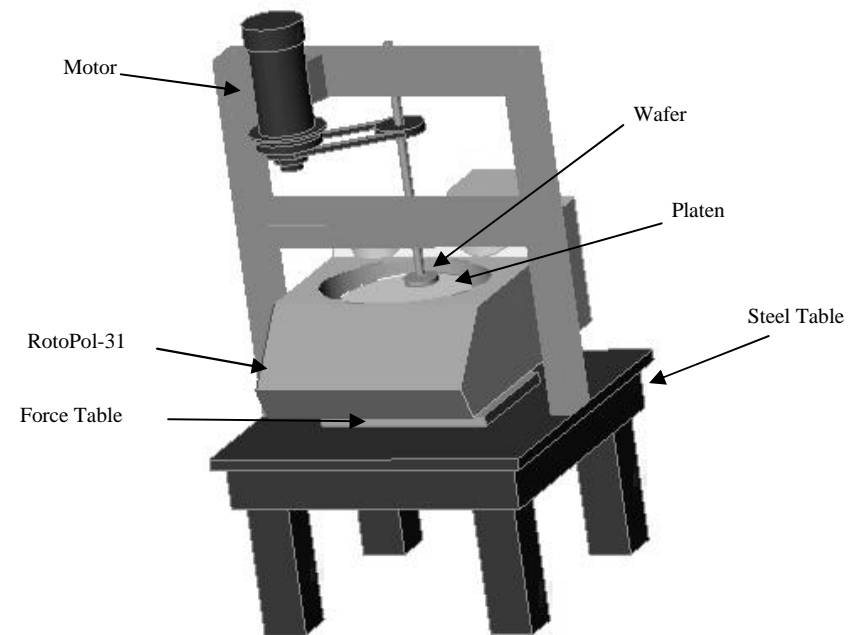
Detecting Pad-Wafer Contact in CMP using DELIF

Caprice Gray

ERC Task # 425.020

PI: C. B. Rogers, V. P. Manno,
and R. D. White

Tufts University
Department of Mechanical
Engineering



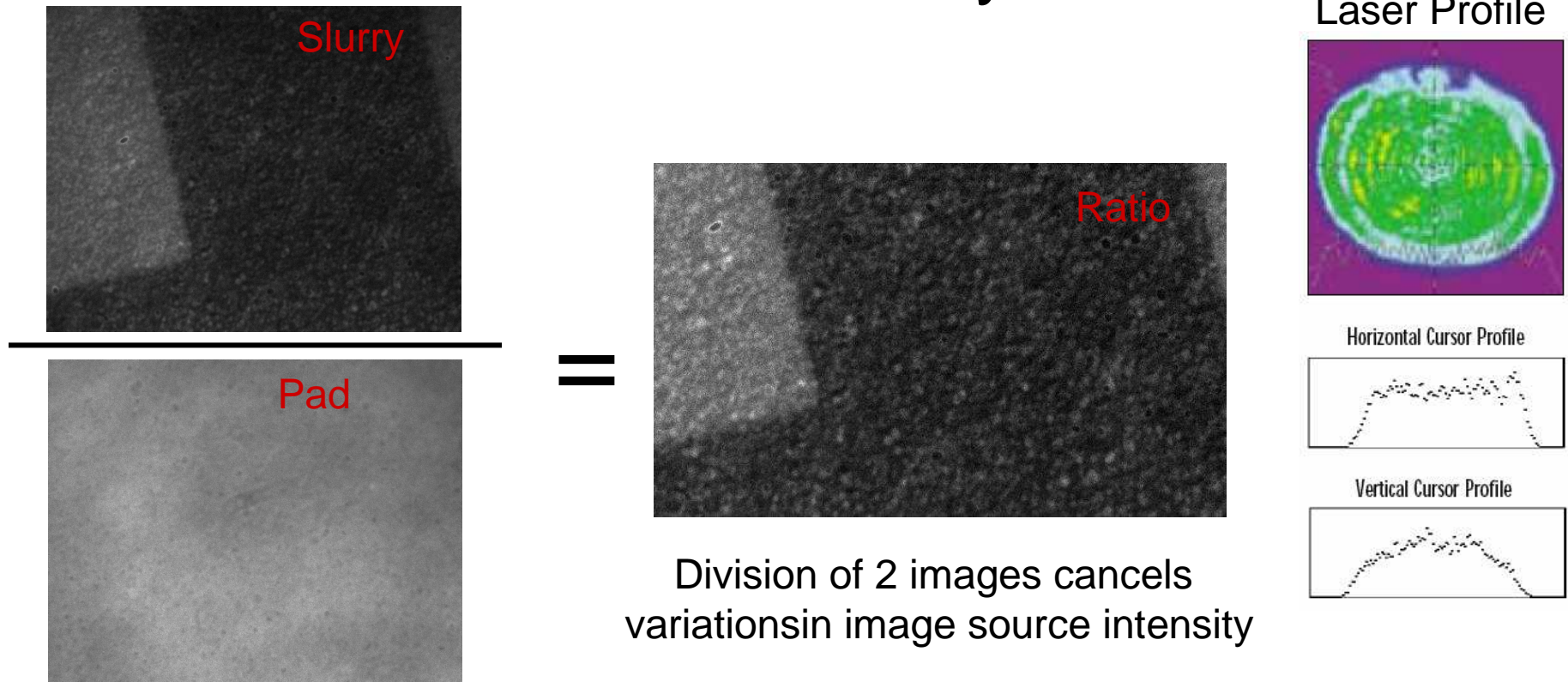
Project Objectives

- Use Dual Emission Laser Induced Fluorescence (DELIF) to attain in-situ images of the slurry layer during CMP
 - Images are instantaneous (6 ns time integration), taken at a rate of 2 images/sec
 - High spatial resolution ($>3 \mu\text{m}/\text{pixel}$) to resolve micron sized features
 - Hi slurry film dept resolution $\rightarrow \pm 0.1 \mu\text{m}$
- Detect in-situ pad-wafer contact
 - Pads (all polyurethane based): CMC D100, CMC D200, Fruedenburg FX9, IC1000
 - Process variables: applied wafer down force, pad-wafer relative velocity, slurry particle concentration, pad conditioning

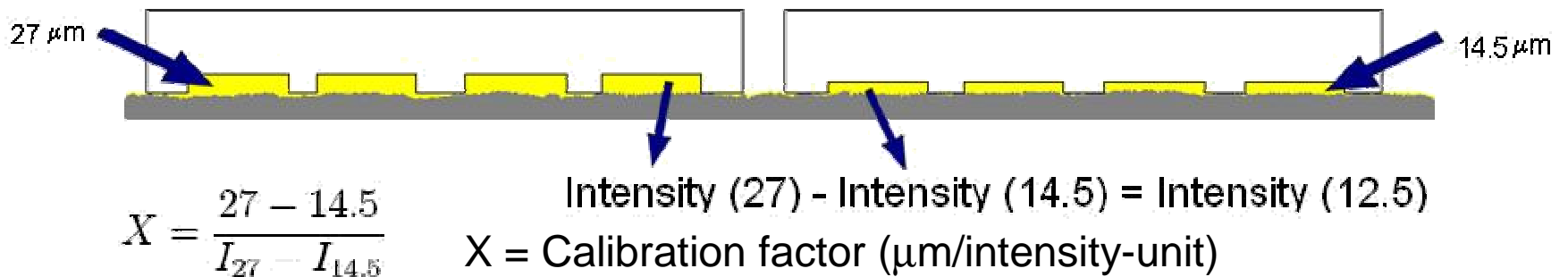
Environmental Safety and Health (ESH) Metrics and Impacts

<u>METRIC</u>		<u>IMPACT</u>
Energy Consumption During Process	→	Understanding wafer-pad interactions during polish leads to reduced time to polish and tool energy consumption
DI Water Consumption During Process	→	Optimized process parameters based on in-situ characterization of contact, and forces leads to reduced time to polish and slurry consumption
Process Chemical Consumption (Slurry Chemicals)		optimization

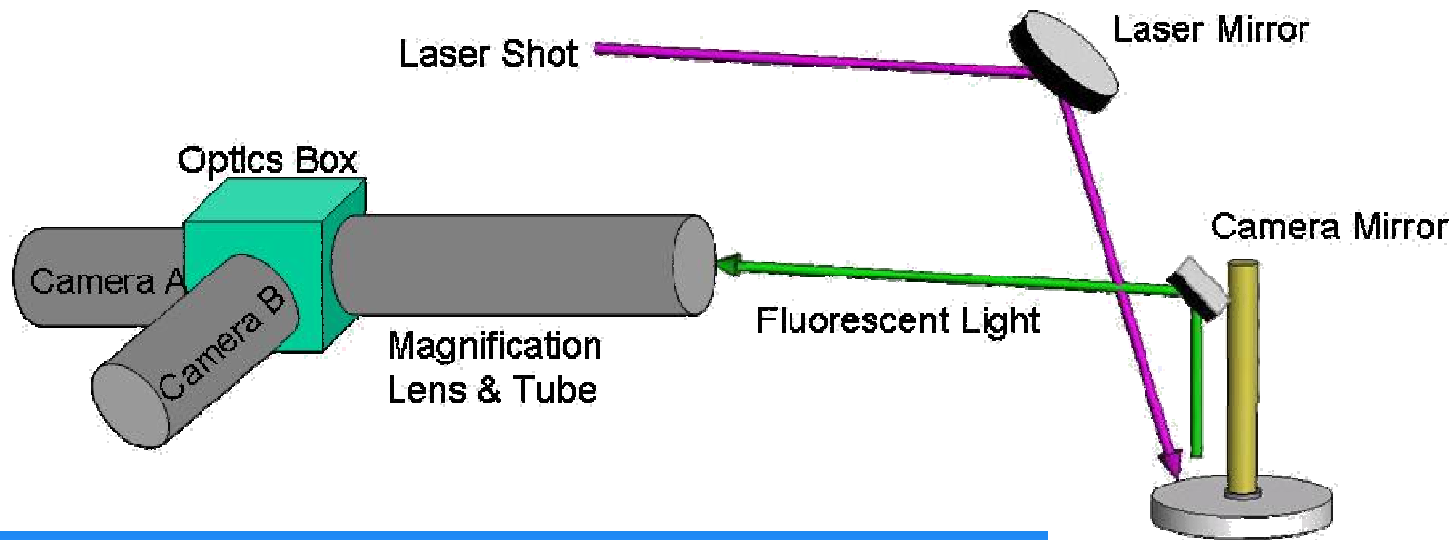
DELIF Theory



Linear calibration technique to correlate image intensity to fluid layer thickness

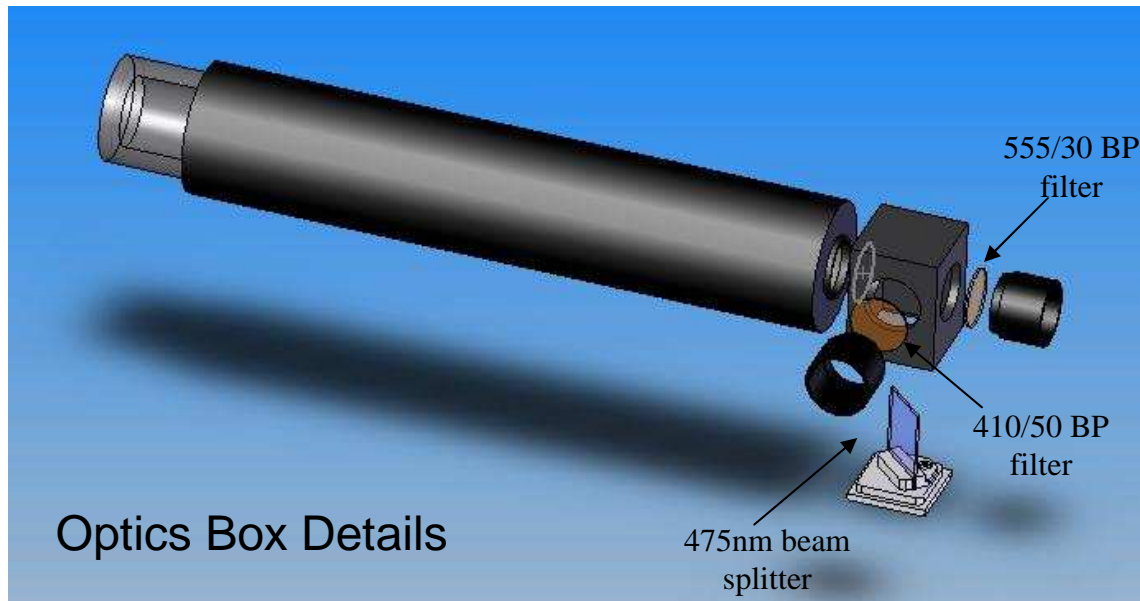


DELIF Data Acquisition



BK7 Optical
Glass Wafer

The laser light produces fluorescent light from the polyurethane polishing pad and the Calcein dye dissolved in the slurry.

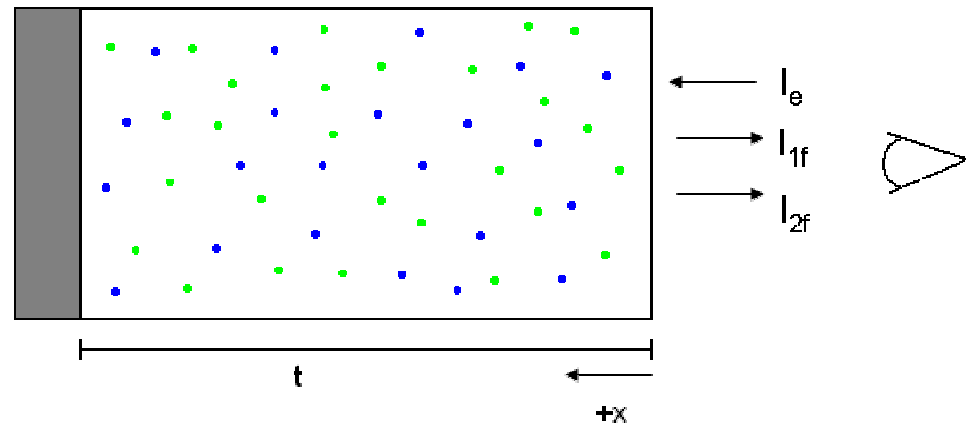


Optics Box Details

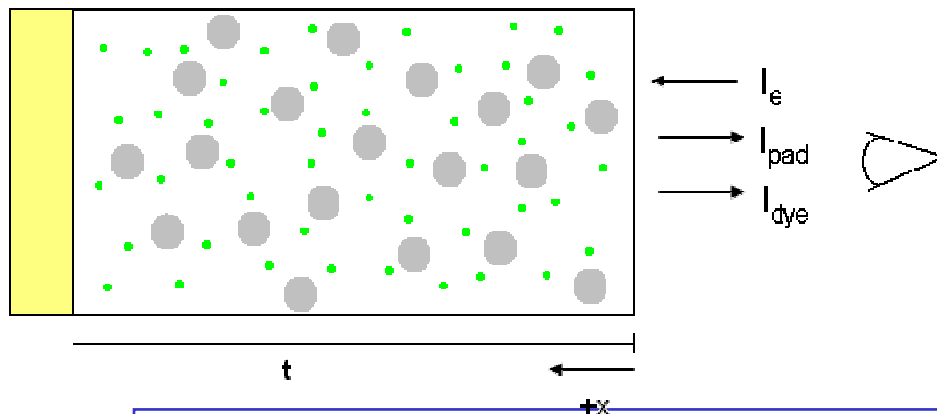
DELIF Modeling

- Goals
 - Examine how comparable our actual system is to existing DELIF models
 - Verify our linear calibration technique (Ratio Intensity \rightarrow Fluid layer thickness)

Existing Model Geometry



CMP Model Geometry



Existing Model Solution $\frac{I_{2f}}{I_{1f}} = At + B$

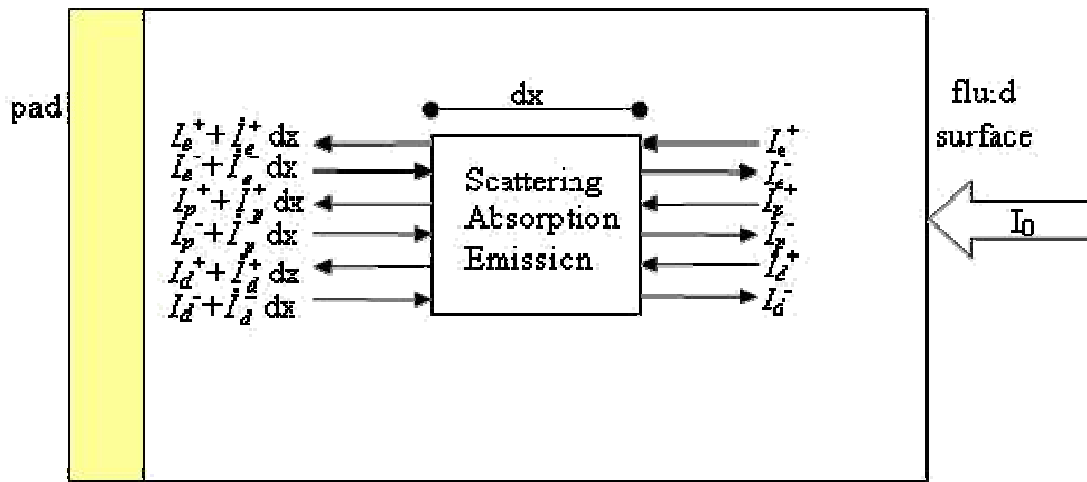
CMP DELIF Model

$$\begin{bmatrix} \dot{I}_e^+ \\ \dot{I}_e^- \\ \dot{I}_p^+ \\ \dot{I}_p^- \\ \dot{I}_d^+ \\ \dot{I}_d^- \end{bmatrix} = \begin{bmatrix} -k_1 & \mu_b C_{Si} & 0 & 0 & 0 & 0 \\ -\mu_b C_{Si} & k_1 & 0 & 0 & 0 & 0 \\ 0 & 0 & -k_2 & \mu_b C_{Si} & 0 & 0 \\ 0 & 0 & -\mu_b C_{Si} & k_2 & 0 & 0 \\ k_4(\lambda_l) & k_4(\lambda_l) & k_4(\lambda_p) & k_4(\lambda_p) & -k_3 & \mu_b C_{Si} \\ -k_4(\lambda_l) & -k_4(\lambda_l) & -k_4(\lambda_p) & -k_4(\lambda_p) & -\mu_b C_{Si} & k_3 \end{bmatrix} \cdot \begin{bmatrix} I_e^+ \\ I_e^- \\ I_p^+ \\ I_p^- \\ I_d^+ \\ I_d^- \end{bmatrix}$$

$$\begin{aligned} k_1 &= (\epsilon_{Si}(\lambda_l) C_{Si} + \mu_f C_{Si} + \epsilon_d(\lambda_l) C_d) \\ k_2 &= (\epsilon_{Si}(\lambda_p) C_{Si} + \mu_f C_{Si} + \epsilon_d(\lambda_p) C_d) \\ k_3 &= (\epsilon_{Si}(\lambda_d) + \mu_f C_{Si}) \\ k_4(\lambda) &= \frac{\phi_d}{2} \eta_d(\lambda) C_d \epsilon_d(\lambda) \end{aligned}$$

Variables

- k_1, k_2, k_3 = extinction coefficients
- k_4 = emission coefficient
- C_{Si} = slurry particle concentration
- μ_b = effective back scattering
- λ = wavelength
- I_e = excitation intensity
- I_p = pad fluorescence intensity
- I_d = dye (slurry) fluorescence



Simplified Model Results

$$\begin{bmatrix} \dot{I}_e^+ \\ \dot{I}_p^- \\ \dot{I}_d^+ \\ \dot{I}_d^- \end{bmatrix} = \begin{bmatrix} -k_1 & 0 & 0 & 0 \\ 0 & k_2 & 0 & 0 \\ k_4(\lambda_l) & k_4(\lambda_p) & 0 & 0 \\ -k_4(\lambda_l) & -k_4(\lambda_p) & 0 & 0 \end{bmatrix} \cdot \begin{bmatrix} I_e^+ \\ I_p^- \\ I_d^+ \\ I_d^- \end{bmatrix} \quad \begin{aligned} k_1 &= \varepsilon_d(\lambda_l)C_d \\ k_2 &= \varepsilon_d(\lambda_p)C_d \\ k_4(\lambda) &= \frac{\phi_d}{2}\eta_d(\lambda)C_d\varepsilon_d(\lambda) \end{aligned}$$

Boundary Conditions

Simplification Assumptions:

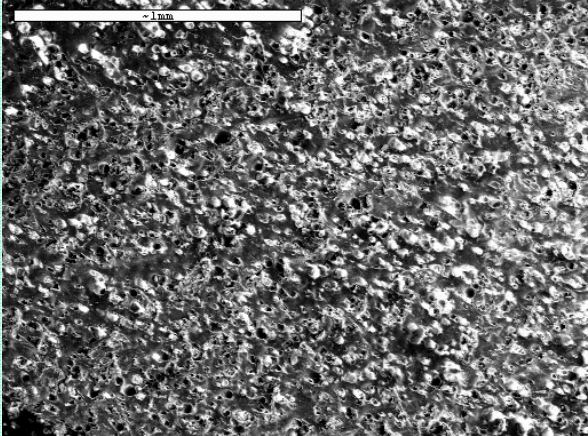
1. No scattering particles
2. All excitation light is absorbed and no excitation light is reflected

1. $I_e^+(0) = I_0$
2. $I_p^-(L) = I_e^+(L)\alpha(\lambda_l)\phi_p\eta_p(\lambda_p)$
3. $I_d^+(0) = 0$
4. $I_d^-(L) = I_d^+(L)$ for 100% reflection of $I_d^+(x)$

Solution:

$$R_{pad} = \frac{I_d^-, pad}{I_p^-} = \left(1 + \frac{1}{\alpha(\lambda_l)\phi_p\eta_p(\lambda_p)}\right) 2k_4L \longrightarrow \text{LINEAR Calibration}$$


Image Quality Benchmarking



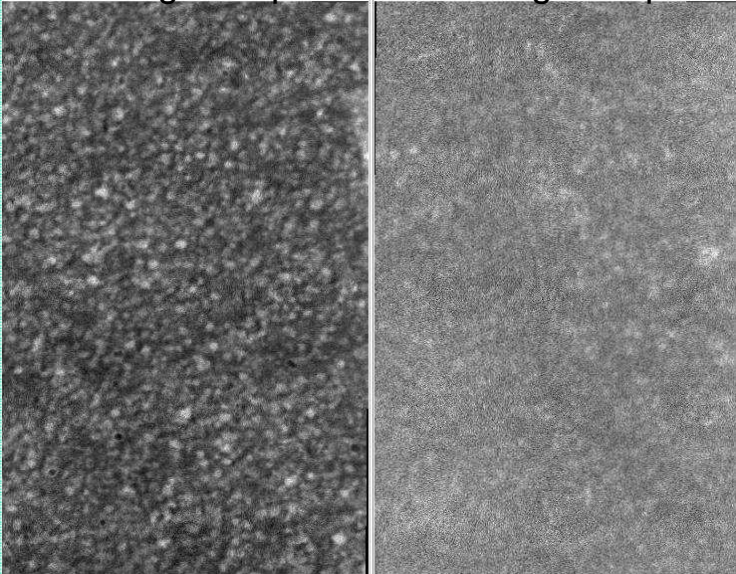
SEM

NO Z
RESOLUTION

Optical Microscope



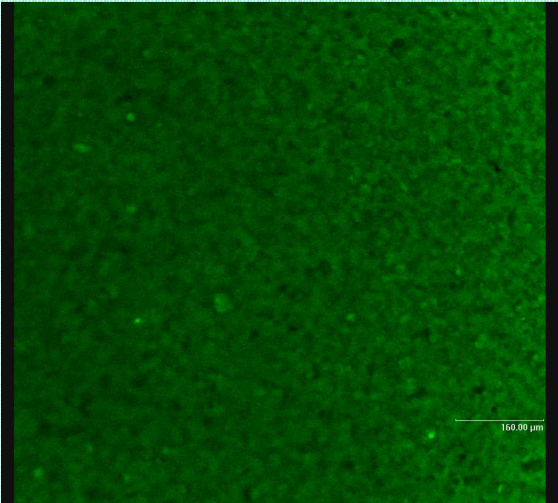
Well aligned optics Poor aligned optics



DELIF

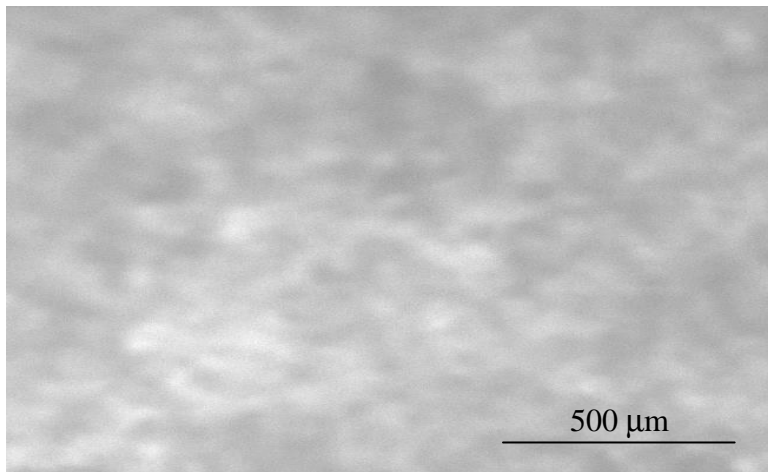
GOOD Z
RESOLUTION

Confocal
Microscope

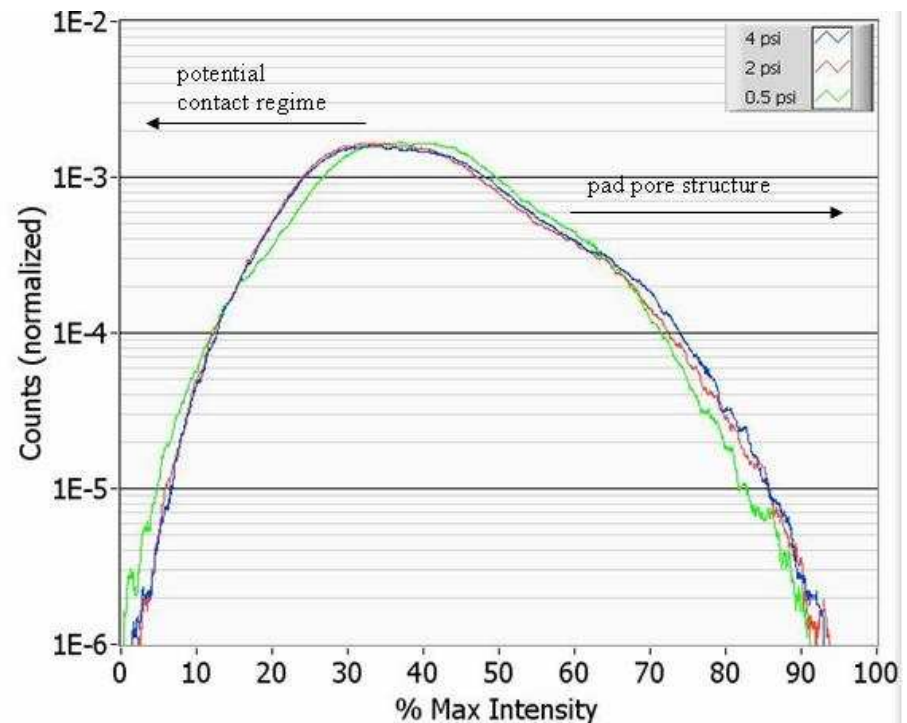


DELIF for Contact

- 360,000+ pixels \rightarrow 2% \sim 7200 pixels
- 50 $\mu\text{m}^2 \sim$ 7-8 pixels (6.7 $\mu\text{m}^2/\text{pixel}$)
 - Focus must be really good
 - We are at the resolution limit for our system
- At this resolution, we are seeing contact region intensity smoothing



Data for static DELIF on CMC D100



Industrial Collaboration/Technology Transfer

- Close collaboration with industry partners – Cabot
Microelectronics and Intel
 - Monthly telecons – secure website for information exchange
 - Semi-annual face-to-face meetings
 - Thesis committees and joint publication authorship
 - Metrology and analysis methodology technology transfer
 - In-kind support – specialized supplies and equipment
 - Student internships (e.g. C. Gray at Intel during Summer 2005)
 - Close coordination with A. Philipossian research group at U of Arizona
- Information and results exchange with MIT (D. Boning)
ERC project
 - Monthly joint meetings of PIs and research students
 - Discussion of findings with other colleagues (e.g. E. Paul – Stockton College on leave at MIT)

Future Work and Conclusions

- Future Work
 - Calculate results of full CMP DELIF model including slurry particle scattering effects
 - Determine pad to pad DELIF variations
 - Choose a slurry for optimal DELIF and polishing
 - Observe pad-wafer contact on various polishing pads and differing CMP run parameters (down-force, pad-wafer speed, etc.)
- Conclusions
 - We had developed an optical model that helps us understand calibration of image intensity to fluid layer thickness.
 - We have made optical system improvements to optimize detection of pad-wafer contact.
 - We have begun to benchmark DELIF method by making pad surface measurements using other techniques
 - We have established a data processing method for detecting pad-wafer contact.

Process Optimization and Modeling of Copper CMP

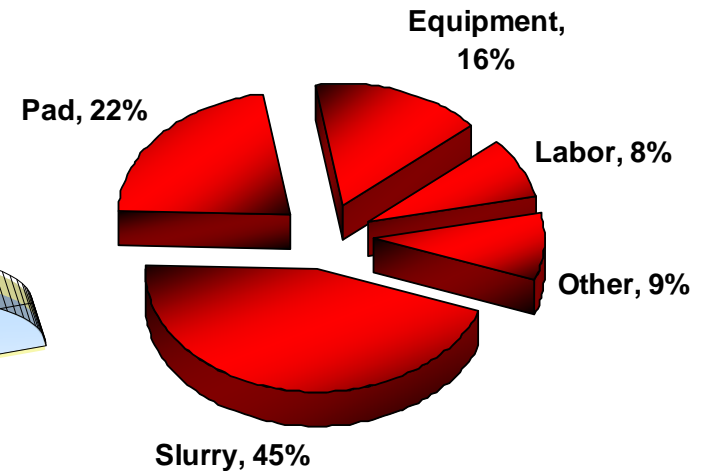
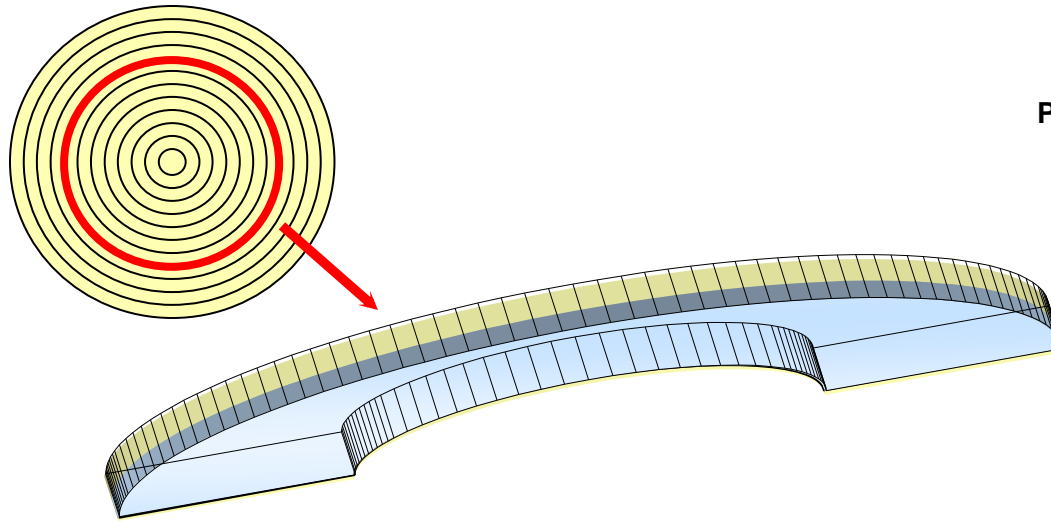
**¹ D. Rosales-Yeomans, ¹ D. DeNardis, ² L. Borucki
and ^{1,2} A. Philipossian**

SRC #425.020

¹ The University of Arizona, Tucson AZ USA

² Araca Incorporated, Tucson AZ USA

Objective and ESH Impact



Stavreva et al., 1997

Pad grooves affect chemical and mechanical mechanisms during CMP:

- **Net flow under the wafer**
- **Process temperature**
- **Reactants and polish debris concentrations**
- **Slurry film thickness under the wafer**
- **Shear force**
- **Pad compressibility**
- **Pad-wafer contact area**

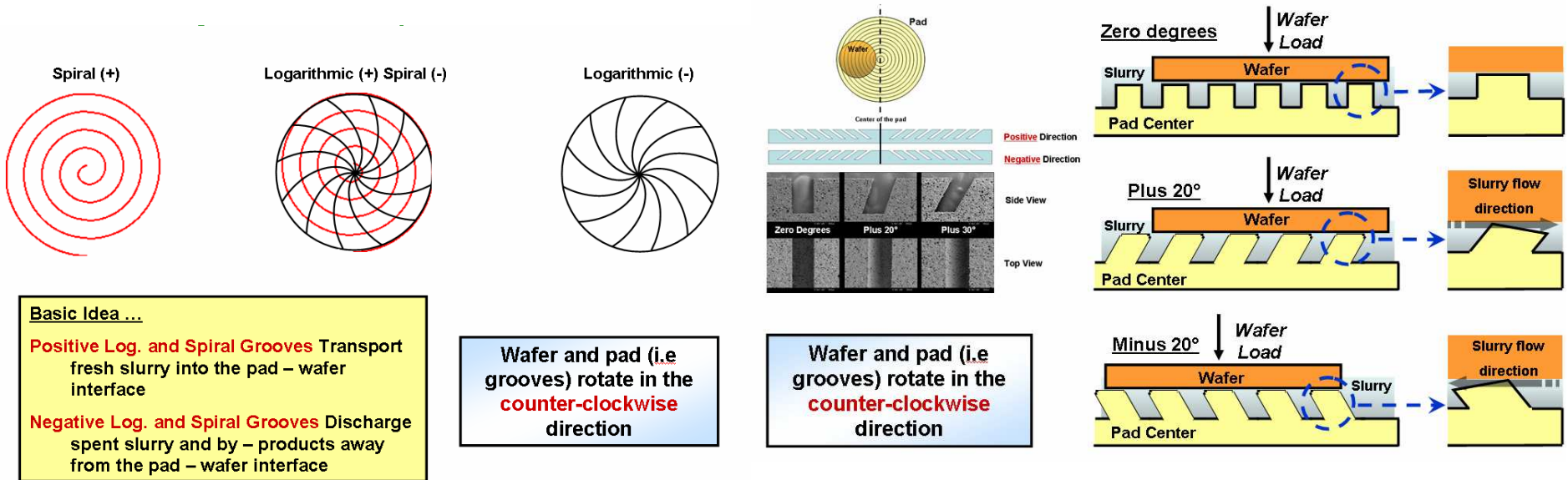
Chemical

Mechanical

Objective: Analyze the effect of novel groove patterns on the kinetic, thermal and tribological attributes of copper CMP in an effort to reduce slurry and pad consumption

Novel Grooves – Groups 1 & 2

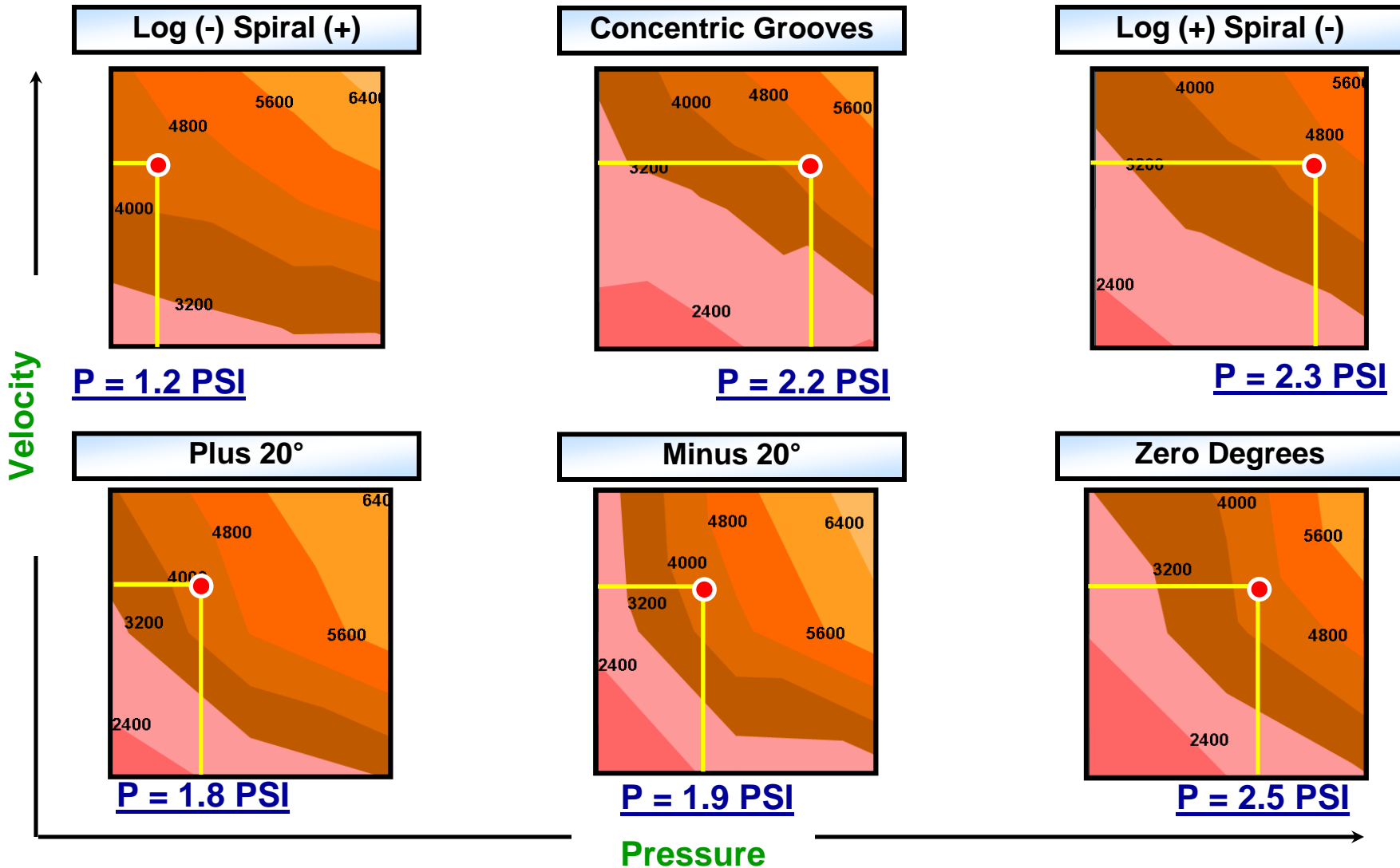
Logarithmic and Spiral (left) and Concentric Slanted (right) Grooves



Experimental Conditions

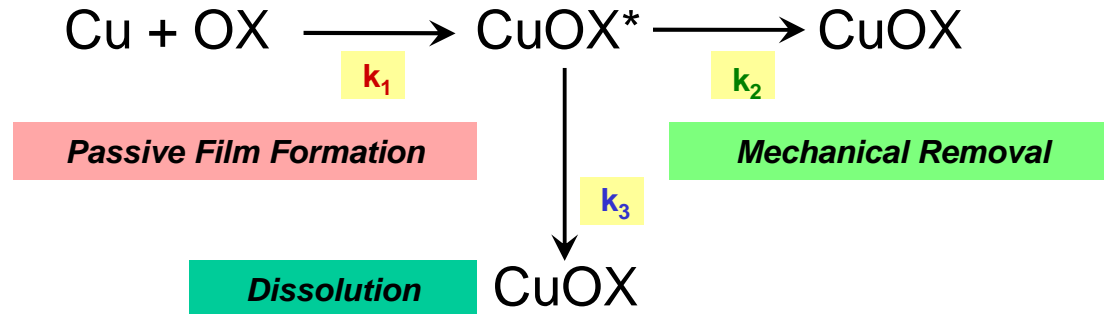
- **Constants:**
 - **Conditioning**
 - 100 grit diamond disc (TBW)
 - 30 min with UPW at 30 rpm disc speed and 20 per min sweep frequency
 - **Break-in**
 - 5 dummy Discs (Cu) with Fujimi PL-7102
 - **Slurry**
 - Fujimi PL-7102
 - 220 cc per minute
 - **Wafers**
 - 200-mm Cu wafers
- **Variables:**
 - **Relative pad-wafer velocity (m/s)**
 - 0.30
 - 0.75
 - 1.20
 - **Wafer pressure (PSI)**
 - 1.0 (6894 Pa)
 - 1.5 (10300 Pa)
 - 2.0 (13780 Pa)
 - 2.5 (17200 Pa)
 - **Pad groove design**
 - Concentric
 - Logarithmic Spiral
- **Variables:**
 - **Relative pad-wafer velocity (m/s)**
 - 0.30
 - 0.75
 - 1.20
 - **Wafer pressure (PSI)**
 - 1.0 (6894 Pa)
 - 2.0 (13780 Pa)
 - 3.0 (20,684 Pa)
 - **Pad groove design**
 - Concentric
 - Concentric Slanted

Decoupling the Effect of P and V on RR



At a given RR, several novel grooves are less dependent on P (at constant V). This is an advantage in polishing ULK materials where low pressures are required. In addition to increase pad life by reducing the applied pressure

3 – Step Model for Cu Removal



$$k_1 = \frac{\rho_{ox}}{Mw_{ox}} (N\Omega f) \exp\left(\frac{-W}{kT_w}\right) \exp\left(\frac{qa}{2kT_w x} V\right)$$

$$k_2 = c_p \cdot \mu_k \cdot (p \cdot V)$$

$$k_3 = \frac{-A \cdot \exp\left(-\frac{E_a}{R \cdot T_w}\right)}{(x_C - X)}$$

$$\Delta \bar{T}_f = \frac{\beta}{V^{1/2+e}} \cdot \mu_k \cdot (p \cdot V)$$

Real-time measurements can be used to predict RR

3 Fitting parameter

k_1 is characterized based on cation migration

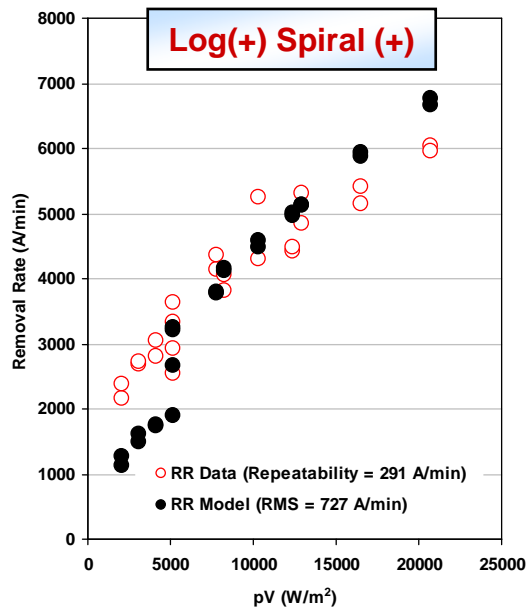
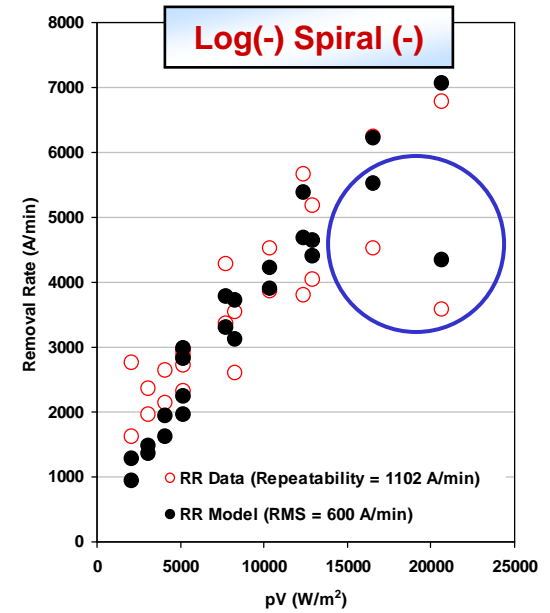
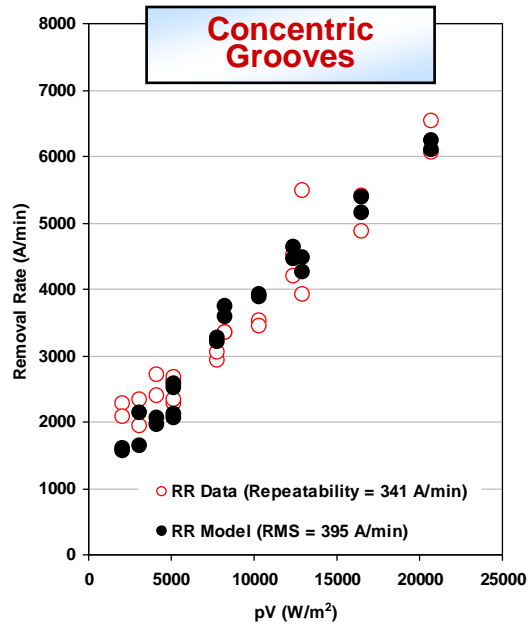
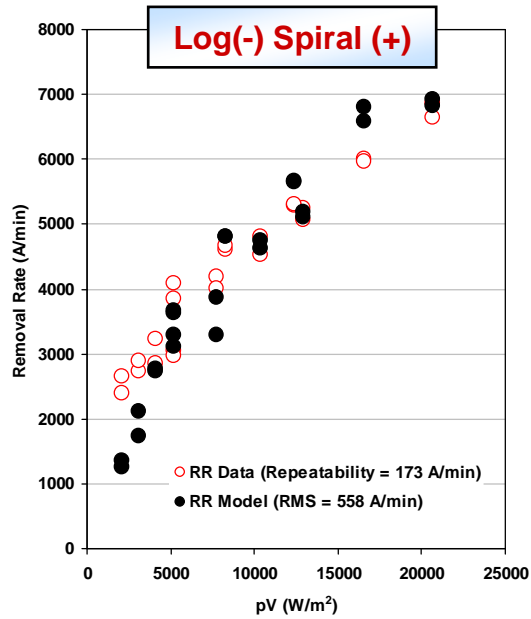
Applicable at $p \cdot V = 0$ due to the addition of a dissolution step (k_3)

k_3 is characterized based on diffusion of complexant through by-product film

Dissolution rate (k_3) was found to be **negligible** for our system (**type of slurry, pressure and velocity conditions**)

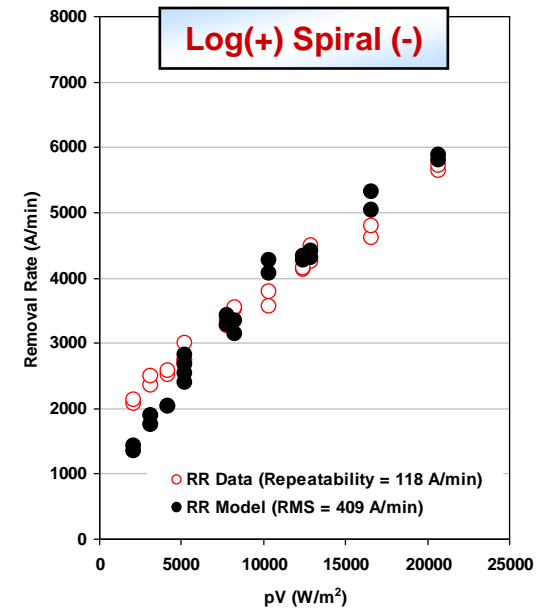
However it becomes more important as **pressure x velocity** approaches zero

3 – Step Model RR

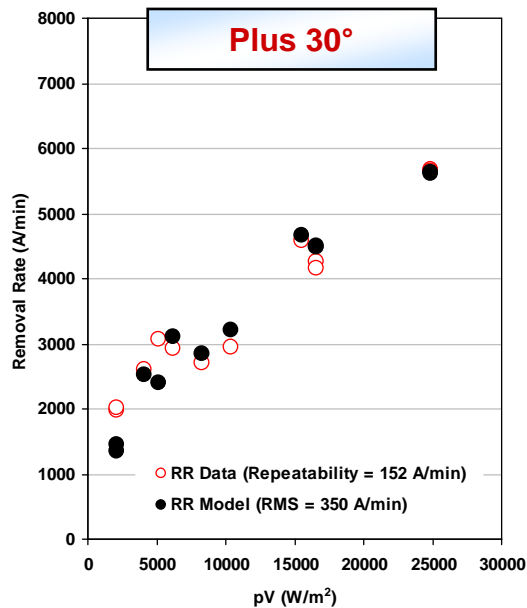
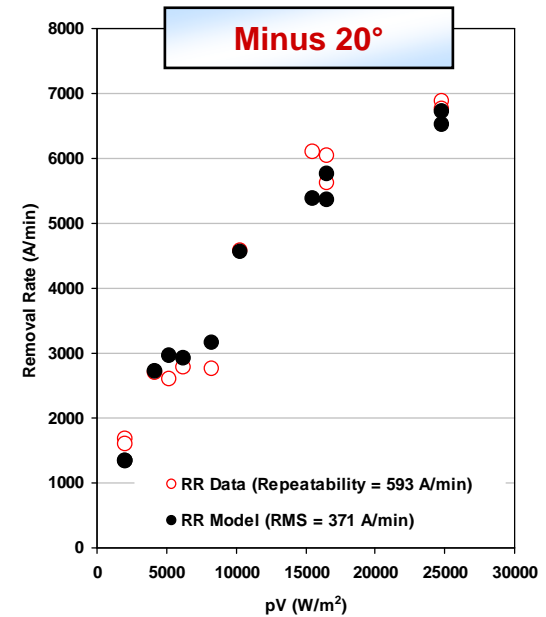
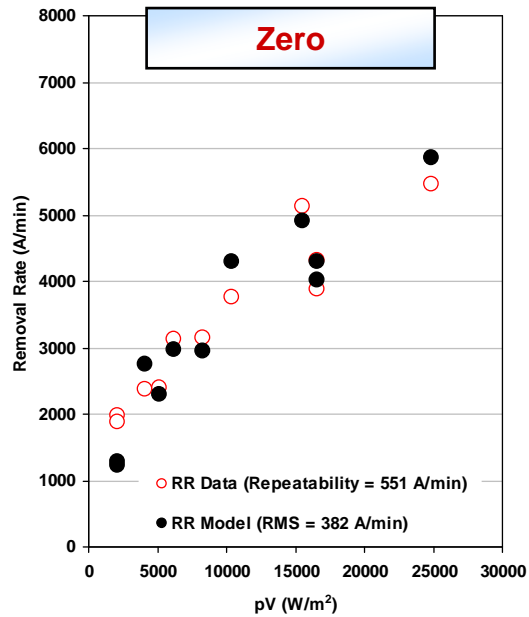
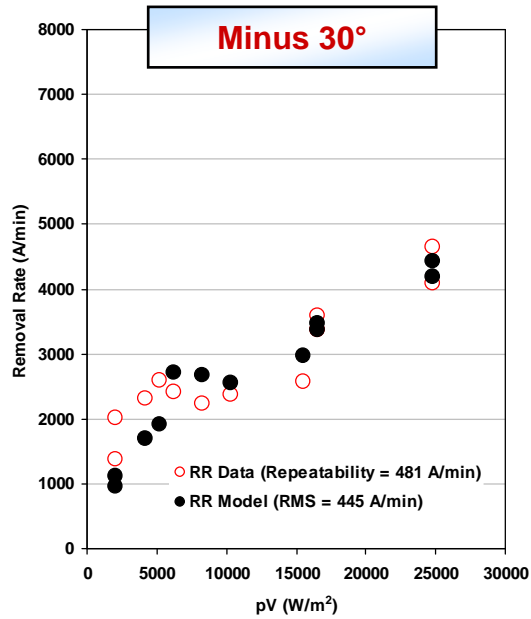


Experimental Repeatability range
120 – 1100 Å/min

Model RMS range
400 – 730 Å/min

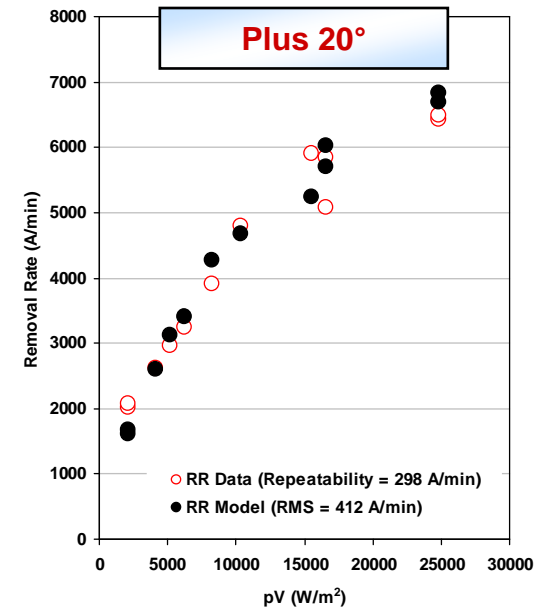


3 – Step Model RR

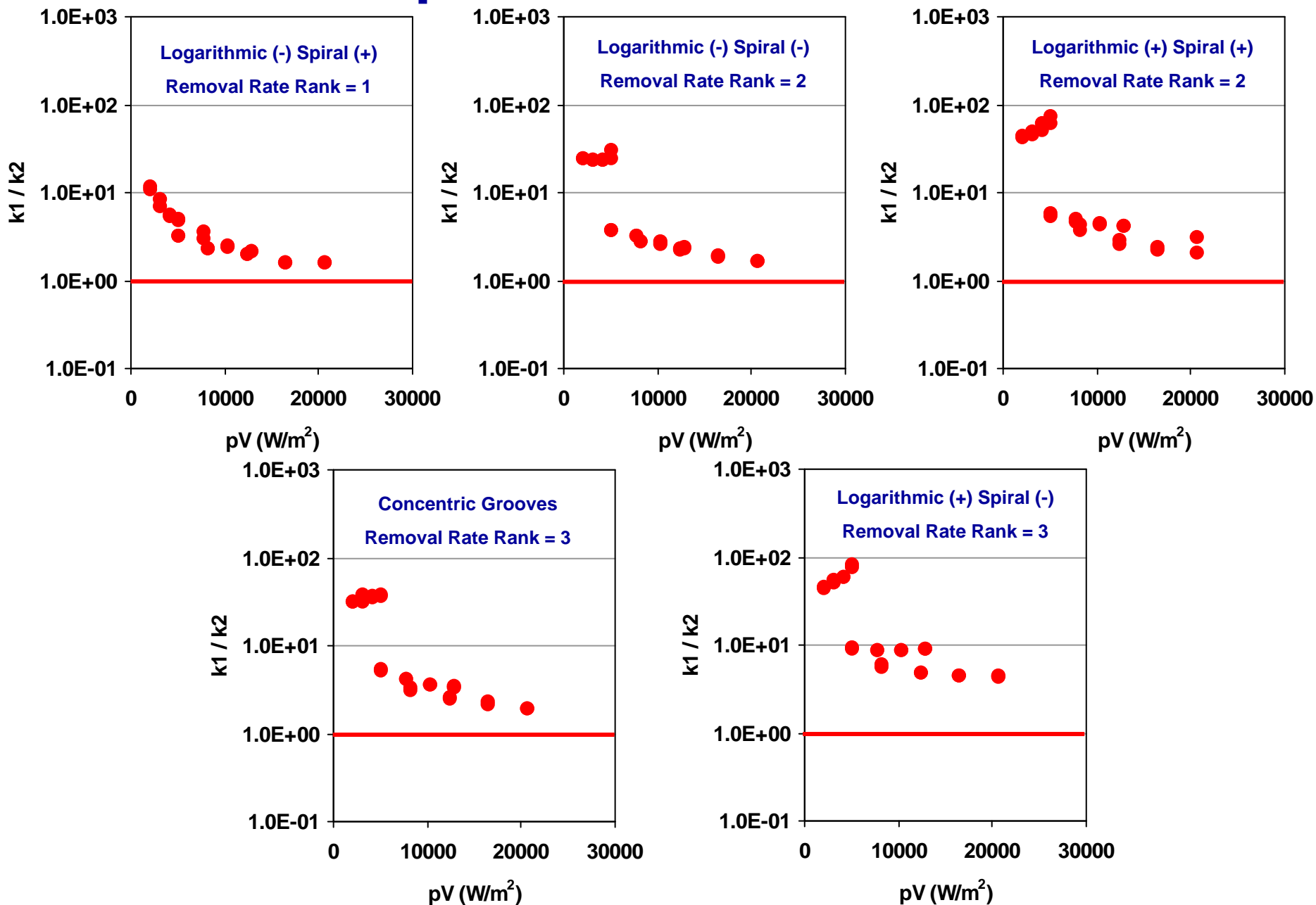


**Experimental
Repeatability range
150 – 590 Å/min**

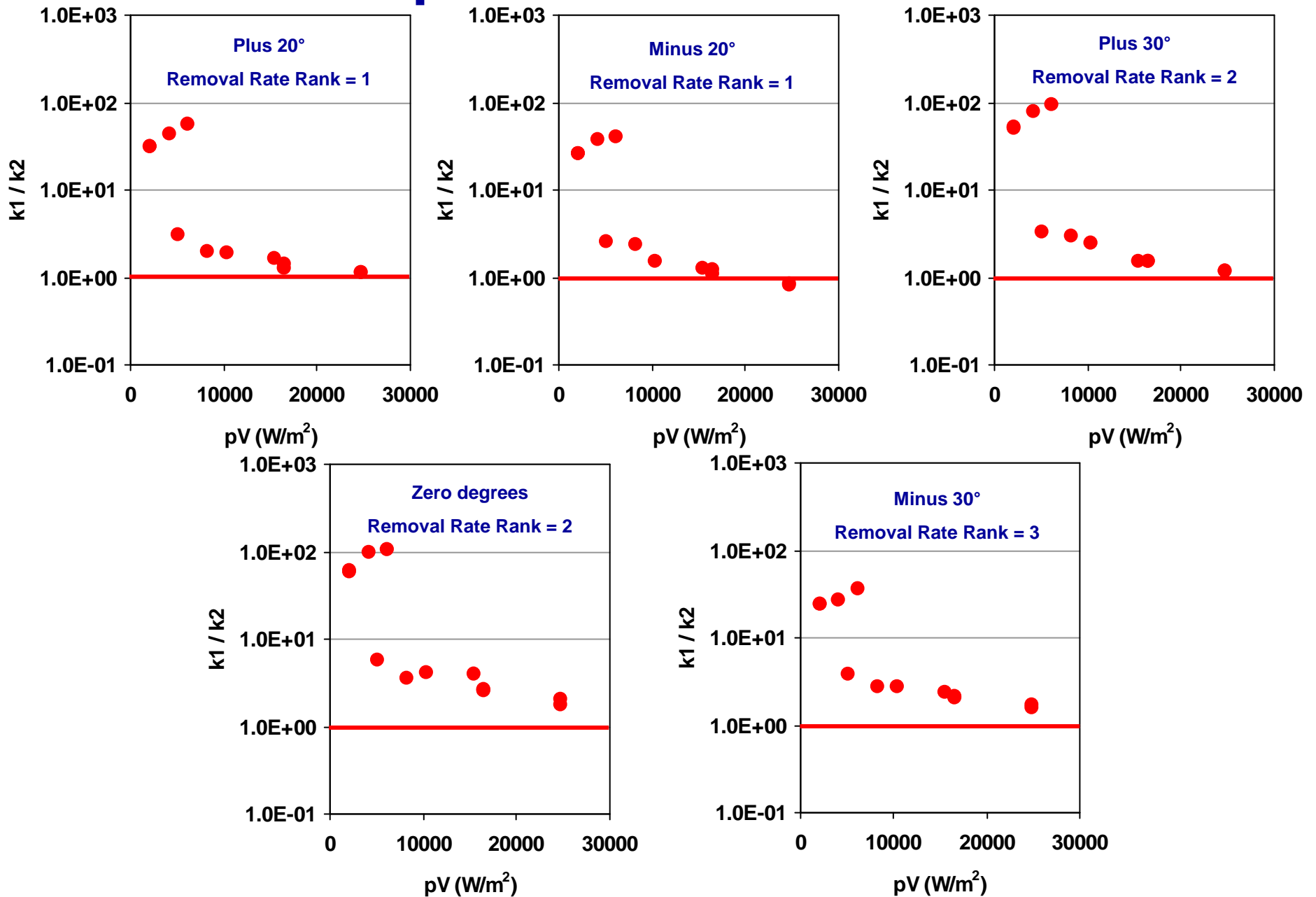
**Model RMS range
350 – 445 Å/min**



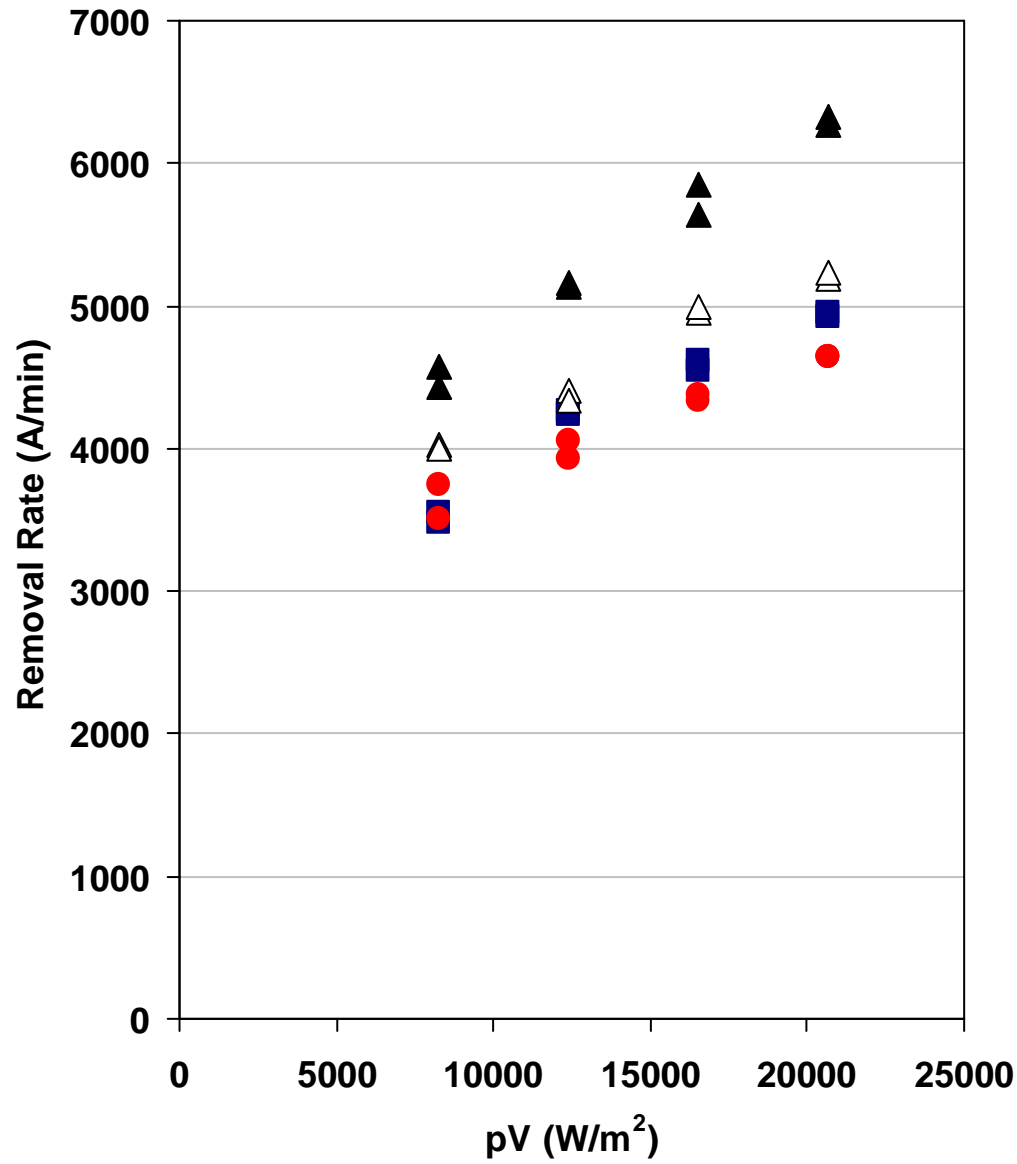
3 – Step Model Rate Constants



3 – Step Model Rate Constants



EHS Impact of Novel Groove Designs



- ▲ Log(-) Spiral(+) 110 cc/min (50% Reduction)
- △ Concentric grooves 110 cc/min (50% Reduction)
- Concentric grooves 165 cc/min (25% Reduction)
- Concentric grooves 220 cc/min

Preliminary results show significant reduction in slurry consumption

Removal rate increases slightly as slurry flow rate is decreased for the pad with concentric grooves

However, the Log(-) Spiral(+) pad results in much higher rates when slurry flow is reduced by 50%

Conclusions and Future Plans

Conclusions:

- Novel grooves allow for **higher removal rates at progressively smaller scales**
- Certain designs can **positively affect COO and EHS via decreasing pad and slurry consumption during copper CMP**
- The 3 – Step model predicts RR well for different types of pads used in copper CMP. **The RMS falls in the range of 350 - 700 A/min whereas the repeatability range is 120 - 1200 A/min for all cases**
- Relative values of k_1 and k_2 as a function of pV show that **the process is more limited by film removal through mechanical abrasion, especially at low pV . However, as pV increases this limitation is reduced and there is a transition to a more balanced process**
- k_1/k_2 seems to indicate that as pV increases, the faster each pad type approaches a **balance between film growth and film removal, the higher the removal rate for that particular pad**

Future Plans:

- Perform rigorous analysis and modeling of the effect of groove design (i.e. Logarithmic-Spiral) under reduced slurry flow rates
- Perform Dual Emission UV Enhanced Fluorescence (DEUVEF) analysis to visualize and evaluate the effect of pads with slanted groove patterns on slurry flow
- Expand the 3 – Step copper removal model by characterizing the dependence of copper oxide film growth on sliding velocity and conditioning process

Experimental Investigation and Numerical Simulation of Pad Stain Formation during Copper CMP

SRC: 425.020

H. Lee, ^{1,2} Y. Zhuang, ² L. Borucki, ³ S. Joh, ³ F. O' Moore, and ^{1,2} A. Philipossian

¹ The University of Arizona, Tucson AZ USA

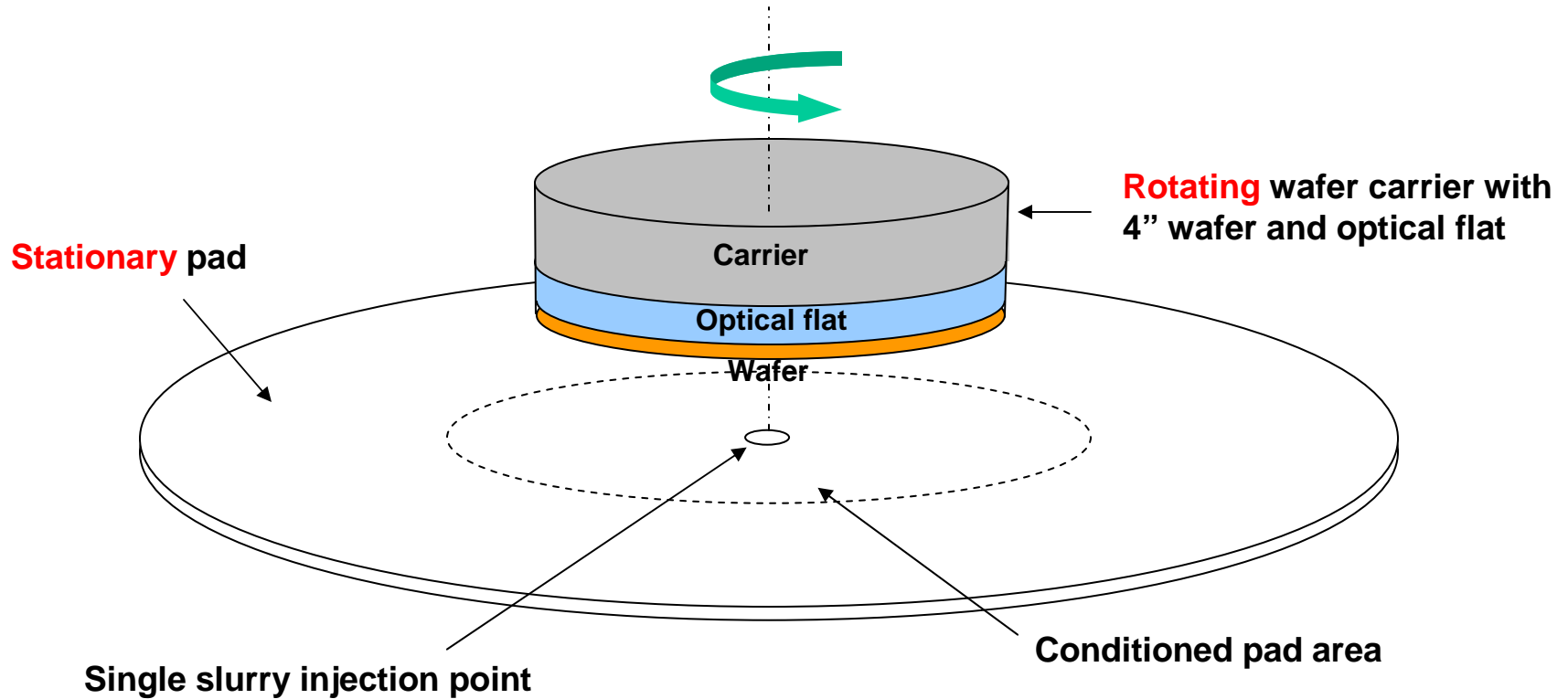
² Araca Incorporated, Tucson AZ USA

³ Novellus Systems, San Jose CA USA

Objectives and EHS Impact

- **Stain is often generated on pad surface due to polishing by-product buildup during copper CMP processing.**
- **Investigate the effects of process parameters on the by-product build up and on polishing performance.**
- **Develop a 3D fluid transport model for fluid flow and couple it with a model for transport and consumption of reactant and for production and deposition of byproducts to predict pad staining and compare with experimental results.**

Axisymmetric Polishing System

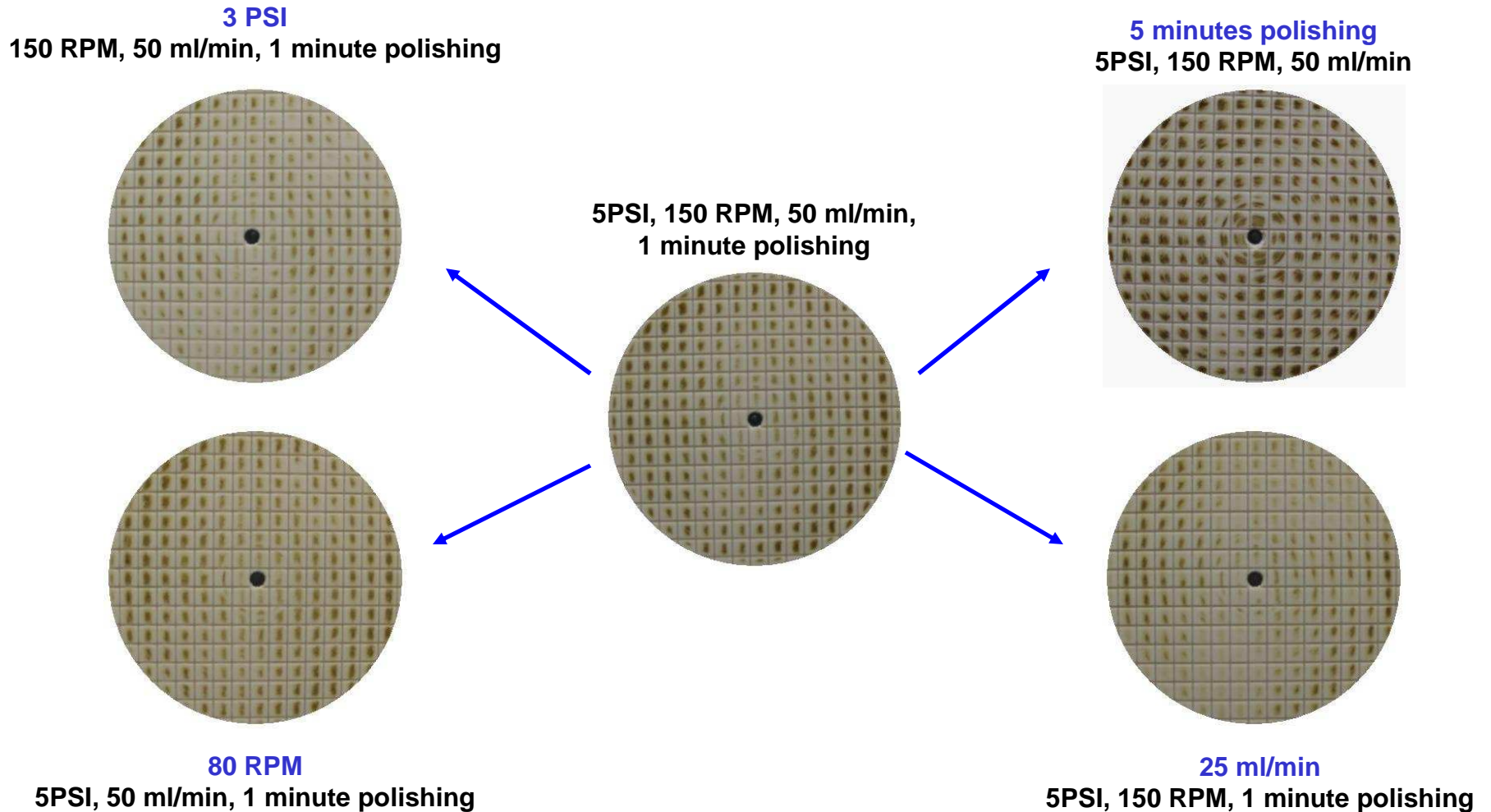


Stain Advection

The generated pad stain on each land area was darker following the direction of wafer rotation, suggesting the stain was affected by slurry advection.



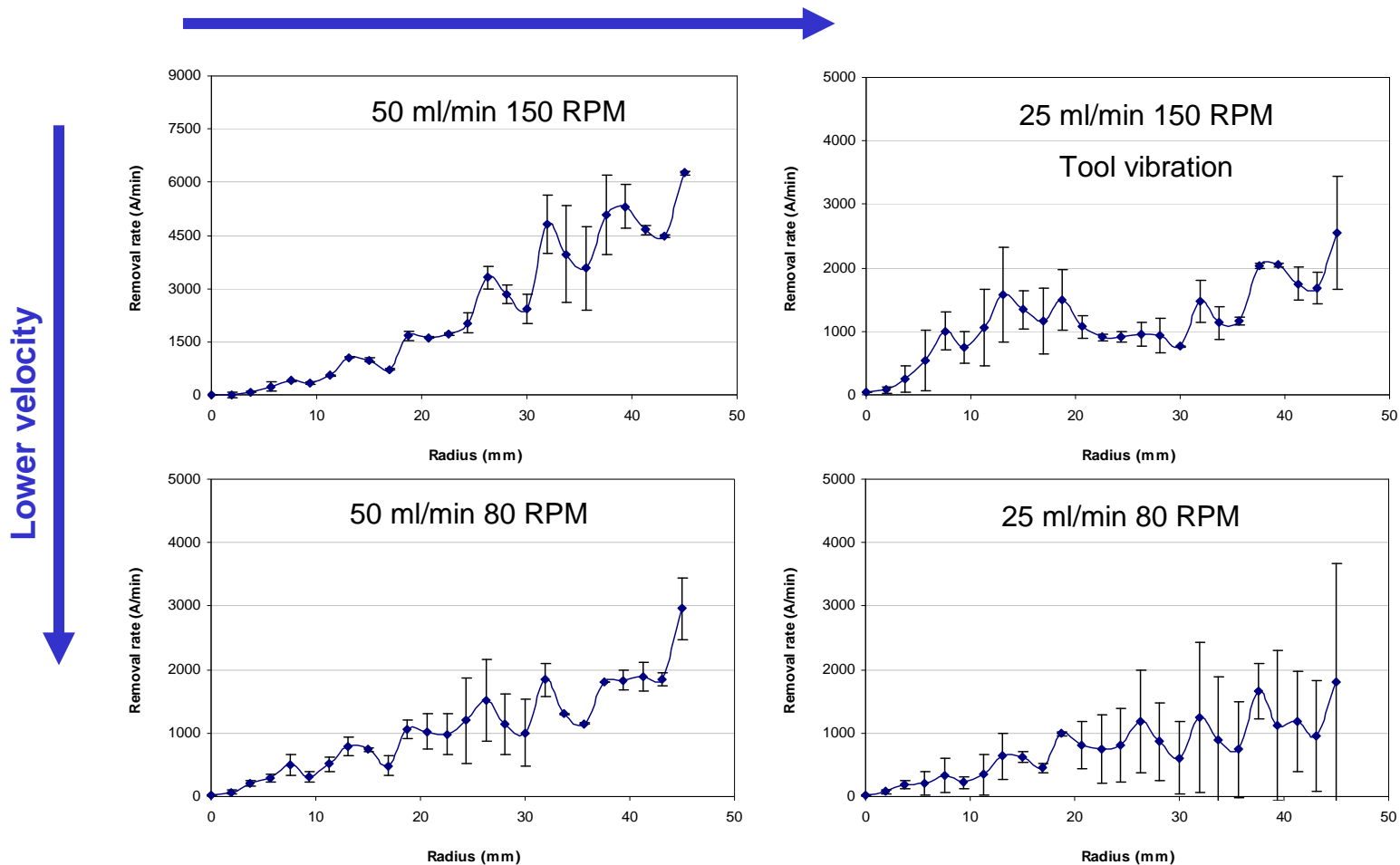
Effect of Polishing Kinematics on Staining



Staining became darker with increasing polishing pressure, wafer rotation rate, slurry flow rate and polishing time.

Copper Removal Rate Profile

Lower flow rate

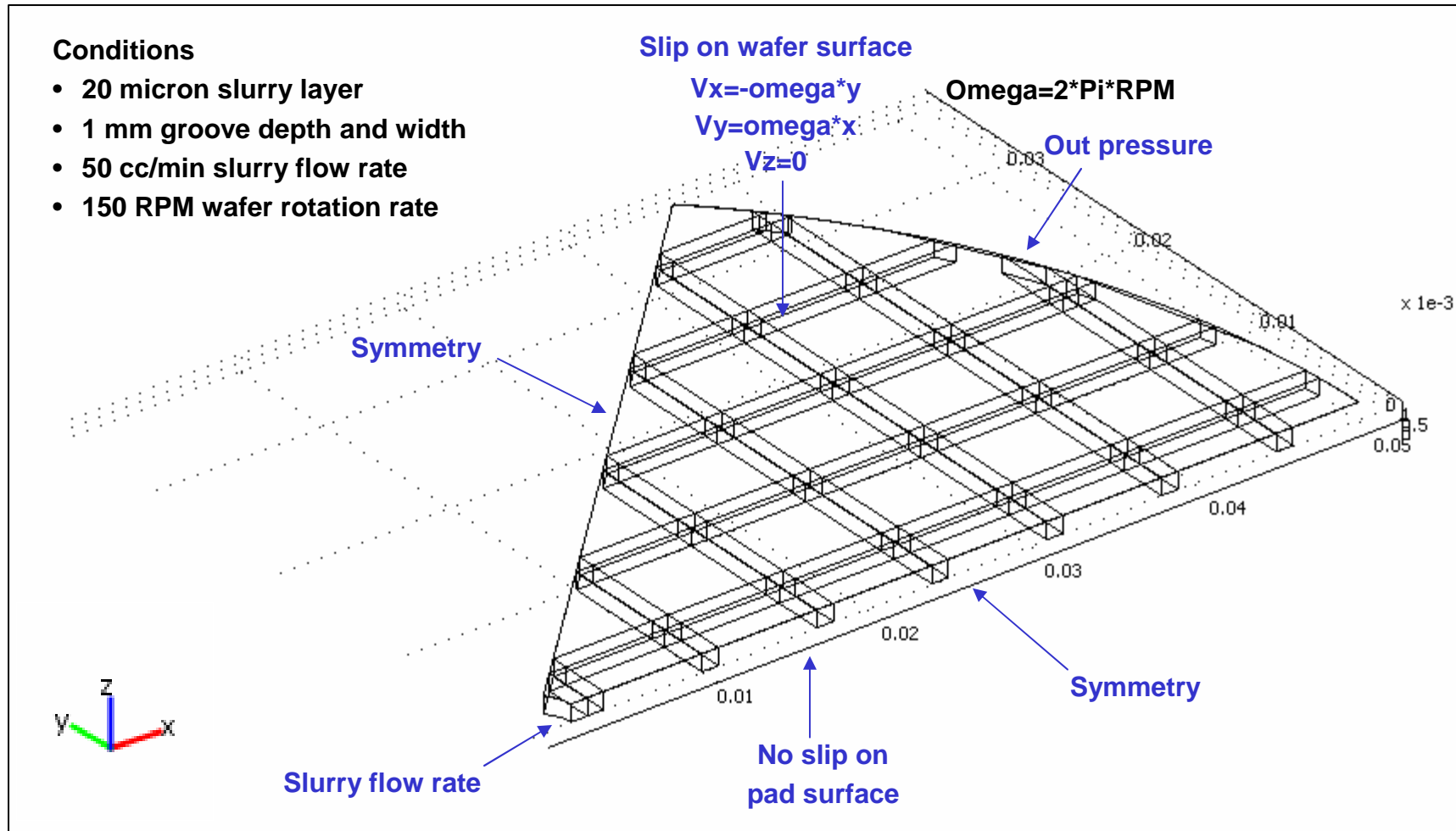


At 50 ml/min, local copper removal rate generally increased linearly with wafer radius, indicating a mechanically controlled process.

At 25 ml/min, local copper removal rate did not increase linearly with the wafer radius and did not increase with wafer rotation rate, suggesting the onset of slurry starvation.

SRC/Sematech Engineering Research Center for Environmentally Benign Semiconductor Manufacturing

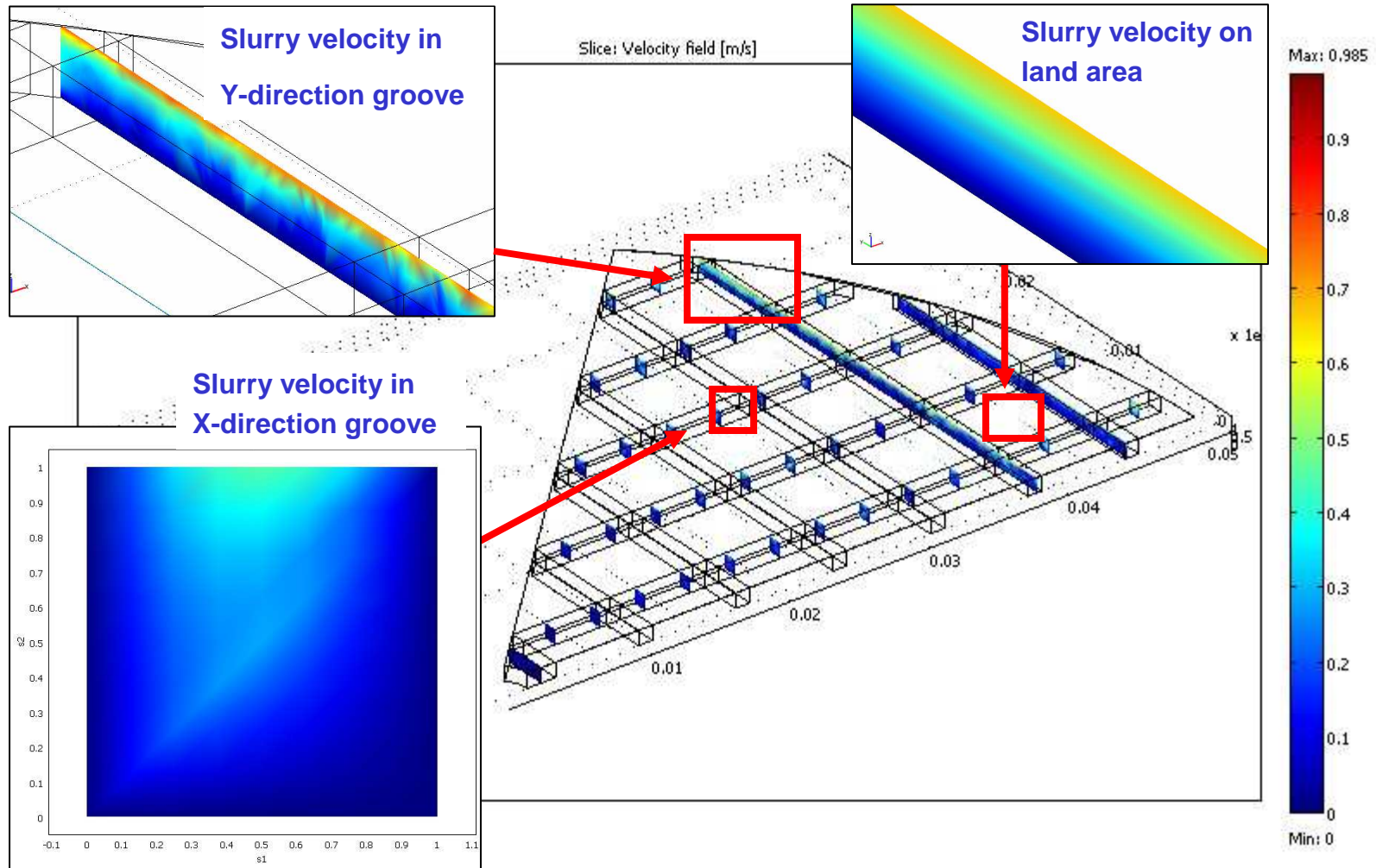
B. C. for Slurry Velocity Simulation in XY groove Pad



The Navier-Stokes equations for the slurry flow were solved only in the grooves and on the land areas.

SRC/Sematech Engineering Research Center for Environmentally Benign Semiconductor Manufacturing

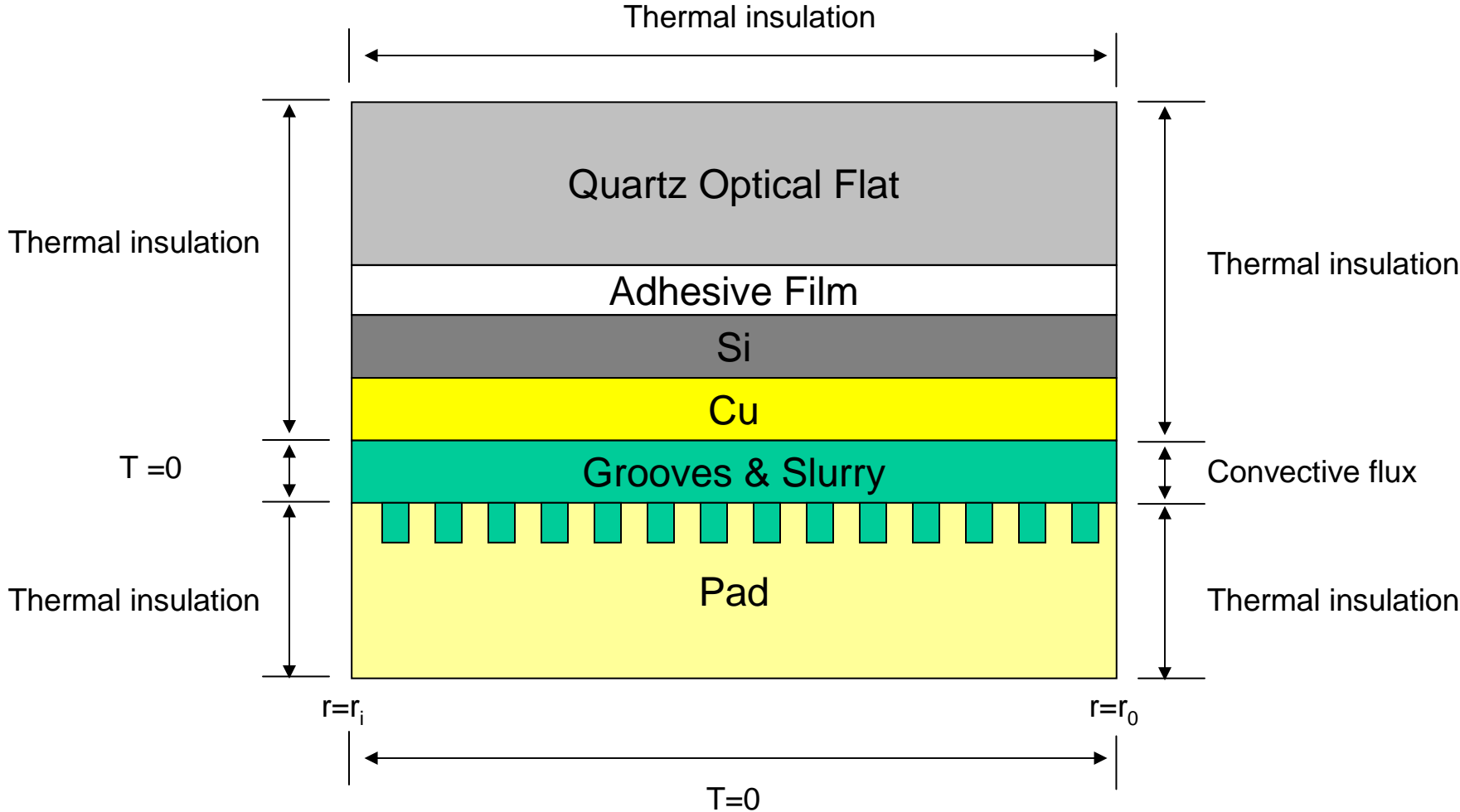
Simulated Slurry Velocity in Grooves and Land Area



Results showed shear flow on the land areas and wafer-driven circulation in the grooves.

SRC/Sematech Engineering Research Center for Environmentally Benign Semiconductor Manufacturing

Material Layers and B. C. for Thermal Model



Initial Condition: $t = 0, T = 0$

Thermal Model Geometry

Heat equation

$$\rho C_p \left(\frac{\partial T}{\partial t} + \vec{V} \cdot \vec{\nabla} T \right) = \vec{\nabla} \cdot (k \vec{\nabla} T) + Q$$

- \vec{V} :
- From Navier-Stokes in slurry layer
 - Rigid body in wafer and above
 - 0 in pad

Q :

- $\frac{\mu_k p_s V_s}{h}$ on land areas

- 0 elsewhere

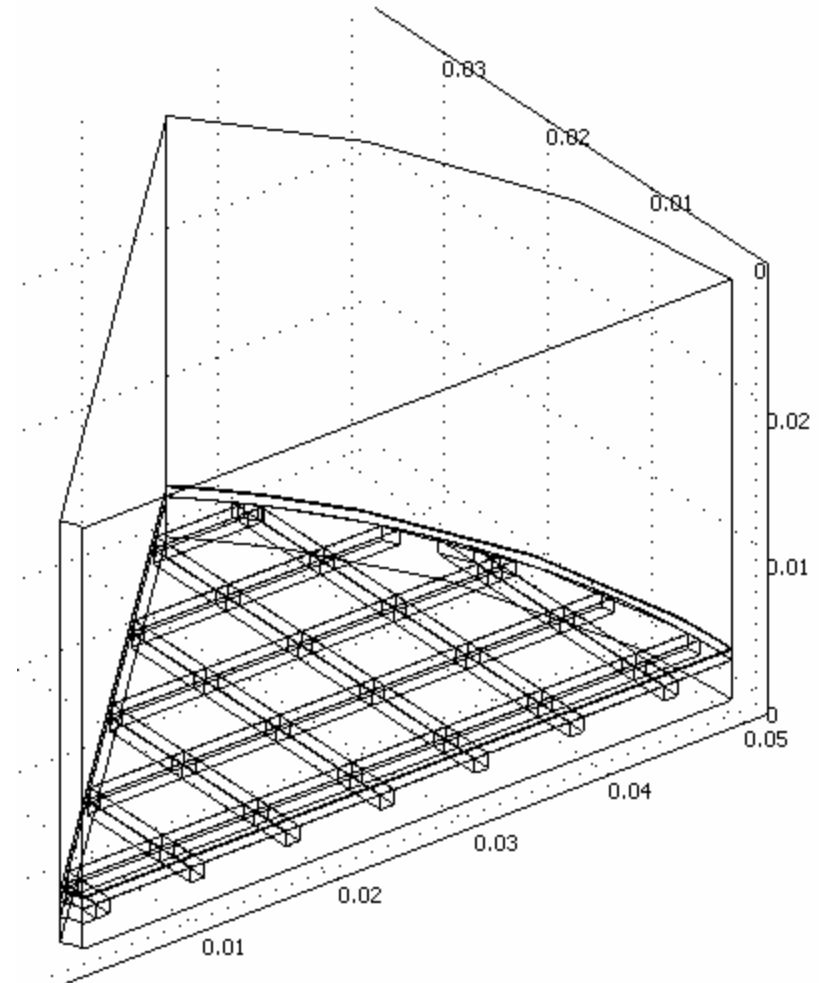
p_s : 34400 Pa (Actual 5PSI)

V_s : $\Omega \cdot r$ (Sliding velocity)

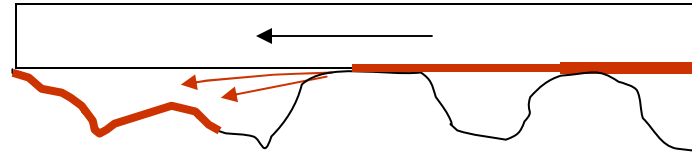
μ_k : COF

Flow rate: 50 cc/min

$\Omega = 2 \cdot \pi \cdot \text{RPM}$



Staining Model



Governing Equation:
$$\frac{\partial c_{ox}}{\partial t} + \vec{V} \cdot \vec{\nabla} c_{ox} = \nabla \cdot (D \nabla c_{ox})$$

Advection by the fluid with a velocity

B.C. at wafer surface:
$$D \vec{\nabla} C_s \cdot \vec{n} = \frac{k_2 k_1}{k_1 + k_2}$$

B.C. at pad surface:
$$-D \vec{\nabla} C_s \cdot \vec{n} = k_4 C_s$$

Conclusions and Future Plan

- **Stain was generated on pad surfaces during copper CMP using a table-top axisymmetric polishing system. Staining agents were produced by mechanical action during polishing and were advected downstream by the slurry flow.**
- **Staining increased with polishing pressure, wafer rotation rate, slurry flow rate and polishing times.**
- **Simulated slurry velocity increased gradually on the wafer surface in the radial direction due to wafer rotation, affecting slurry velocity in the grooves. Also, simulation results showed shear flow on the land areas and wafer-driven circulation in the grooves.**
- **With simulated slurry velocity and temperature profile, byproduct generation, transport, and deposition on pad will be simulated to illustrate the mechanism of stain formation on pad surface.**

Friction Studies in Chemical Mechanical Planarization

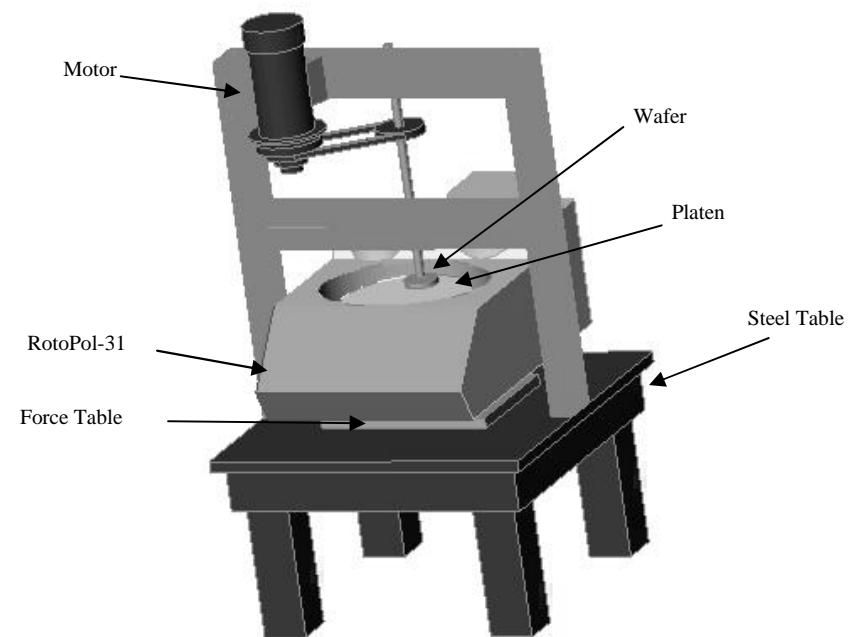
Jim Vlahakis, PhD Candidate

ERC Task # 425.020

February 2007

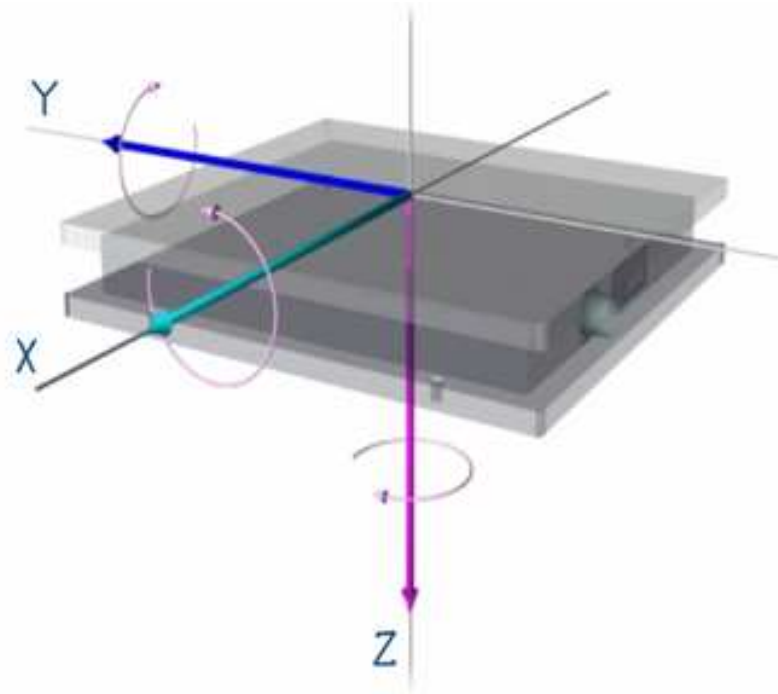
PI: C. B. Rogers, V. P. Manno,
and R. D. White

Tufts University



CMP Friction Studies

1. ESH Metrics and Impacts
2. Industrial Collaboration & Technology Transfer
3. Progress in 2006
 - Past issues & solutions
4. Latest data
 - CoF and Drag Forces vs. Slurry Dilution
 - Development of Stick-Slip during polishing
5. Modeling
6. Laser displacement sensor tests
 - Feasibility
7. Future work



The force table is capable of data acquisition up to 10kHz and measures forces and moments in the x, y and z directions.

Environmental Safety and Health (ESH) Metrics and Impacts

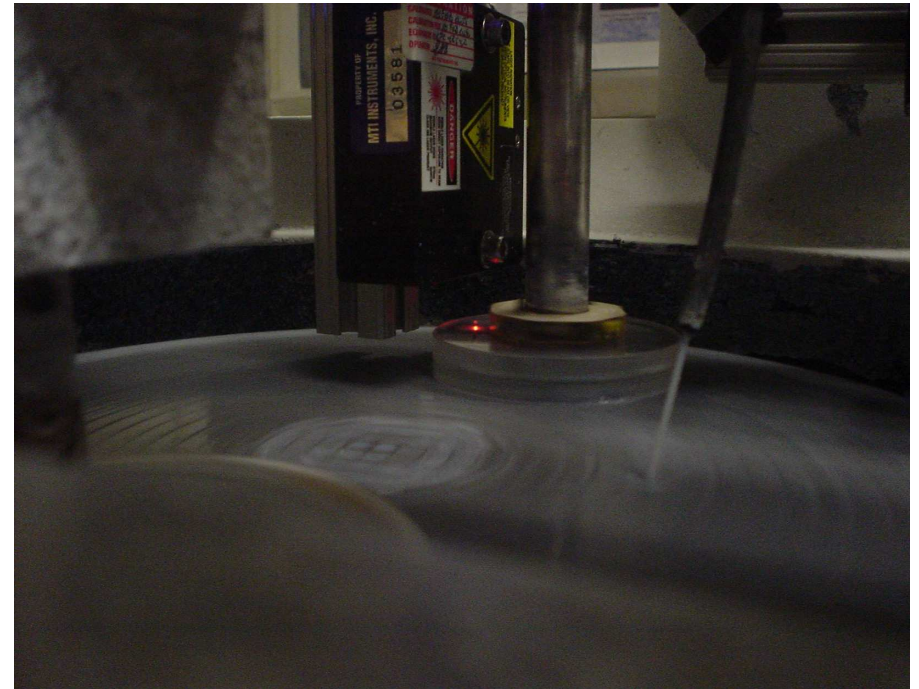
<u>METRIC</u>		<u>IMPACT</u>
Energy Consumption During Process	→	Understanding wafer-pad interactions during polish leads to reduced time to polish and tool energy consumption
DI Water Consumption During Process	→	Optimized process parameters based on in-situ characterization of contact, and forces leads to reduced time to polish and slurry consumption
Process Chemical Consumption (Slurry Chemicals)		optimization

Industrial Collaboration/Technology Transfer

- Close collaboration with industry partners – Cabot
Microelectronics and Intel
 - Monthly telecons – secure website for information exchange
 - Semi-annual face-to-face meetings
 - Thesis committees and joint publication authorship
 - Metrology and analysis methodology technology transfer
 - In-kind support – specialized supplies and equipment
 - Student internships (e.g. C. Gray at Intel during Summer 2005)
 - Close coordination with A. Philipossian research group at U of Arizona
- Information and results exchange with MIT (D. Boning)
ERC project
 - Monthly joint meetings of PIs and research students
 - Discussion of findings with other colleagues (e.g. E. Paul – Stockton College on leave at MIT)

CMP Friction Studies – Progress in 2006

- Previous data runs at 30/60rpm
 - Now using 60/120rpm (.5 & 1m/s), more in line with industry practice
- Polishing pressures up to 2.5psi easy achievable
- Irregularities due to changes in wafer shape
 - Controls in place to monitor wafer shape
- Issues concerning slurry dilution
 - Moved from 9:1 to 3:2 dilution of Cabot SC1 slurry for general experiments, more in line with industry practice

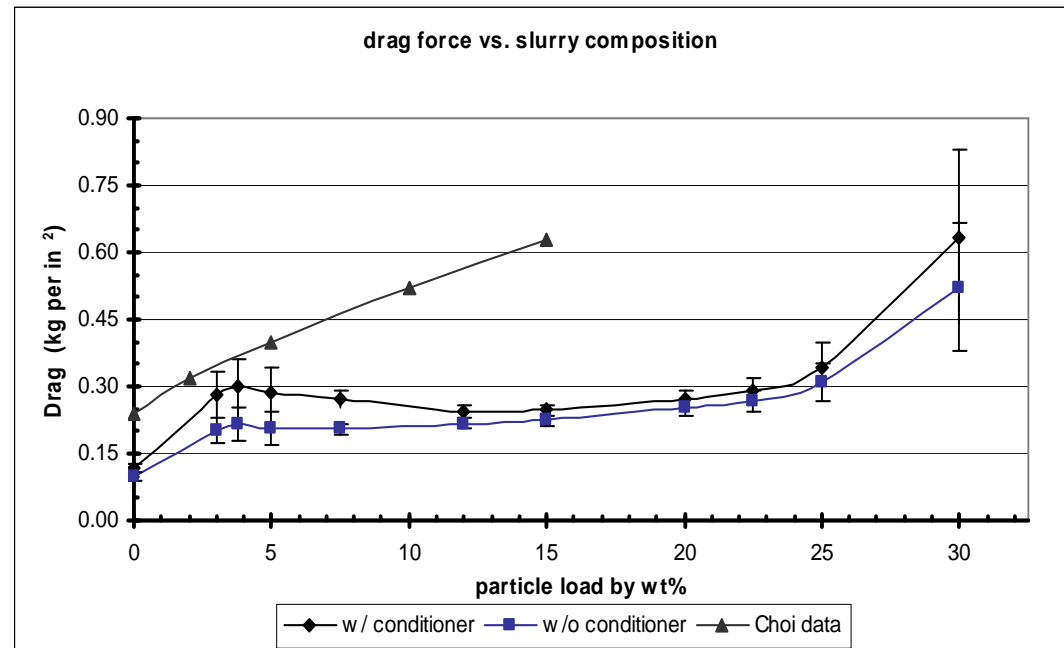


CMP Friction Studies – Latest Data

- Drag Force vs. slurry dilution

- 60rpm (~.5m/s) & 1.7psi
- Note large CoF (and large σ) for pure slurry. A result of shear thickening?
- CoF remains fairly constant over a wide range of slurry dilutions
- Our experiments indicate that for pure H₂O, pH plays a role in determining CoF
- Next steps

- Explore particle loadings in the 0 - 5% range. Specifically, where does the “up and over” nature of the curve begin to manifest?
- Investigate pH dependence for H₂O
- Perform experiment “backwards” – if we begin with pure slurry and work towards pure H₂O, would we see different results than if we started with pure H₂O and worked towards pure slurry? If so, what does this tell us about slurry/pad interactions?



Choi data – Choi, Lee and Singh, “Effects of Particle Concentration in CMP,” Mat. Res. Soc. Symp. Proc. Vol. 671, 2001

Choi’s parameters

2psi
 Particle size ~.2 μ m
 $V_{relative} = 2.2$ m/s
 .64in² sapphire

Our parameters

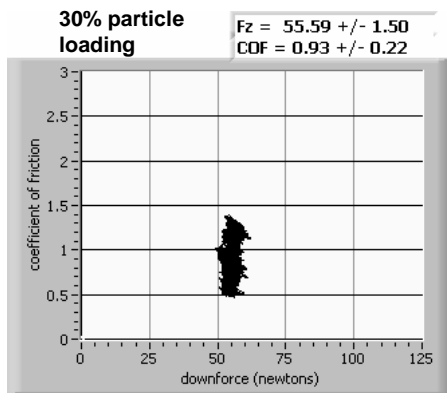
1.7psi
 Particle size ~.09 μ m
 $V_{relative} = .5$ m/s
 7in² BK7 glass

CMP Friction Studies – Latest Data

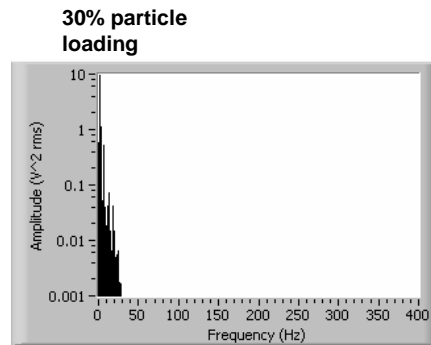
CoF vs. slurry dilution,

- stick-slip response grows as we dilute the slurry
- note how CoF plots and spectra develop as stick-slip grows

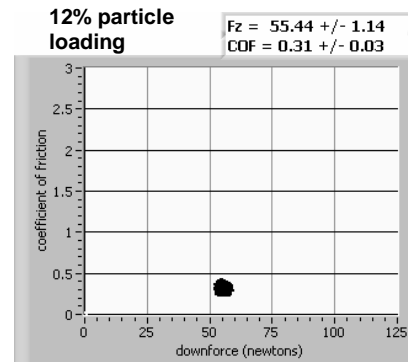
CoF vs. Downforce



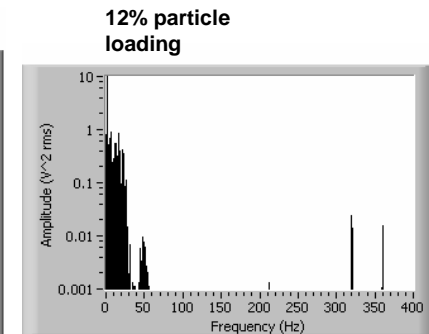
Fx Spectra



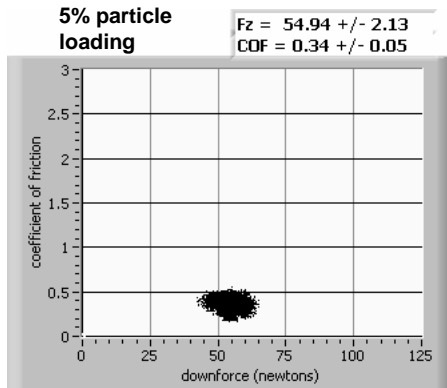
CoF vs. Downforce



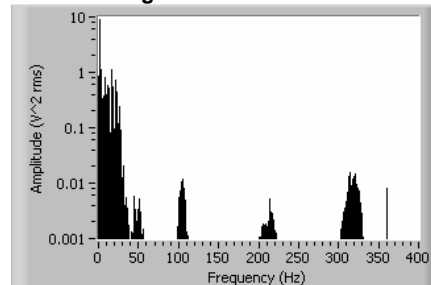
Fx Spectra



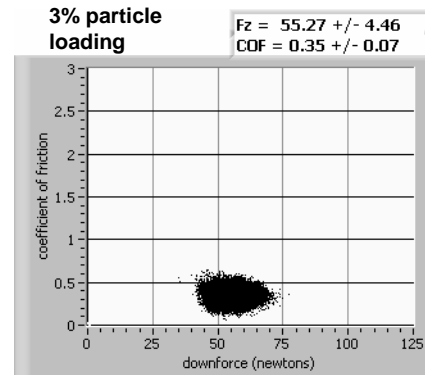
5% particle loading



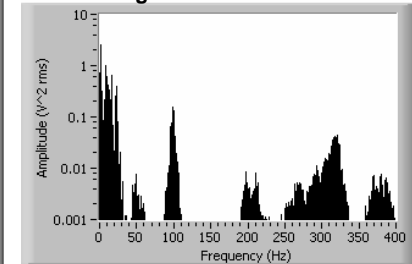
5% particle loading



3% particle loading



3% particle loading



CMP Friction Studies – Modeling

Goal – To develop a predictive, microscale model of CMP and a corresponding series of macroscale experiments that serve to both inform and develop our model

- **Lets consider the force required to drag a wafer across a polishing pad. We can consider three separate components and break them down individually.**
 1. **Fluid forces associated with flow underneath the wafer**
 2. **Mechanical forces associated with dragging pad asperities (and particles?) across the wafer**
 3. **Chemical forces associated with actual material removal**

CMP Friction Studies – Modeling

Goal – To develop a predictive, microscale model of CMP and a corresponding series of macroscale experiments that serve to both inform and develop our model

1. Forces associated with fluid flow underneath the wafer

- Under normal polishing parameters, its safe to assume that these forces are small compared with other forces involved. Indeed, in hydroplaning cases the drag force is small.
- Unless we have a particle loading beyond ~20% at which point, we believe shear thickening becomes important

2. Mechanical forces associated with dragging pad asperities (and particles?) across the wafer

- Dependent on
 - Downforce
 - Actual contact area
 - $V_{relative}$
 - Mechanical properties of wafer and pad (modified by slurry exposure)
 - Other pad properties?
 - Porosity
 - conditioning

CMP Friction Studies – Modeling

Goal – To develop a predictive, microscale model of CMP and a corresponding series of macroscale experiments that serve to both inform and develop our model

3. Chemical forces associated with actual material removal

- F_p = force due to wafer-pad interaction
- F_a = force due to wafer-abrasive interaction
- We can write

$$\mu = \frac{F_p + F_a}{(\text{pressure} \times \text{area}_{\text{wafer}})}$$

- We can separate the terms so that

$$F_p = \mu_p (\text{press} \times \text{area}_{\text{pad}})$$

$$F_a = \mu_a (\text{press} \times \text{area}_{\text{abrasive}})$$

- The area fraction has been shown to be

$$\frac{A_{\text{abrasive}}}{A_{\text{pad}}} = \frac{[A]}{K_{\text{pad}} + [A]}$$

- Ultimately, this simple, preliminary analysis arrives at

$$F_{\text{drag}} = \left(\frac{\mu_p K_{\text{pad}} + \mu_a [A]}{K_{\text{pad}} + [A]} \right) F_z$$

[A] – abrasive concentration

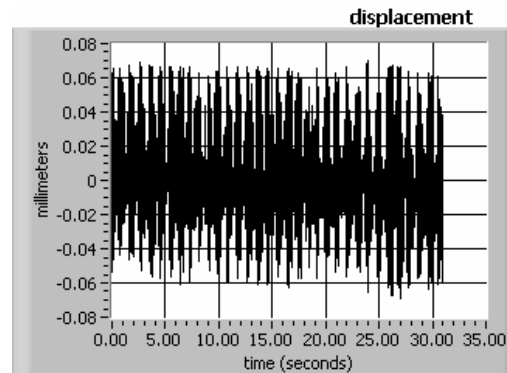
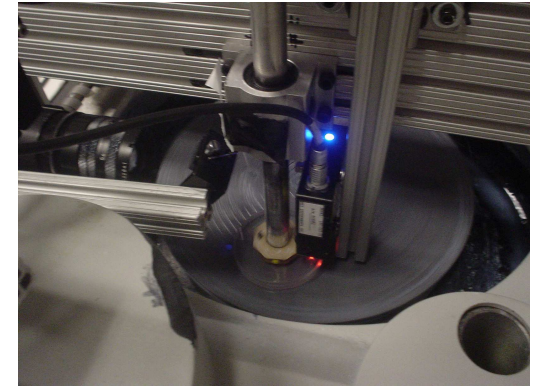
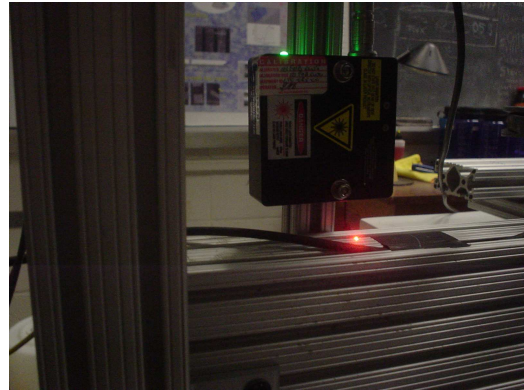
K_{pad} – fitting parameter dependent on pad properties

- Now we must develop some experiments that can reveal whether or not this sort of modeling is on the right track

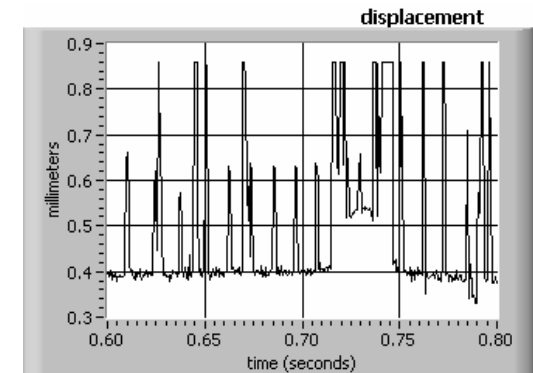
CMP Friction Studies – Laser Sensor

Feasibility of using multiple laser sensors to monitor wafer displacement

- **Support frame displacement during worst case polishing?**
 - 60rpm–2.5psi–pure H₂O (strong stick-slip)
 - Frame displacements are on the order of .1mm
- **Wafer displacement during polishing?**
 - Standard experimental conditions
 - Displacements on the order of 1mm
- **Safe to say that wafer displacement will not be lost in the frame displacement**



Frame displacement vs. time



Wafer displacement vs. time

CMP Friction Studies – Future Work

High Level View

1. Continue microscale model development leveraging or the knowledge base that exists among this and other SRC groups
2. Identify the experiments that will show the accuracy (or inaccuracy) of our models and adjust our models accordingly
3. Perform the experiments and, if necessary, iterate until our models can explain our data

Low Level View

1. Continue CoF vs. slurry dilution experiments
2. Explore the low particle (0-5%) loading regime
3. Purchase and begin installation of laser displacement package
4. Prepare for various conferences and papers

Thanks to both the SRC and to our industrial partners Cabot Microelectronics and Intel

Surface Characterization and Flow Resistance Estimates for CMP Pads

SRC 425.020

T. Sun ¹, L. Borucki ², Y. Zhuang ^{1,2}, D. Marks ³, T. Clark ³, A. Philipossian ^{1,2}

¹ Dept. of Chemical & Environmental Engineering University of Arizona, Tucson, AZ, USA

² Araca, Inc., Tucson, AZ, USA

³ psiloQuest Corporation, Orlando, FL, USA

Project Overview

Project Objectives:

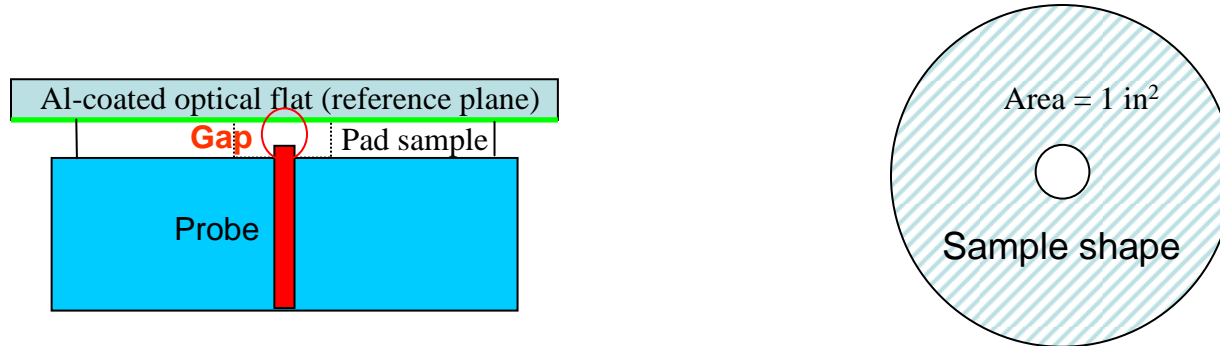
The objective is to investigate the fluid carrying capacity of CMP pads by quantifying their surface topography through both contact and non-contact methods. By better understanding how pad surface asperities resist or assist slurry flow during CMP, pads with engineered surfaces can be produced to yield lower slurry flow rate processes.

ESH Impact:

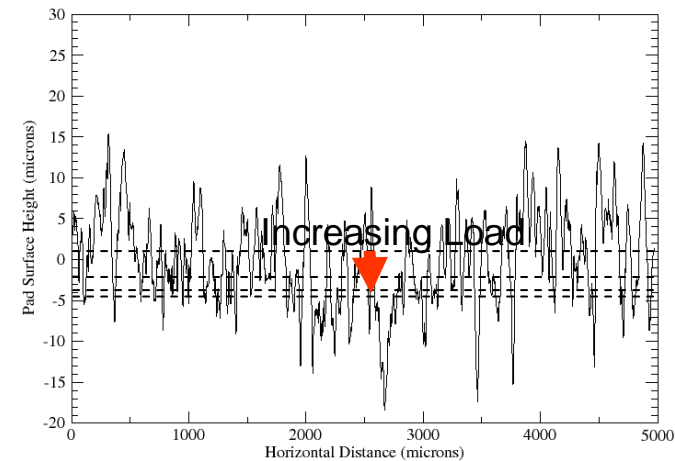
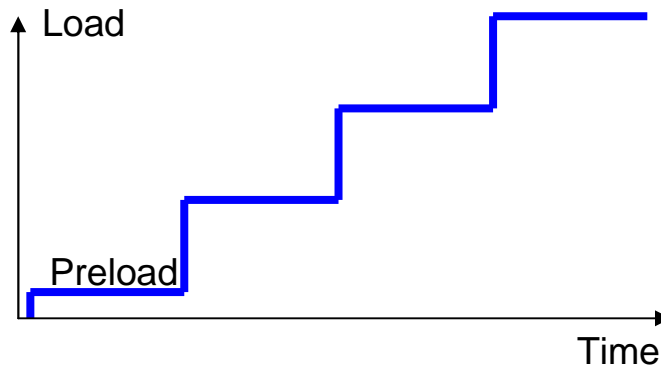
A method was developed to study fluid flow features on the land areas of pad surfaces. This method can be used to assess and novel designs of pad materials and surface texture, which would reduce slurry usage. As a result, the waste volume produced by CMP process would be reduced.

Probing the Surface with Incremental Loading

The loading device measures the **gap** between a reference plane in contact with the pad sample and a capacitance probe. The gap changes with loading.



Starting with a light preload, the load is increased by equal increments at equal time intervals. The reference plane displacement probes the pad surface mechanically.



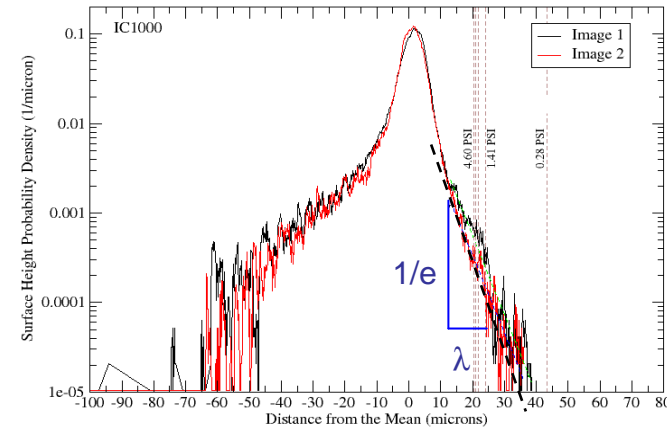
Modeling Pad/Wafer Contact

Greenwood and Williamson pressure-displacement relationship

+

A surface with exponentially distributed summit heights in the contacting tail

$$p = \frac{4\eta \cdot E \cdot R^{1/2}}{3(1-\nu^2)} \int_d^\infty (z-d)^{3/2} \phi_s(z) dz$$



together imply an exponential relation between displacement d and pressure p :

$$p = (\text{Parameters})e^{-d/\lambda}$$

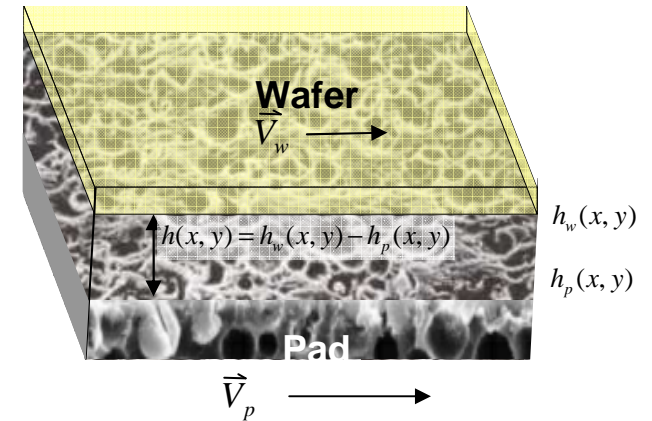
$$\frac{p_1}{p_2} = e^{-(d_1-d_2)/\lambda}$$

so A log plot of p_1/p_2 vs. displacement increment should be linear.

Fluid Transport Analysis

Slurry flow under the wafer in the land areas can be modeled with the **Reynolds equation**:

$$\nabla \cdot \left(\frac{h^3}{12\mu} \nabla p_f \right) = \frac{1}{2} (\vec{V}_p + \vec{V}_w) \cdot \nabla h_w + \frac{1}{2} (\vec{V}_p - \vec{V}_w) \cdot \nabla h_p$$



For non-isotropic surface roughness, the **corrected** form of the Reynolds equation for boundary lubrication is:

$$\frac{\partial}{\partial x} \left(\phi_x \frac{\langle h \rangle^3}{12\mu} \frac{\partial \bar{p}_f}{\partial x} \right) + \frac{\partial}{\partial y} \left(\phi_y \frac{\langle h \rangle^3}{12\mu} \frac{\partial \bar{p}_f}{\partial y} \right) = \frac{1}{2} (\vec{V}_p + \vec{V}_w) \cdot \nabla \langle h \rangle + \frac{\sigma}{2} (\vec{V}_p - \vec{V}_w) \cdot \nabla \phi_s$$

Here, \bar{p}_f is a mean approximation to the fluid pressure field p_f
 $\langle h \rangle$ is the local mean separation between the pad and wafer.
 ϕ_x and ϕ_y are **pressure flow factors** - identical for isotropic surfaces.
 ϕ_s is a **shear flow factor** for fluid transport in the direction of sliding.
 σ is the surface height standard deviation of the pad surface.

Connection Between Flow Factors and Transport

Flow factors quantify the effect on fluid flow of the pad surface roughness.

For example, for sliding in the y-direction with velocity magnitudes v_p and v_w for the pad and wafer, respectively, the fluid flux in the y direction is

$$q_y = \int_{h_1}^{h_2} v dz = -\phi_y \frac{\langle h \rangle^3}{12\mu} \frac{\partial \bar{p}_f}{\partial y} + \frac{1}{2} (v_p + v_w) \langle h \rangle + \frac{1}{2} (v_p - v_w) \sigma \phi_s$$

We can see from this that

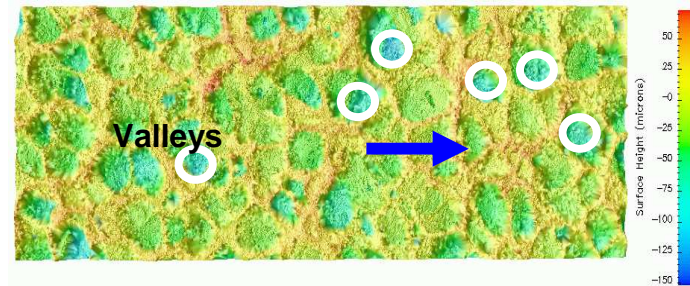
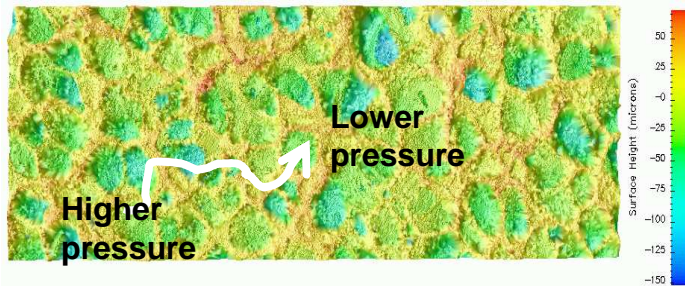
When $\phi_y < 1$, the pad surface *impedes flow* due to fluid pressure gradients. This factor is 1 for a perfectly smooth surface. For a rough pad surface, the factor becomes smaller as the surface is compressed.

When $\phi_s > 0$, the pad surface *enhances transport*. For a perfectly smooth pad surface, this factor is 0. For a rough surface, the factor is a measure of the ability of the surface to carry fluid directly in topographical valleys.

For grooved pads, there is very little fluid pressure development, so the most important measure is the product of the shear flow factor and σ .

Flow factors can be calculated with the *method of homogenization*.

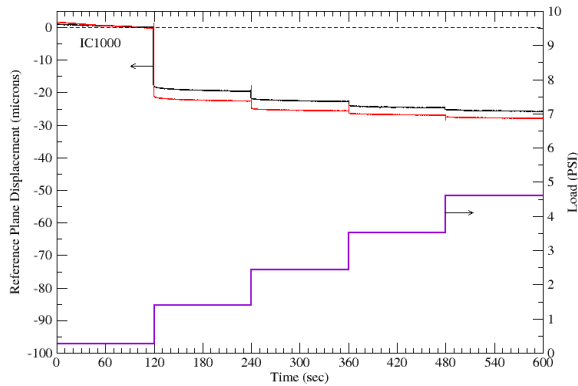
Pad Surfaces and Fluid Flow



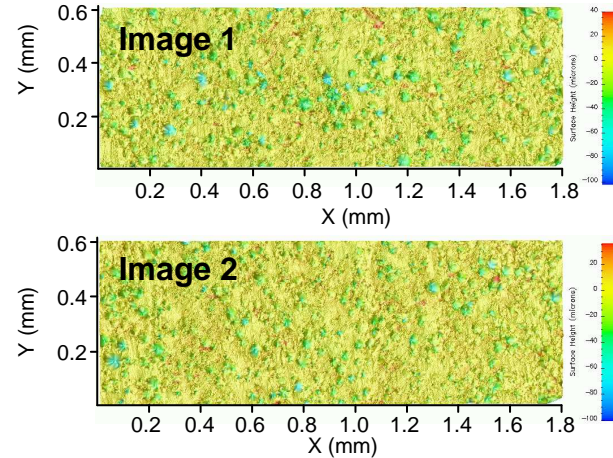
Pad surface topography can present an obstacle to fluid flow when pressure differences exist in the fluid. Resistance to pressure-driven flow can be quantified by a **pressure flow factor**. The pressure flow factor can be calculated directly from interferometry data. The factor is 1 when the surface is perfectly smooth and 0 when no flow occurs.

Valleys in the pad surface topography carry fluid directly. The effect of valleys on fluid transport can be quantified from interferometry with a **shear flow factor**. The shear flow factor is 0 for a smooth surface and increases as valleys become deeper. The total fluid flux is proportional to the product of the shear flow factor and the surface height standard deviation σ . **The shear flow factor is relevant for evaluating transport by the land areas of grooved pads.**

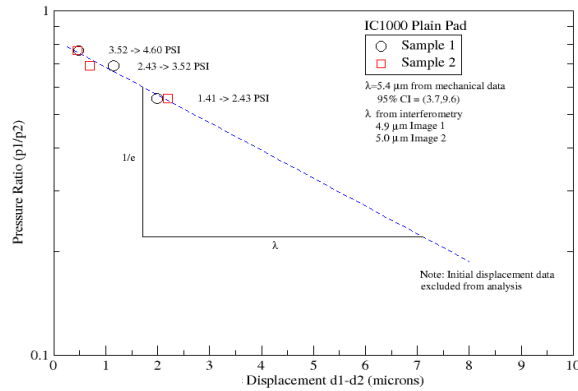
Rohm and Haas IC1000 Pad



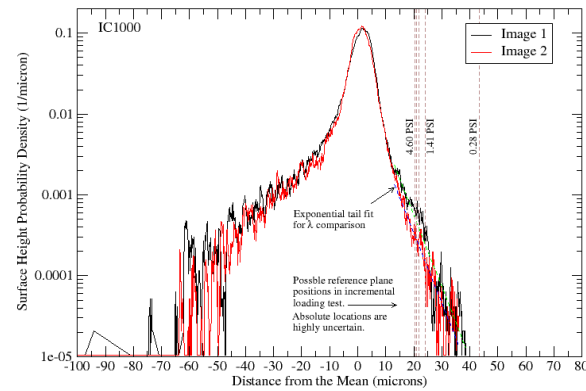
Incremental Loading Results



Interferometry

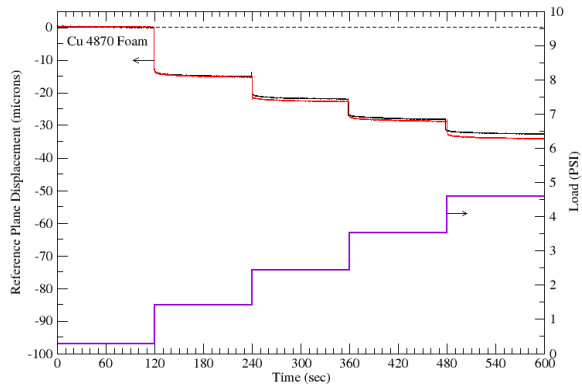


Incremental Load vs. Elastic-Plastic Displacement

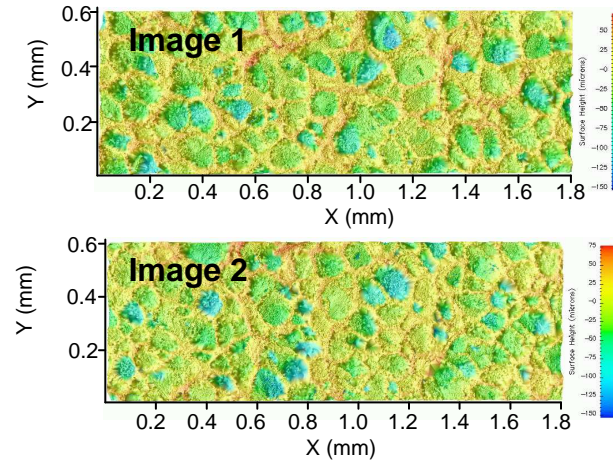


Surface Height Histograms (PDFs) Derived from Interferometry

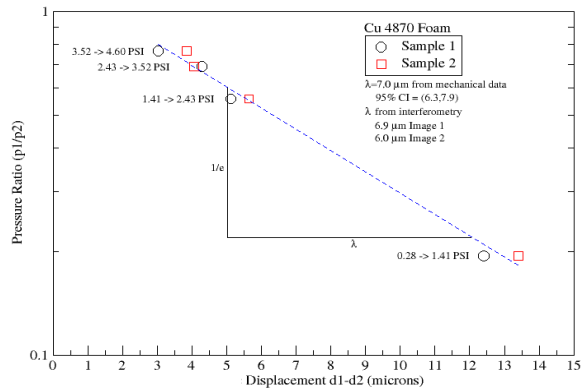
psiloQuest Cu 4870 Pad



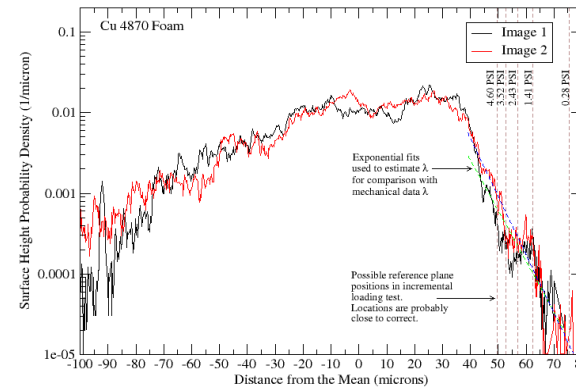
Incremental Loading Results



Interferometry



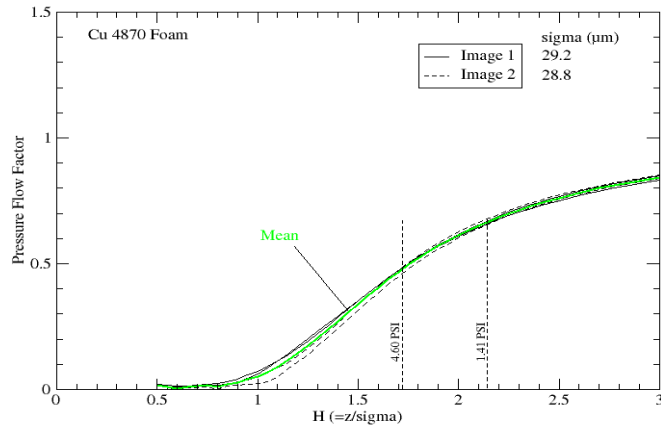
Incremental Load vs. Elastic-Plastic Displacement



Surface Height Histograms (PDFs) Derived from Interferometry

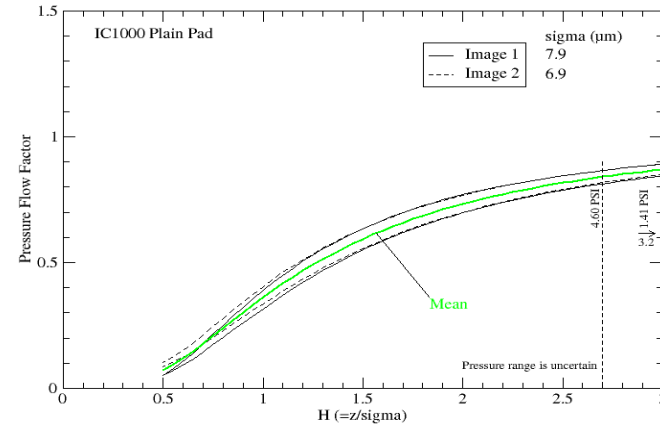
Flow Resistance Estimation

psiloQuest Cu 4870 Pad

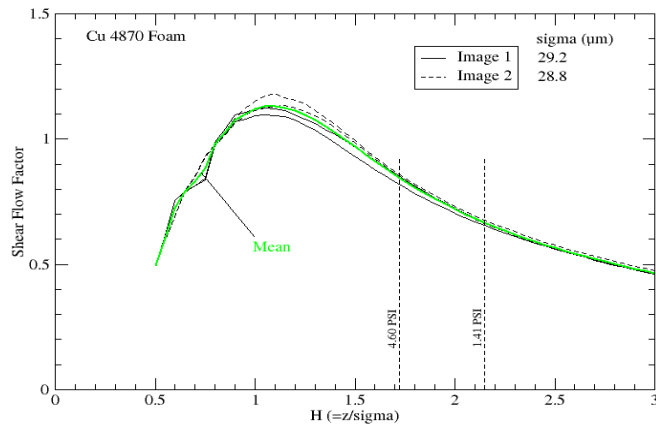


Pressure Flow Factor

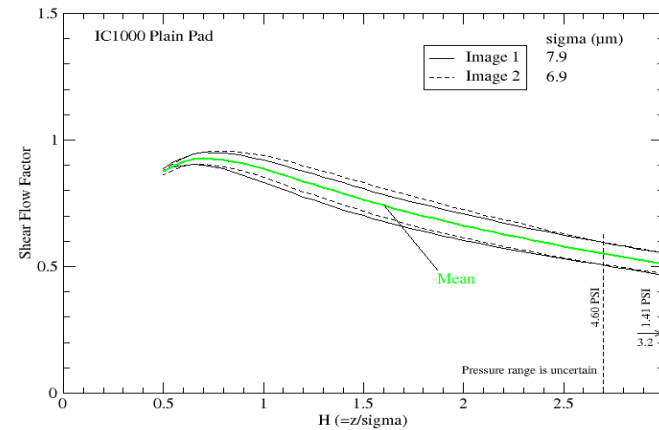
Rohm and Haas IC1000 Pad



Pressure Flow Factor



Shear Flow Factor



Shear Flow Factor

Summary and Conclusions

λ measures both the slope of the contacting tail in pad surface height PDF data and the displacement that occurs when the load is changed by a factor of e.

Pad surfaces exhibit a nonlinear mechanical response to incremental loading, as predicted by theory: increasing the load by equal increments has an *exponentially diminishing* effect on elastic-plastic surface compression; decreasing the load by equal increments has an *exponentially magnified* effect.

Shear flow factor estimation results show that the psiloQuest Cu 4870 pad has about *5 times* more capacity to transport fluid in topographical valley relative to the Rohm and Haas IC1000 pad, thereby suggesting that much *lower slurry flow rates* might be possible with the philoQuest Cu 4870 pad.

Future Plans:

- Determine whether ILD can be used with **moist pad samples**. Study of moist pad samples is more realistic, and not possible with interferometry. Quantify and explain differences between moist and dry pad samples.
- Modify the ILD to allow samples to be analyzed at different temperature.
- Investigate the effect of **temperature** on pad surface topography.

Industrial Collaboration/Technology Transfer:

- Dan Marks and Tony Clark (psiloQuest)
- Jam Sorooshian, Darren DeNardis and Don Hooper (Intel)

Detection of Slurry Abnormality during ILD CMP Using Real-Time Frictional Force Measurement and Analysis

SRC: 425.020

**Y. Sampurno ¹, Y. Zhuang ^{1,2}, F. Sudargho ^{1,2}, M. Goldstein ³
and A. Philipossian ^{1,2}**

¹ The University of Arizona, Tucson, Arizona USA

² Araca Incorporated, Tucson, Arizona USA

³ Intel Corporation, Santa Clara, California USA

Motivation, Goal and Methodology

Motivation

- **Large abrasive particles and abrasive particles agglomeration** in slurries can cause scratch defects on wafer surfaces during CMP. Scratch defects significantly affect die yield. Effective methodologies are needed to identify such slurry abnormalities before its usage.

Goal and Methodology

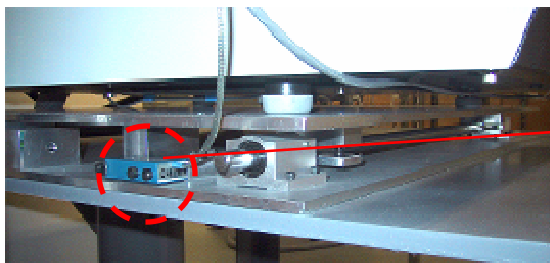
- Small amounts of large particles were added to a commercial slurry to create slurry contamination.
- Determine whether **real-time shear force measurement and analysis** can detect the above slurry contamination.

Experimental Apparati

100-mm Wafer Polisher



200-mm Wafer Polisher



Load
Cell



Shear force was measured in real-time by load cells installed in 100-mm and 200-mm wafer polishers during polishing.

Experimental Conditions

Contamination with Large Alumina Particles

100-mm Wafer Polish

– Slurries

- Fujimi PL-4217 slurry with 12.5% (weight percent) silica particles
- Fujimi PL-4217 slurry with 12.4% (weight percent) silica particles and 0.1% (weight percent) 0.9 μm alumina particles
- Flow rate: 80 ml/min

– Wafers

- 100-mm blanket oxide wafers

– Pad

- 12-inch IC1000 plain pad

– Wafer Polishing

- Polishing pressure: 4 PSI
- Sliding velocity: 1.12 m/s
- Polishing time: 30 s

– Pad Conditioning

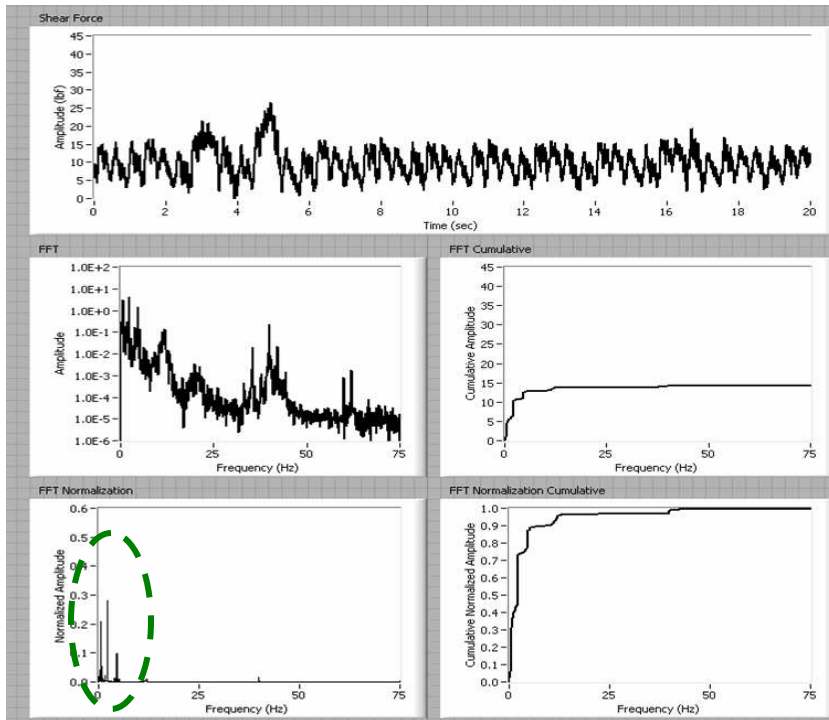
- 2-inch TBW 100-grit diamond disc rotating at 30 RPM and sweeping at 20 times/min
- In-situ conditioning at 0.5 PSI

Shear Force Spectral Comparison

Contamination with Large Alumina Particles

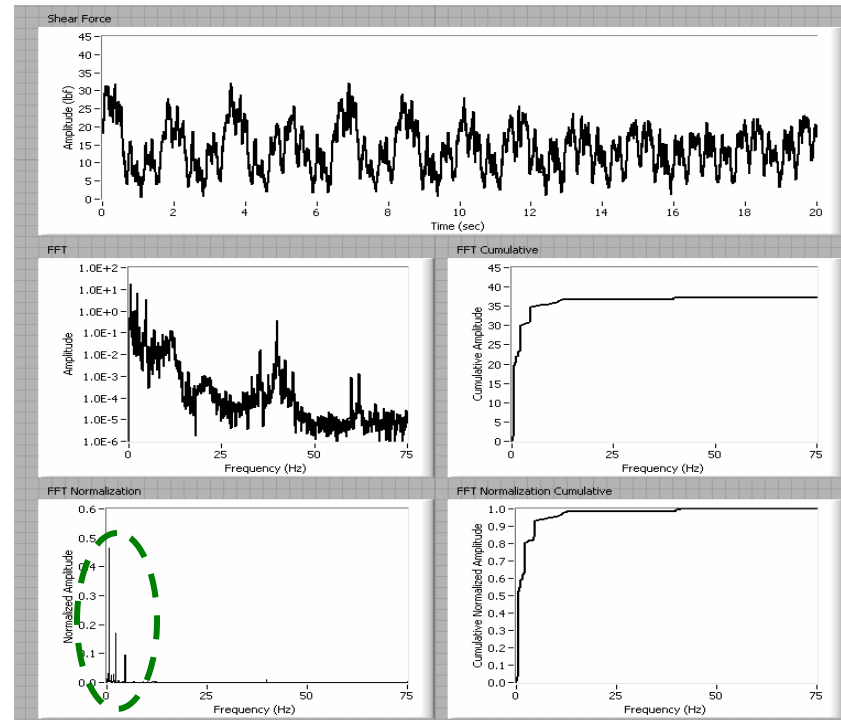
100-mm Wafer Polish

Uncontaminated Slurry



Mean COF: 0.186; Mean RR: 1321 Å/min
Mean variance of shear force: 18 lb_f²

Contaminated Slurry



Mean COF: 0.249; Mean RR: 1362 Å/min
Mean variance of shear force: 36 lb_f²

The addition of large alumina particles induced a significantly higher COF and variance of shear force. Shear force spectral amplitude shifted towards lower frequency ranges for the contaminated slurry.

Experimental Conditions

Contamination with Large Silica Particles

100-mm Wafer Polish

– Slurries

- Fujimi PL-4217 slurry with 10% (weight percent) silica particles
- Fujimi PL-4217 slurry with 9.9% (weight percent) silica particles and 0.1% (weight percent) large silica particles
- Flow rate: 80 ml/min

– Wafers

- 100-mm blanket oxide wafers

– Pad

- 12-inch IC1000 plain pad

– Wafer Polishing

- Polishing pressure: 4 PSI
- Sliding velocity: 1.12 m/s
- Polishing time: 75 s

– Pad Conditioning

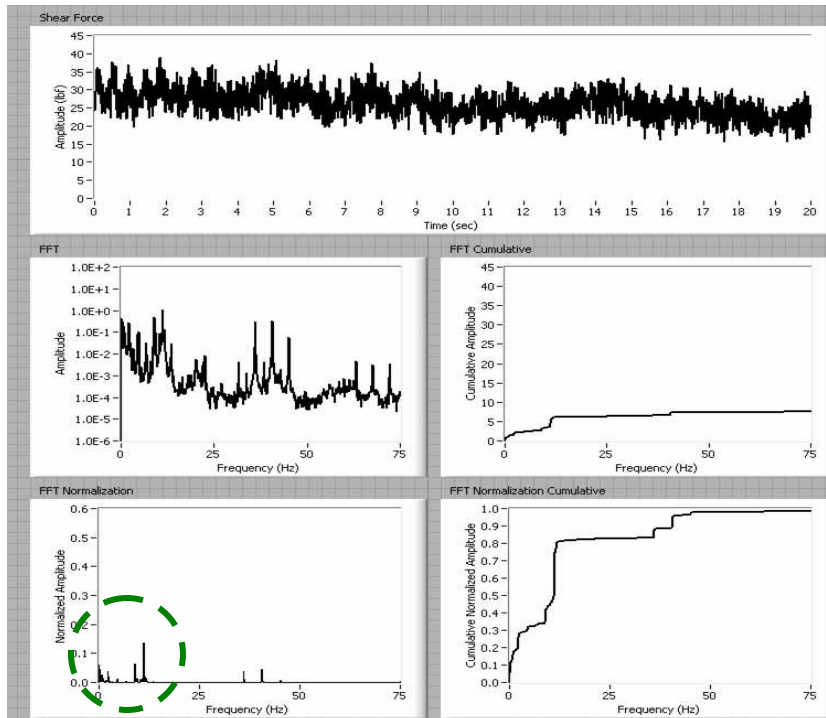
- 2-inch TBW 100-grit diamond disc rotating at 30 RPM and sweeping at 20 times/min
- In-situ conditioning at 0.5 PSI

Shear Force Spectral Comparison

Contamination with Larger Silica Particles

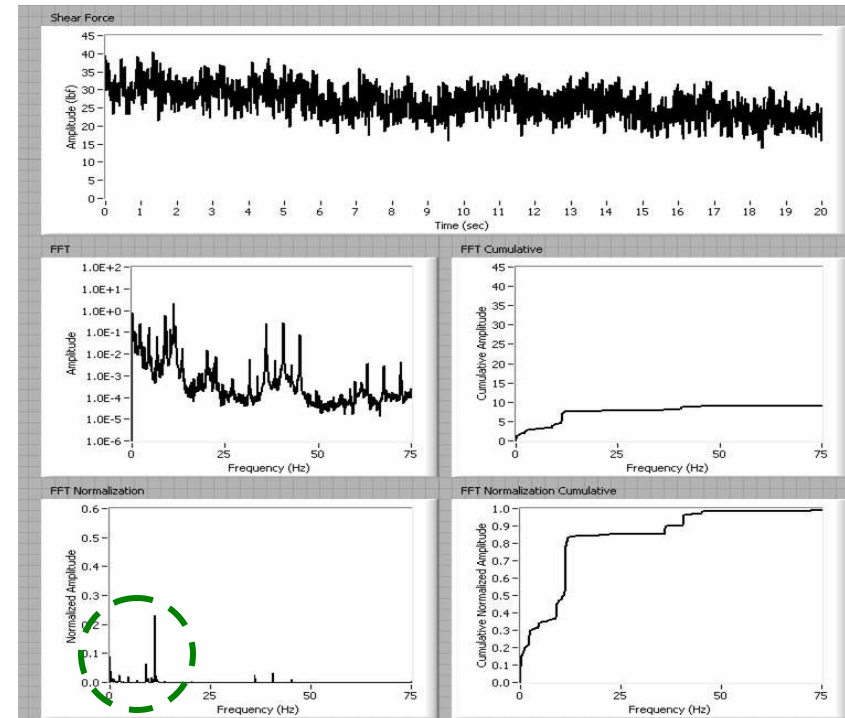
100-mm Wafer Polish

Uncontaminated Slurry



Mean COF: 0.452; Mean RR: 2732 Å/min
Mean variance of shear force: 14 lb_f²

Contaminated Slurry



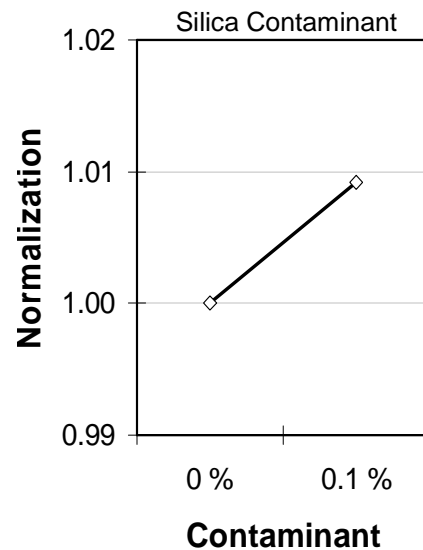
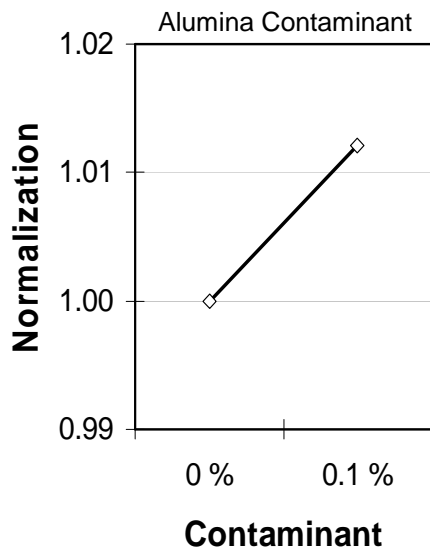
Mean COF: 0.463; Mean RR: 2768 Å/min
Mean variance of shear force: 15 lb_f²

The addition of large silica particles induced a slightly higher COF and variance of shear force. Shear force spectral amplitude shifted towards lower frequency ranges for the contaminated slurry.

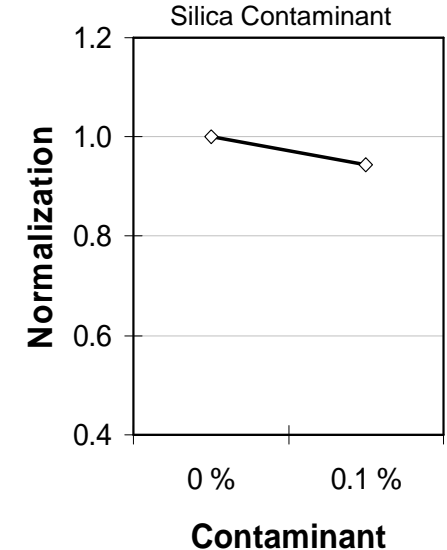
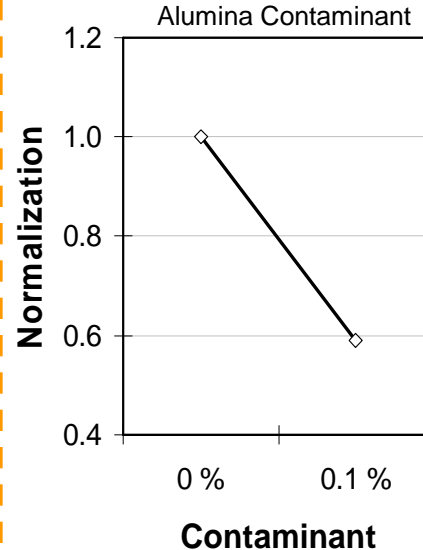
Normalized Spectral Amplitude Comparison

100-mm Wafer Polish

Frequency Range 0 – 15 Hz



Frequency Range 0 – 15 Hz



The addition of 0.1% large particles caused:

- a larger shear force spectral amplitude distribution in 0 – 15 Hz
- a smaller shear force spectral amplitude distribution in 30 – 50 Hz.

Experimental Conditions

Contamination with Large Silica Particles

200-mm Wafer Polish

– Slurries

- Fujimi PL-4217 slurry with 10% (weight percent) silica particles
- Fujimi PL-4217 slurry with 9.9% (weight percent) silica particles and 0.1% (weight percent) large silica particles
- Flow rate: 200 ml/min

– Wafers

- 200-mm blanket oxide wafers

– Pad

- 20-inch IC1000 A2 K-groove pad

– Wafer Polishing

- Polishing pressure: 4 PSI
- Sliding velocity: 1.12 m/s
- Polishing time: 75 s

– Pad Conditioning

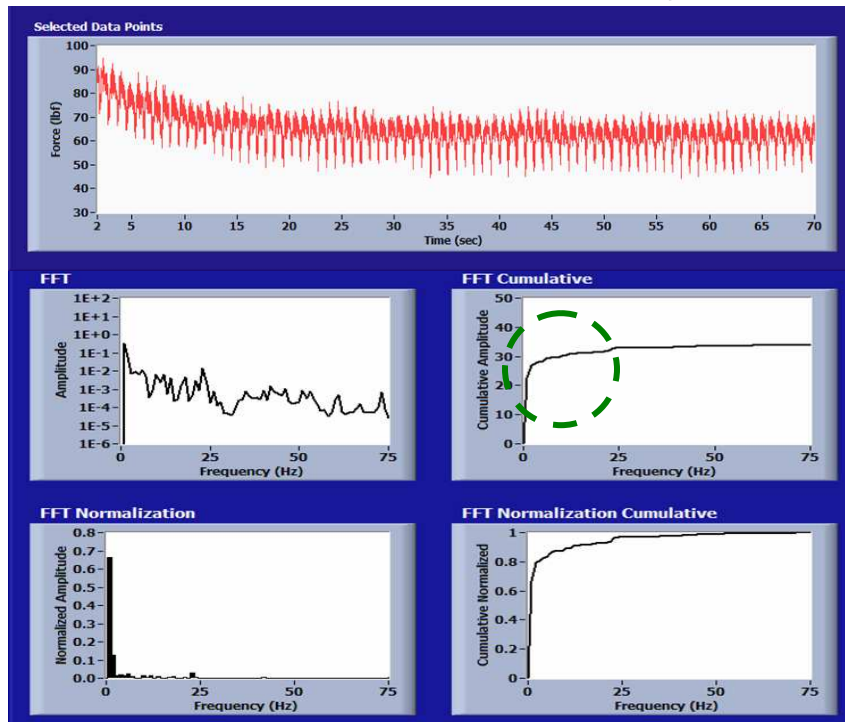
- 4-inch Mitsubishi Materials Corporation 100-grit diamond disc rotating at 30 RPM and sweeping at 20 times/min
- In-situ conditioning at 0.5 PSI

Shear Force Spectral Comparison

Contamination with Larger Silica Particles

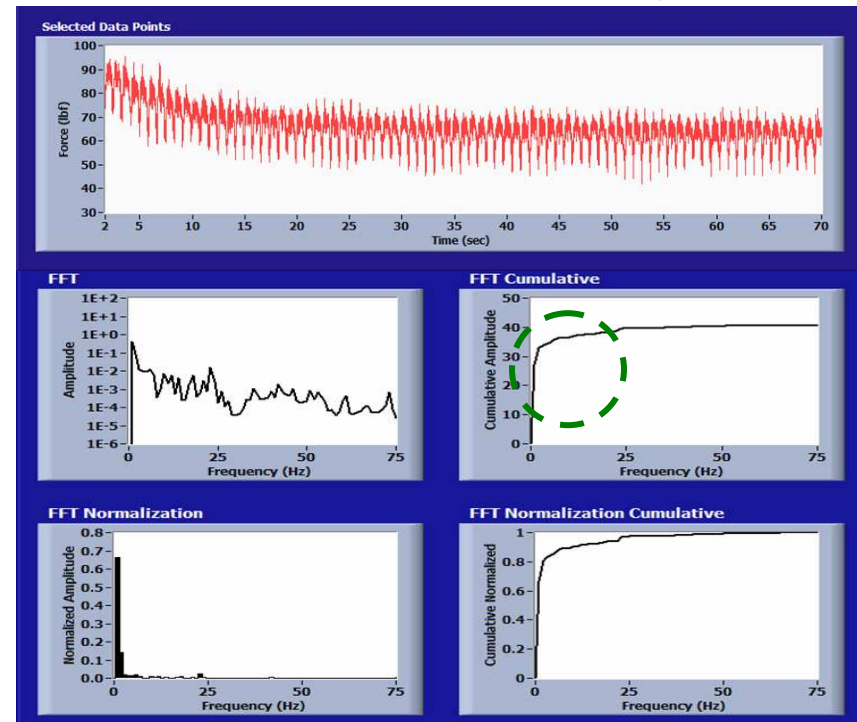
200-mm Wafer Polish

Uncontaminated Slurry



COF: 0.321; Variance of shear force: 65 lb_f^2

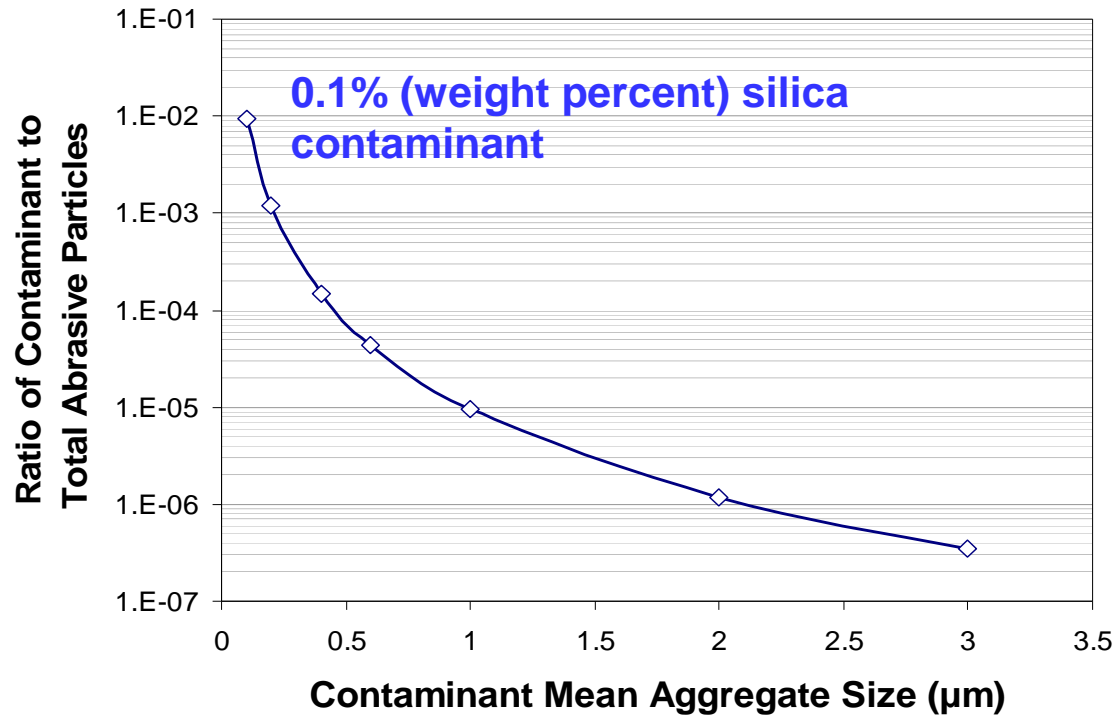
Contaminated Slurry



COF: 0.323; Variance of shear force: 110 lb_f^2

The addition of large silica particles induced a **significantly higher variance of shear force** for the contaminated slurry.

Ratio of Contaminating Silica Particles to Total Abrasive Particles



Size of the primary abrasive particles is assumed to be 0.1 μm .

In a slurry containing 0.1% (weight percent) 2 μm contaminant silica particles, the ratio of the contaminant particles to the total abrasive particles is **1:1,000,000**.

Shear force measurement and analysis are able to detect this level of slurry contamination!

Summary

Real-time shear force measurement and analysis were able to detect slurry contamination caused by small amounts of large abrasive particles:

- **Slurry contaminated with large alumina particles generated a significantly higher COF and variance of shear force. Compared with uncontaminated slurry, shear force spectral amplitude shifted towards lower frequency ranges for the contaminated slurry.**
- **For 100-mm wafer polish, shear force spectral amplitude shifted towards lower frequency ranges for slurry contaminated with large silica particles.**
- **For 200-mm wafer polish, slurry contaminated with large silica particles generated a significantly higher variance of shear force.**

Low-Water and Low-Energy Rinsing and Drying of Patterned Wafers and Nanostructures

Jun Yan, Kedar Dhane, Farhang Shadman
University of Arizona

Bert Vermeire
Arizona State University

Joint work with Freescale:
Hsi-An Kwong, Tom Roche, Jack Shively

Industrial Liaisons: Marie Burnham (Freescale) and
Douglas Goodman (Environmental Metrology Corp.)

Objective and Approach

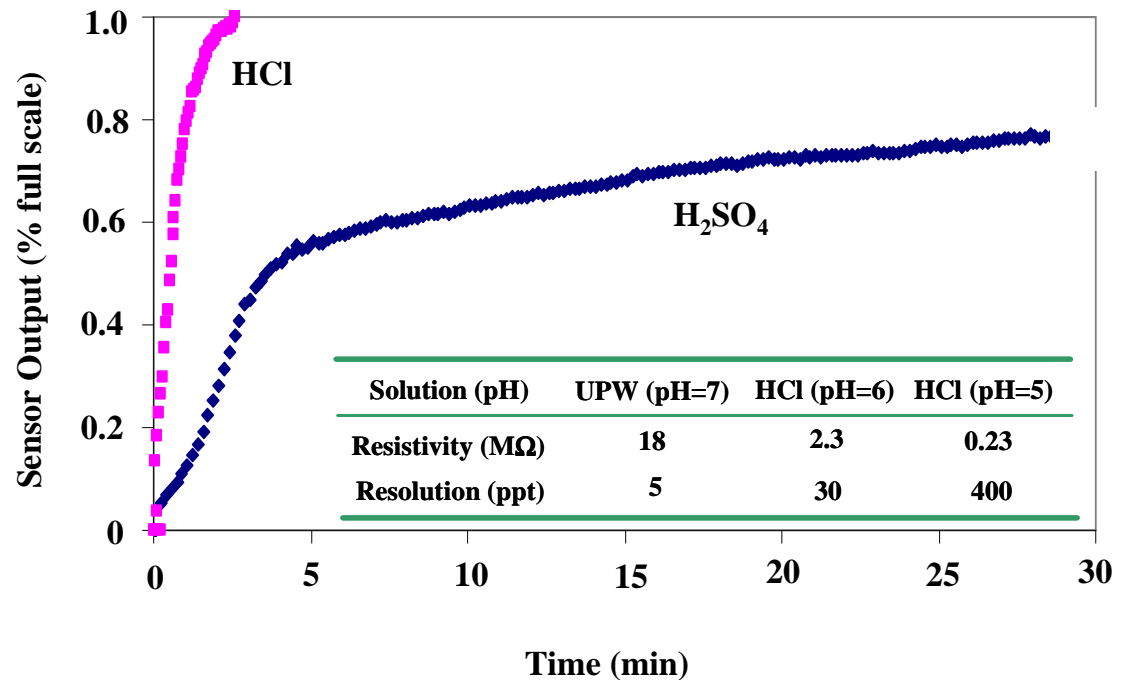
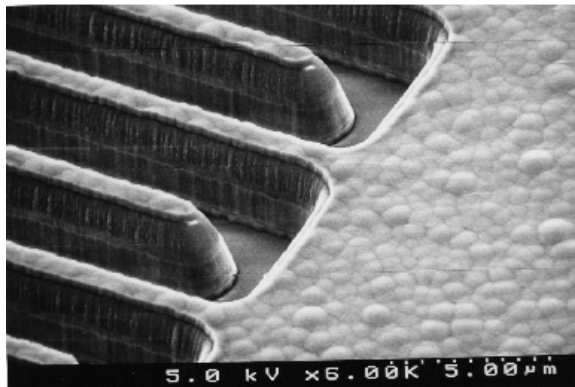
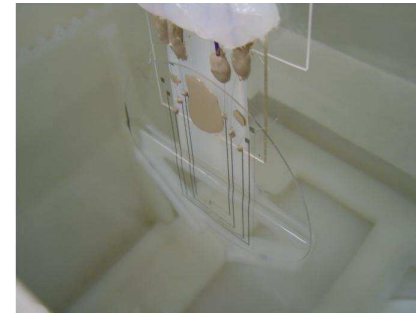
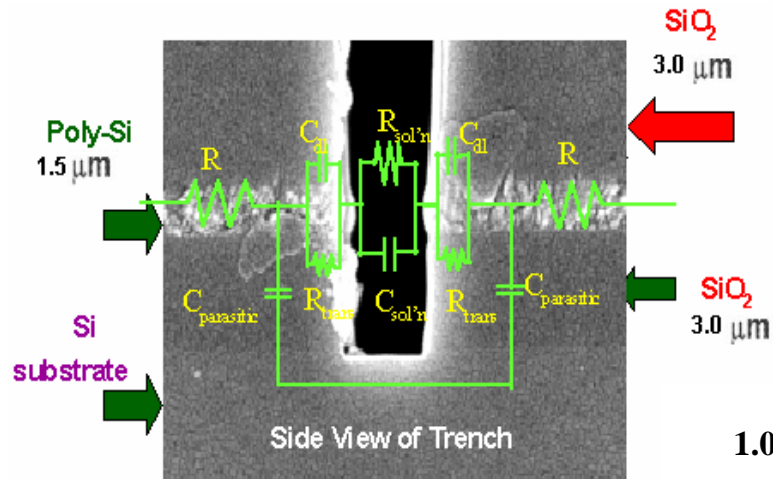
Objectives:

- **Develop technology for reducing water, energy, and chemicals used during cleaning of patterned wafers, without sacrificing the cleaning performance**

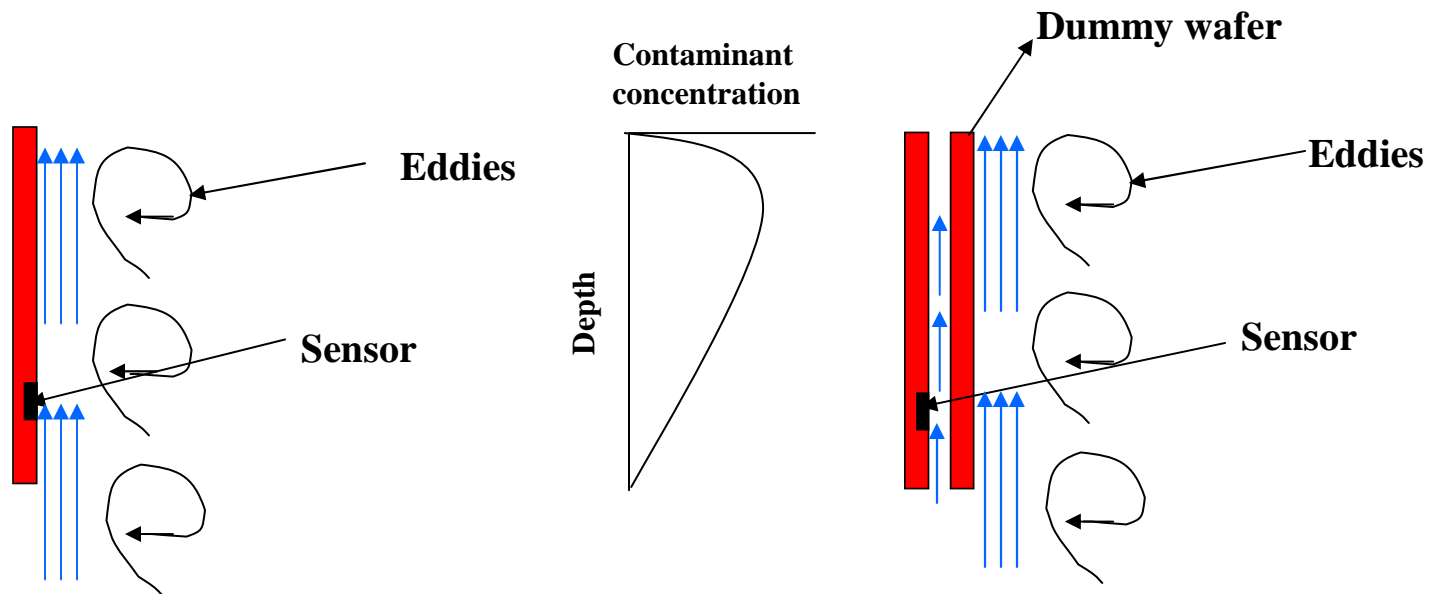
Approach:

- **Develop a novel sensor for in-situ and real-time measurement of residual contamination in microstructures during wafer cleaning, rinsing, and drying**
- **Develop new cleaning methods, using sensor measurements and process modeling**

On-Line Metrology for Low-Water Rinsing and Cleaning



Effect of Mixing on Cleaning

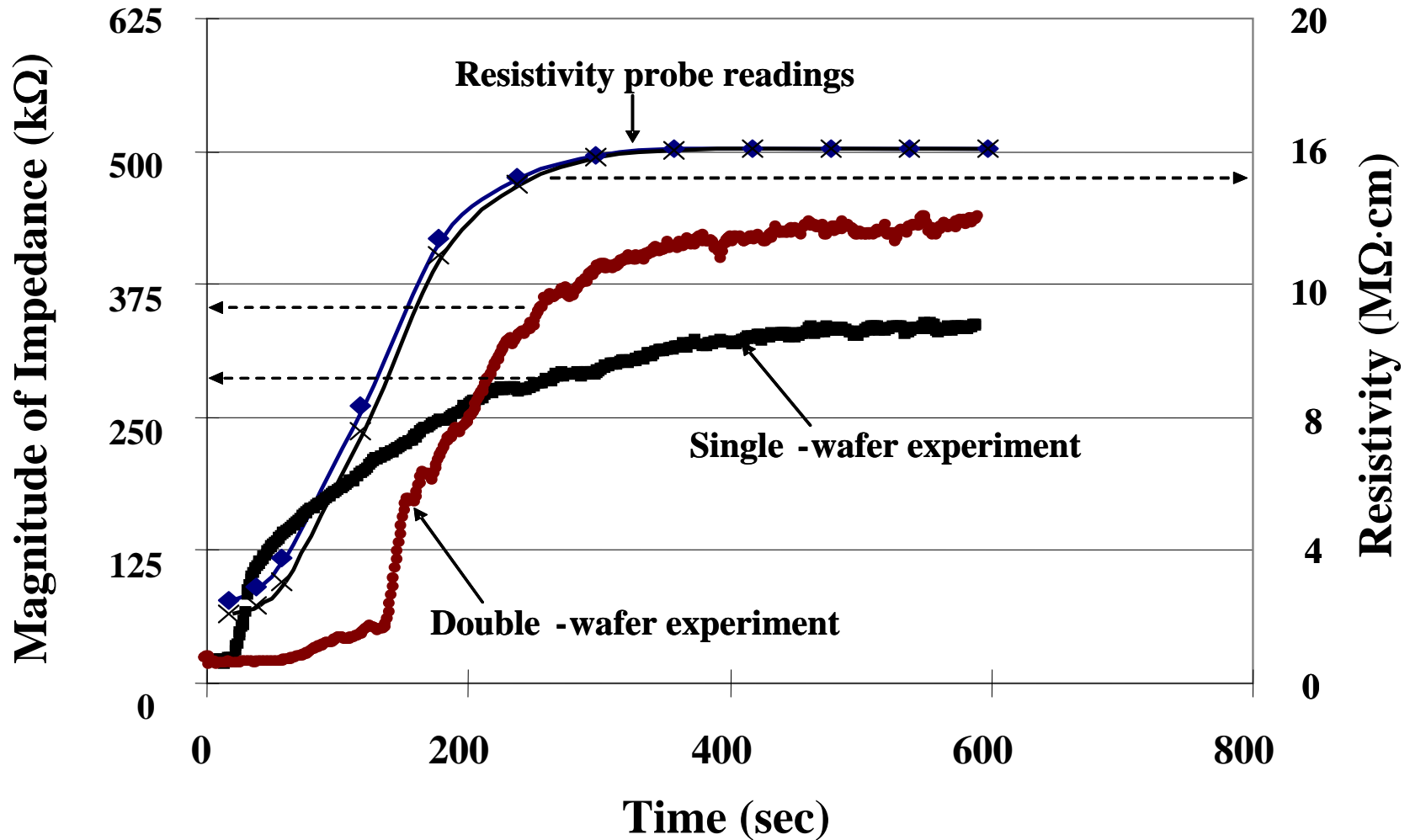


- **Single-wafer configuration**
- **High convective and turbulent flow**
- **Good mixing**

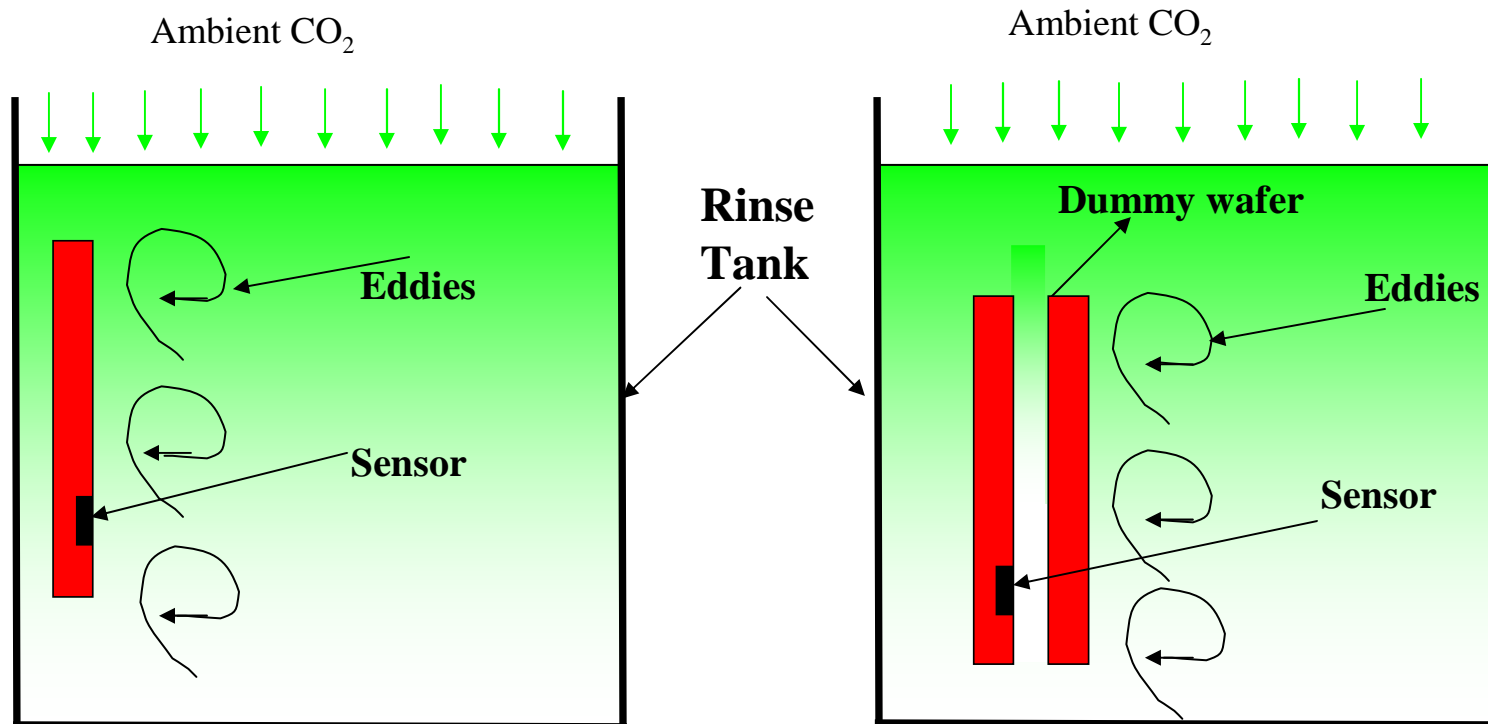
- **Multi-wafer configuration**
- **Slow laminar flow between wafers**
- **Poor mixing**

Sensor Performance and Capabilities

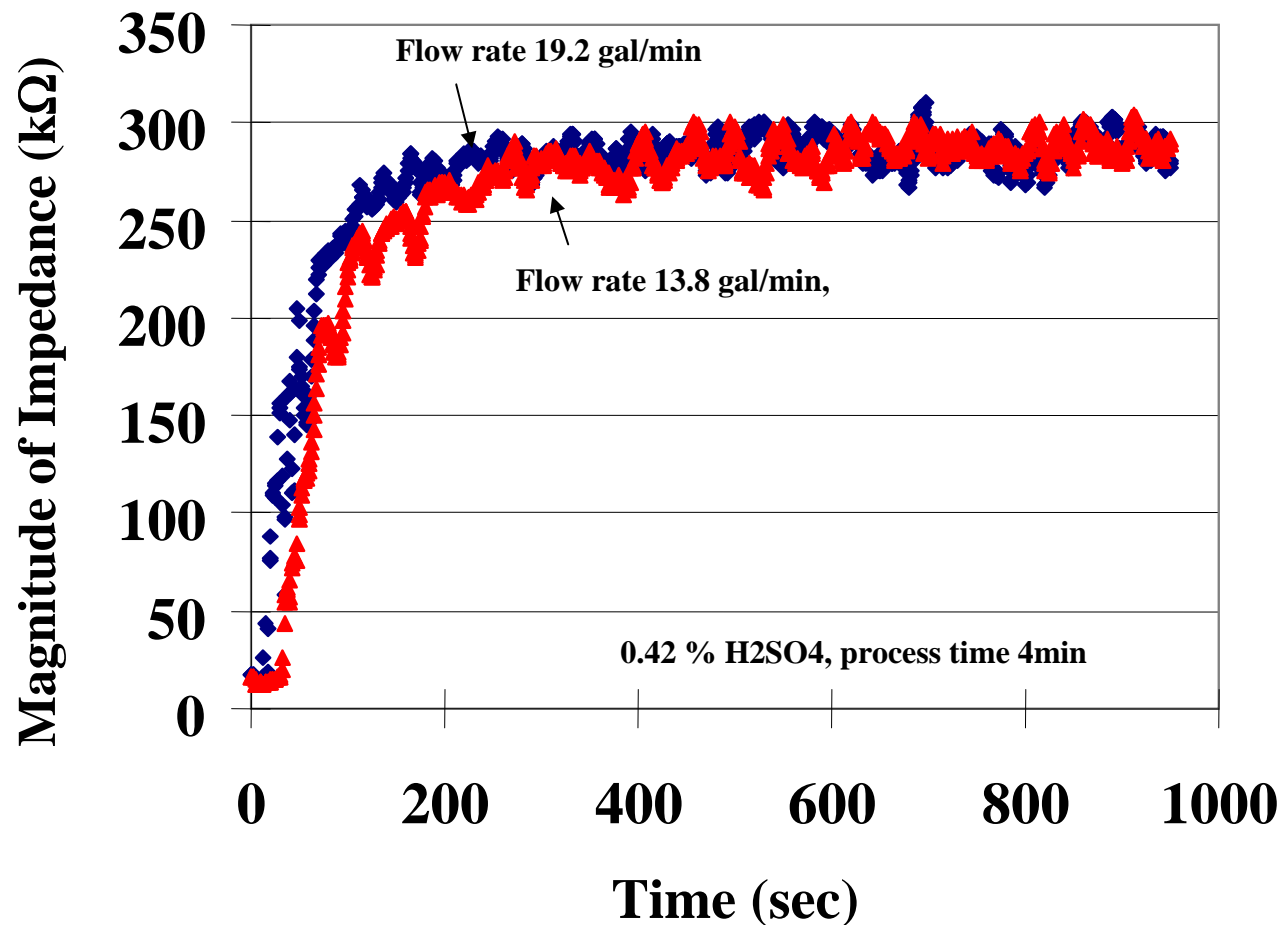
H₂SO₄ Rinsing



Dissolution and Dispersion of Ambient CO₂ in Rinse Tank

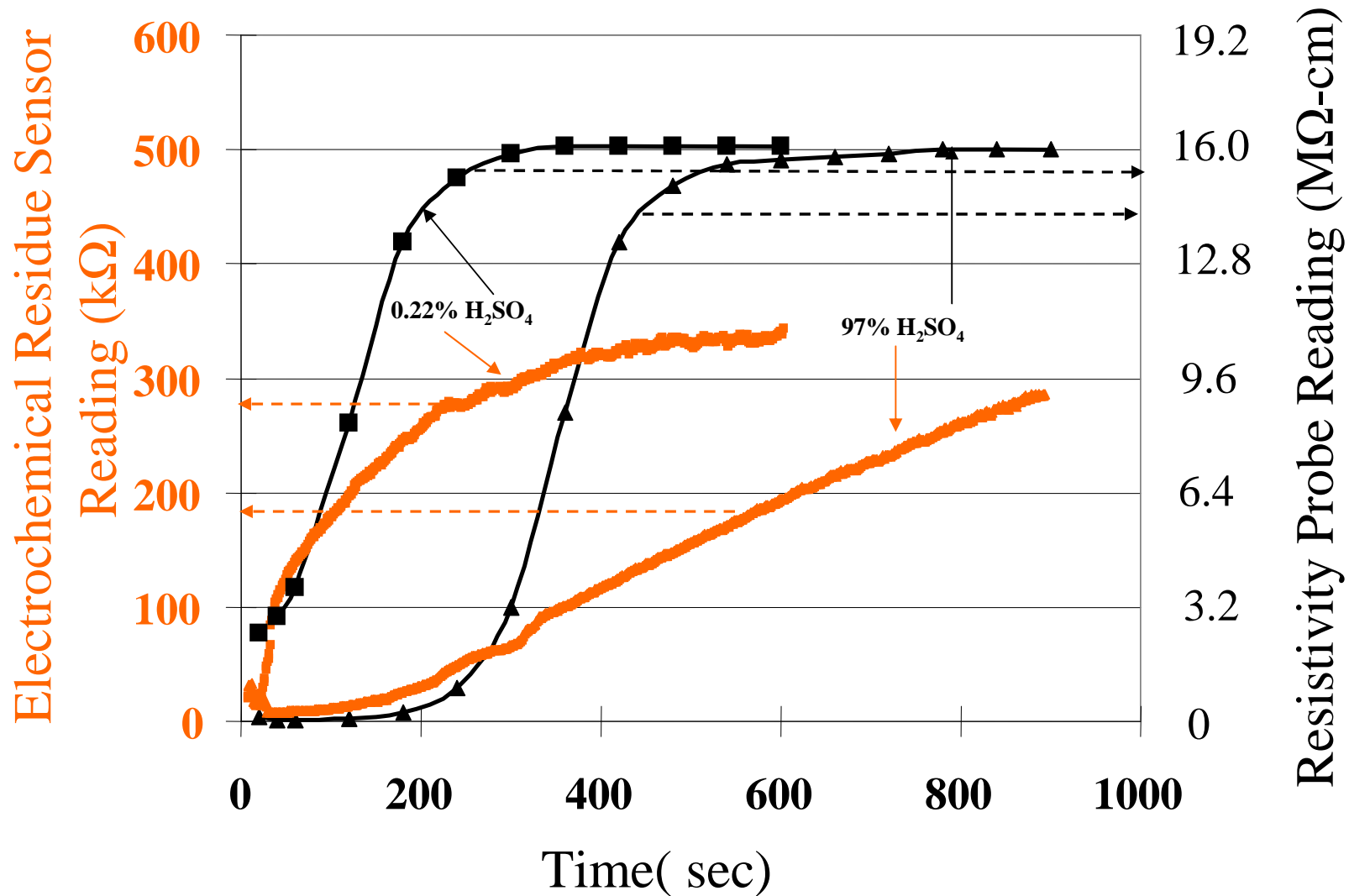


Effect of Flow Rate on H₂SO₄ Rinsing

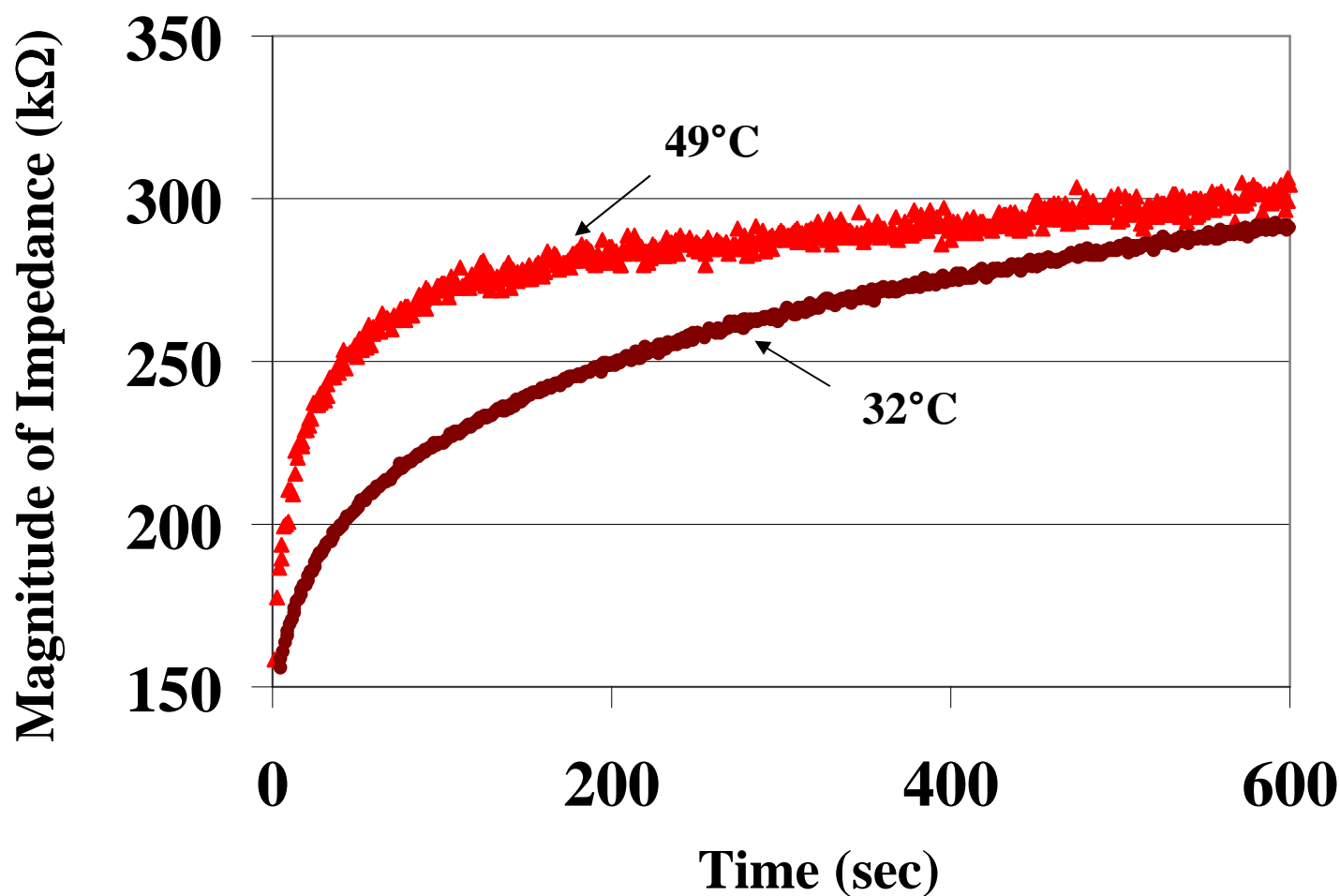


No Significant gain in cleaning by increasing the flow rate

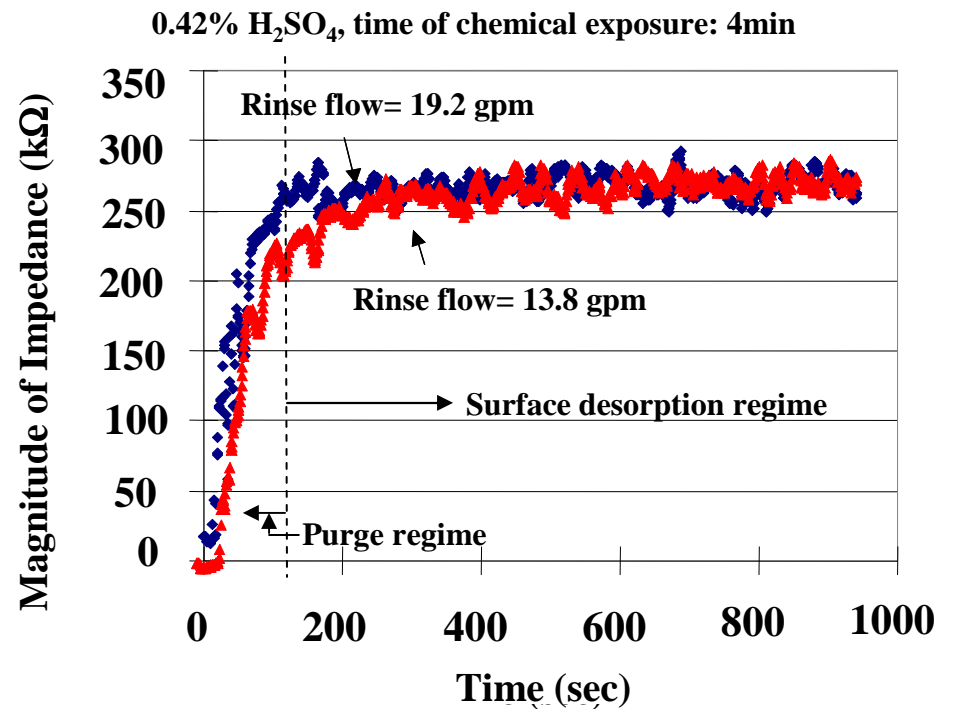
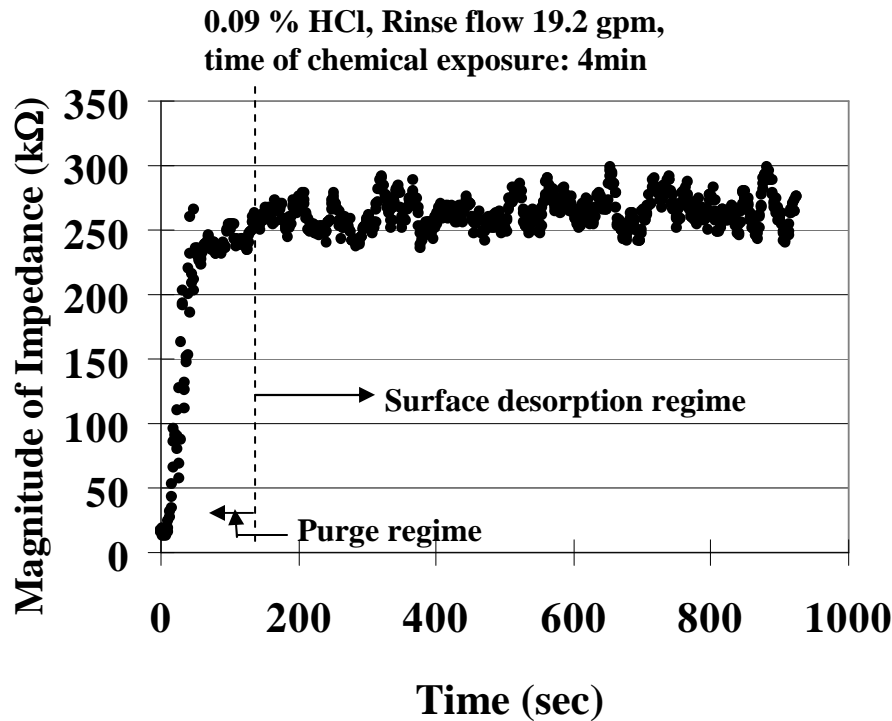
Effect of Concentration on H₂SO₄ Rinsing



Effect of Temperature on H₂SO₄ Rinsing



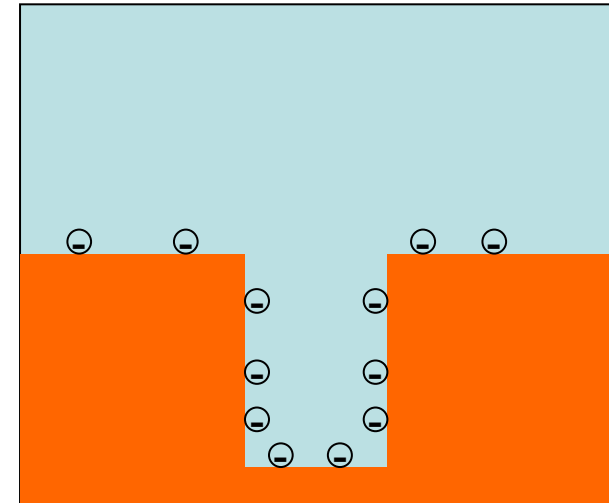
Rinse Optimization Implications



- Transitions from *tank purge regime* to *surface desorption regime* after 2-3 min.
- High flow-rate does not help rinse during the surface desorption regime.

Fundamental Processes During Cleaning and Rinsing of Patterned Wafers

- Transport of the cleaning chemical from the bulk phase into the boundary (migration and diffusion)
- Transport of the cleaning chemical into the feature (diffusion, charge effect, side-wall effect)
- Surface processes (dissolution, adsorption, and desorption)
- Reverse of the above steps for the removal of by-products out of the trench



Comprehensive Simulation of Rinse Process

Transport equation for H^+ , OH^- , NH_4^+ and SO_4^{2-} :

$$\frac{\partial C_i}{\partial t} = \nabla \cdot (D_i \nabla C_i + z_i \mu_i F C_i \nabla \phi)$$

Surface adsorption and desorption :

$$\frac{\partial C_{s2}}{\partial t} = (k_{a2} C_i (S_o - C_{s2}) - k_d C_{s2})$$

Poisson equation, relating charge distribution in the trench and boundary layer:

$$\nabla^2 \phi = -\frac{\rho}{\epsilon}$$

where charge density,

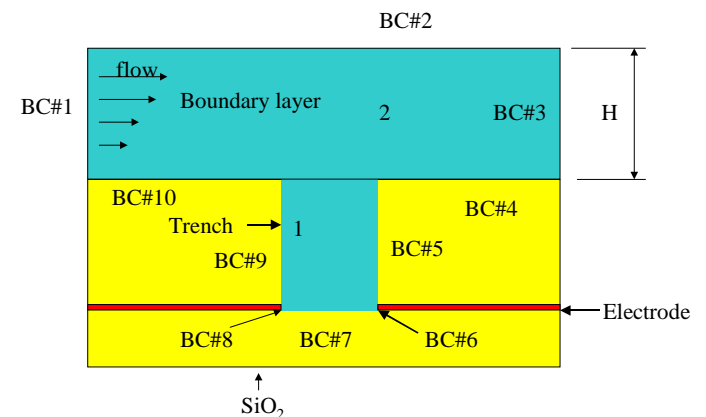
$$\rho = F \sum_i z_i C_i$$

Ohm's law to relate concentration to the impedance:

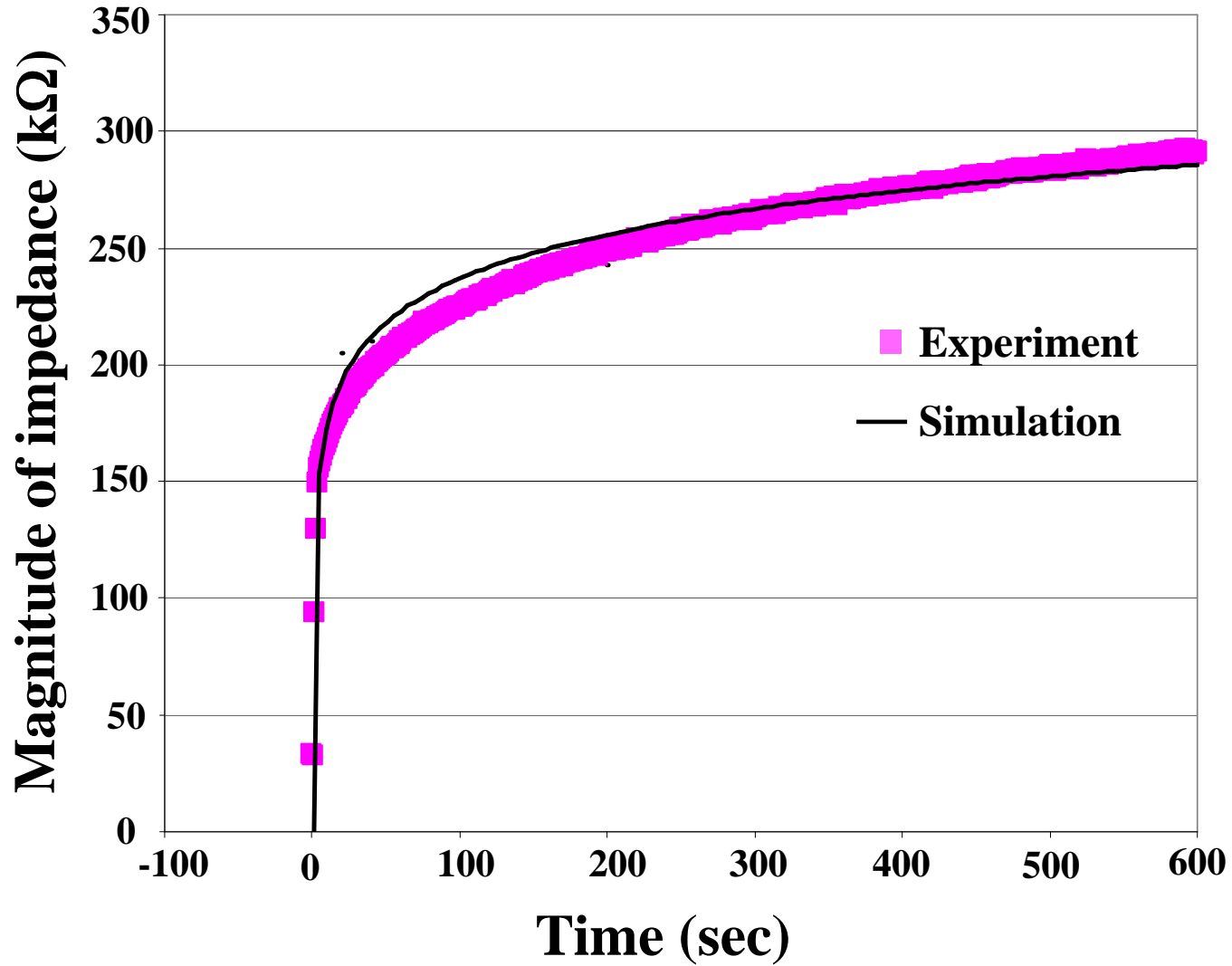
$$\sigma E = J \quad \text{and} \quad \nabla E = 0$$

where electrical conductivity,

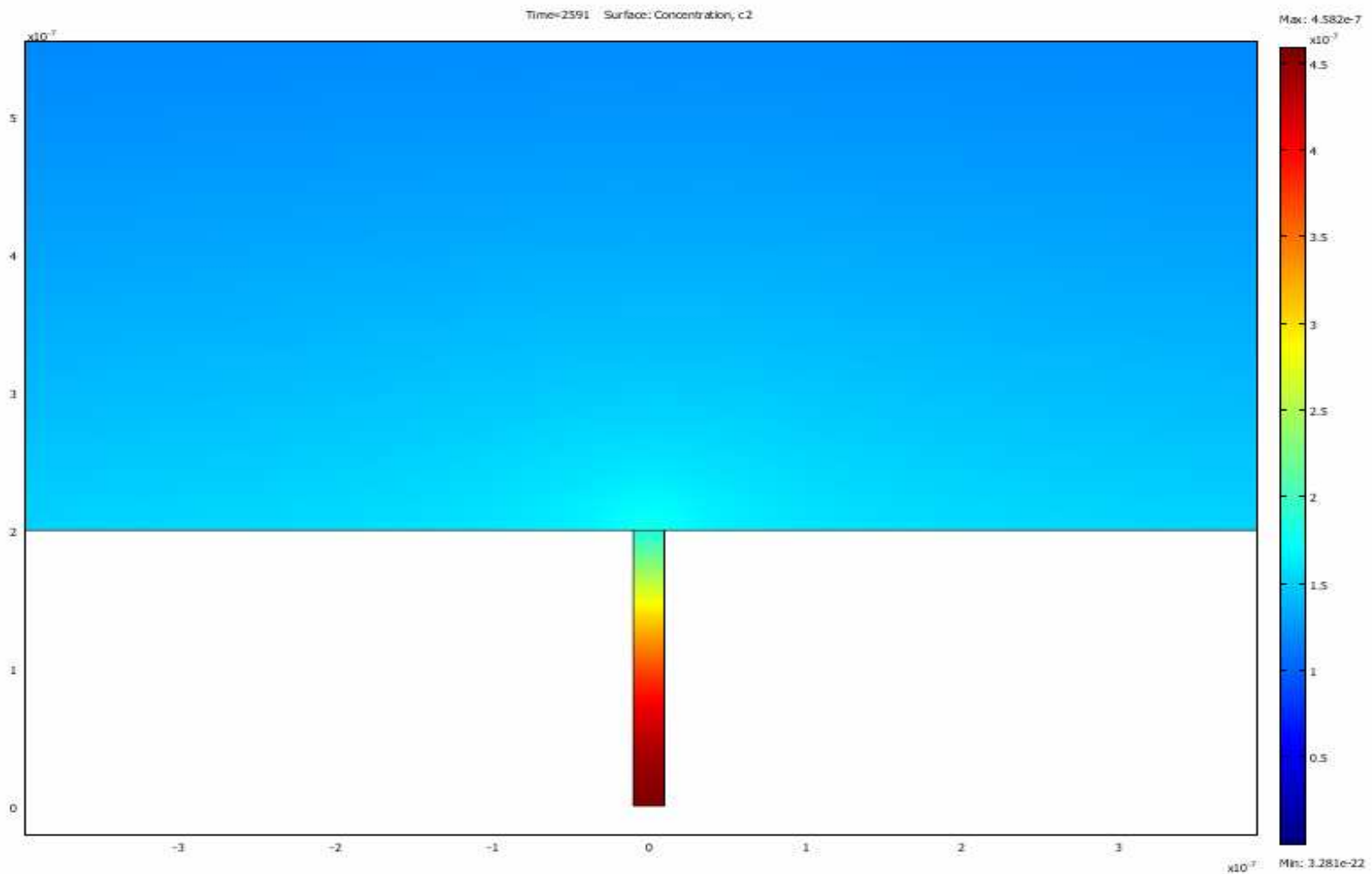
$$\sigma = \sum_i \lambda_i C_i$$



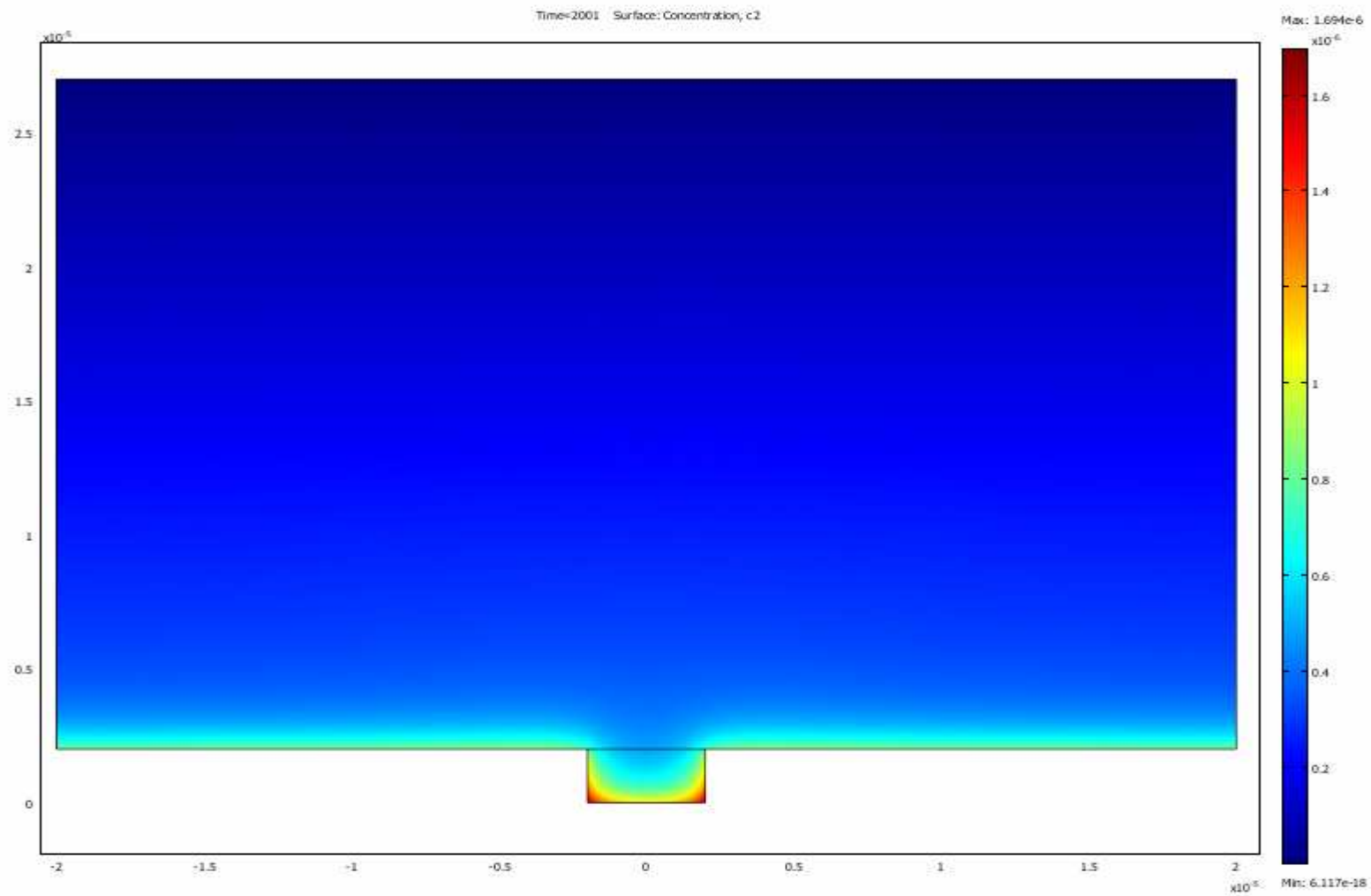
Model Fit to the Experimental Data



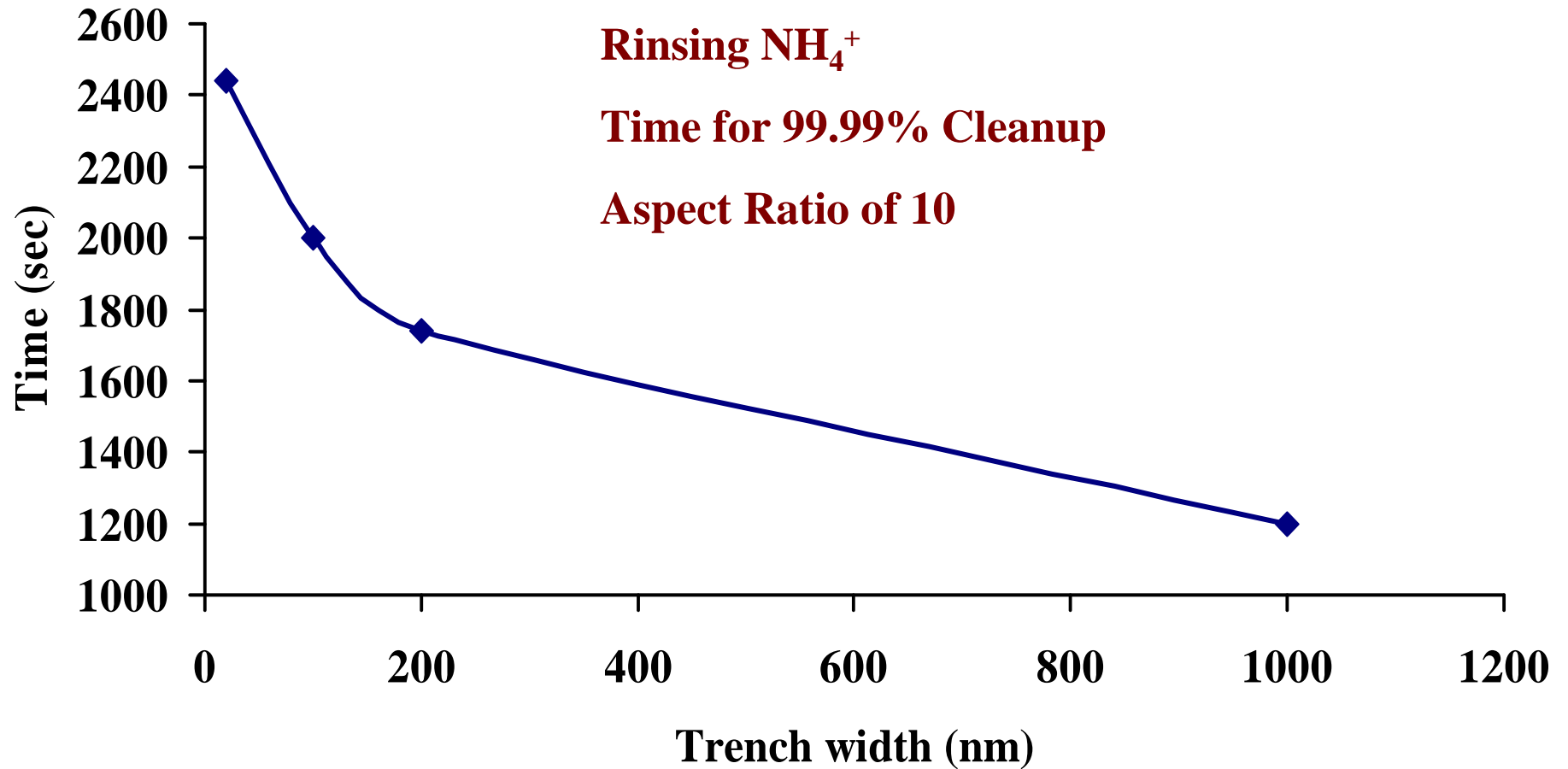
NH₄⁺ Rinse out of 20nm Trench



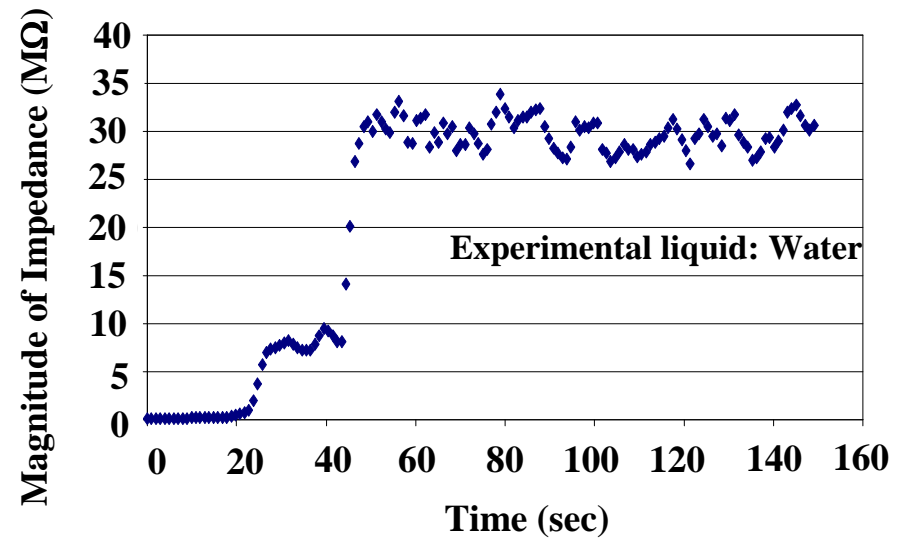
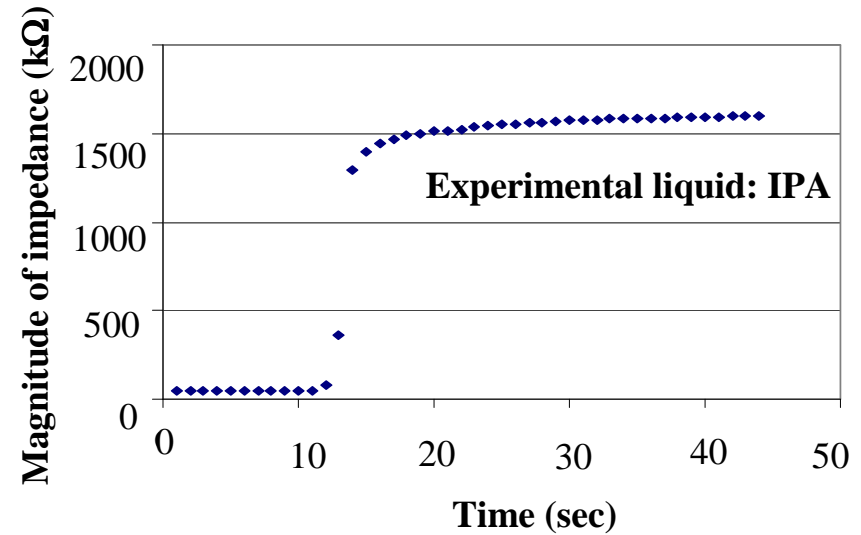
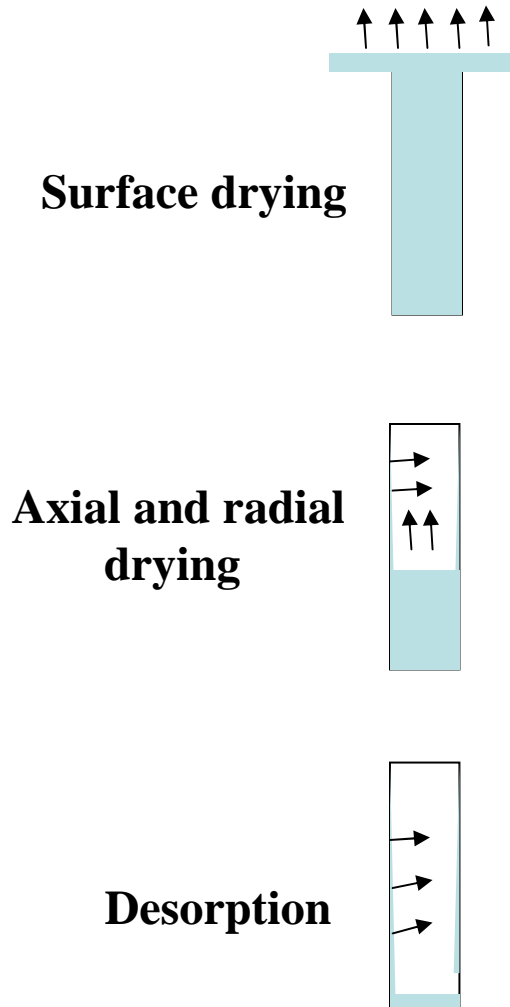
NH₄⁺ Rinse out of 4 Micron Trench



Effect of Feature Size on Cleaning



Material and Energy Use Reduction in Drying Processes



Conclusions

- **Improved the ECSR design for better S/N and direct tool integration**
- **Developed and verified a comprehensive process model; the model is applicable to rinsing and cleaning of fine structures on patterned wafers.**
- **Used ECRS measurements and process modeling to develop rinse processes that require significantly less water and energy.**
- **Have been working with Freescale team towards developing a new rinse recipe based on staged flow rate.**
- **Based on preliminary tests, concluded that water use reduction of 40% (cold rinse) and 50% (hot rinse) is achievable.**

Future Plans and Technology Transfer

- **Investigate the application of ECRS technology for other applications (drying and post-etch cleaning of sidewalls)**
- **Continue joint work with Sematech and the Freescale task force to validate and implement the project results.**
- **Commercialize the ECRS through joint work with Environmental Metrology Corp.**
- **Continue collaboration and technology transfer that has been initiated with other members (e.g. Samsung)**

Acknowledgement

- **Primary Funding by SRC/Sematech ERC**
- **Partial Funding by Environmental Metrology Corp**
- **Technology Transfer and Industrial Liaisons:**
 - **Marie Burnham (Freescale Semiconductor, Inc.)**
 - **Douglas Goodman (Environmental Metrology Corp.)**
- **Fabrication Assistance:**
 - **MFC (University of Arizona)**
 - **CSSER (Arizona State University)**
 - **SNF (Stanford University)**

**Environmentally-Friendly Cleaning of New
Materials and Structures for Future Micro- and
Nano-Electronics Manufacturing**

Drying of Thin Porous Low- k Films

**Asad Iqbal*, Junpin Yao*, Harpreet Juneja*, Farhang Shadman*, and
Ting Tsui#**

***Chemical and Environmental Engineering, University of Arizona**

#Texas Instruments, Austin, Texas

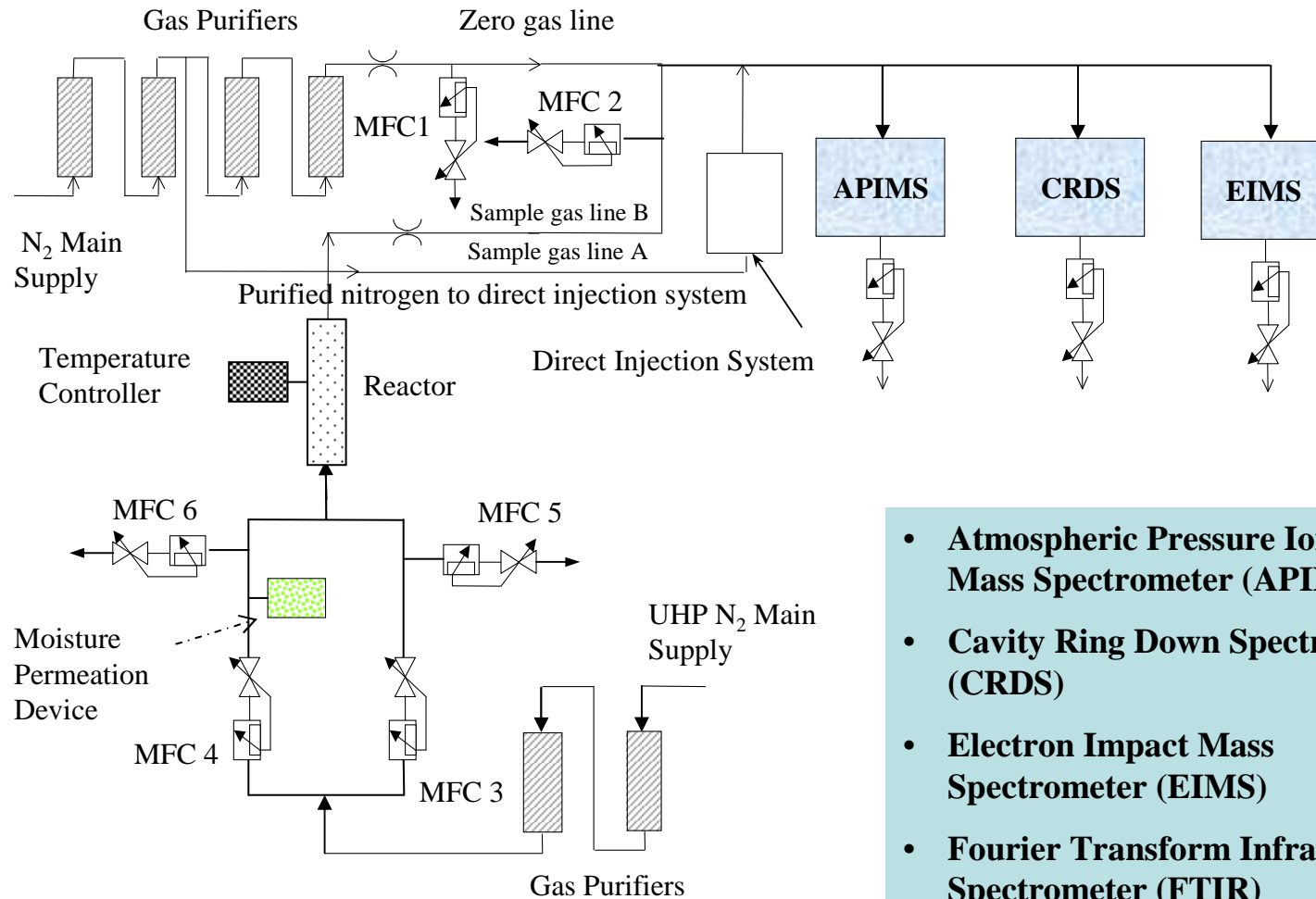
Background

- **Moisture can deteriorate the k value, create adhesion problems, and cause reliability issues.**

Objectives

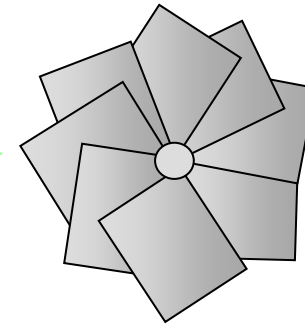
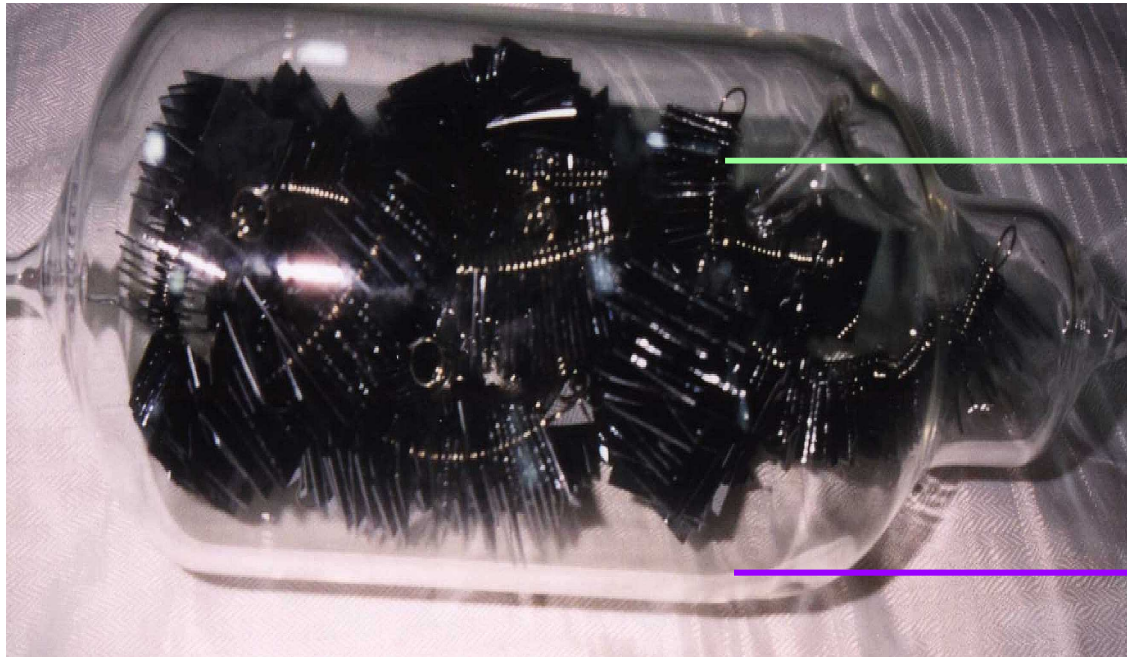
- **Determine the fundamentals of moisture interactions and outgassing in both uniform and non-uniform porous low- k films:**
 - loading
 - molecular transport
 - chemical interactions
 - removal
- **Develop experimental and process modeling techniques for minimizing the chemical and energy usage during cleaning and purging of low- k films.**

Experimental Setup



- **Atmospheric Pressure Ionization Mass Spectrometer (APIMS)**
- **Cavity Ring Down Spectroscopy (CRDS)**
- **Electron Impact Mass Spectrometer (EIMS)**
- **Fourier Transform Infrared Spectrometer (FTIR)**

Experimental Reactor

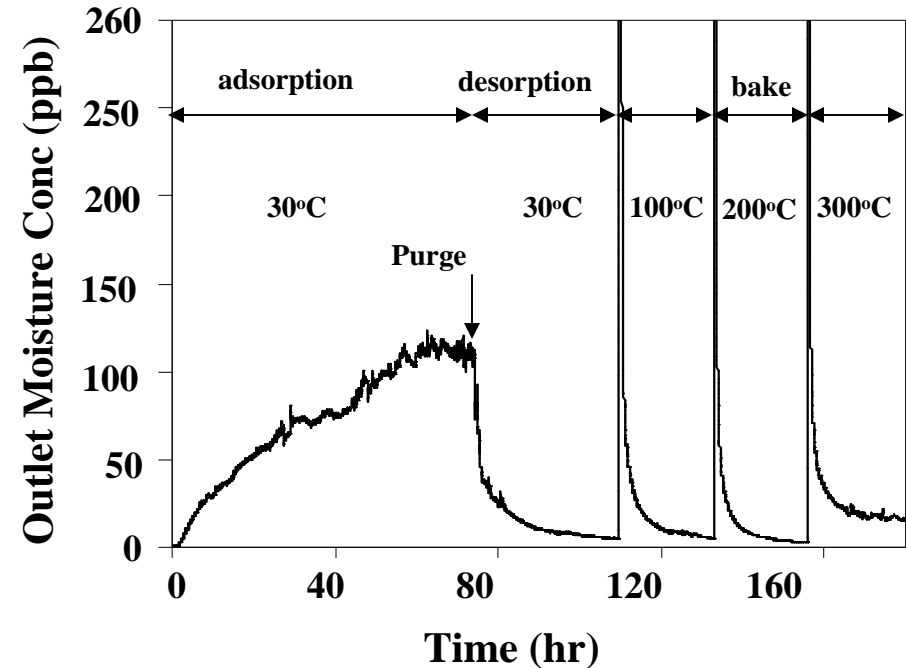
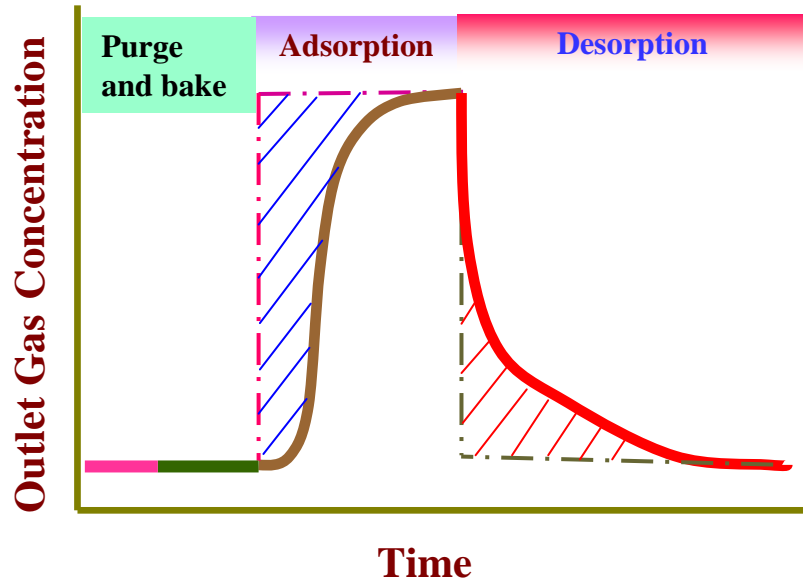


Wafer coupons loaded
on springs

Pyrex reactor

- 1 x 2 cm coupons
- Random orientation results in adequate gas mixing
- High wafer to glass surface area ratio

Experimental Procedure



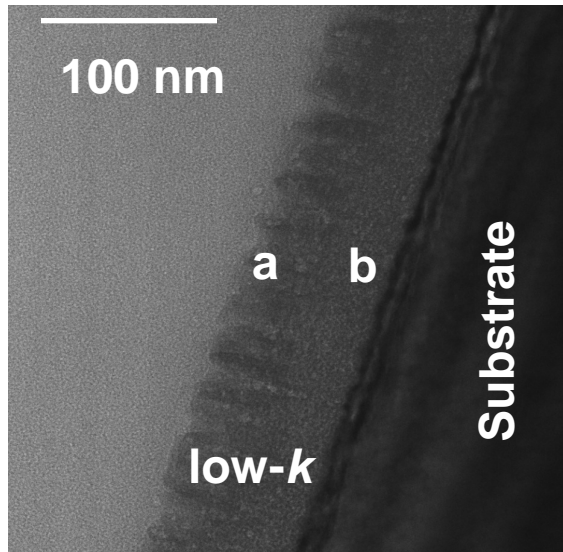
Experimental procedure

Adsorption at 30°C; then desorption at 30°C; followed by bake-out at 100, 200 & 300°C

Temporal profile

Exposure to 110 ppb moisture; followed by temperature-programmed desorption

TEM Images

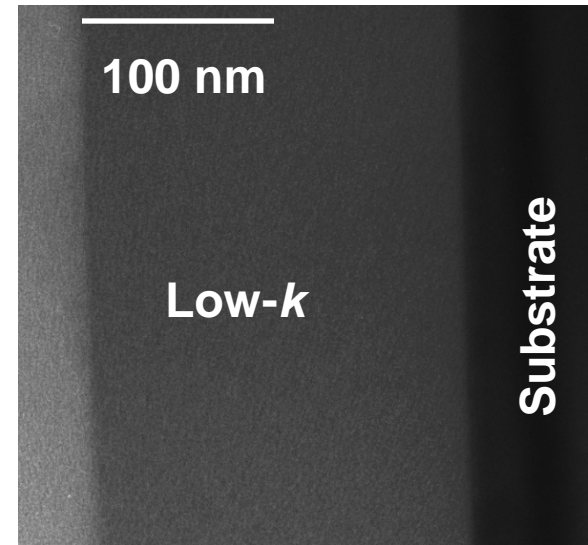


a – Damaged low-*k* layer, 50 nm

b – Bulk low-*k* layer, 50 nm

Low-*k* thickness ~ 100 nm

p-MSQ -- Partial etch, N₂H₂ ash

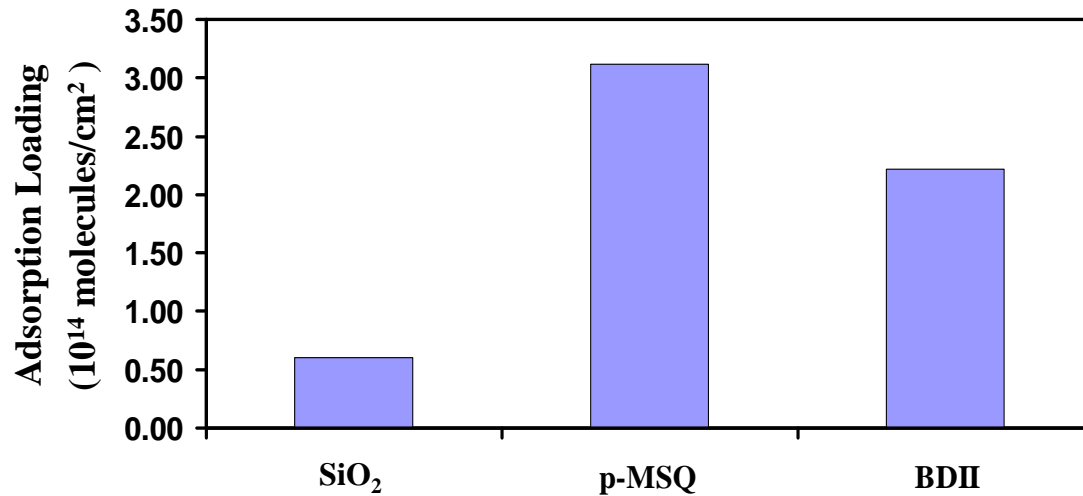


Low-*k* thickness ~ 200 nm

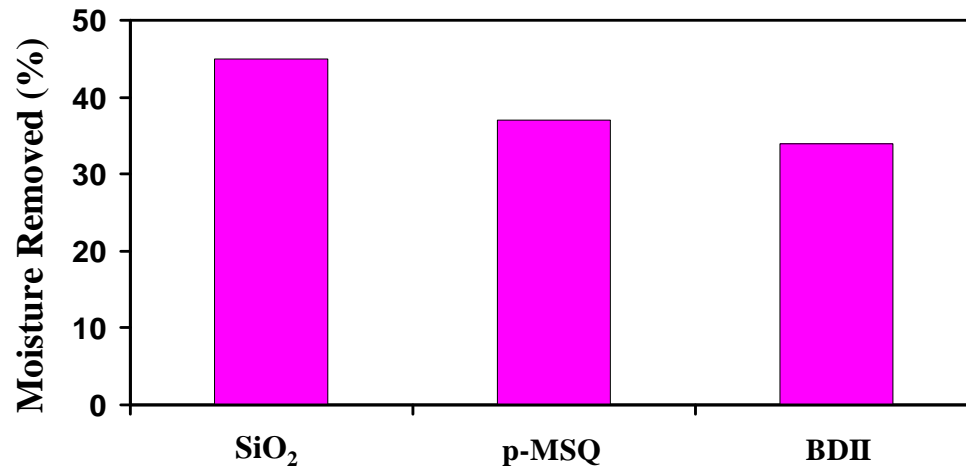
p-MSQ -- blanket and cure only

Moisture Loading and Retention Comparison

Challenge Concentration: 56 ppb; Purge Time: 10 hr

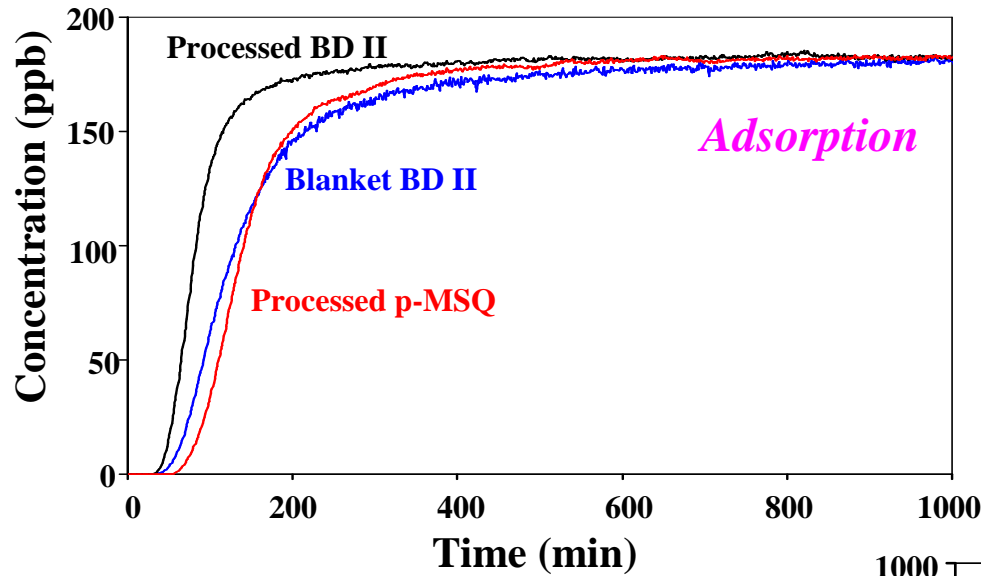


Porous low-*k* films have much higher sorption loading than SiO₂



Moisture removal is a very slow process

Comparison between p-MSQ & BD II



Challenge Conditions:

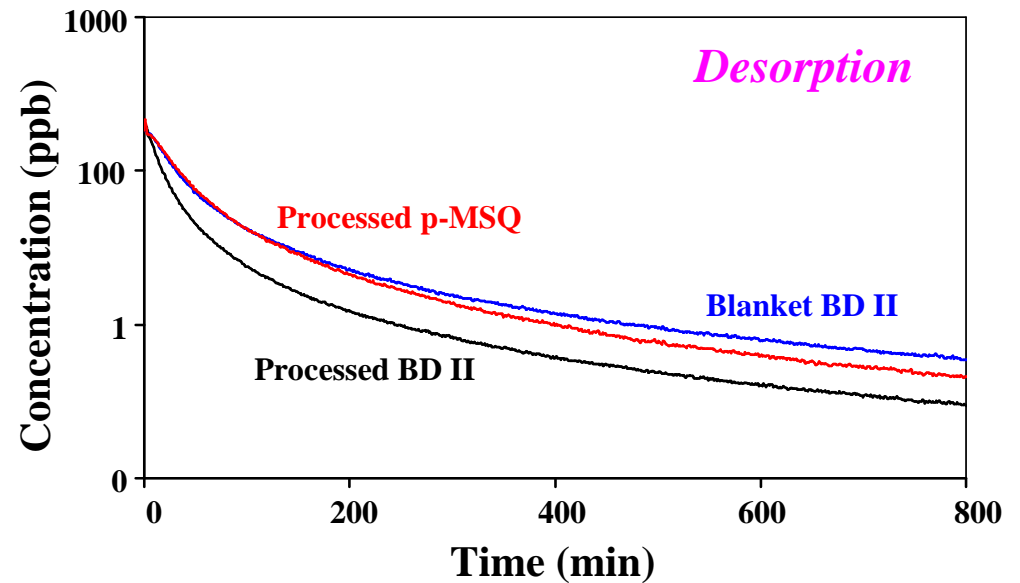
Concentration: 181 ppb

Temperature: 30°C

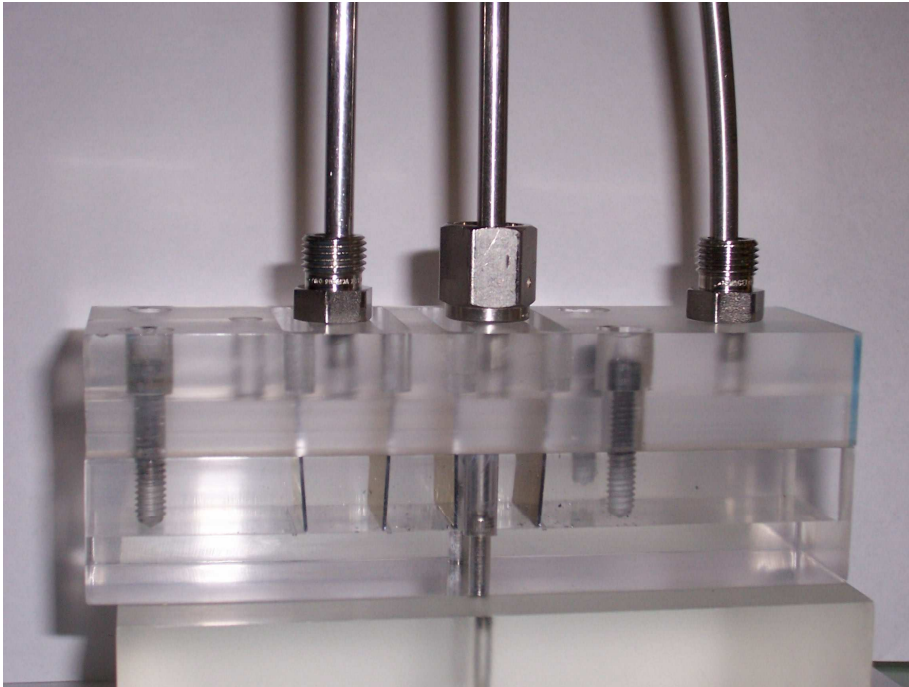
Purge Conditions:

Temperature: 30°C

Purge Purity: 1 ppb

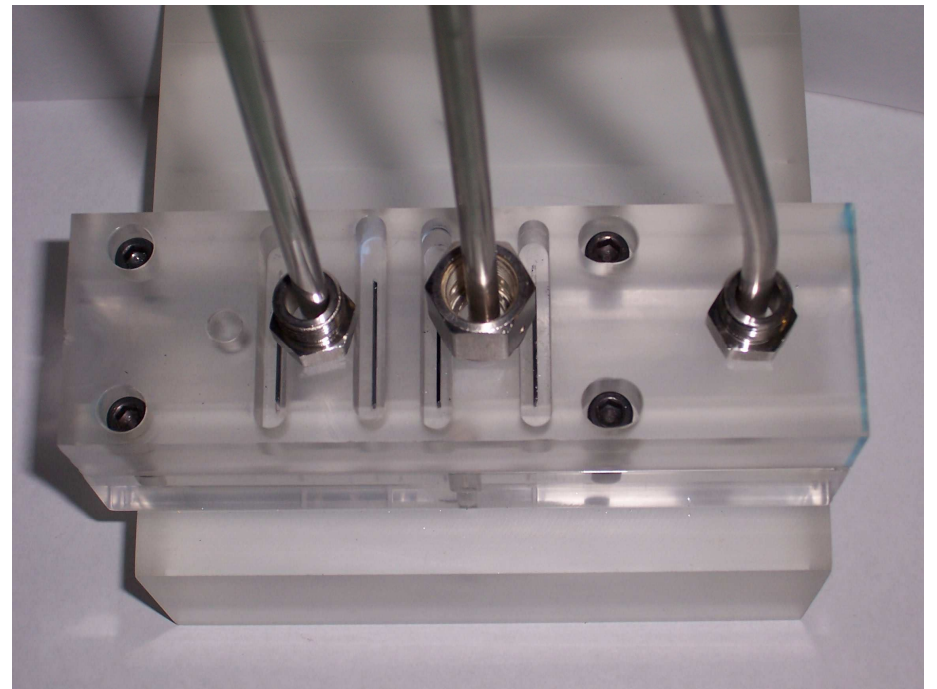


FTIR Cell Design

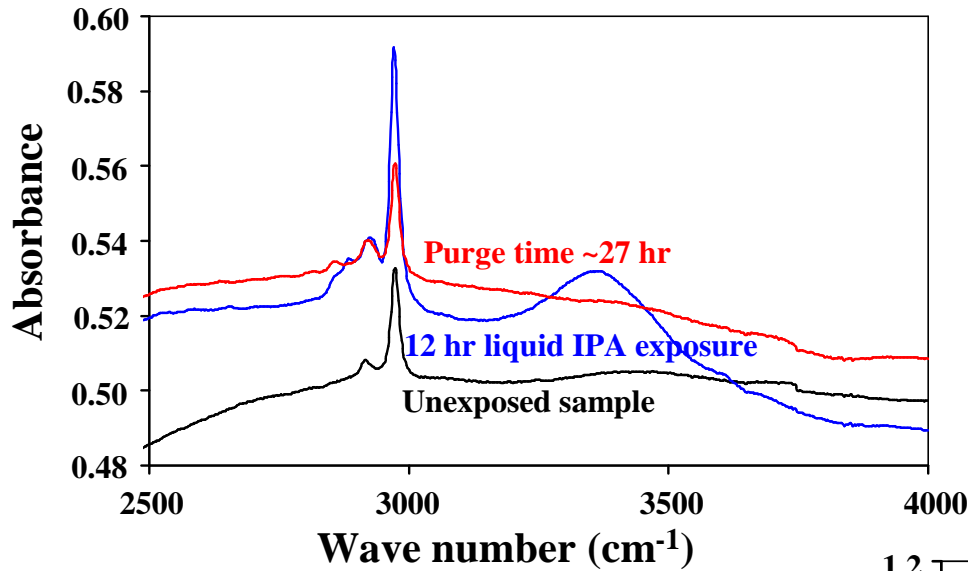


Side View

Top View

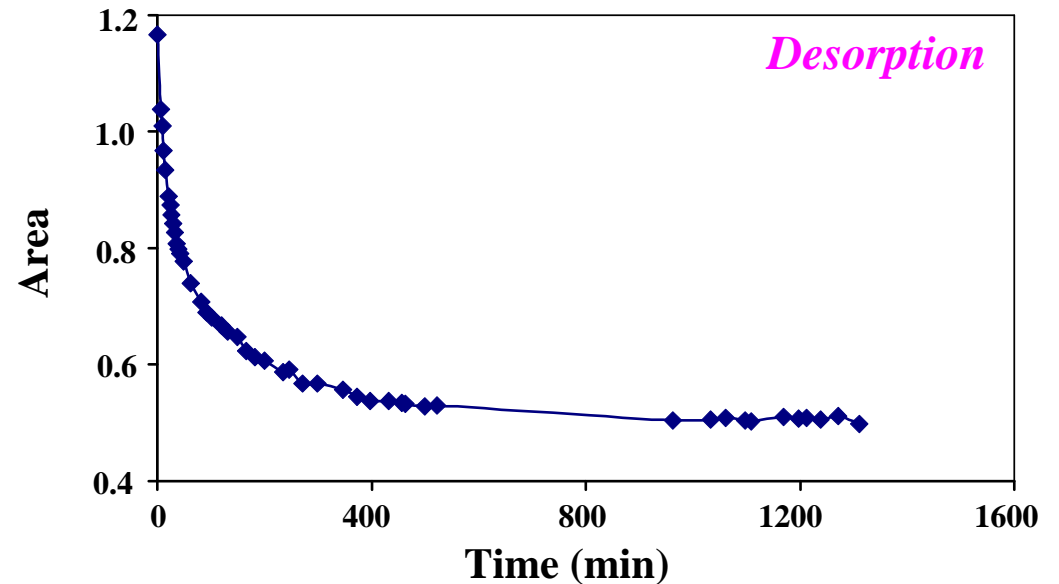


Outgassing Dynamics of IPA using FTIR

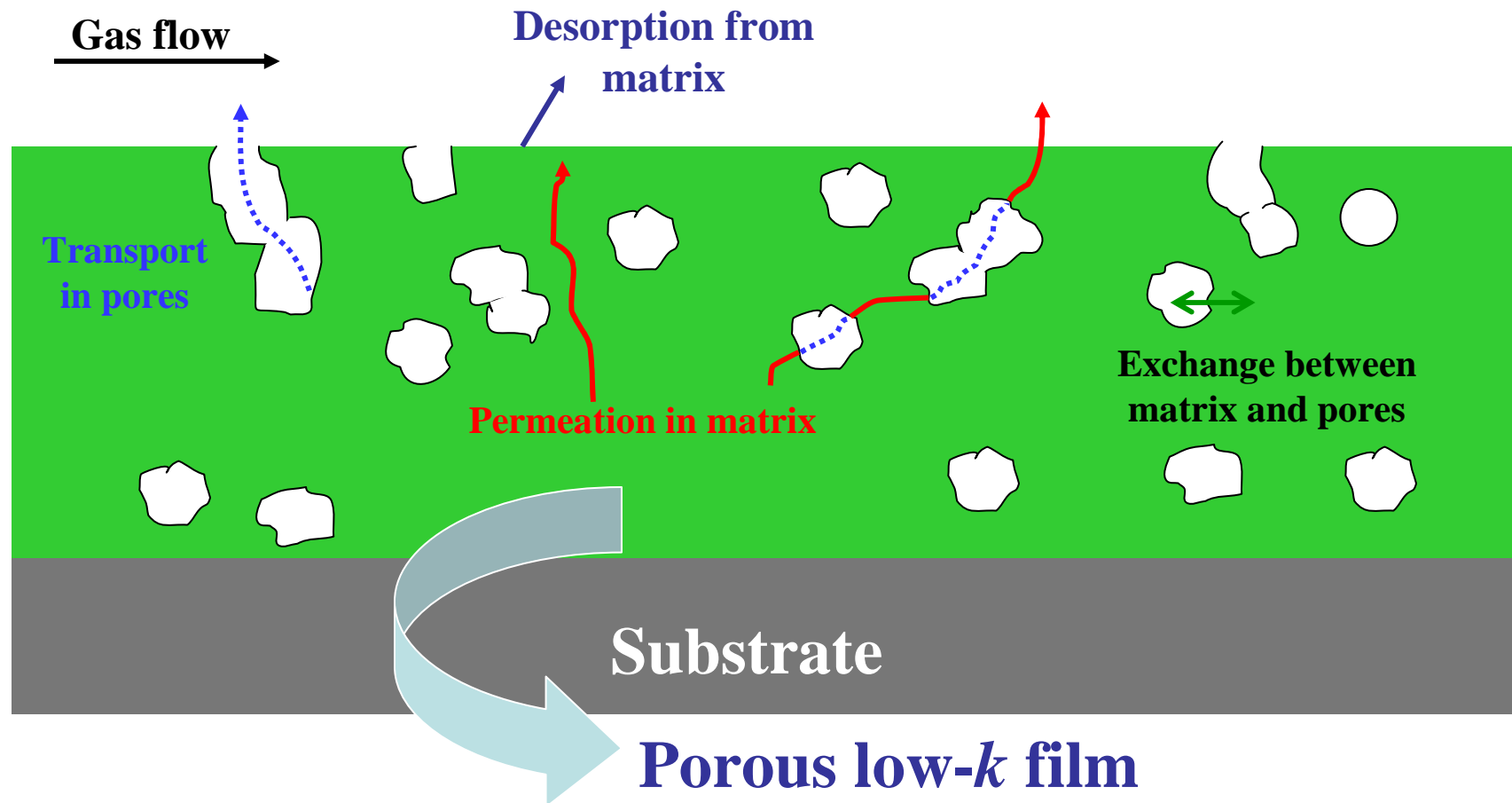


FTIR Spectra for IPA Exposure

Peak Area: 2950 – 3000
Wave number



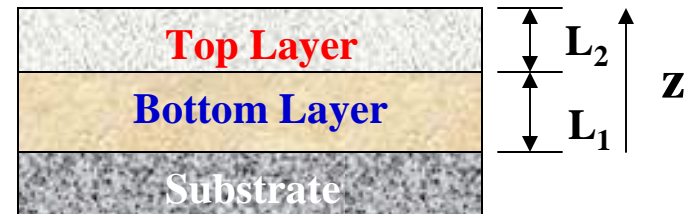
Moisture Transport Pathways in Porous Low- k Film



Process Model for Non-Uniform Films

Transport of moisture in matrix:

$$\frac{\partial C_s}{\partial t} = \frac{1}{1-\varepsilon} \frac{\partial}{\partial z} \left[(1-\varepsilon) D_s \frac{\partial C_s}{\partial z} \right] - \frac{\varepsilon}{1-\varepsilon} k_m S_p \left(\frac{C_s}{S} - C_g \right)$$



Transport of moisture in pore:

$$\frac{\partial C_g}{\partial t} = \frac{1}{\varepsilon} \frac{\partial}{\partial z} \left[\varepsilon D_g \frac{\partial C_s}{\partial z} \right] + k_m S_p \left(\frac{C_s}{S} - C_g \right)$$

C_s / C_g : Moisture concentration in matrix / pore;

D_s / D_g : Moisture diffusivity in matrix / pore;

ε : Film porosity;

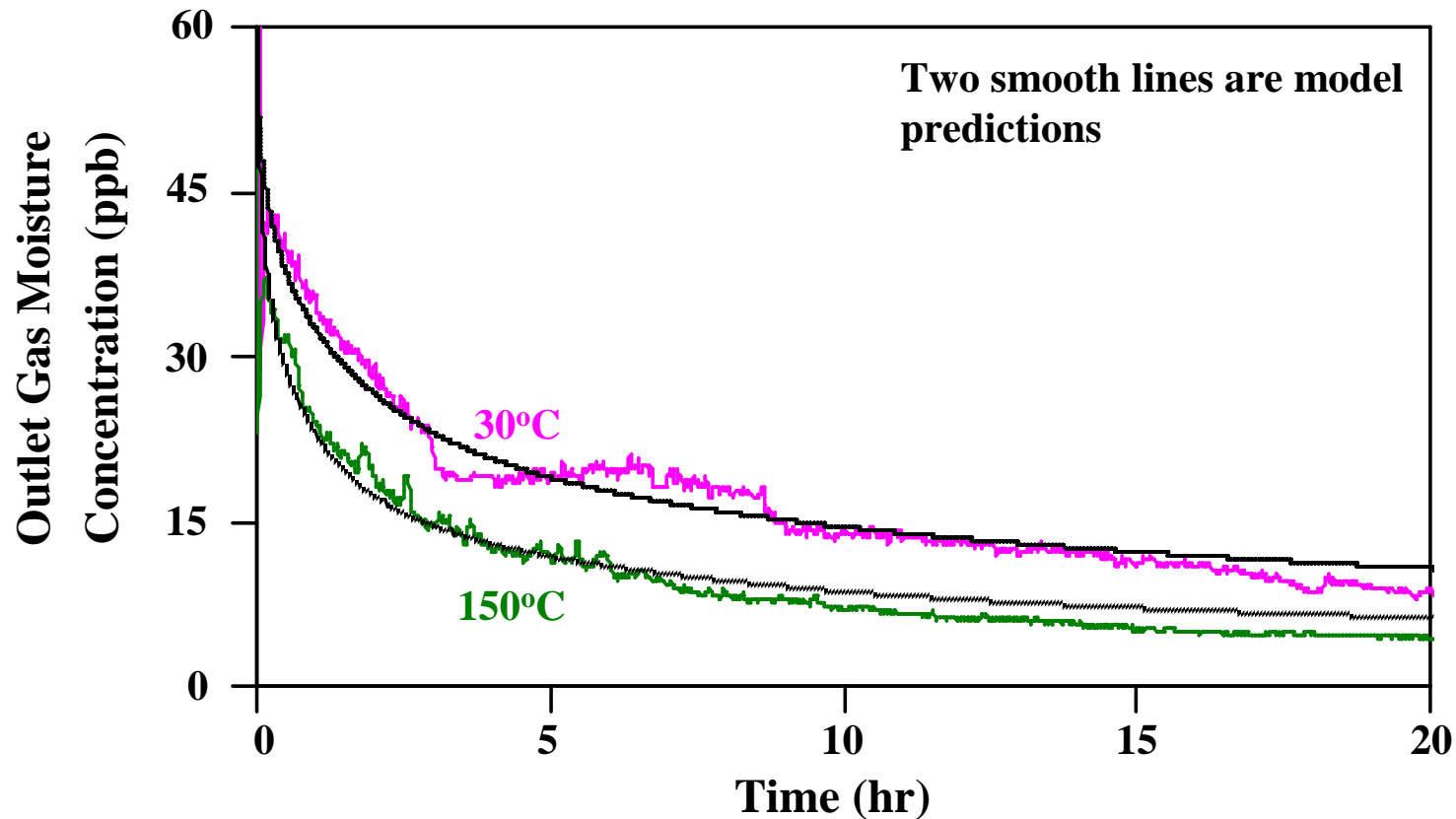
S_p : Specific surface area;

S : Moisture solubility in matrix;

k_m : Interphase transport coefficient between pore and matrix;

Validation of Model

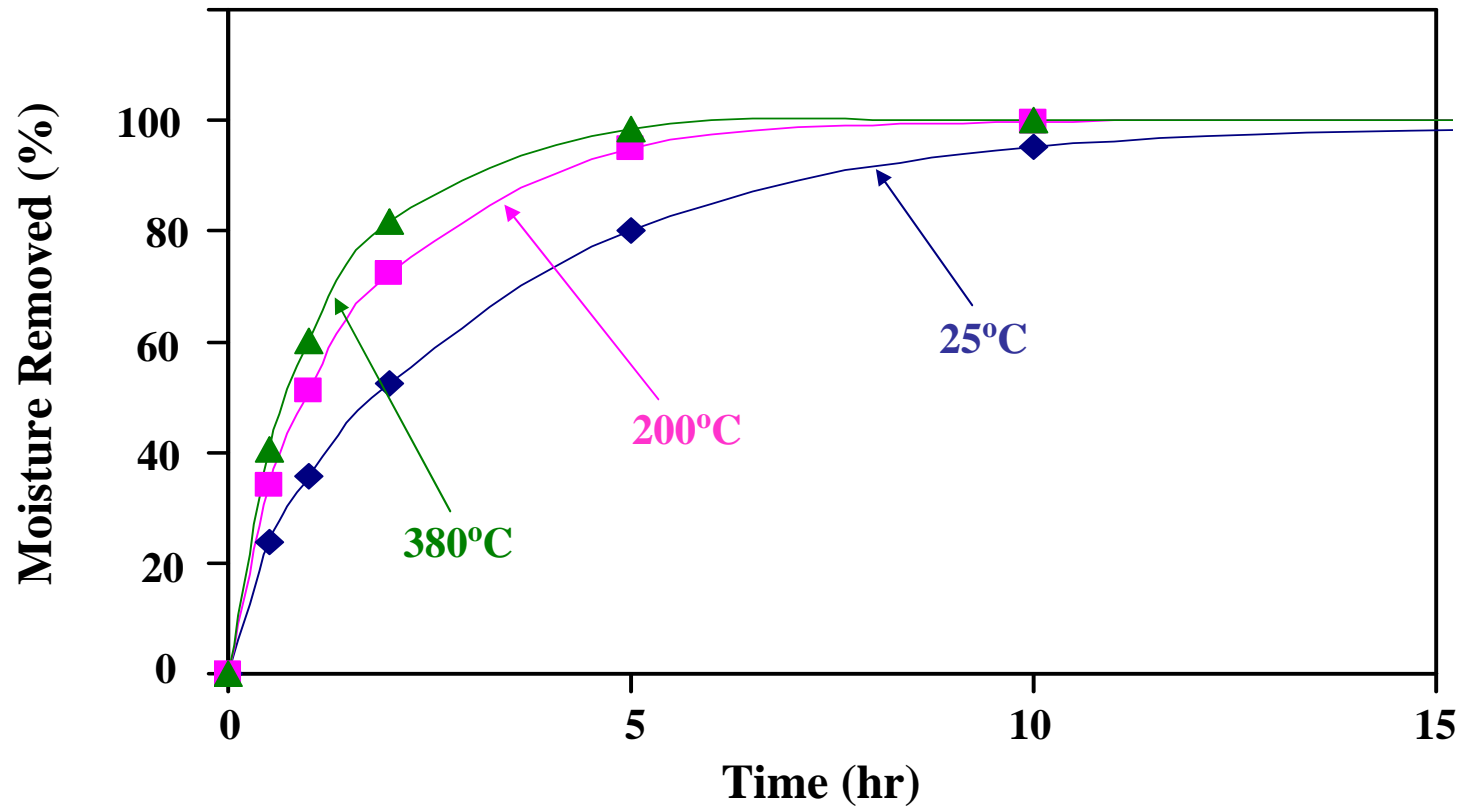
p-MSQ (JSR LKD 5109); Challenge Concentration: 56 ppb;
Purge Gas Purity: 1 ppb; Purge Gas Flow Rate: 318 sccm;
Film Thickness: 4000 Å



Good agreement between the model and the experimental data

Effect of Temperature on Moisture Removal

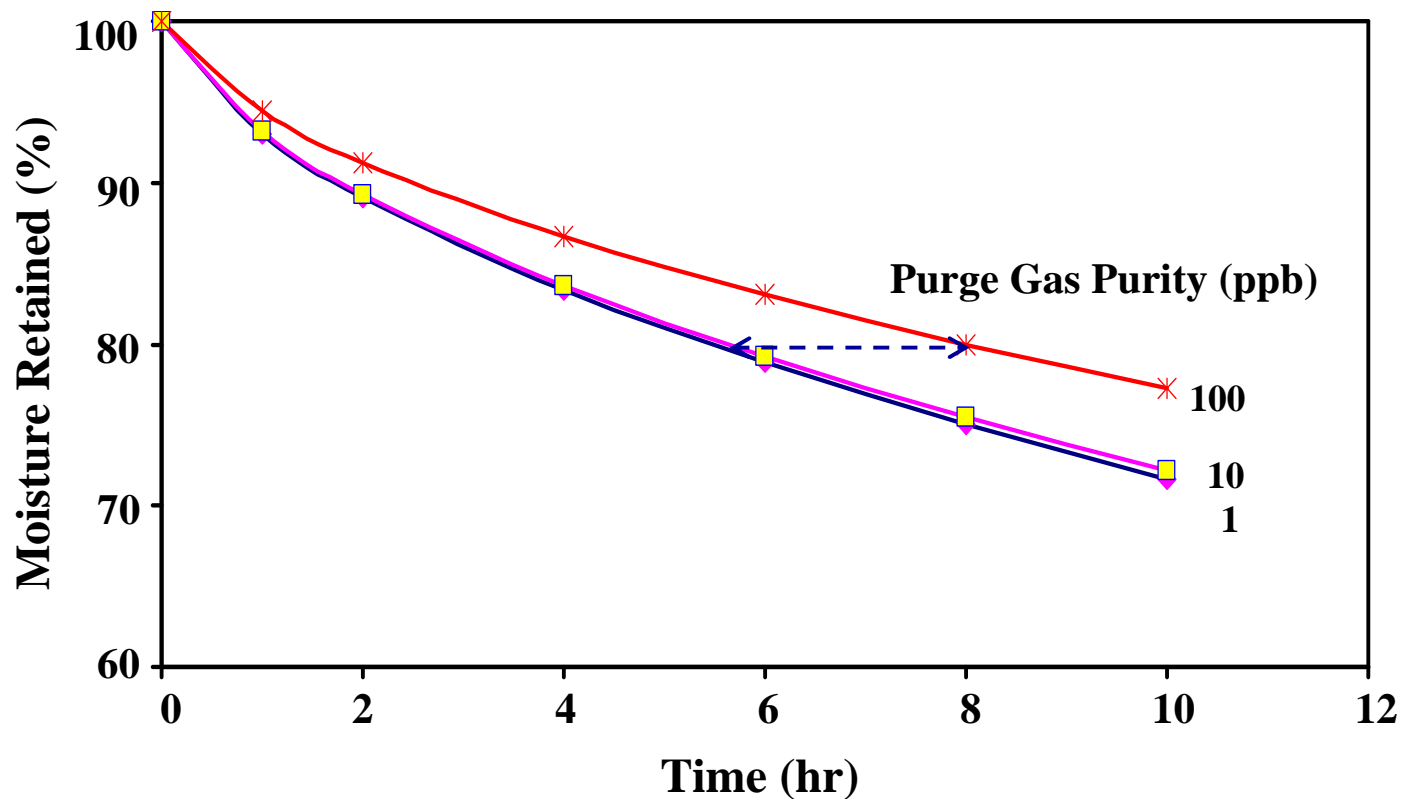
p-MSQ (partial etch, N₂H₂ ash); Challenge Concentration: 1500 ppm;
Purge Gas Purity: 1 ppb; Purge Gas Flow Rate: 350 sccm;
Film Thickness: 1000 Å



There is an optimum extent of heating for enhancing the desorption

Dependence of Moisture Removal on Purge Purity

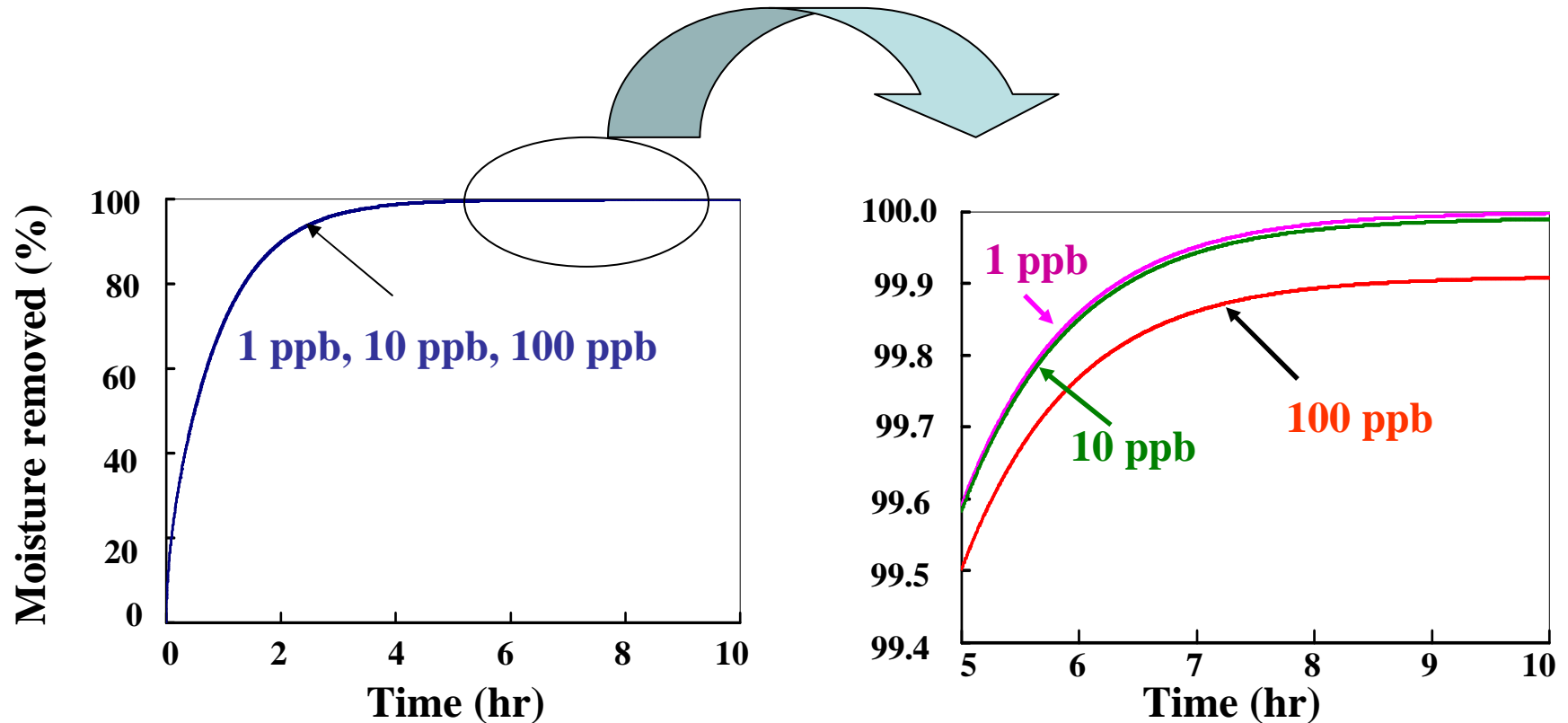
p-MSQ (LKD 5109); Challenge Concentration: 500 ppb; Temperature: 250°C;
Film Thickness: 4000 Å; Purge Gas Flow Rate: 600 sccm



Purge purity enhances drying primarily at the late stages of desorption

Effect of Purge Gas Purity

p-MSQ (partial etch, N₂H₂ ash); Challenge Concentration: 100 ppm;
Temperature: 25 °C; Film Thickness: 1000 Å; Purge Gas Flow Rate: 350 sccm



Purge purity enhances drying primarily at the late stages of desorption

Moisture Uptake in Capped and Uncapped p-MSQ Films

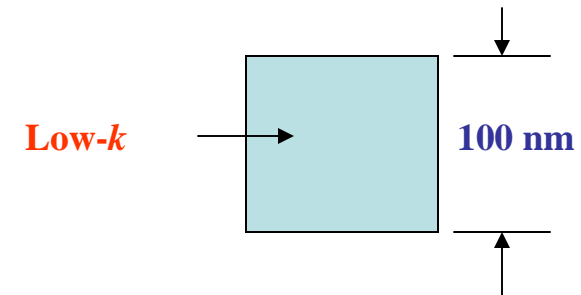
(I) Uncapped p-MSQ film:

Film Thickness: 100 nm

Porosity: 0.3

$D_s = 7.0 \times 10^{-15} \text{ cm}^2/\text{sec}$

$S = 1.3 \times 10^5 \text{ cm}^3(\text{gas})/\text{cm}^3(\text{solid})$



(II). Capped p-MSQ films:

Thickness of low- k layer: 100 nm

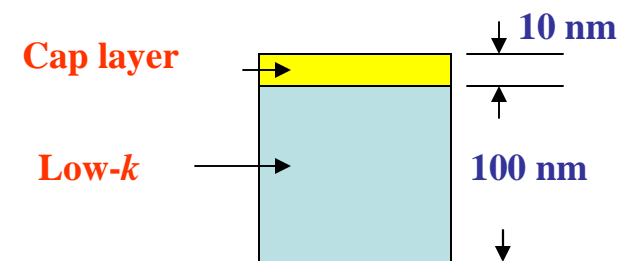
Thickness of cap layer: 10 nm

Porosity of low- k layer: 0.3

Porosity of cap layer: ~ 0

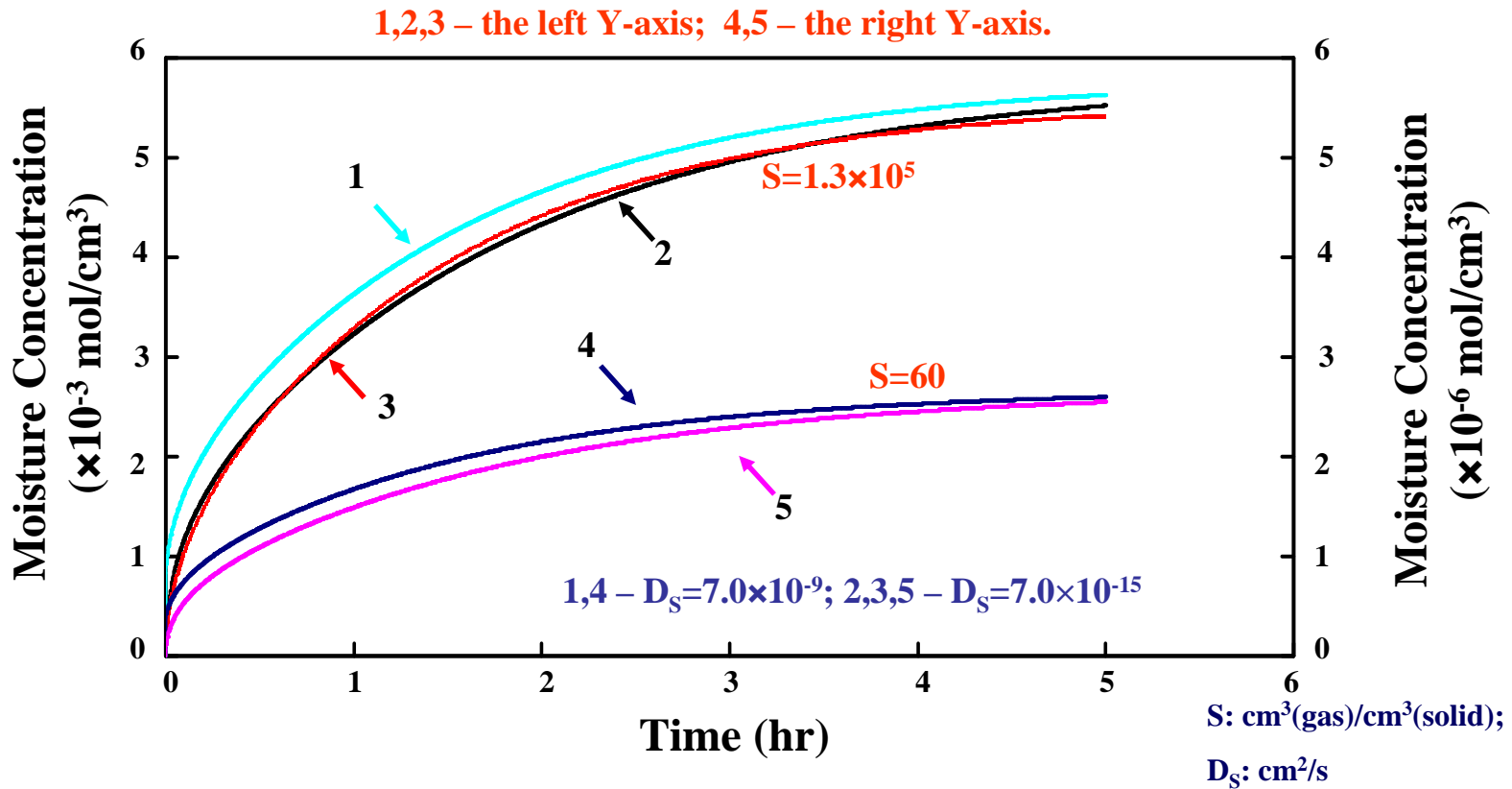
$D_s = 7.0 \times 10^{-9} - 7.0 \times 10^{-15} \text{ cm}^2/\text{sec}$

$S = 60 - 1.3 \times 10^5 \text{ cm}^3(\text{gas})/\text{cm}^3(\text{solid})$



Moisture Uptake in Capped and Uncapped p-MSQ Films

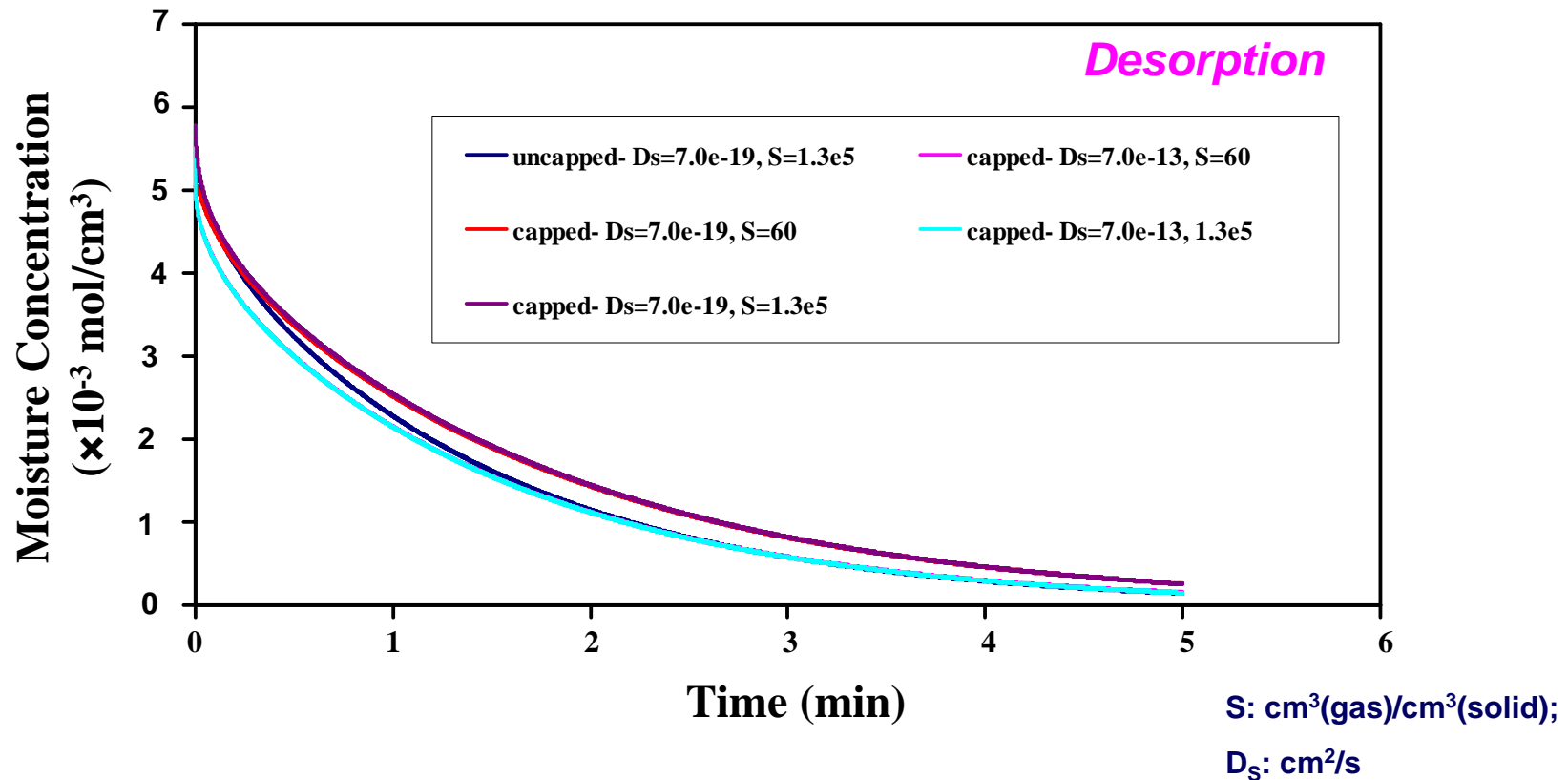
Challenge Concentration: 1500 ppm; Temperature: 25 °C



Cap layer with low moisture solubility prevents moisture intrusion

Moisture Removal in Capped and Uncapped p-MSQ Films

Temperature: 25 °C; Purge Gas Concentration: 1 ppb;
Initially all the films were equilibrated with 1500 ppm of moisture

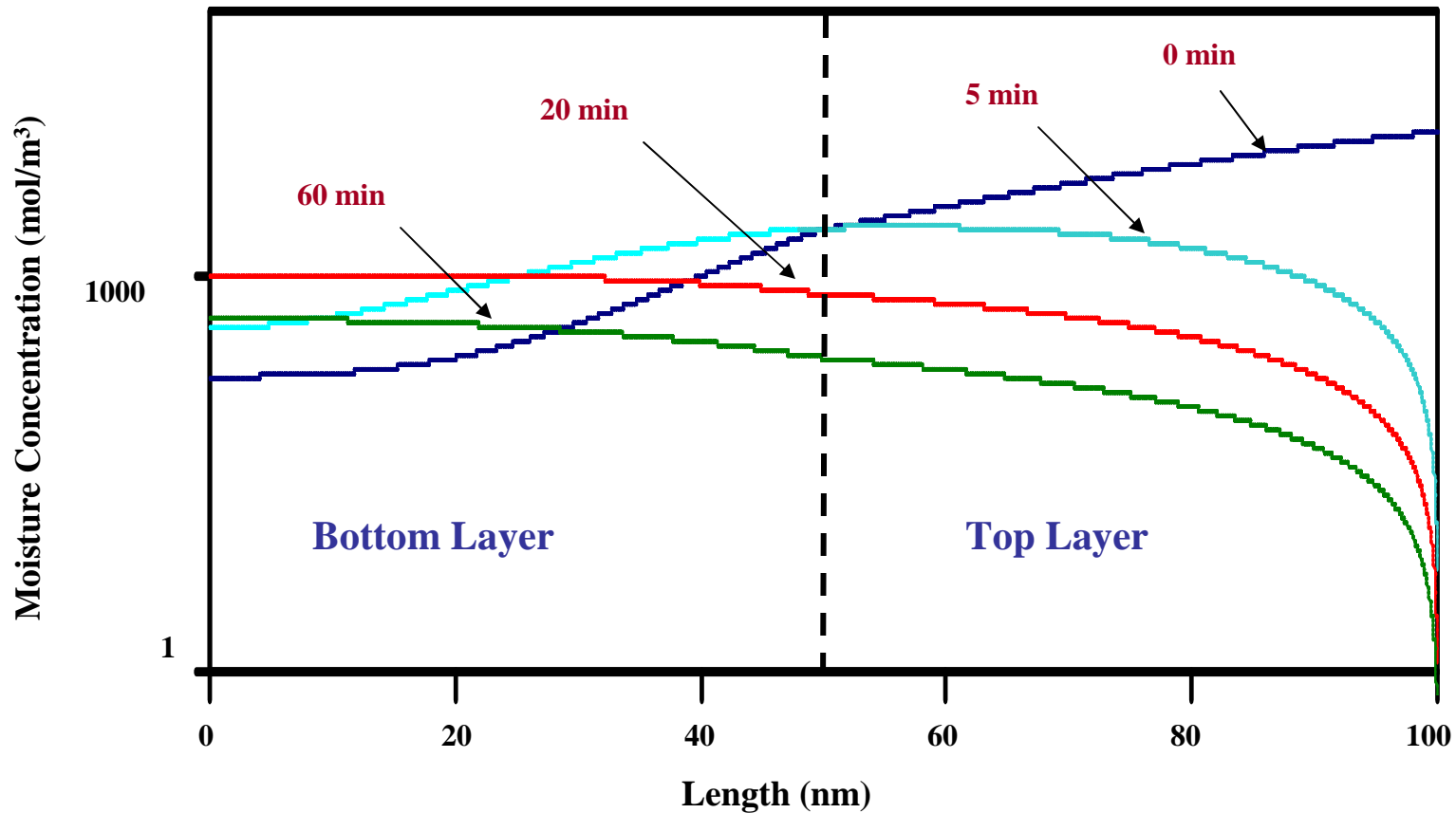


Cap layer with low moisture solubility does not prevent moisture removal

Moisture Profile within Low-*k* Film

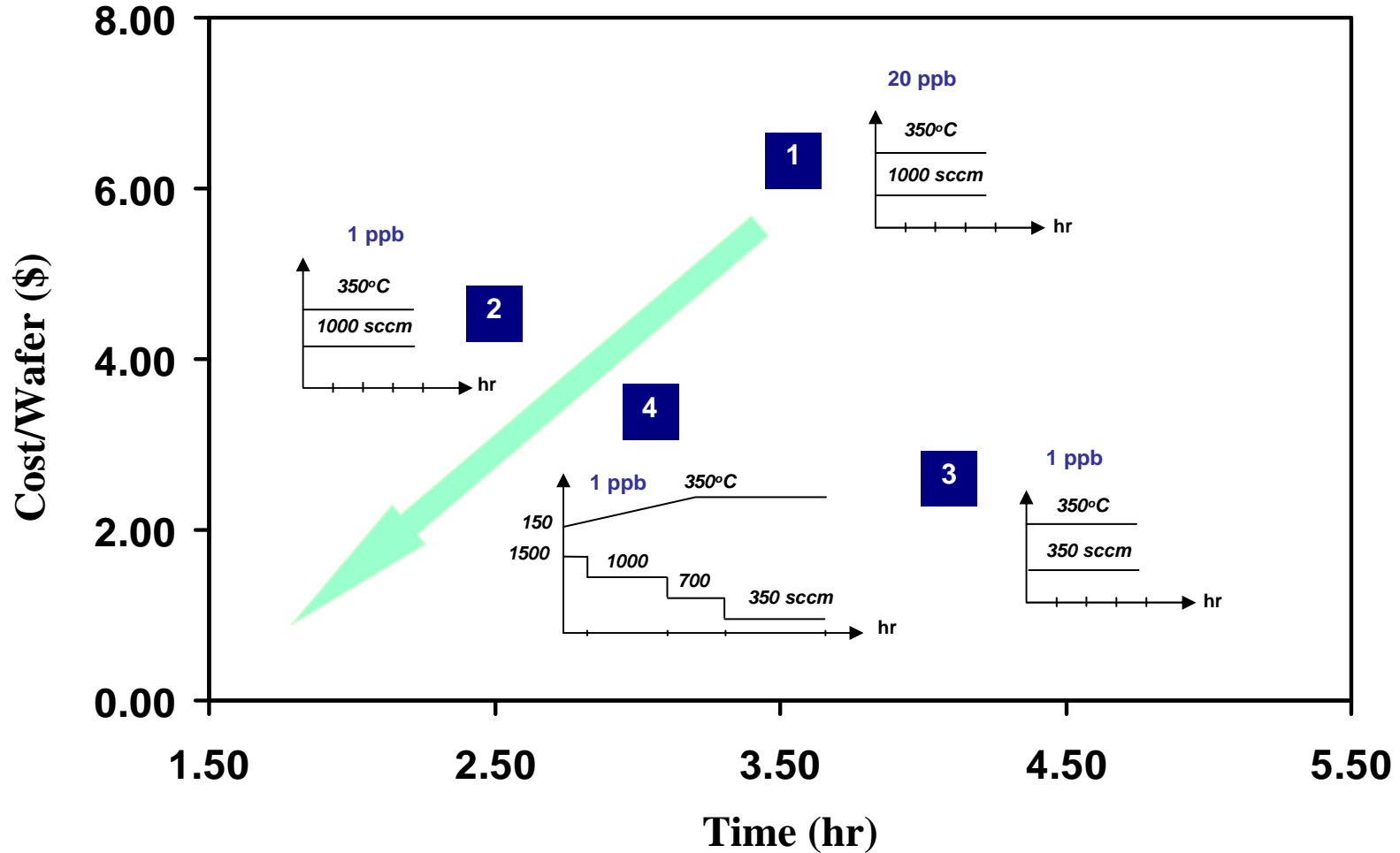
p-MSQ (partial etch, N₂H₂ ash); Purge Temperature: 25°C;
Challenge Concentration: 1500 ppm

First challenge for 5 mins, then switch to purge



ESH Gain in Optimizing the Purge Process

Challenge Conditions: 500 ppb moisture at 30°C for 1 hr. Purge for 80% moisture removal



Conclusions

- **Moisture removal is a slow and highly activated process.**
- **Porous low- k films has a higher uptake capacity as compared to SiO_2 .**
- **There is an optimum extent of heating for enhancing the desorption.**
- **Purge gas purity primarily help the late stages of outgassing.**
- **Cap layer with low moisture solubility prevents moisture intrusion, but does not affect moisture removal.**
- **A process model is developed for data analysis and purge optimization. This model can be used to minimize the chemical and energy consumption, reduce the purge time, and increase the throughput.**

ESH Metrics and Impact

I) Basis of Comparison:

Current best technology. Purge and drying is done by best quality gas available in the fab. Very little is known about the actual dynamics of outgassing and purge requirements for cleaning and drying of porous low-k.

II) Manufacturing Metrics

More effective purge process will lower chemical (mainly pure gas) and energy usage. Purge sequence to lower the drying time leading to ESH gain as well as lower down time, higher throughput, and lower cost.

III) ESH Metrics

	Usage Reduction			Emission Reduction			
Goals/ Possibilities	Energy	Water	Chemicals	PFCs	VOCs	HAPs	Other Hazardous Wastes
Purge and outgassing with lower ESH impact	Lower temperature and lower energy	N/A	Lower purge gas	N/A	N/A	N/A	N/A

Acknowledgement

University of Arizona

Dr. Farhang Shadman

Advisor, Regents Professor in Chemical Engineering and Optical Sciences Department, U of A

Dr. Supapan Seraphin

Professor in Materials Science and Engineering Department, U of A for helping with TEM Images

Dr. Roger Sperline

Professor in Chemistry Department, U of A for helping with FTIR Analysis

Sematech (Interconnect Group) and Texas Instruments (SiTD)

For partial support of this research and providing samples

SRC/Sematech

Engineering Research Center for Environmentally Benign Semiconductor Manufacturing

Ge Surface Clean and Passivation

J. Kim, J. McVittie, K. Saraswat and Y. Nishi

Stanford University

1. Introduction
2. Etch Rate Aspects/Surface Roughness
3. Native Oxide Removal and Passivation
4. Metal Removal
5. Environmental Considerations
6. Conclusions

1. Introduction

2. Etch Rate Aspects/Surface Roughness

3. Native Oxide Removal and Passivation

4. Metal Removal

5. Environmental Considerations

6. Conclusions

Why Germanium ?

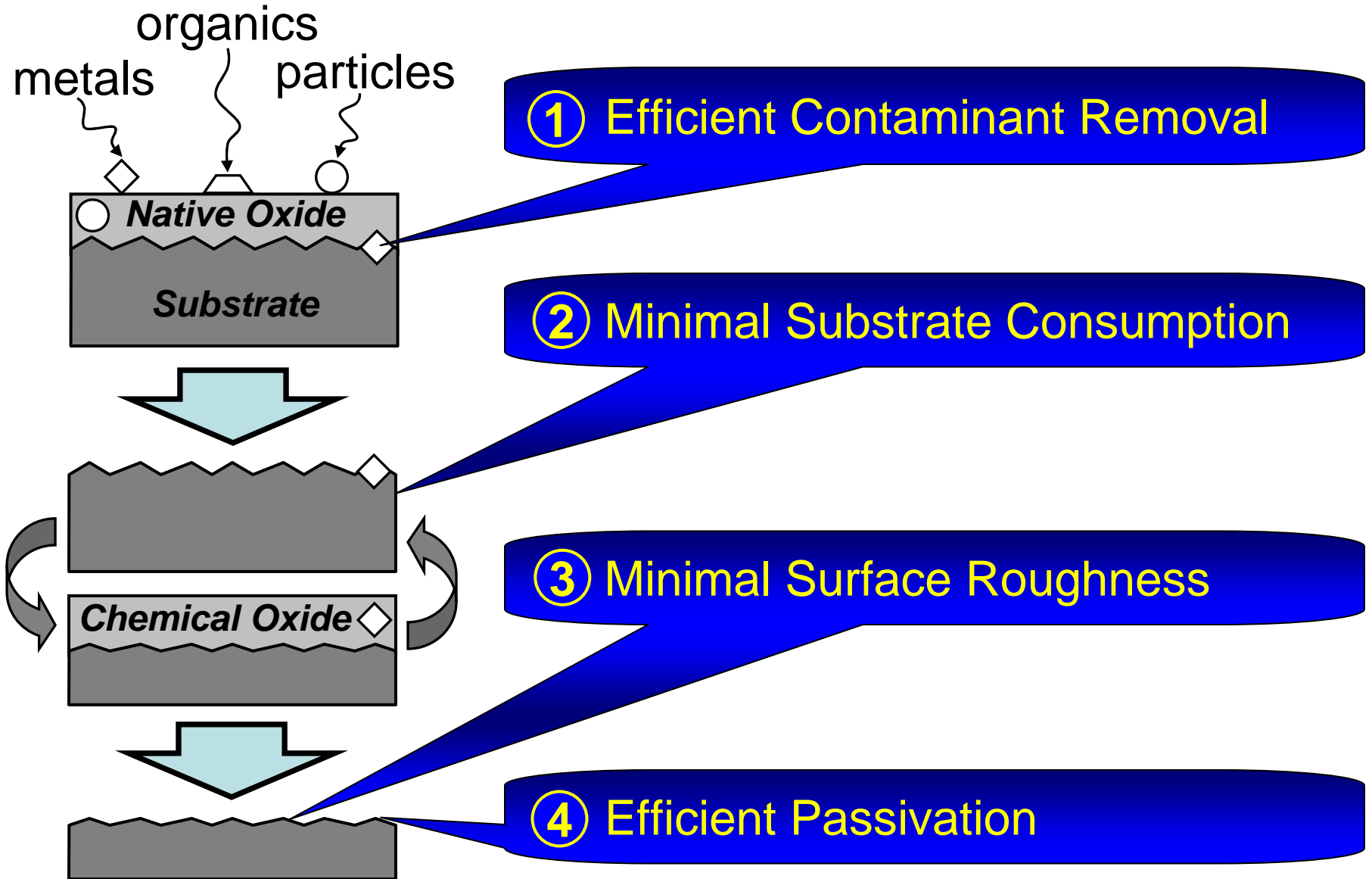
- ▶ Ge is gaining interest as a substrate for high mobility applications because of higher carrier mobility.
(2X electron & 4X hole mobility of Si)

(cm ² V ⁻¹ s ⁻¹)	Si	Ge
Electron	1450	3900
Hole	505	1800

Schäffler et al, *Semiconductor Sci. Tech.* (1997)

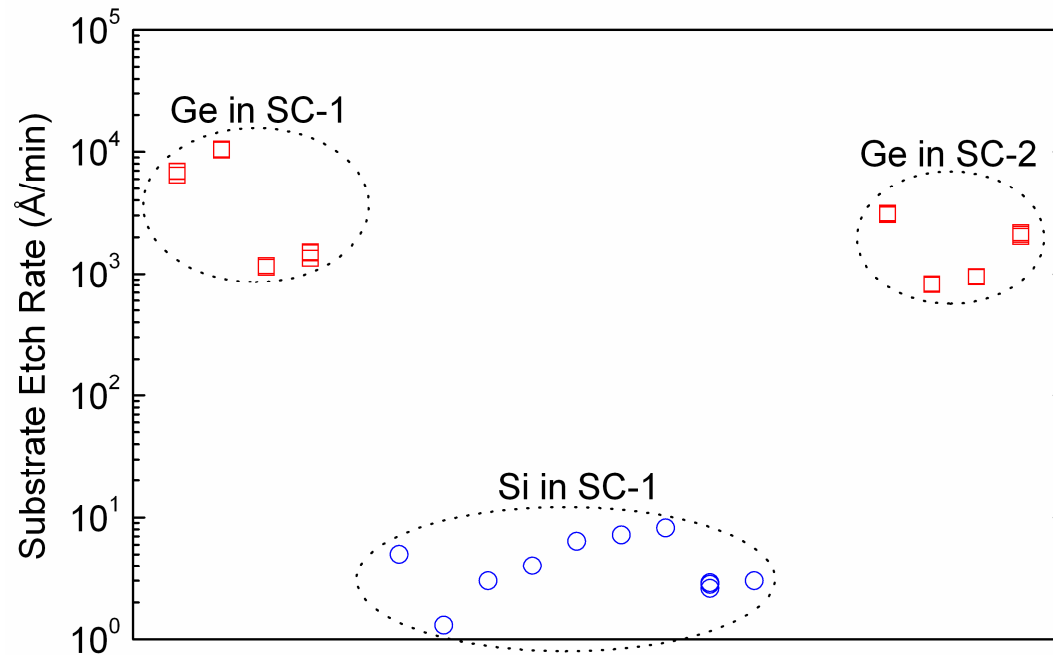
- ▶ Effective surface preparation is required to fully utilize the high mobility properties of Ge in process integration.

Wet Cleaning of Germanium Surface

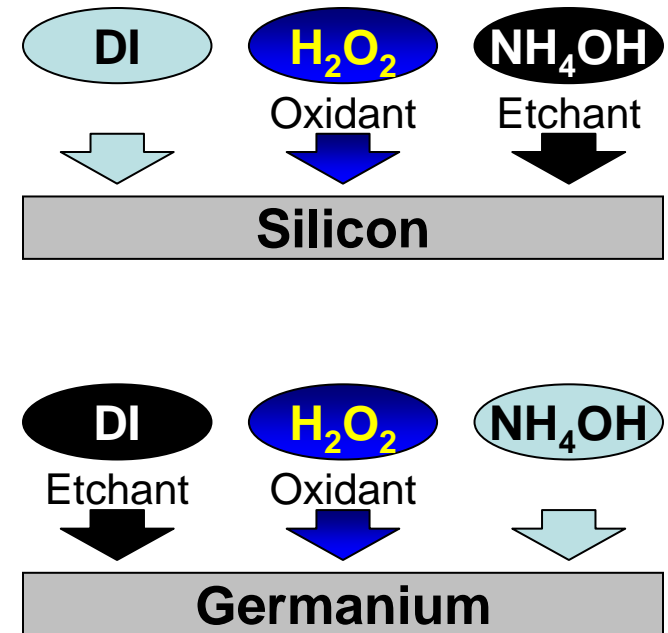


1. Introduction
- 2. Etch Rate Aspects/Surface Roughness**
3. Native Oxide Removal and Passivation
4. Metal Removal
5. Environmental Considerations
6. Conclusions

Etch Rate in Standard Clean Solutions

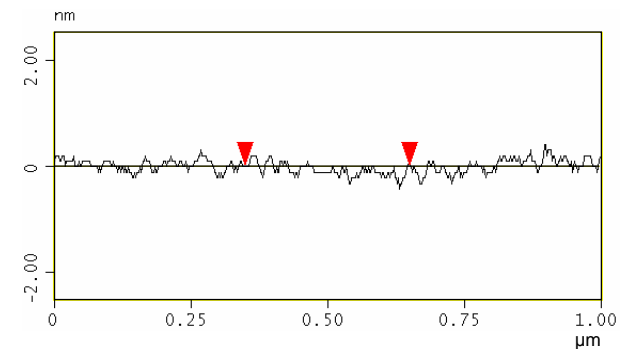
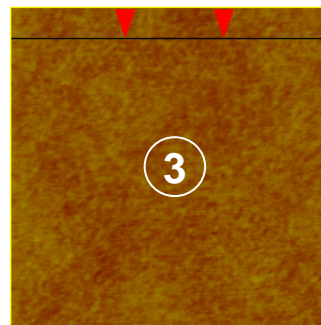
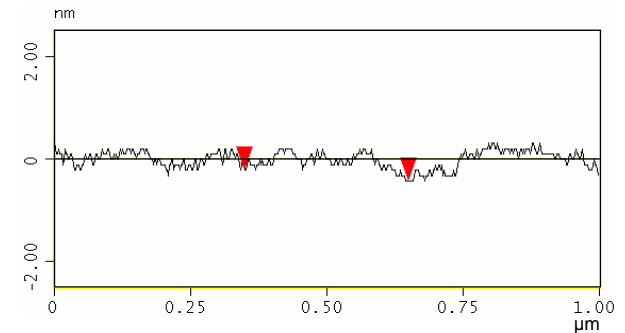
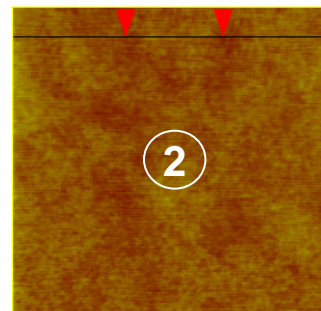
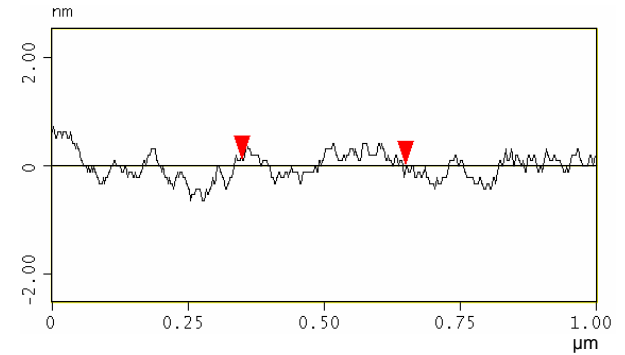
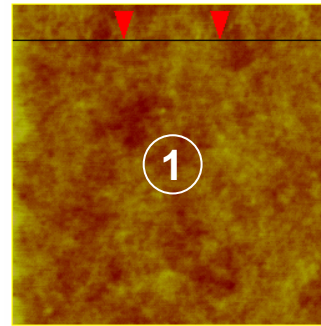
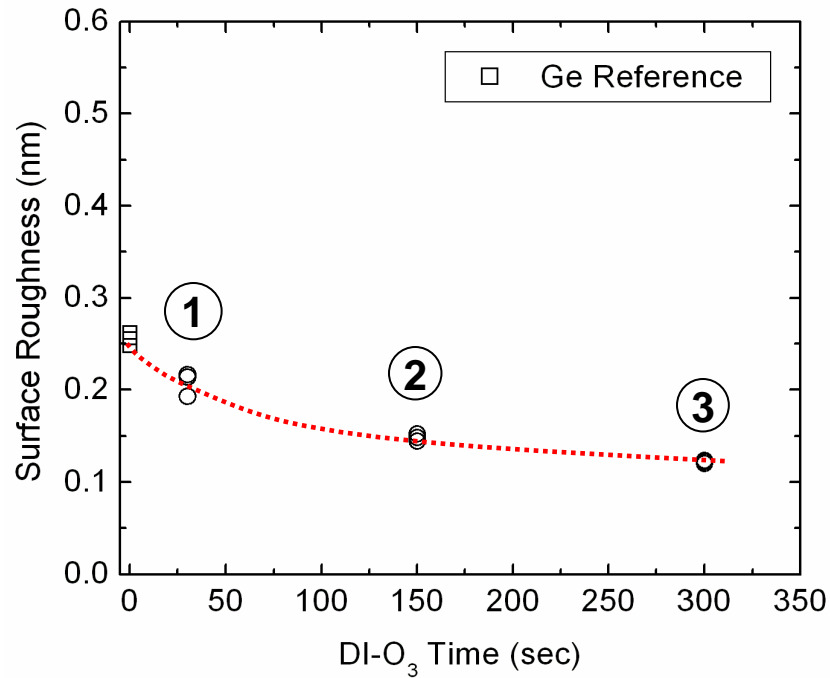


(Si etch rates from Kobayashi et al, *Jpn.J. Appl.Phys.*)



- ▶ Water solubility of GeO₂ (2 μm/min) results in high Ge etch rates for room temp SC-1 & SC-2. (Si etch rates <10 Å/min)
- ▶ Need alternative **minimal-etching** clean solution for Ge.

Roughness Improvement with DI-O₃

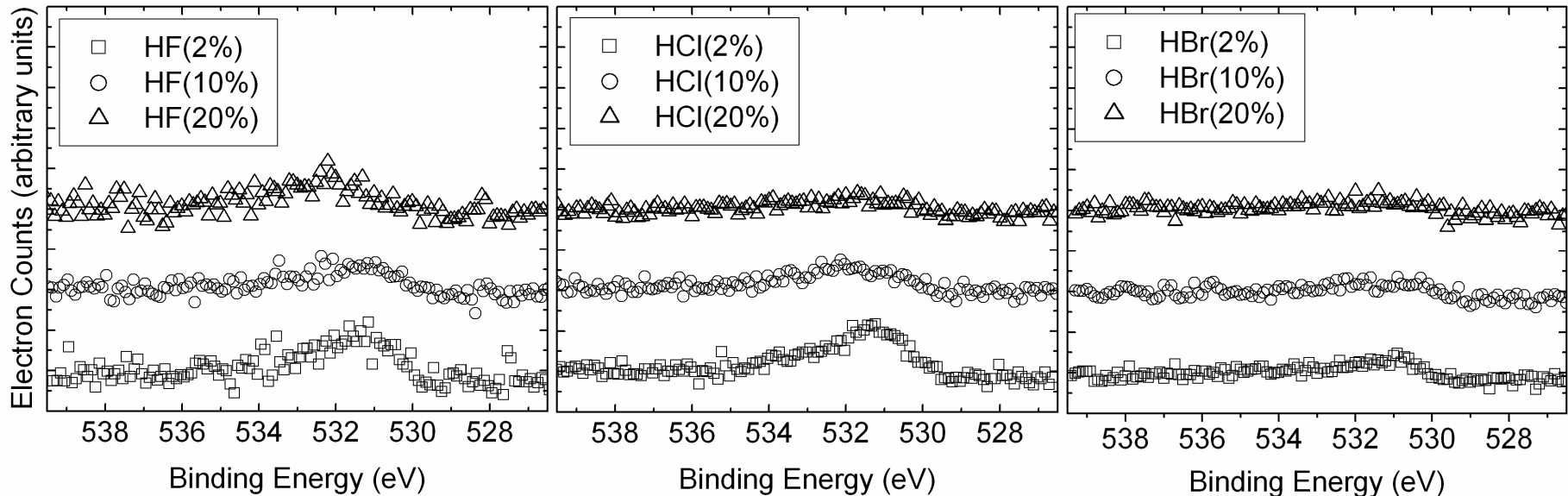


- ▶ Ozonated DI water (DI-O₃) smoothens Ge surface while etching.

1. Introduction
2. Etch Rate Aspects/Surface Roughness
- 3. Native Oxide Removal and Passivation**
4. Metal Removal
5. Environmental Considerations
6. Conclusions

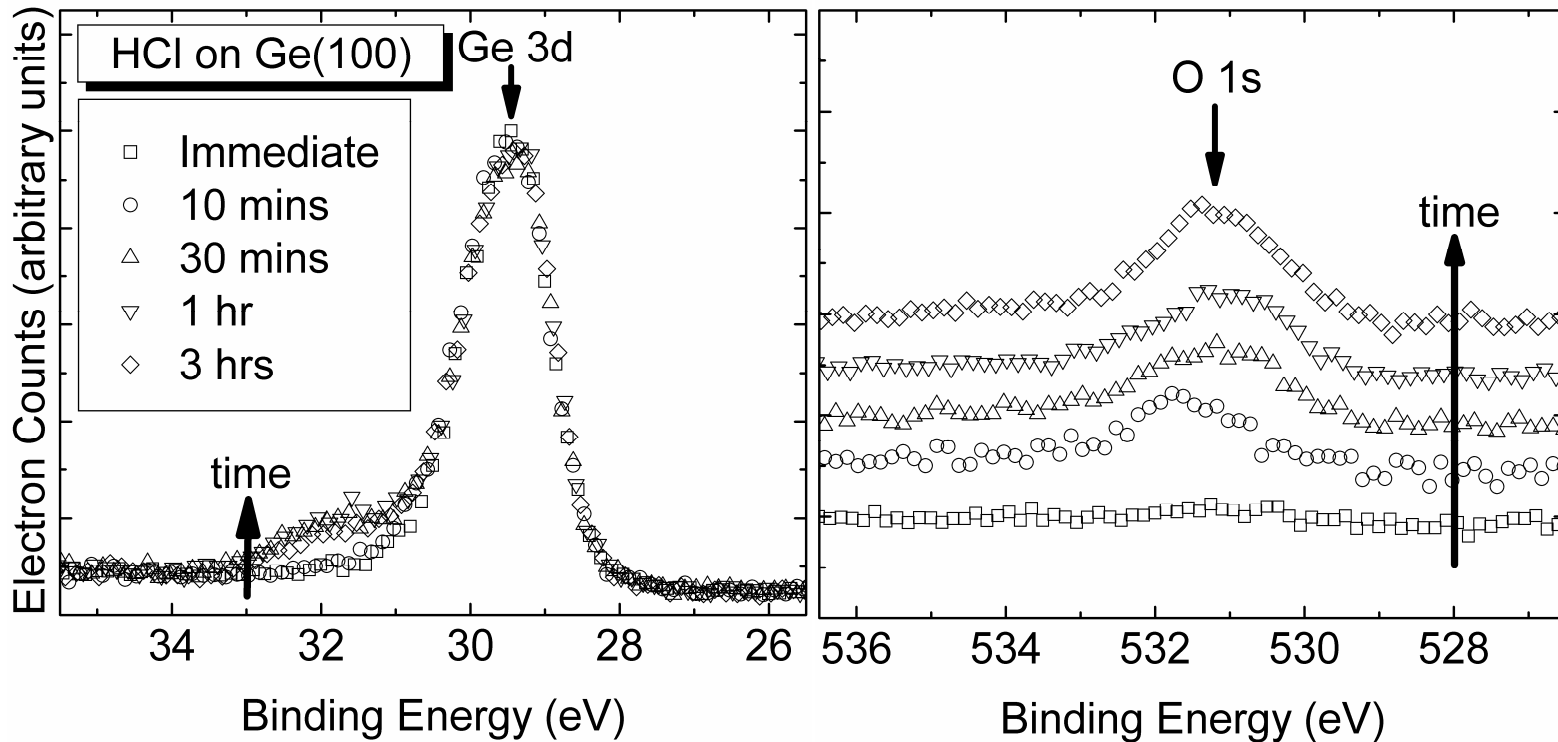
Native Oxide Removal

High Resolution Scans of Oxygen (1s) on Ge



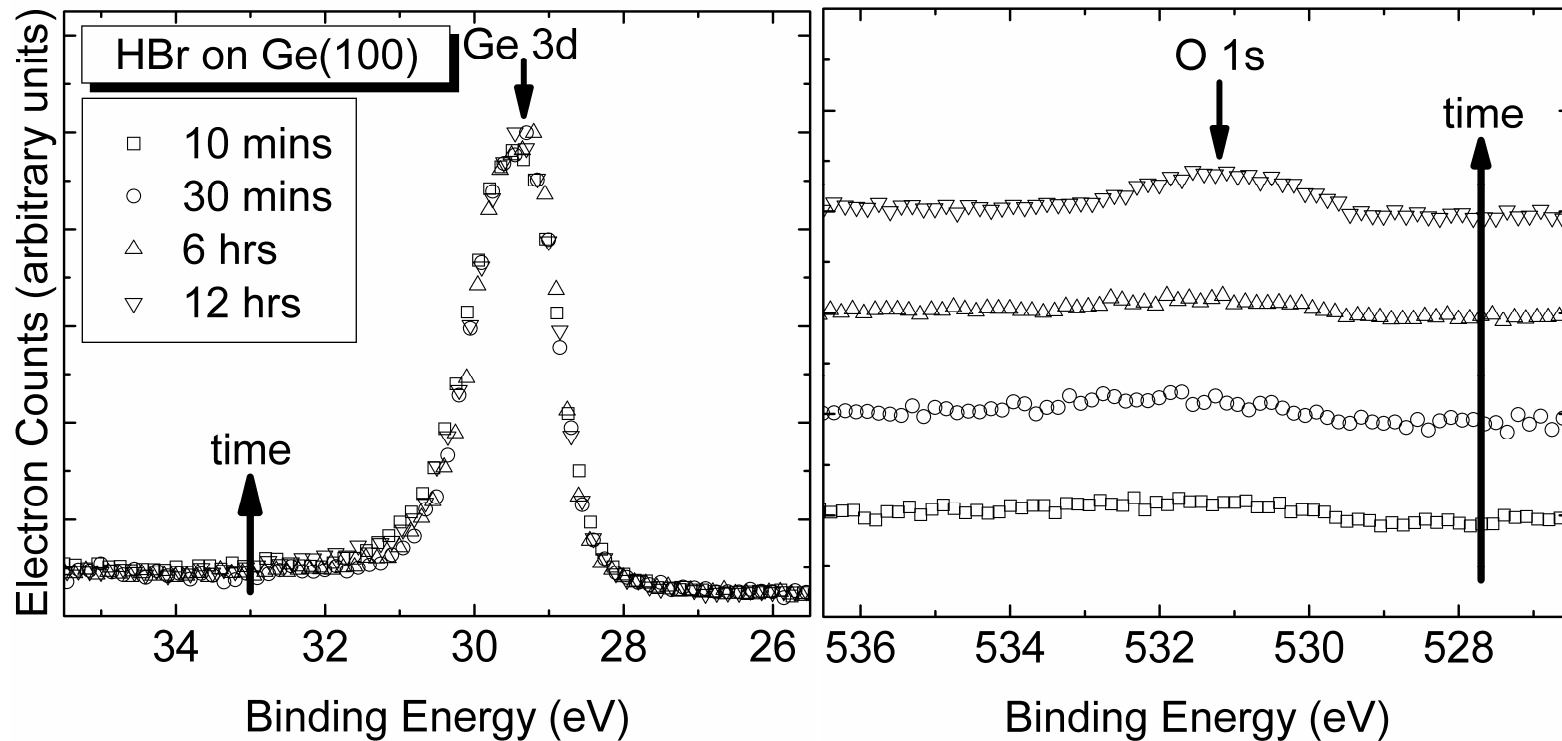
- ▶ Relative O(1s) signal represent remaining oxide.
- ▶ HF (all concentration @2mins) does not remove oxide layer.
- ▶ Concentrated HCl and HBr gives complete removal of the contaminant containing native oxide.

Passivation of HCl Treated Ge Surface



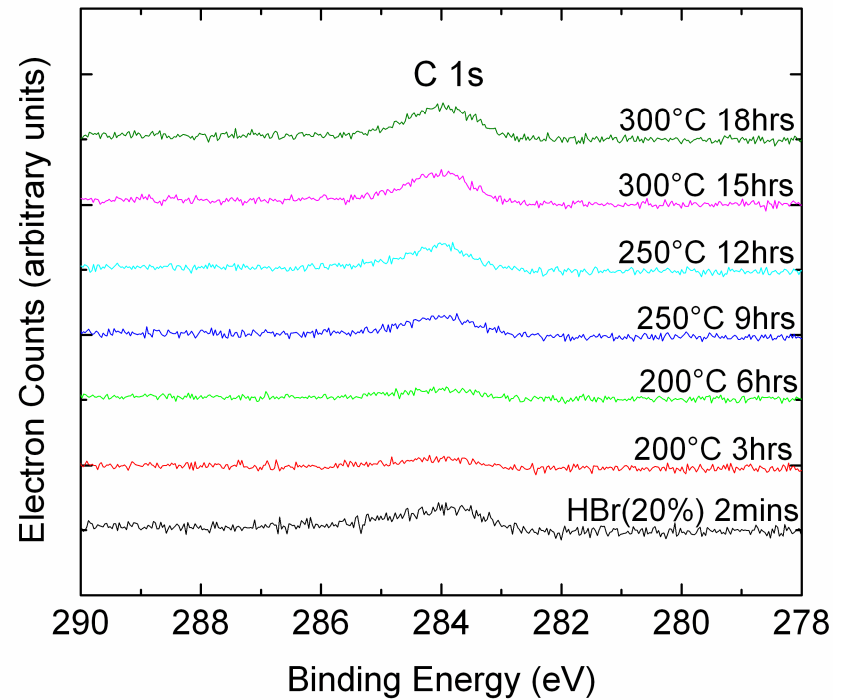
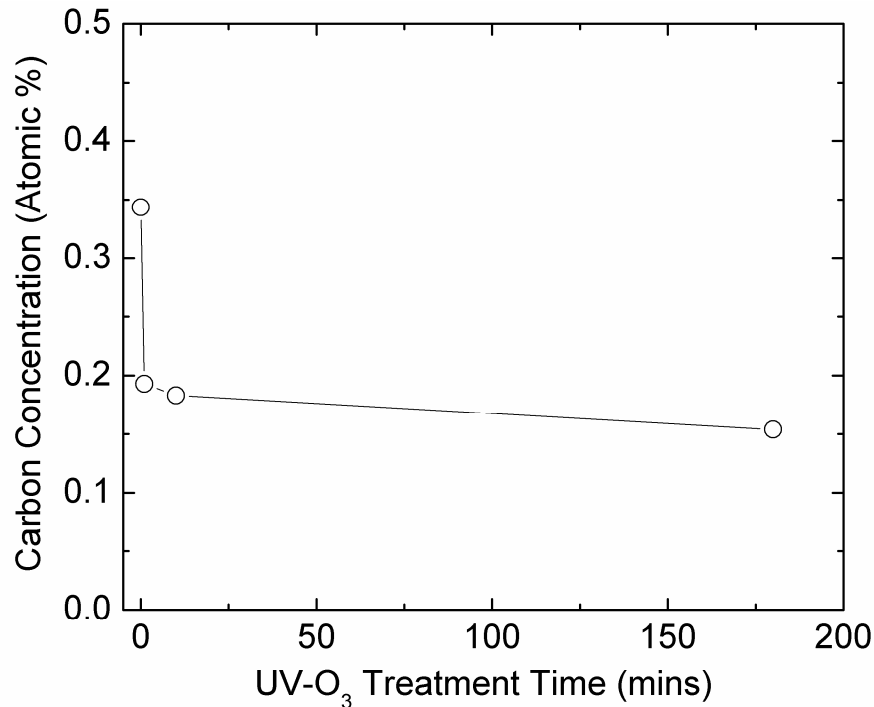
- ▶ Complete removal of oxide achieved.
- ▶ Oxide re-growth in 10mins.

Passivation of HBr Treated Ge Surface



- ▶ Complete removal of oxide achieved.
- ▶ Passivation effective for 6 hours

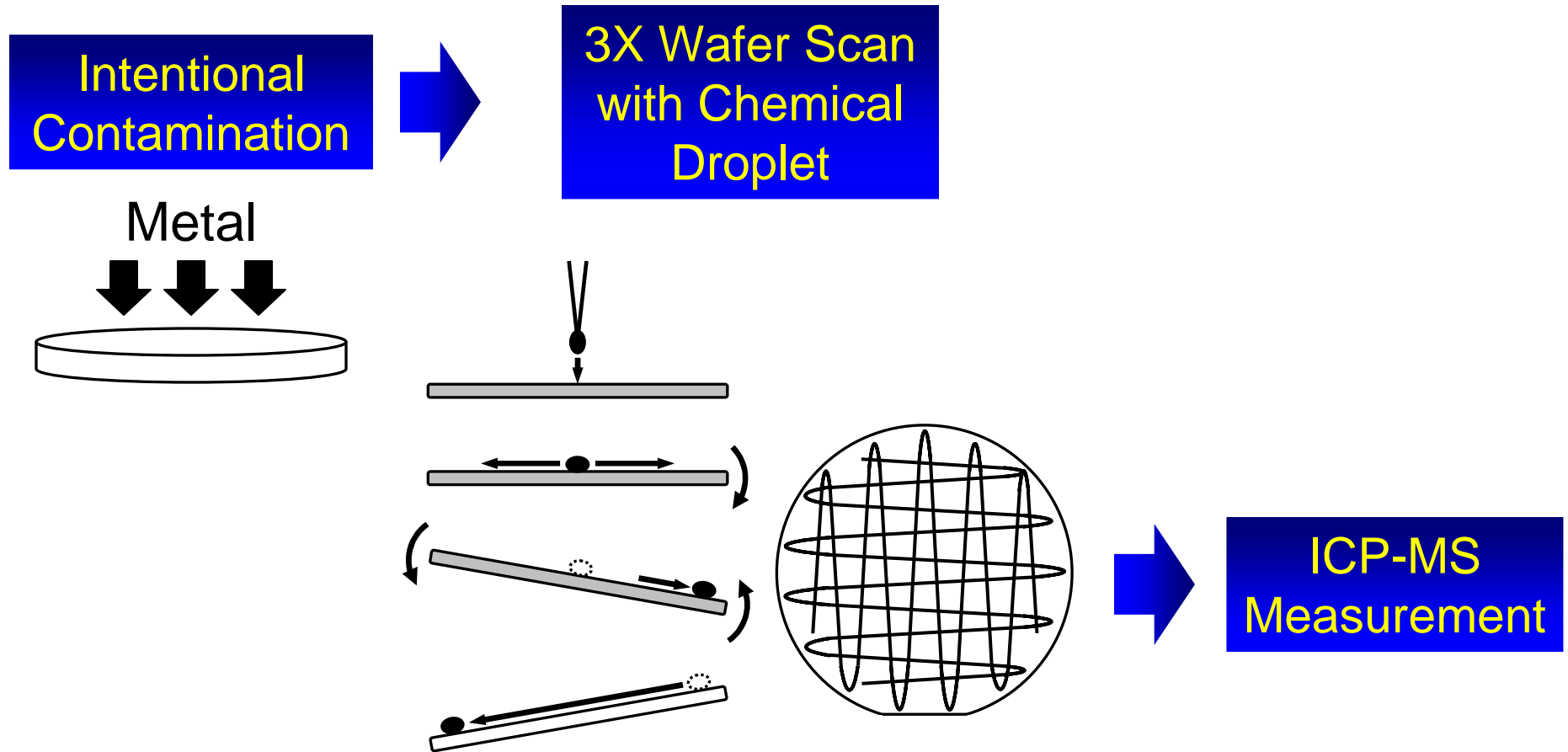
Organic Removal



- ▶ UV-O₃ decrease the carbon contamination level
- ▶ Thermal treatment decreases the carbon level but prolonged treatment at high temperatures redeposit carbon.

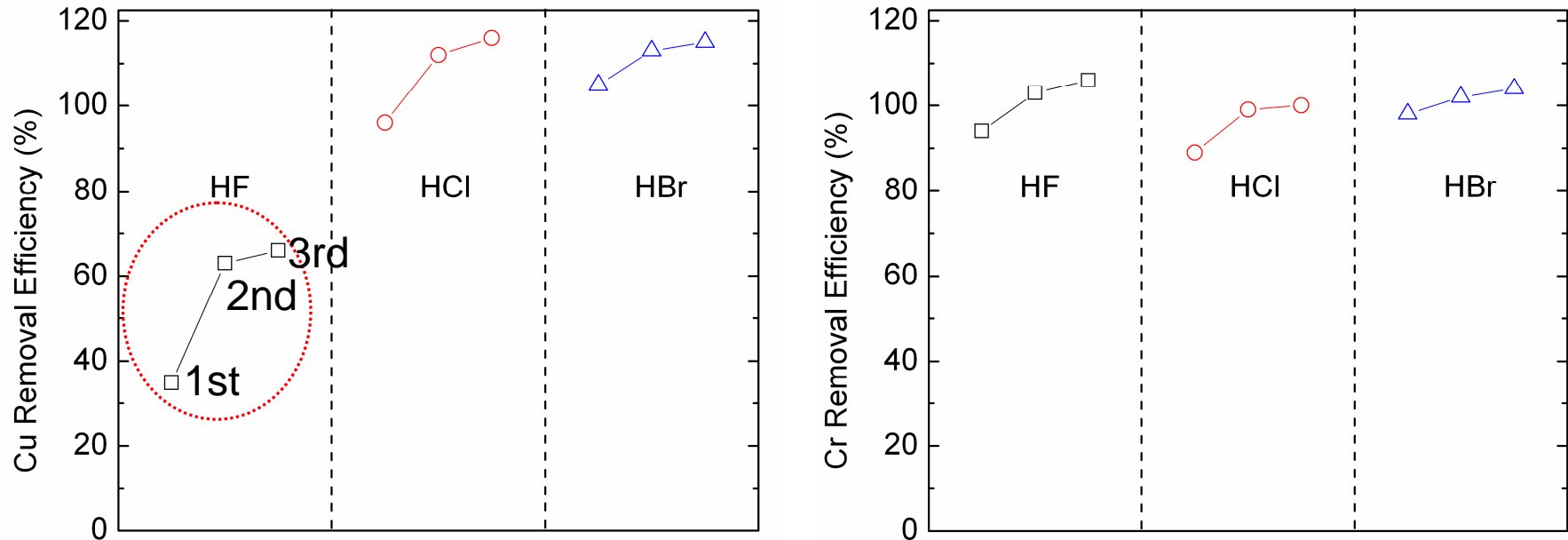
1. Introduction
2. Etch Rate Aspects/Surface Roughness
3. Native Oxide Removal and Passivation
- 4. Metal Removal**
5. Environmental Considerations
6. Conclusions

Wafer Surface Analysis (WSA) Method



- ▶ ICP-MS : Inductively Coupled Plasma Mass Spectroscopy

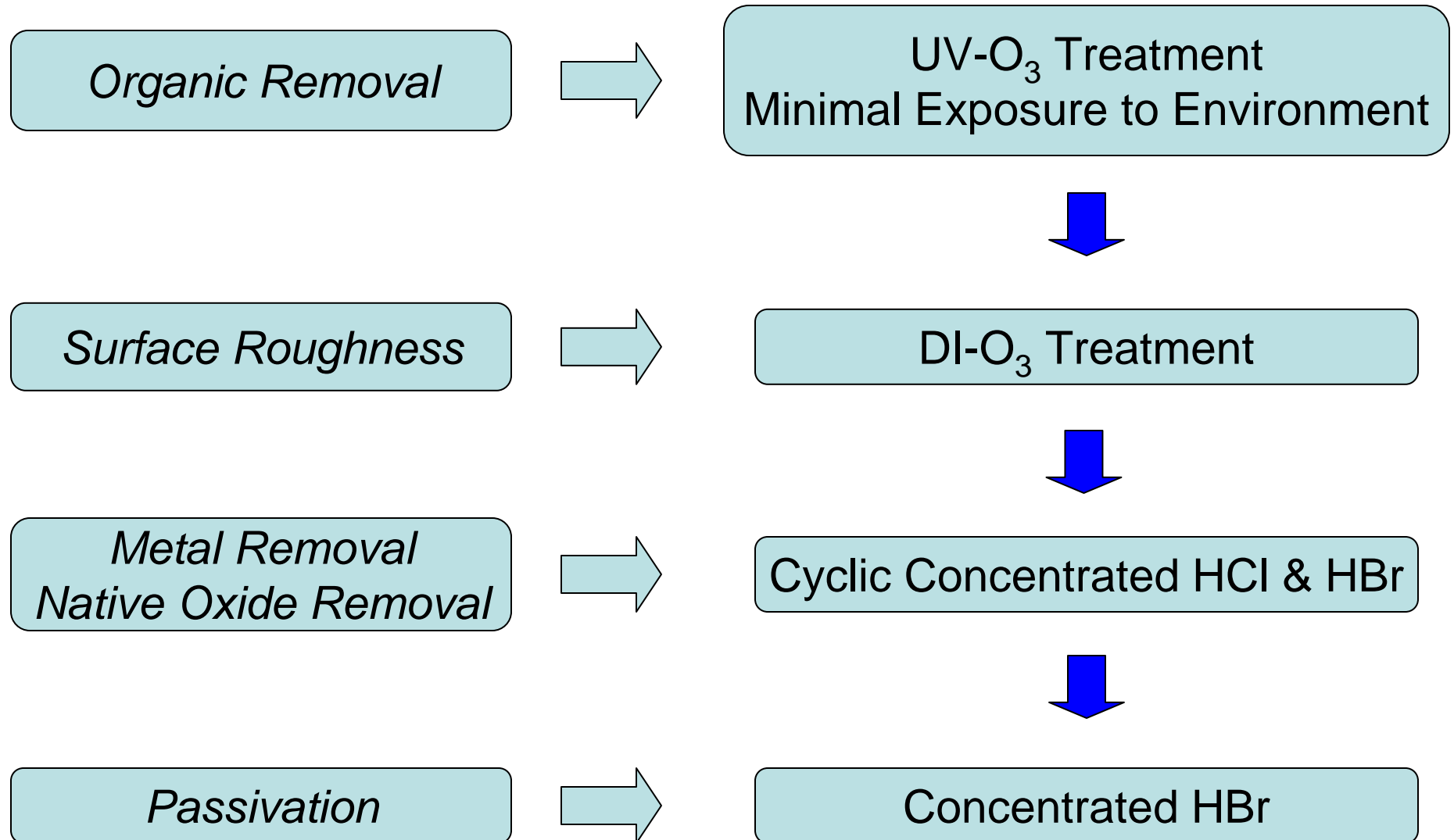
Metal Removal Efficiency (MRE)



$$\text{Metal Removal Efficiency} = \frac{\text{Metal Recovered by WSA Method}}{\text{Initial Contamination on Wafer}} \times 100$$

- ▶ MRE → “Effectiveness of Clean”
- ▶ Fe, Al, Ni, Ti, Co, Cr, Cu show >80% MRE for HF, HCl and HBr except Cu with HF solution.

Proposed Ge Cleaning Solution



1. Introduction
2. Etch Rate Aspects/Surface Roughness
3. Native Oxide Removal and Passivation
4. Metal Removal
- 5. Environmental Considerations**
6. Conclusions

ESH Benefits of Ge Cleaning Solution

Process	Advantages
<ul style="list-style-type: none">•UV-O₃ (Organics)•DI-O₃ (Surface Roughness)	O ₃ breaks down naturally to O ₂ . (non-toxic by-product)
<ul style="list-style-type: none">•Cyclic HCl (Metal)	Room temp process: does not require heat as in SC-2 (65~85°C) for Si. (energy conservation)

- ▶ Water-soluble GeO₂ allows the use of DI water instead of HF as oxide etchant. HF usage can be eliminated.

1. Introduction
2. Etch Rate Aspects/Surface Roughness
3. Native Oxide Removal and Passivation
4. Metal Removal
5. Environmental Considerations
- 6. Conclusions**

Conclusions

1. Ge has abnormally high etch rates in room temp. SC-1 & SC-2.
2. Surface roughness is improved with DI-O₃.
3. Native oxide is efficiently removed with conc. HCl & HBr.
4. Ge is passivated efficiently by HBr.
5. Metals are removed efficiently by HCl & HBr.
6. Proposed Ge clean process uses O₃ chemistry and room temp processes.

Future Work

- ▶ Further work with DI-O₃ and DI-O₃/Acid mixtures on contamination removal of Ge surfaces.
- ▶ Establish correlation of contaminants on electrical properties of Ge surfaces.
- ▶ *ab-initio* modeling of oxidation of halide-passivated surface.

Lowering Purge-Gas Consumption during Dry-down of Gas Distribution Systems

A Joint ERC-Intel Seed Project

Junpin Yao*, Harpreet Juneja*, Asad Iqbal*, Farhang Shadman*, and
Carl Geisert#

*Department of Chemical and Environmental Engineering
University of Arizona

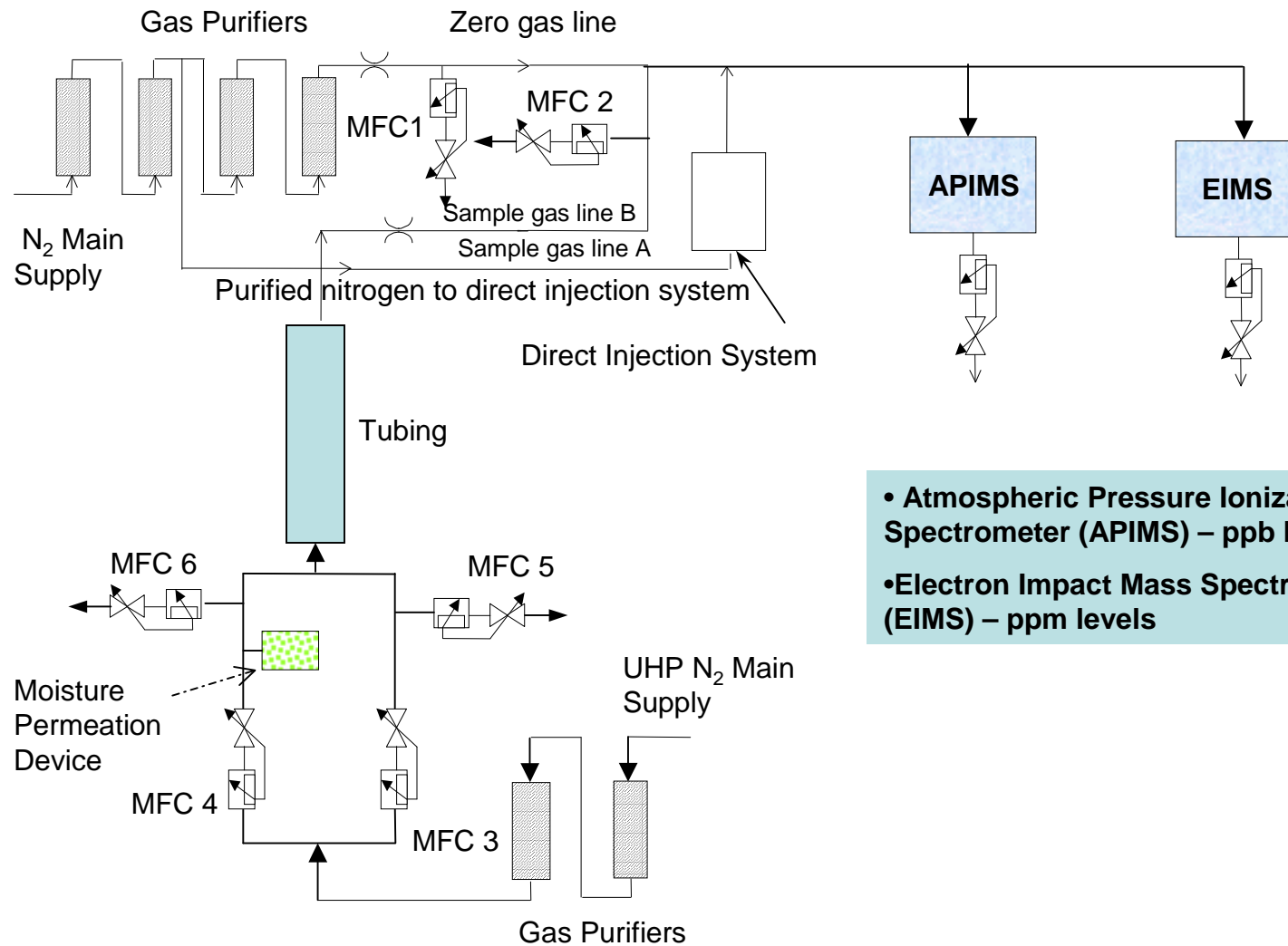
#Intel Corporation, Chandler, Arizona

February 2007

Outline

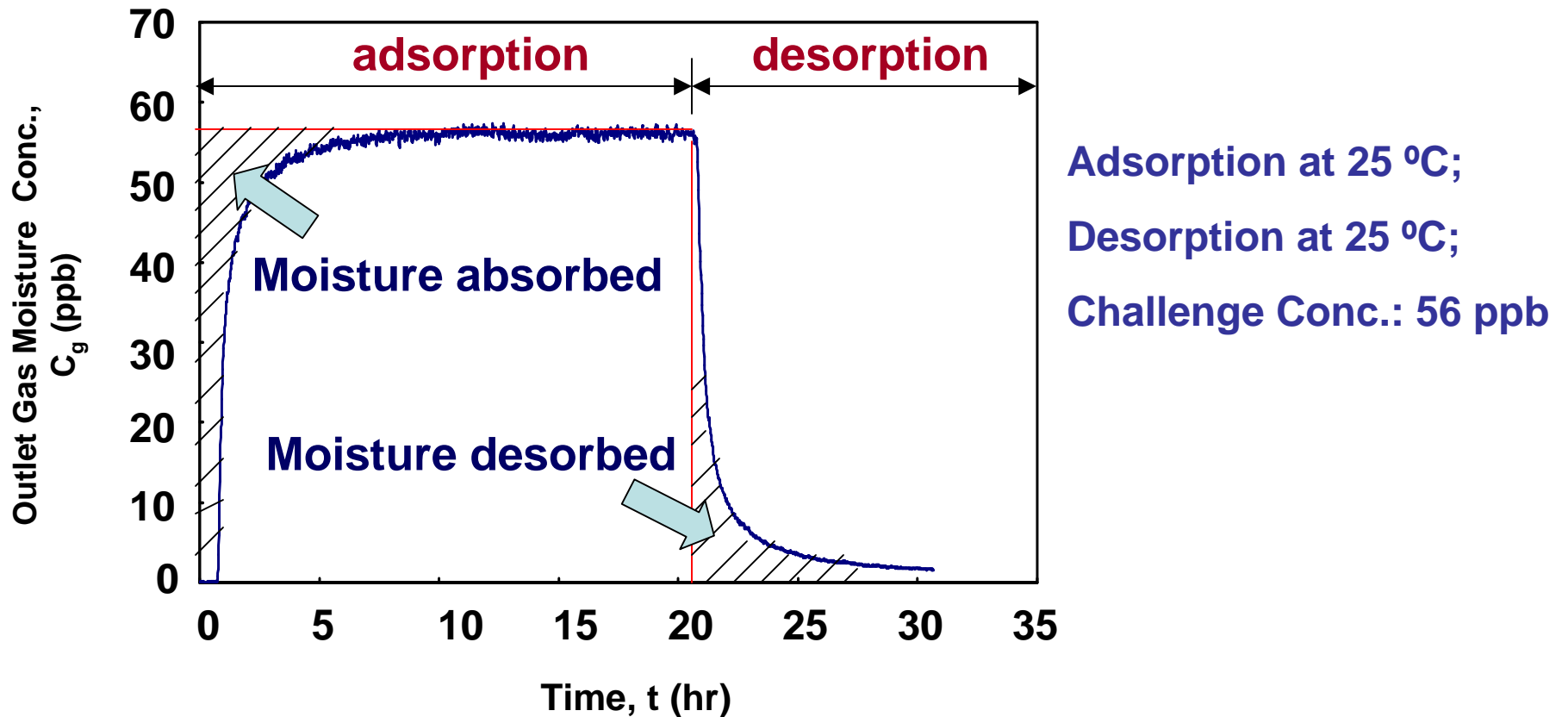
- **Experimental procedure and model development**
- **Experimental results and model validation**
- **Parametric study and model application**
- **Summary and Conclusion**

Experimental Setup



- Atmospheric Pressure Ionization Mass Spectrometer (APIMS) – ppb levels
- Electron Impact Mass Spectrometer (EIMS) – ppm levels

Experimental Procedure

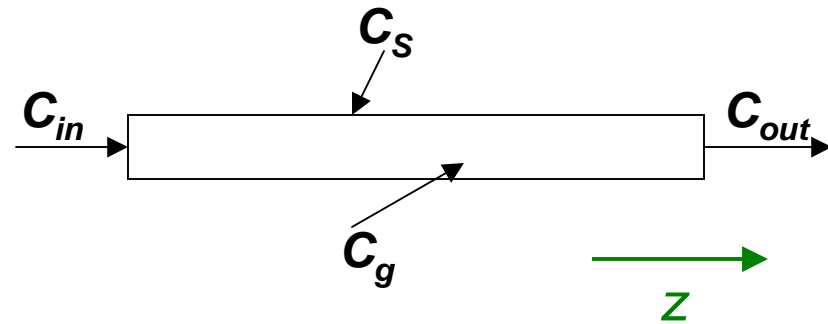


Temporal profile of moisture adsorption/desorption

Model Development for Mass Transport in Cylindrical Tubing

Moisture sorption on tubing wall:

$$\frac{\partial C_S}{\partial t} = k_{ads} C_g (S_0 - C_S) - k_{des} C_S$$



Governing equation for gas phase:

$$\frac{\partial C_g}{\partial t} = D_L \frac{\partial^2 C_g}{\partial z^2} - u \frac{\partial C_g}{\partial z} + \frac{A_S}{V} (k_{des} C_S - k_{ads} C_g (S_0 - C_S))$$

C_S : Moisture concentration on wall, mol/cm²;

C_g : Moisture concentration in gas, mol/cm³;

k_{ads} : Adsorption rate constant, cm³/mol/s

k_{des} : Desorption rate constant, 1/s

S_0 : Site density of surface sorption, # of sites/cm²;

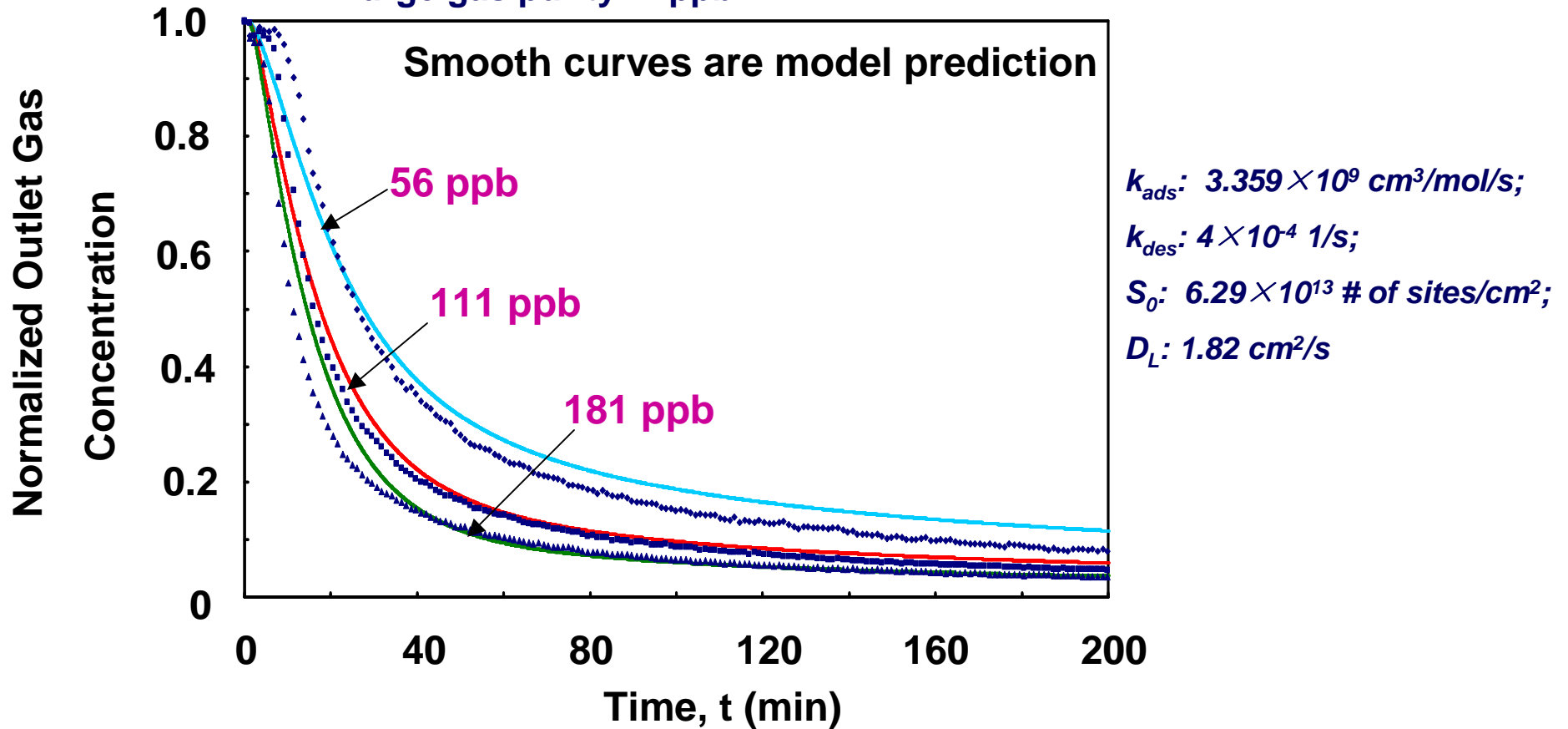
D_L : Dispersion coefficient, cm²/s;

u : Velocity, m/s; A_S : Surface area of wall, m²; V : Volume of tubing, m³

Experimental Data and Model Validation at Different Concentrations

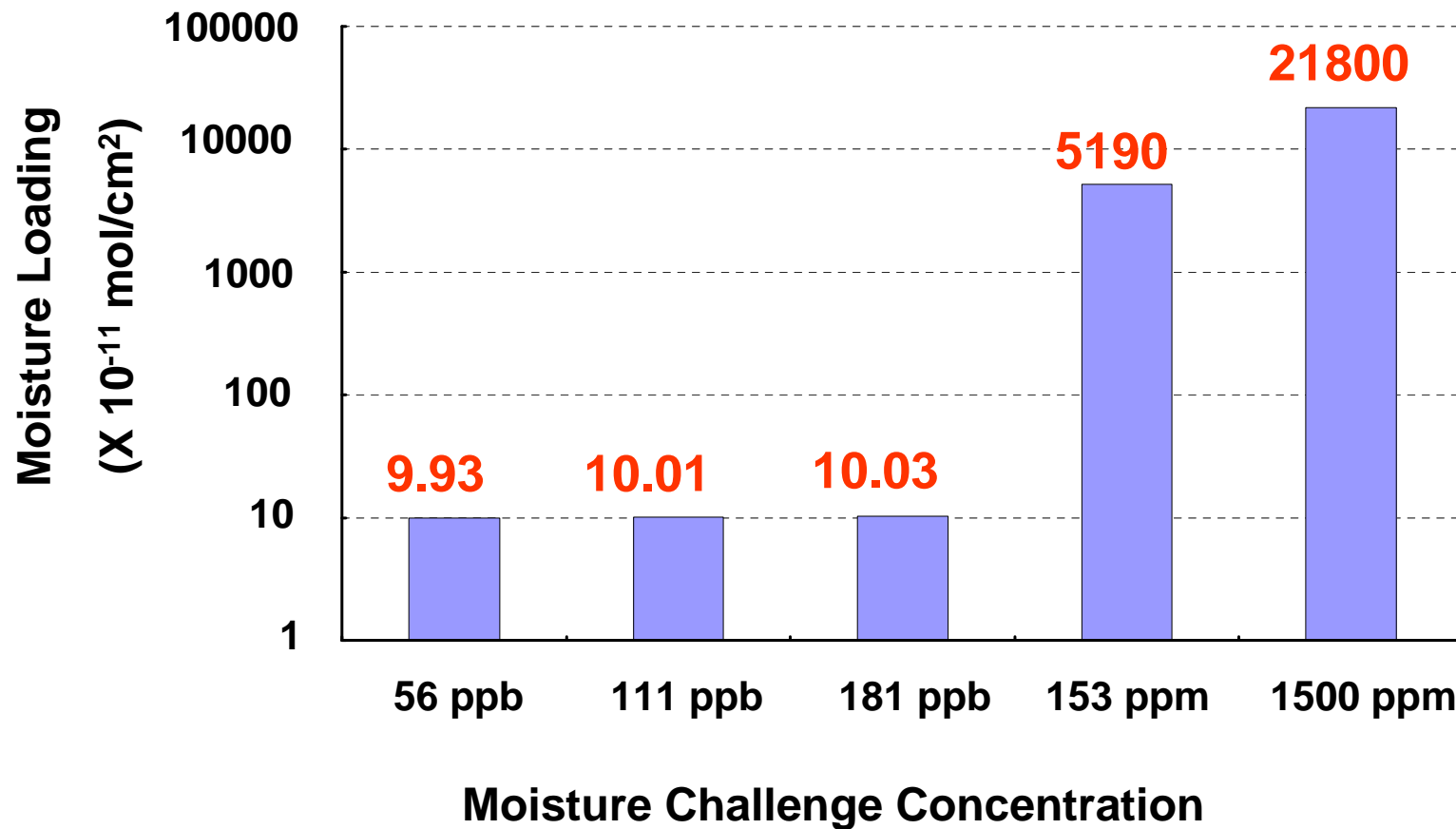
Purge gas flow rate: 350 sccm; Temperature: 25 °C

Purge gas purity: 1 ppb



Moisture Loading

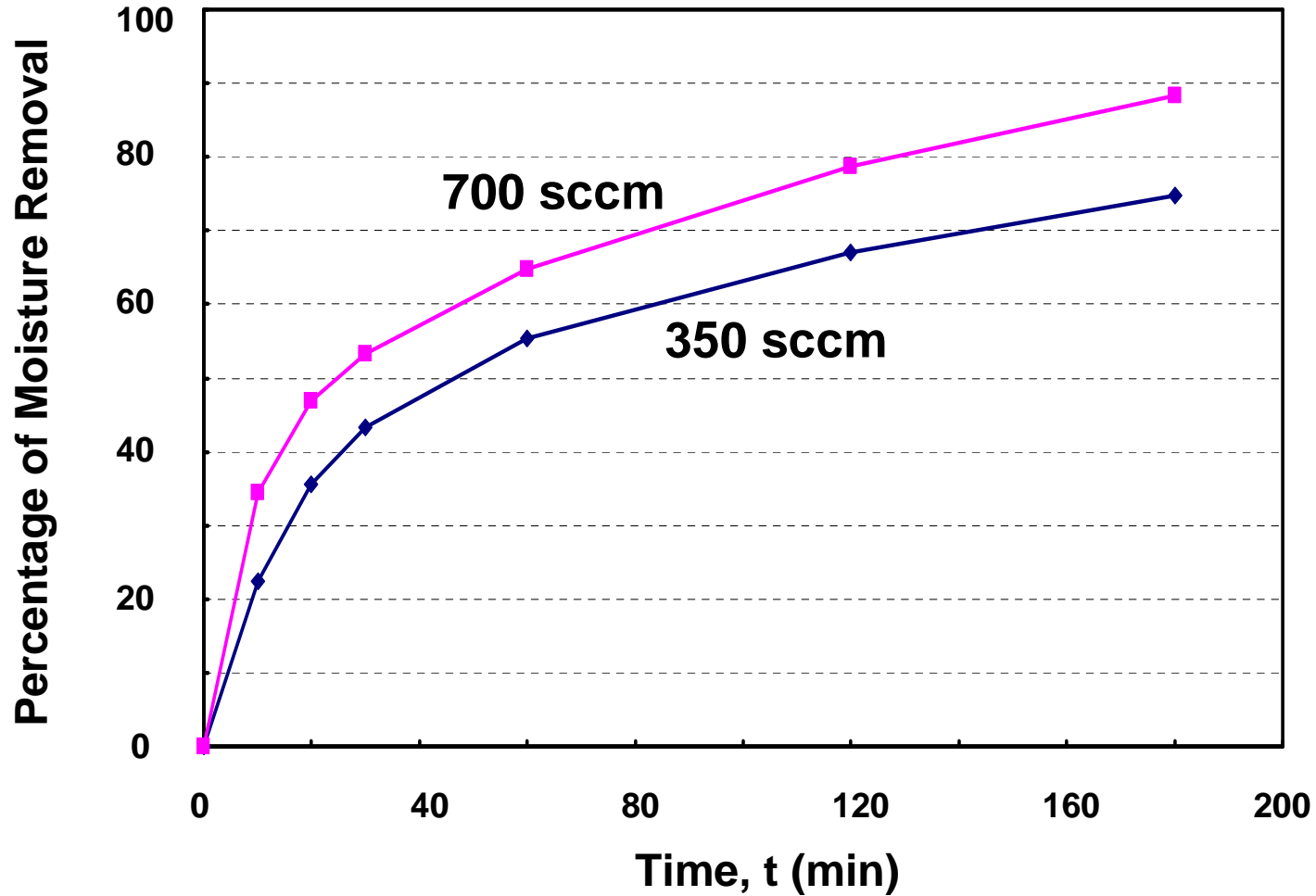
Temperature: 25 °C



Effect of Purge Flow Rate

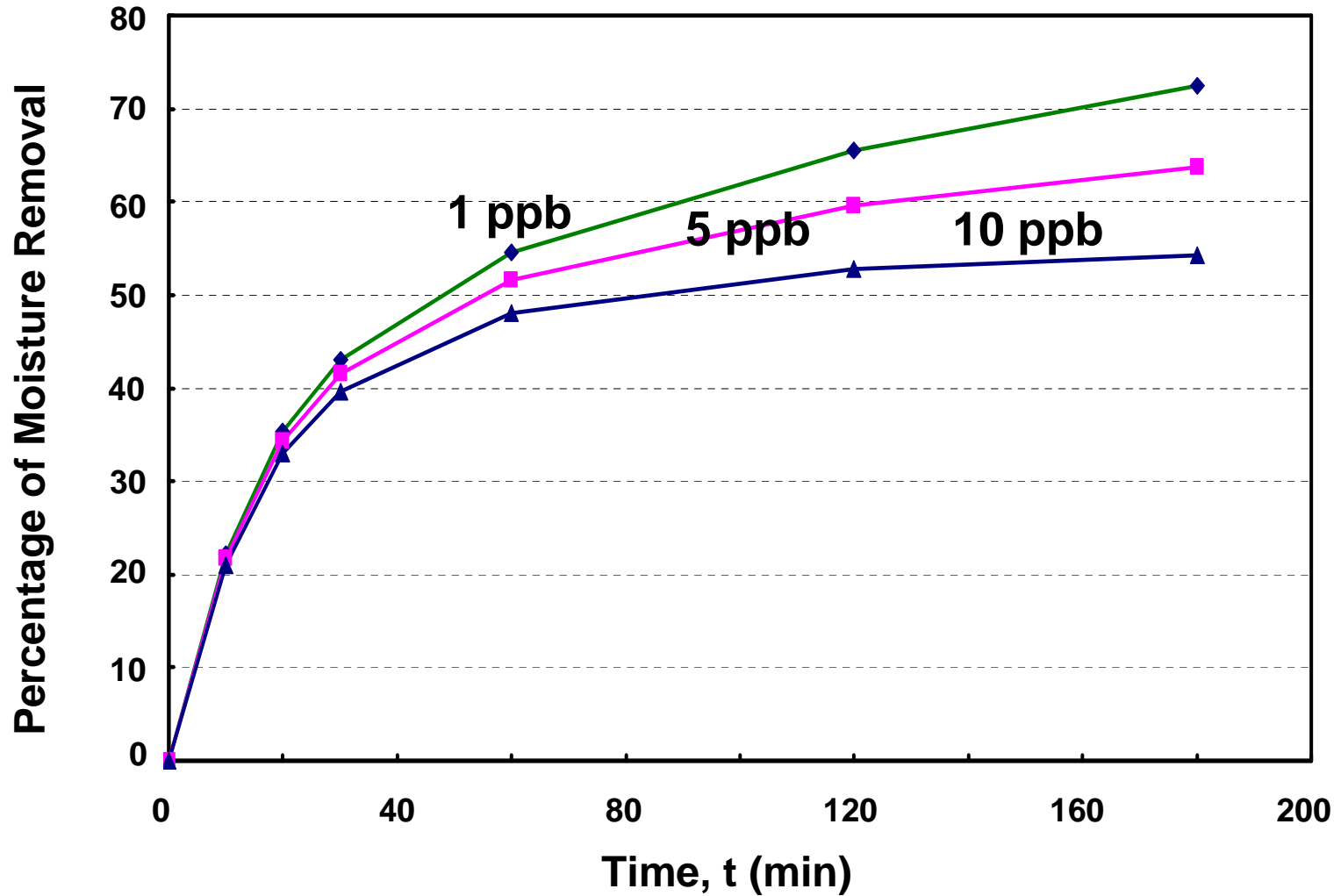
Challenge conc.: 181 ppb; Temperature: 25 °C

Purge gas purity: 1 ppb



Effect of Purge Gas Purity

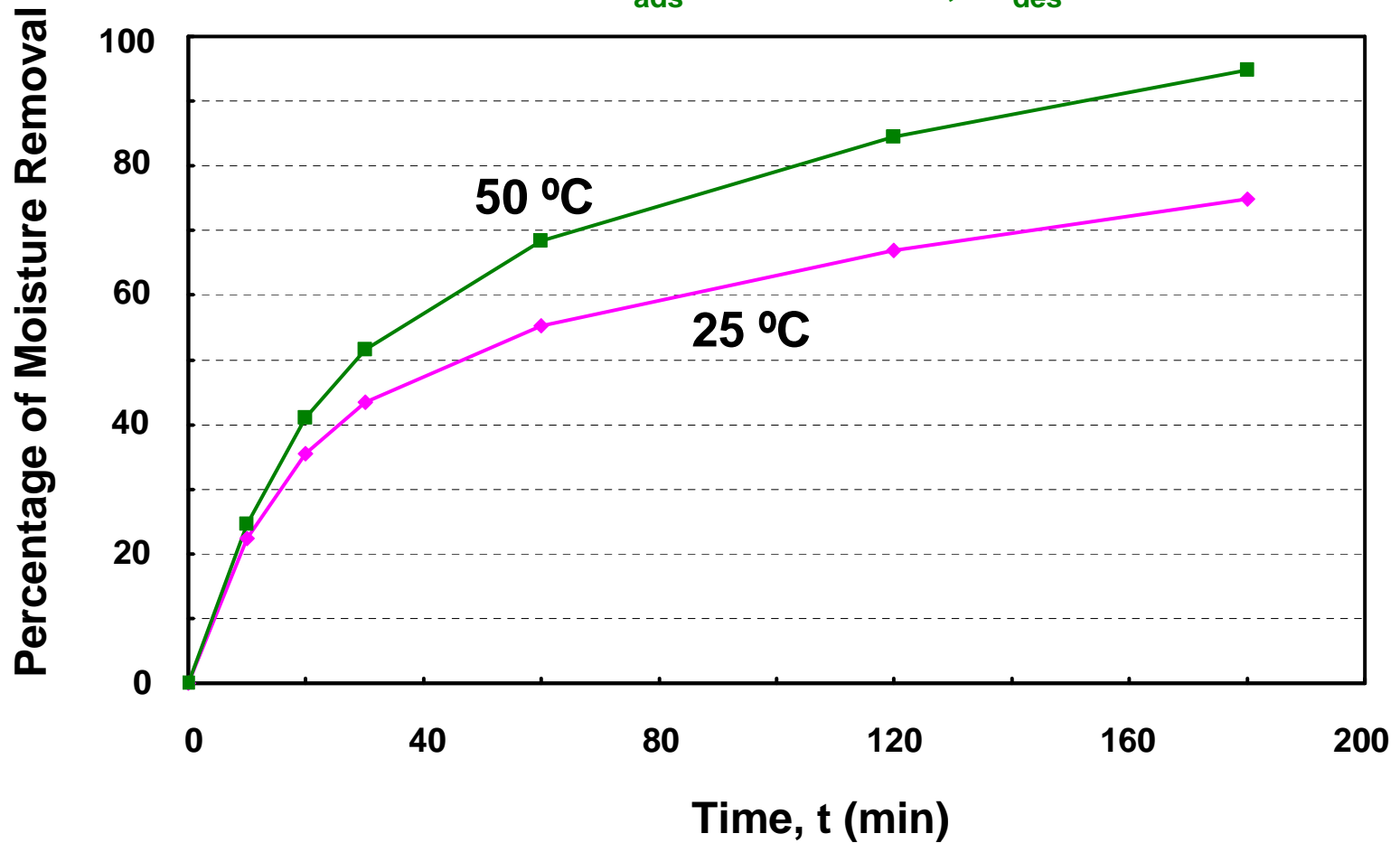
Challenge conc.: 181 ppb; Temperature: 25 °C; Flow rate: 350 sccm



Effect of Purge Gas Temperature

Challenge conc.: 181 ppb; Adsorption temperature: 25 °C;
Flow rate: 350 sccm; Purge gas purity: 1 ppb

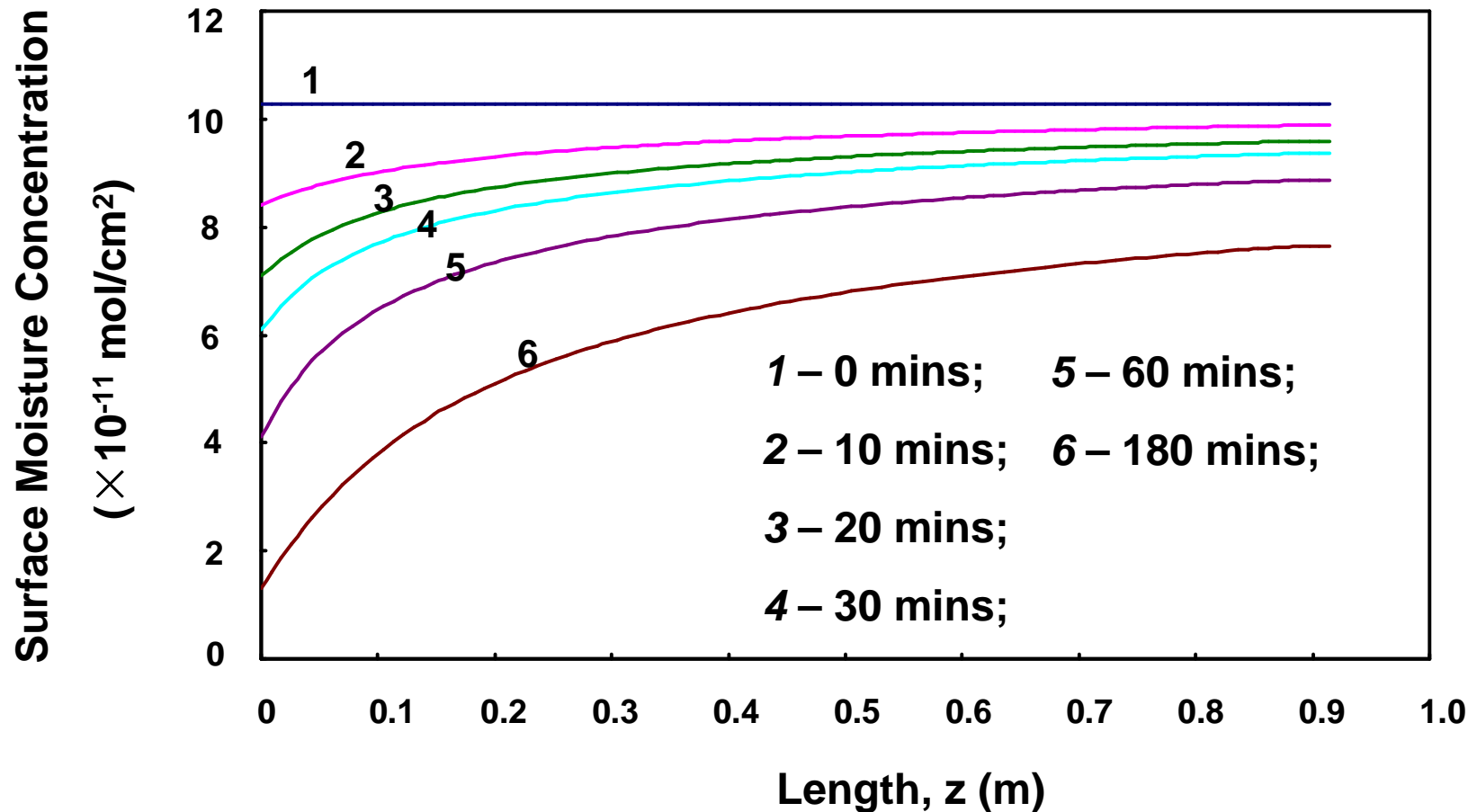
E_{ads} : ~ 19 kJ/mol; E_{des} : ~ 47 kJ/mol



Moisture Distribution along the Tubing at Different Purge Times

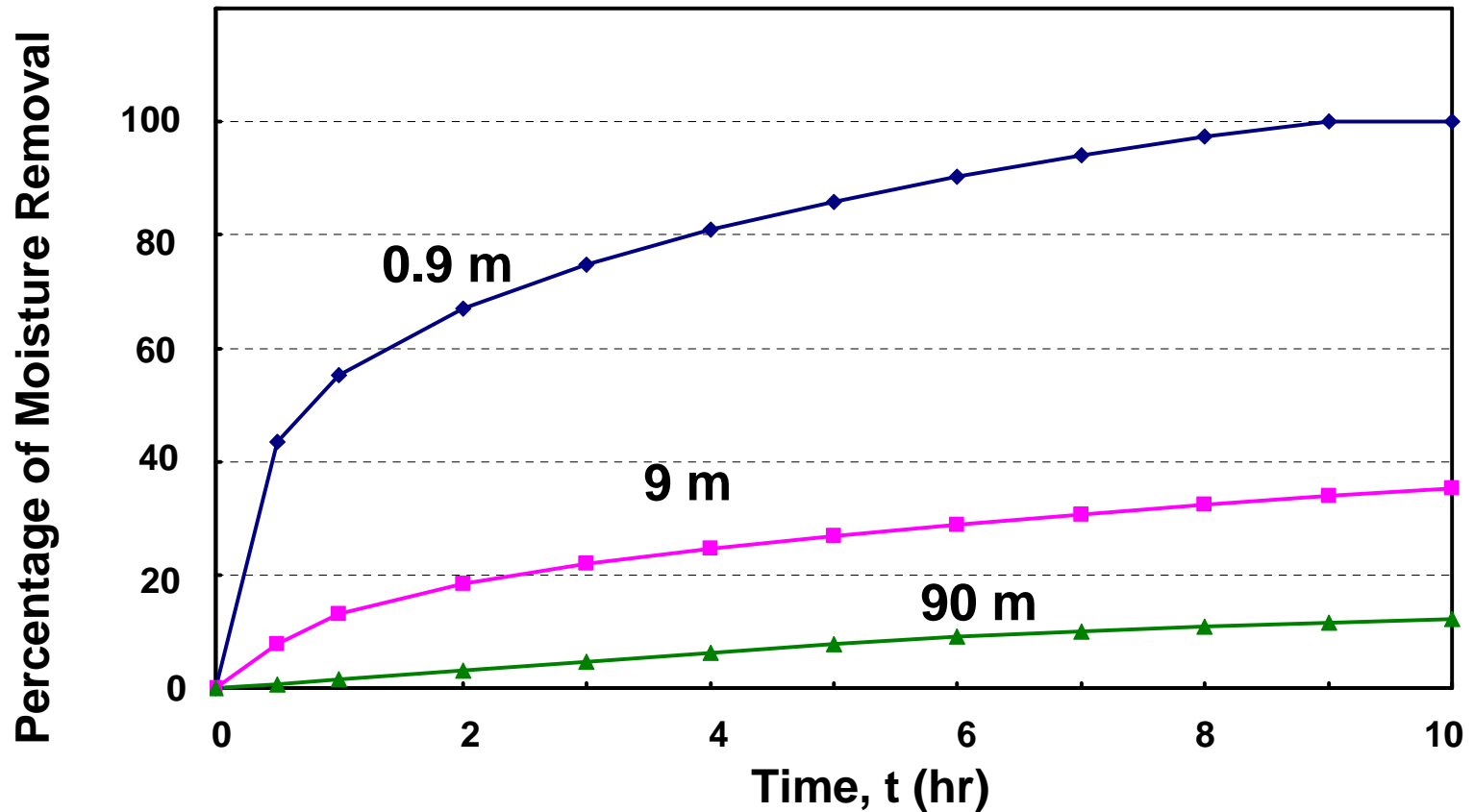
Challenge conc.: 181 ppb; Temperature: 25 °C;

Flow rate: 350 sccm; Purge gas purity: 1 ppb



Extension of Transfer Line

Challenge conc.: 181 ppb; Temperature: 25 °C;
Flow rate: 350 sccm; Purge gas purity: 1 ppb



Summary and Conclusions

- **Moisture removal from stainless steel surfaces is a slow and activated process.**
- **A technique, that combines measurement and process modeling, is developed to study the dynamics of moisture absorption and desorption, moisture loading, and moisture profile in a gas distribution network.**
- **The technique can be used to optimize the dry-down time and lower the purge-gas consumption during system start-up or recovery.**



**Subtask C-1-5 : *Research report on the screening of
of four options for PFOS removal from litho-track wastewater***

-1 year Sematech seed project -

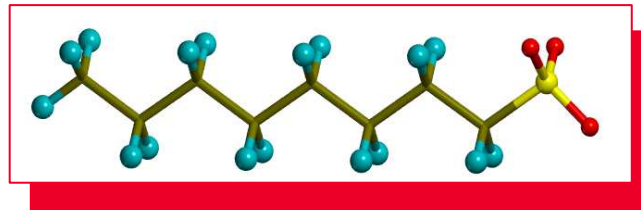
Valeria Ochoa, Jim A Field and Reyes Sierra

***Chemical and Environmental Engineering
University of Arizona***

Introduction



Perfluorinated surfactants are attracting increasing attention from environmental regulatory agencies due to recent reports of their world-wide distribution, environmental persistence and bioaccumulation potential.



PFOS

Feasible methods for the removal of PFOS and related compounds from industrial effluents are needed to minimize environmental discharges. Activated carbon (AC) is a well-known method for removal of halogenated organic contaminants in wastewaters. Although published data on the adsorption of fluorinated compounds onto AC is very scarce, there is some evidence that PFOS [1] and other alkyl sulfonated compounds [2, 3] can be adsorbed onto AC.

- (1) Lampert, D. J. et al., Practice Periodical Hazard. Tox. Radioactive Waste Managem. 2007. p. 60;
- (2) Ihara, Y., J. Appl. Polym. Sci., 1992. 44:1837. (3) Zor, S. J. Serbian Chem. Soc., 2004. 69:25..

Objectives



This seed project funded by Sematech evaluated the effectiveness of four different approaches for the removal of PFOS, *i.e.*,

- 1) Anaerobic reductive dehalogenation.
- 2) Biomimetic dehalogenation (vitamin B₁₂-Ti(III)-citrate).
- 3) Biosorption (by aerobic and anaerobic sludge).
- 4) Activated carbon adsorption.

Results obtained in studies performed to evaluate the feasibility of sorption of PFOS from effluents generated in the semiconductor manufacturing onto granular activated carbon (GAC) and other adsorbents such as wastewater treatment (WWT) sludge, NaY zeolite and poly(vinylpyrrolidone) (PVP).

ESH Metrics and Impact



I) Basis for comparison:

Reverse osmosis (RO)

II) ESH metrics

Goals/ Possibilities	Usage Reduction			Emission Reduction			
	Energy	Water	Chemicals	PFCs	VOCs	HAPs	Other Hazardous Wastes
Decrease PFOS/PFAS concentration in liquid streams by > 98% by adsorption onto granular activated carbon (GAC)	> 85% reduction	N/A	100% reduction in RO aids	>98%	N/A	N/A	No brine generation

Experimental conditions



- Adsorption isotherms determined in pH-7.2 buffer at constant ionic strength and temperature (30°C).

Compounds assayed:

- PFOS
- Perfluorobutane sulfonate (PFBS, $\text{CF}_3(\text{CF}_2)_3\text{SO}_3^-$, a compound proposed to replace PFOS)
- Perfluorooctanoic acid (PFOA, $\text{CF}_3(\text{CF}_2)_6\text{COOH}$, a common perfluorinated surfactant)

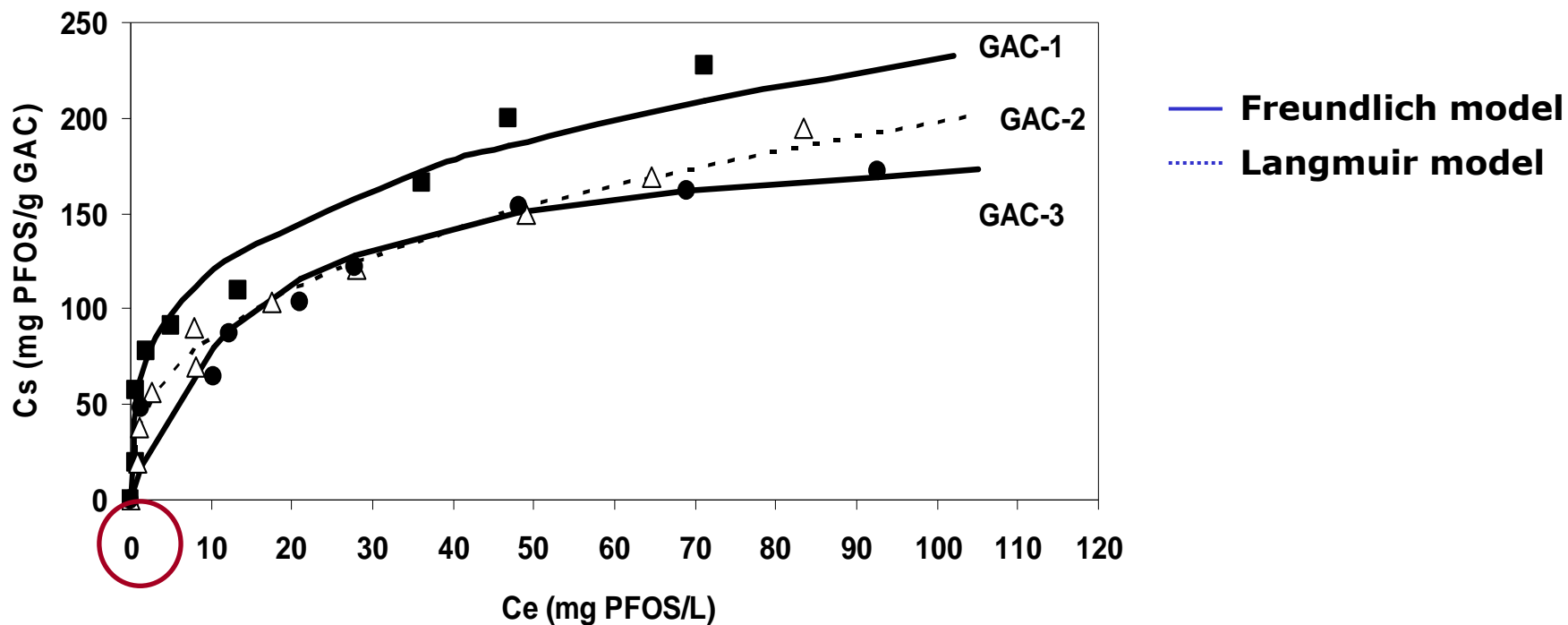
- Isotherms were fitted to:
 - Freundlich model
 - Langmuir model



Results



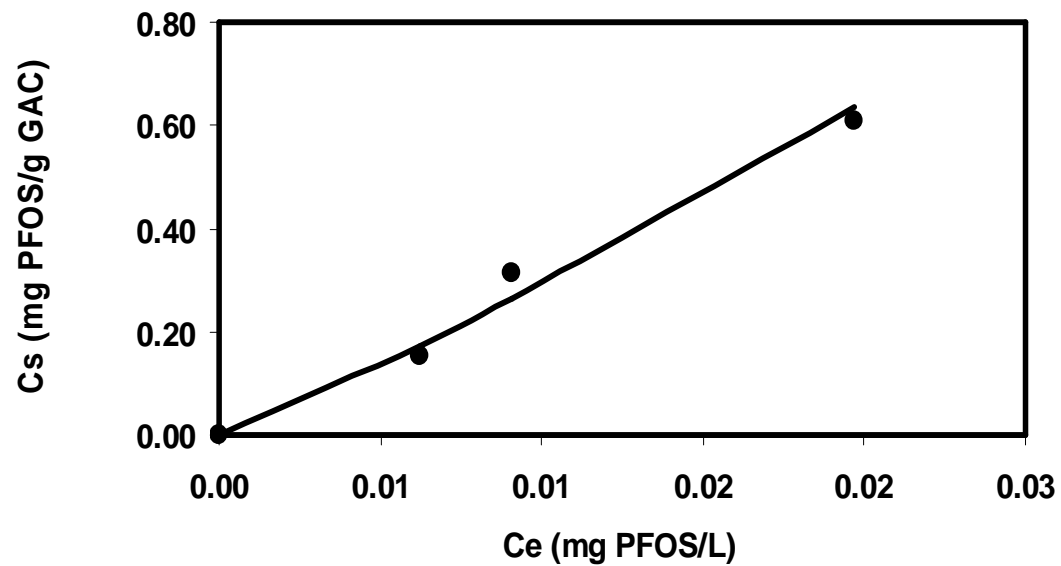
Adsorption isotherms of PFOS on GAC



Results



PFOS adsorption isotherms on GAC-1 in the low concentration range



Results



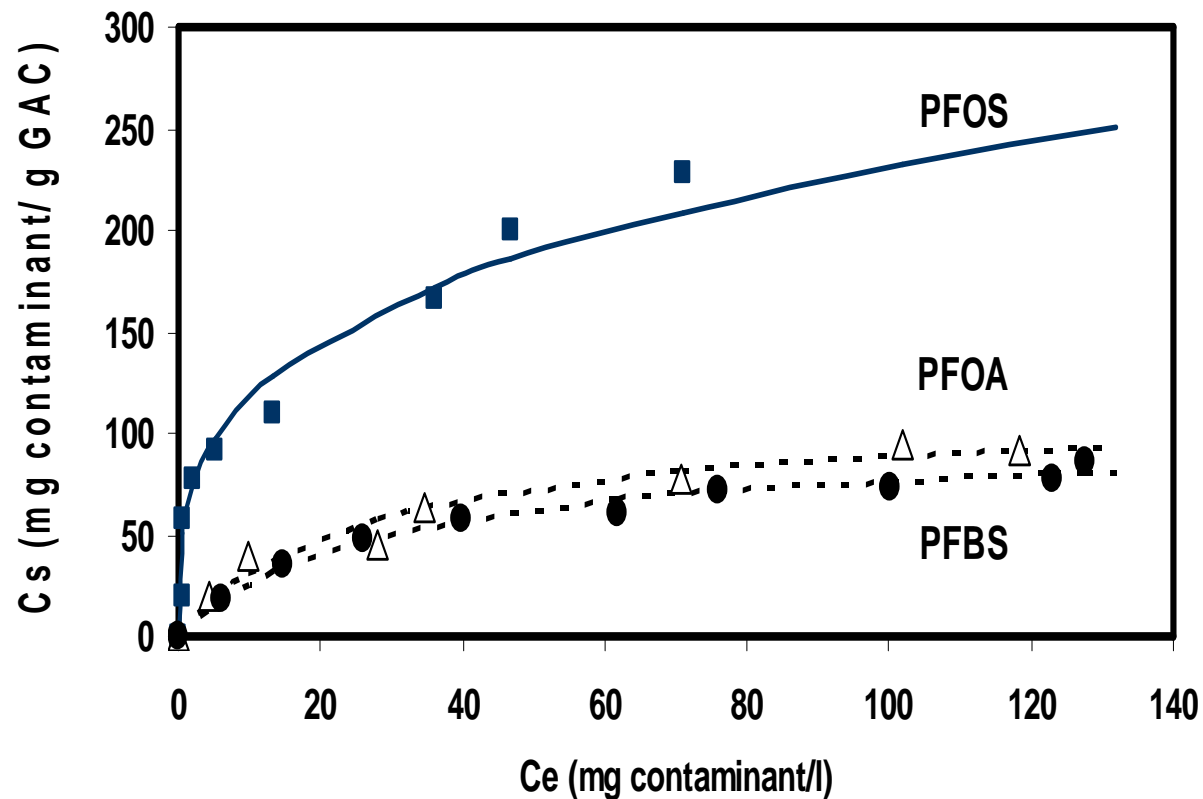
Langmuir and Freundlich isotherm constants for the adsorption of PFOS onto GAC.

Granular activated carbon	Langmuir isotherm			Freundlich isotherm		
	<i>a</i>	<i>b</i>	<i>r</i> ²	<i>K_f</i>	<i>n</i>	<i>r</i> ²
GAC-1	236.4	0.124	0.959	60.9	0.289	0.969
GAC-2	202.5	0.088	0.965	37.2	0.364	0.982
GAC-3	196.2	0.068	0.977	38.5	0.332	0.939

Results



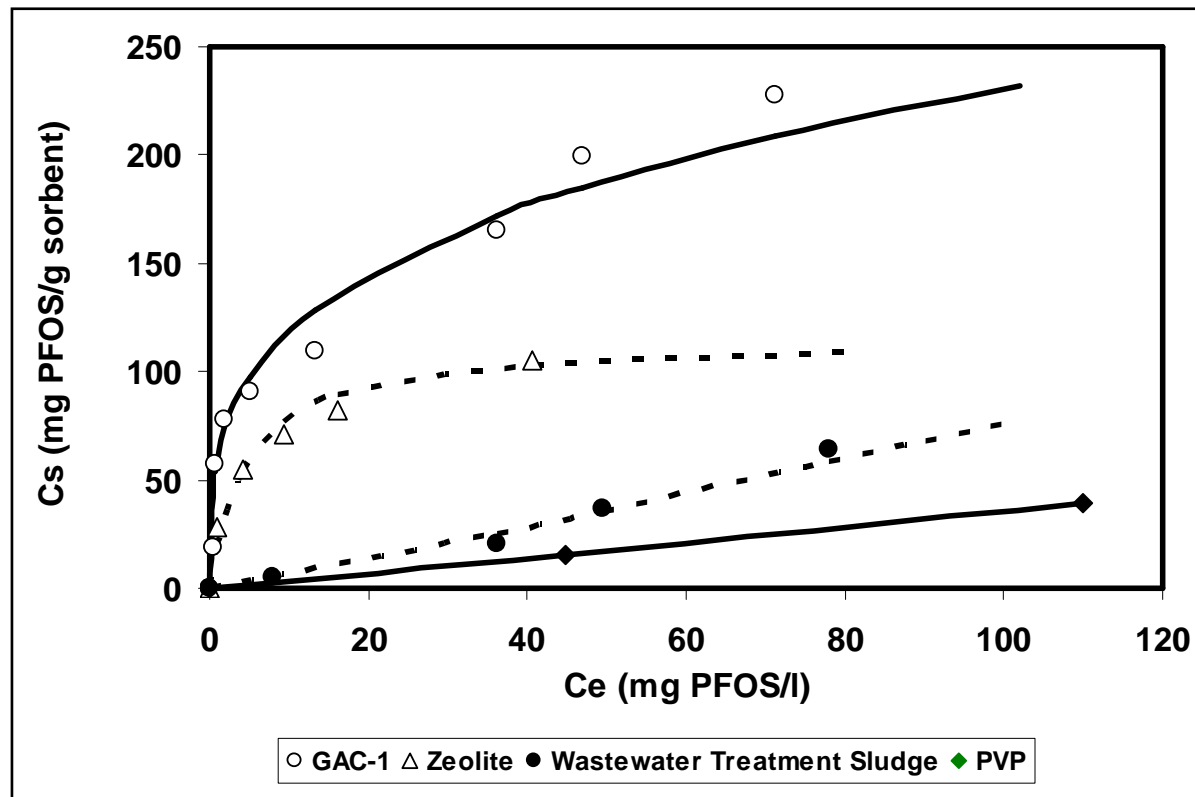
Adsorption isotherm of PFOS and related compounds on GAC-1



Results



Adsorption isotherm of PFOS on various adsorbents



Conclusions



- ❖ GAC adsorption is a promising method for the removal of PFOS from dilute aqueous streams.
- ❖ The removal efficiency for PFOS was 3-fold higher compared to that of PFOA and PFBS.
- ❖ Among all adsorbents evaluated in this study, GAC showed the highest affinity for PFOS.
- ❖ Partial removal of PFOS should be expected during wastewater treatment due to biosorption.

Industrial Collaboration/Technology Transfer

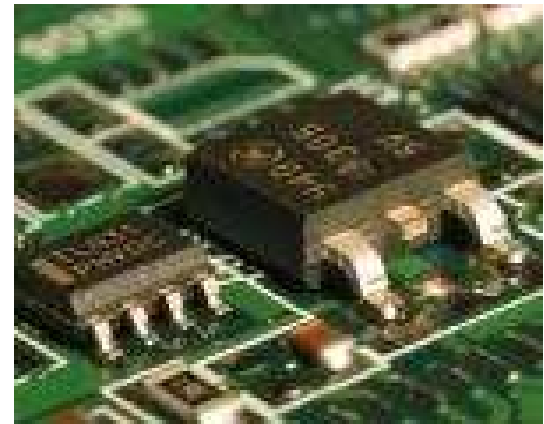
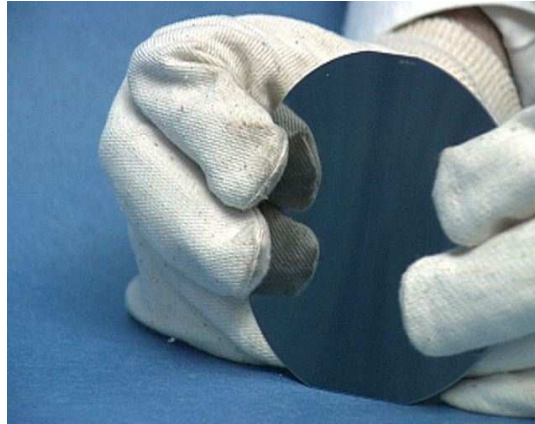
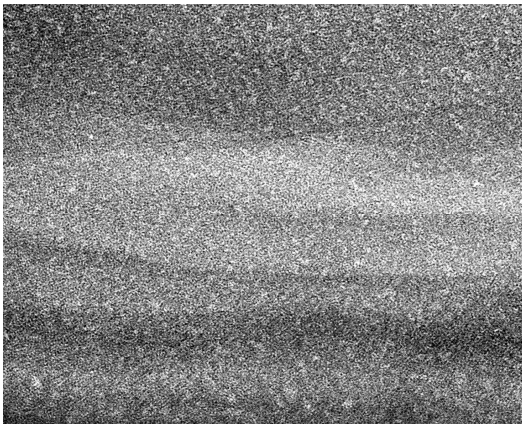


Industrial Liaisons:

Walter Worth - Sematech

Tim Yeakley – TI

Ultra Low- k Film Repair and Pore Sealing Using Supercritical Fluids Sematech Project Thrust D, Task 425.010



Lieschen Hatch and Anthony Muscat

lchoate@email.arizona.edu, muscat@erc.arizona.edu

Department of Chemical & Environmental
Engineering

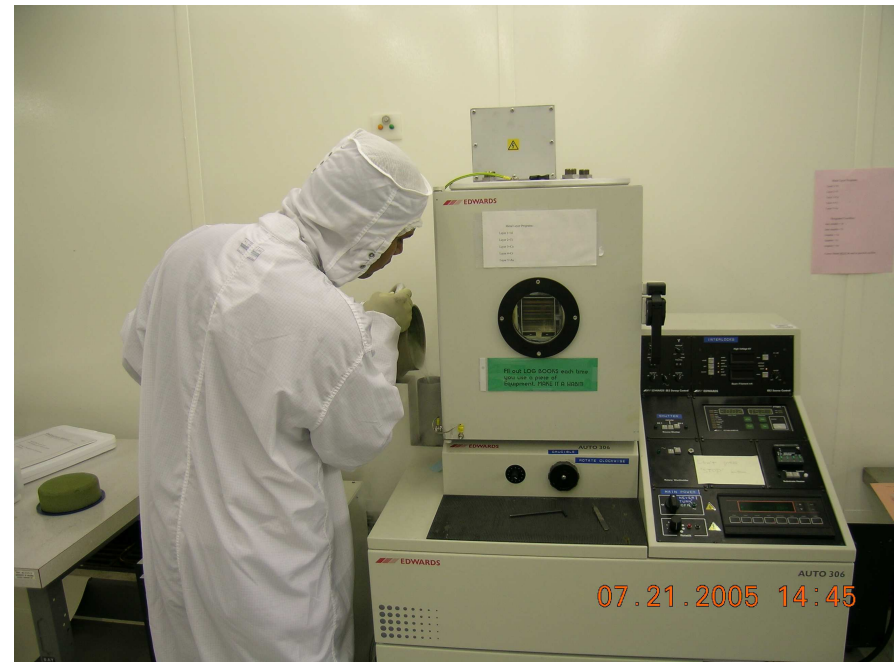
University of Arizona, Tucson, AZ 85721



SRC/Sematech Engineering Research Center for Environmentally Benign Semiconductor Manufacturing

Project Objectives

- Repair porous ultra low- k films
- Seal mesoporous films
- Minimize sealing layer thickness
- Restore hydrophobicity
- Minimize solvent volume
- Maintain mechanical strength

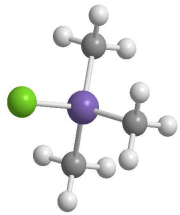


ESH Impact and Metric

Goals/ Possibilities	Usage Reduction			Emission Reduction			
	Energy	Water	Chemicals	PFCs	VOCs	HAPs	Other Hazardous Waste
Reduce organic solvent usage in processing	separations	up to 100%	up to 100% of org. sol.	N/A	capture cosolvents	CO ₂ is non-hazardous	up to 100% reduction in liquid waste
Reduce processing time and temperature	up to 50%	N/A	N/A	N/A	N/A	N/A	overheating system
Compatible with vacuum processing	up to 100%	N/A	N/A	N/A	N/A	N/A	develop one tool with multiple functions
Reduce worker exposure to vapors	ventilation	N/A	up to 50% of chlorine vapors	N/A	volatiles during chemical input	N/A	N/A

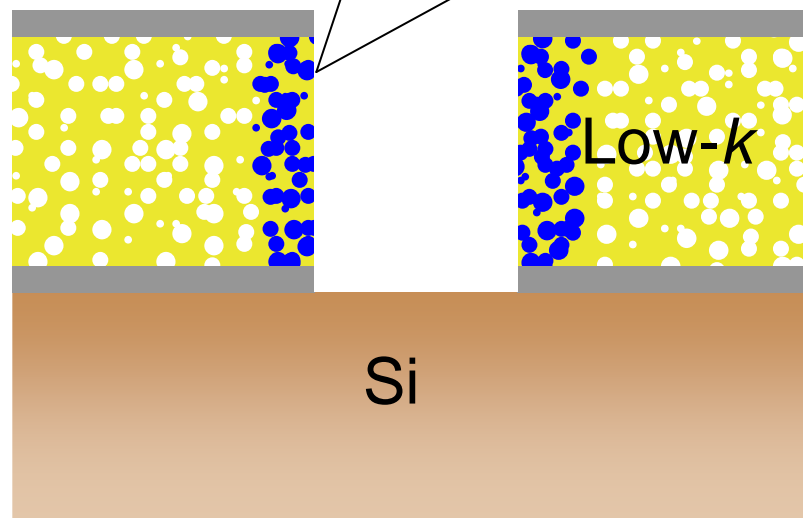
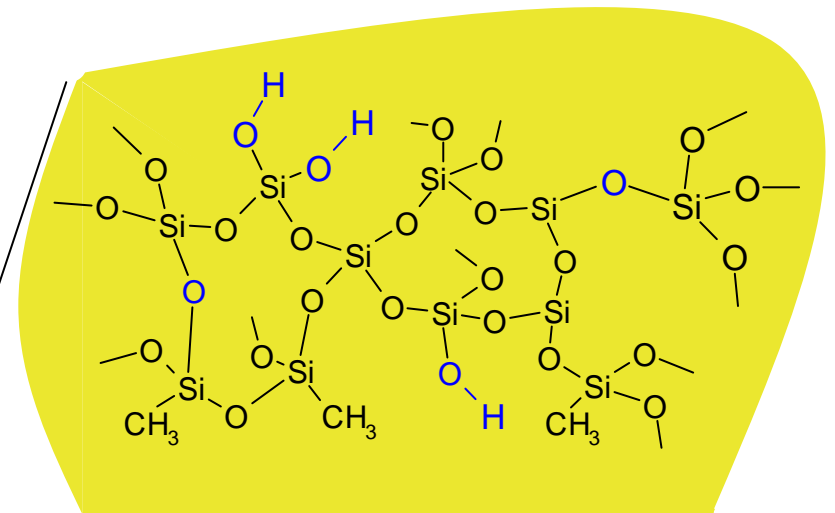
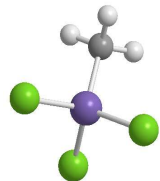
Chemistry of Chlorosilanes and p-MSQ

When silicon wafers are plasma ashed, silanol (SiO-H) groups form in the low-*k* film. These SiO-H groups cause the film to be hydrophilic, increasing the dielectric constant.



Trimethylchlorosilane
(TMCS, 0.44 nm)

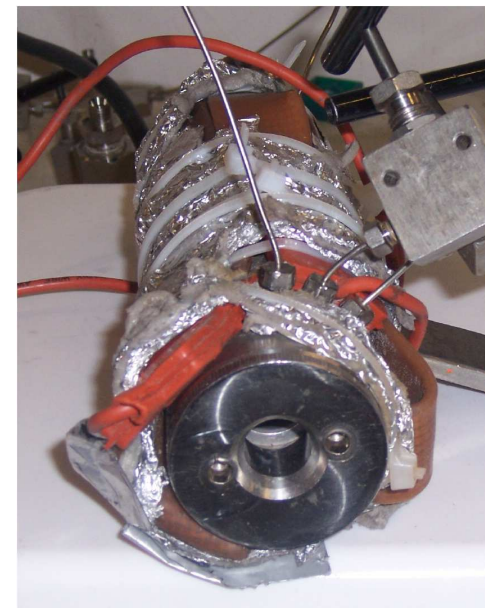
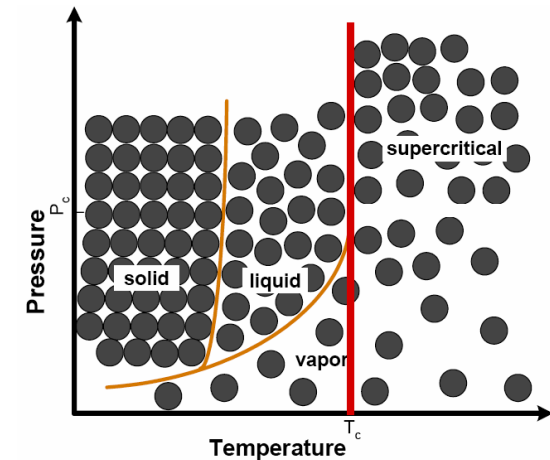
Methyltrichlorosilane
(MTCS, 0.43 nm)



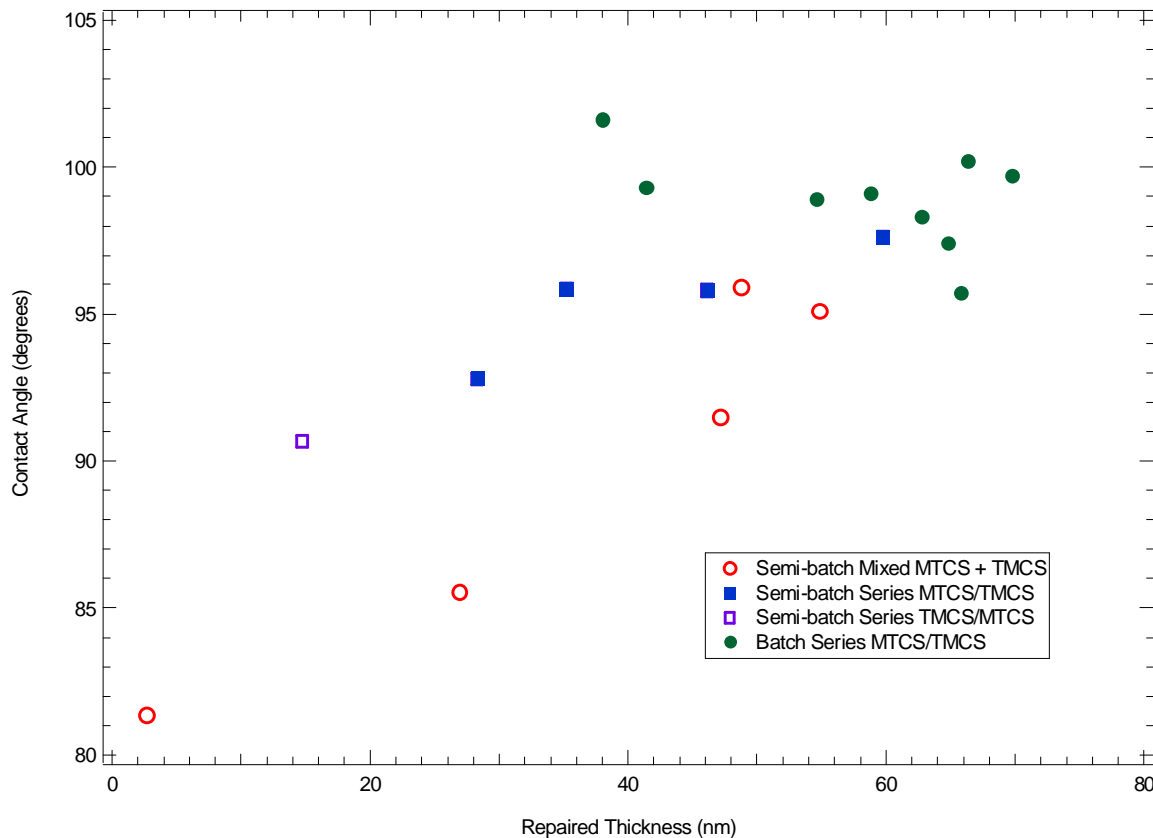
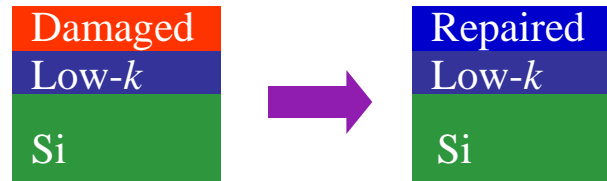
Experimental Method

P-MSQ: 40% porosity, $< 10^\circ$ contact angle, 360 nm thick, $k = 2.4$

- P-MSQ samples loaded into solubility cell, rinsed with CO_2
- CO_2 pumped into cell to 87 bar
- Chlorosilanes pumped in at 90 bar
- Processed for 3 min, then evacuated
- Final $T = 33, 38$ or $43 \pm 1^\circ\text{C}$
- Final $P = 90 \pm 1$ bar
- CO_2 $T_c = 32^\circ\text{C}$
- CO_2 $P_c = 72$ atm

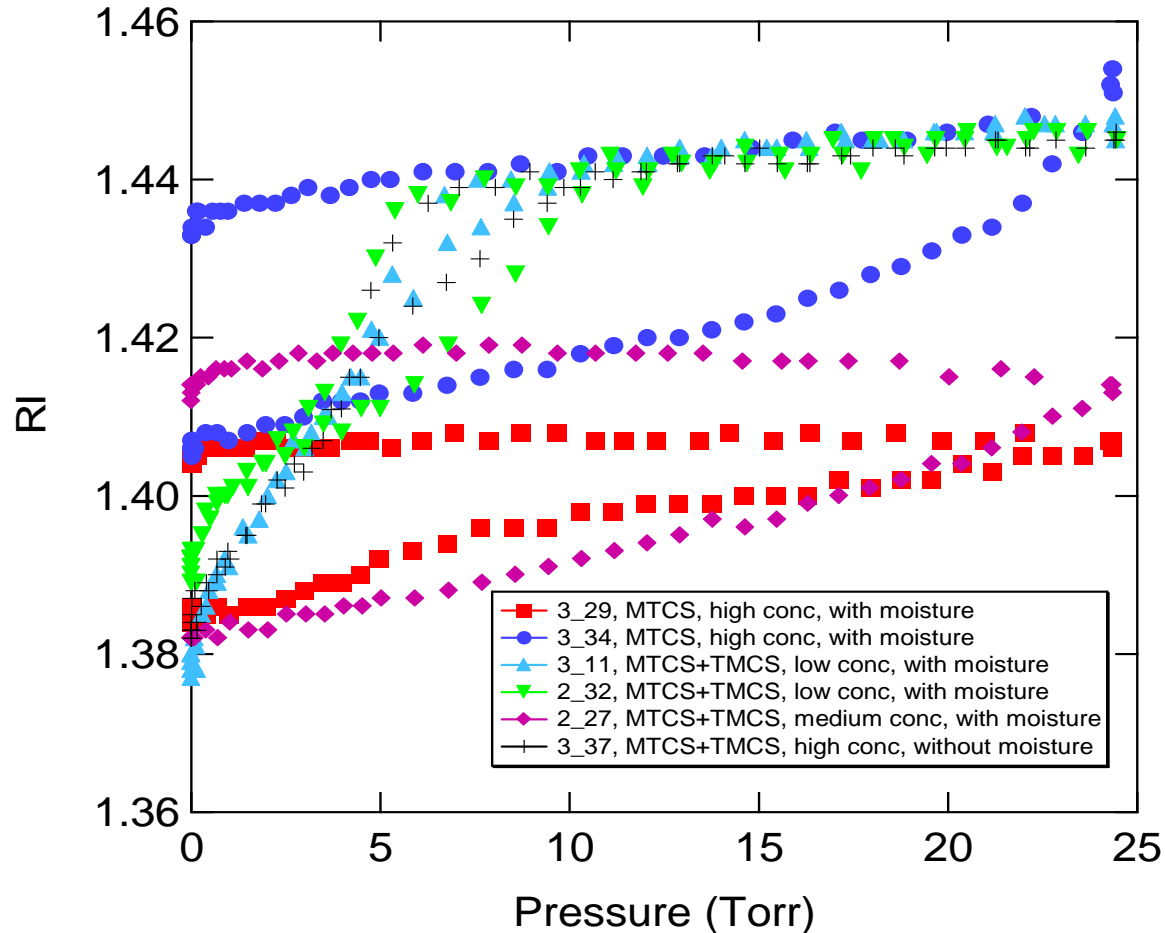


Results: Chlorosilane Repair of p-MSQ



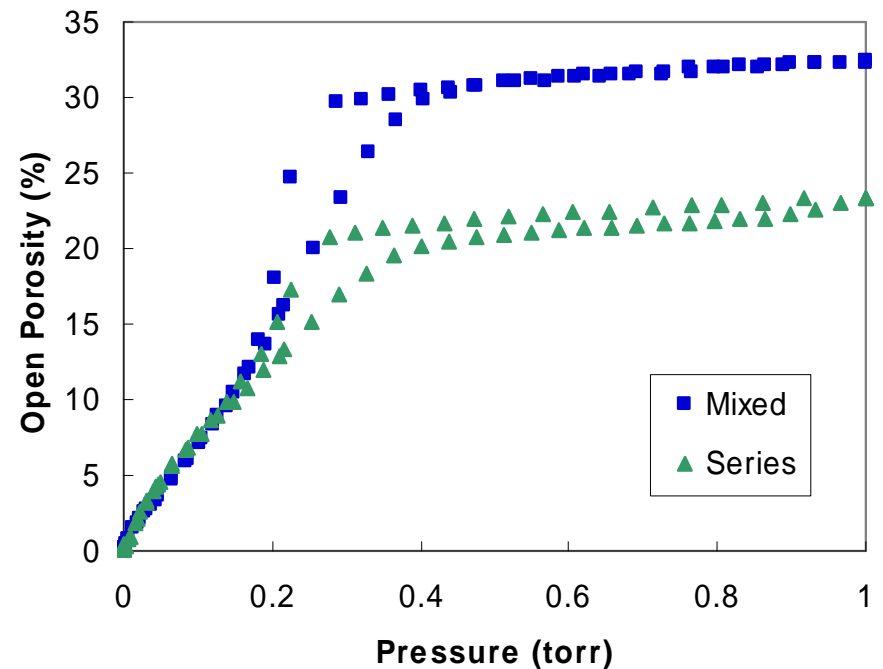
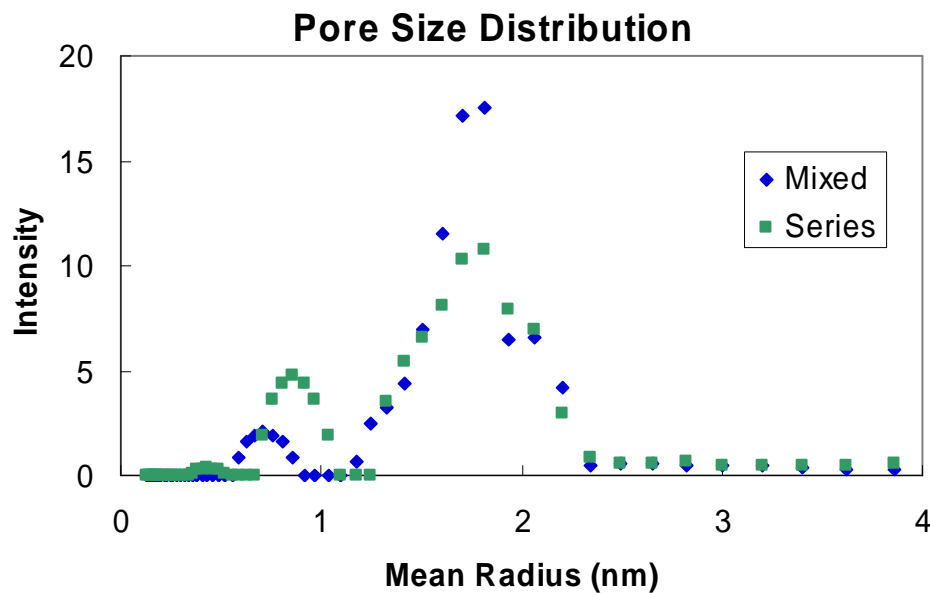
- Series MTCS/TMCS led to higher contact angles with less thickness added
- Goal: MTCS/TMCS to decouple contact angle and thickness

Results: Ellipsometric Porosimetry



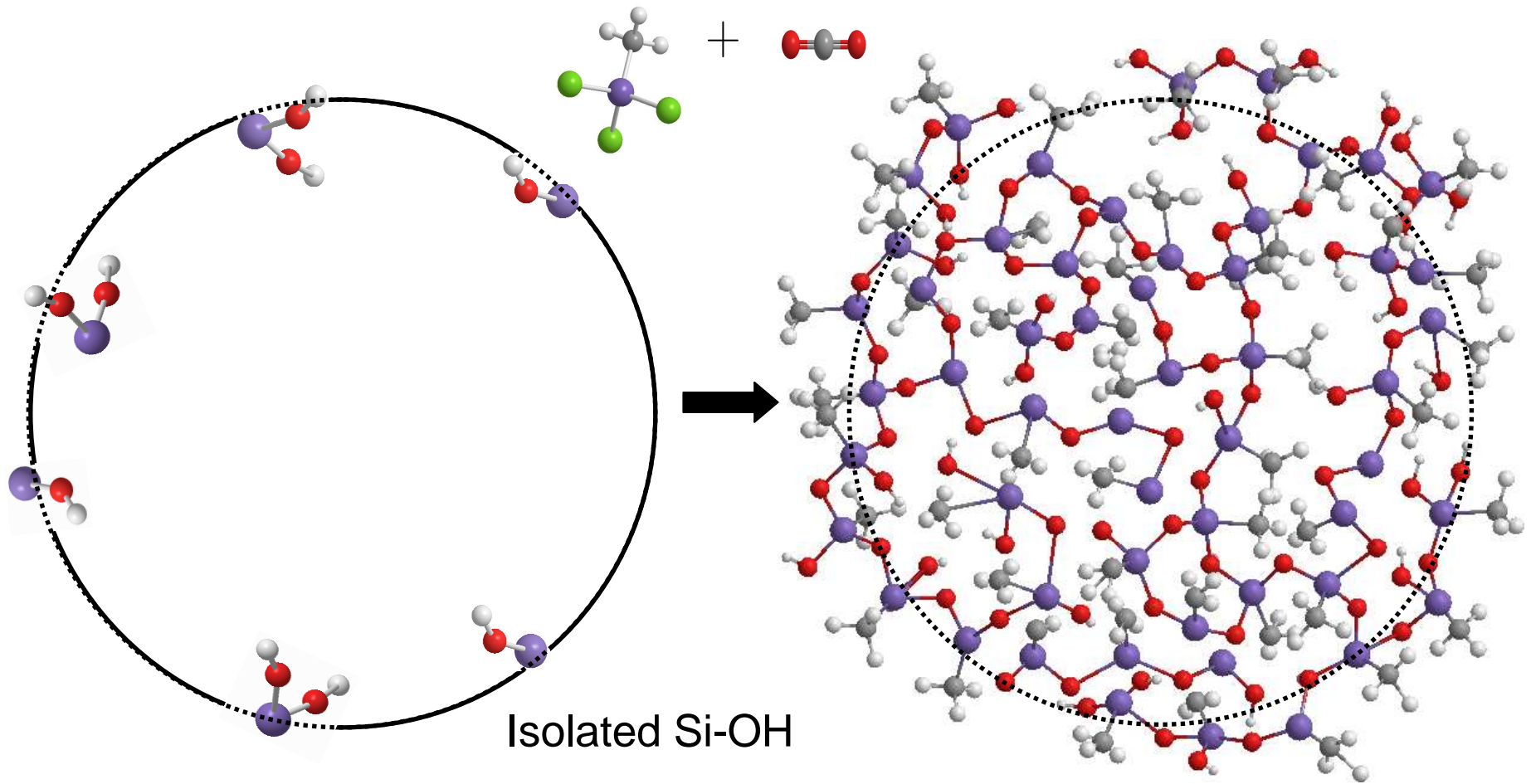
- Pore capped after MTCS/TMCS with moisture
- Pore not capped after MTCS/TMCS without moisture

Results: Pore Size Distribution and EP



- Series MTCS/TMCS decreases porosity by 50 %
- Series MTCS/TMCS better at capping pores than Mixed MTCS + TMCS

Pore Sealing Process

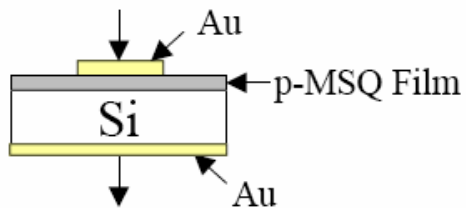
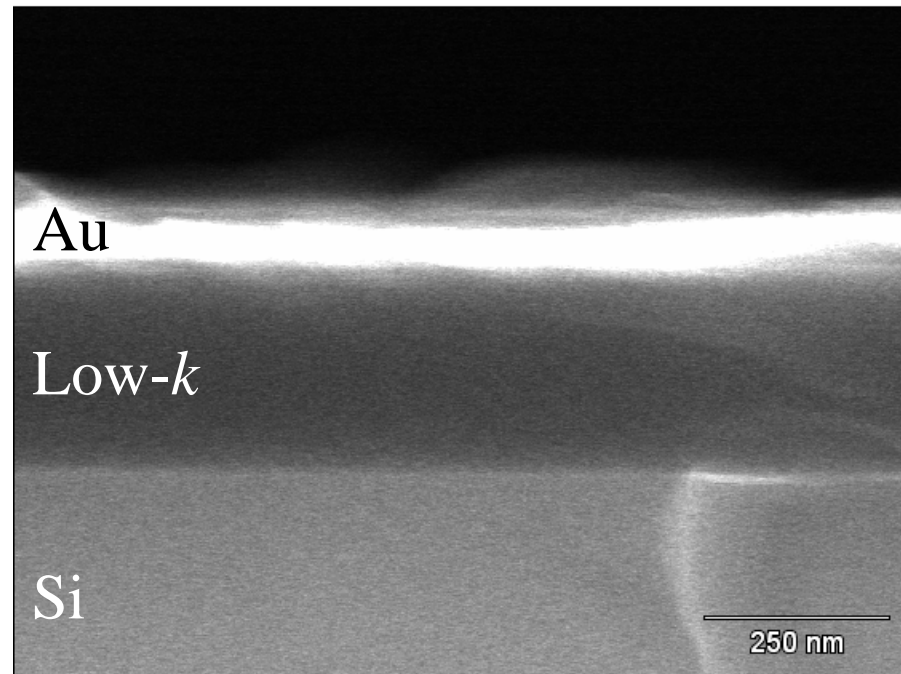
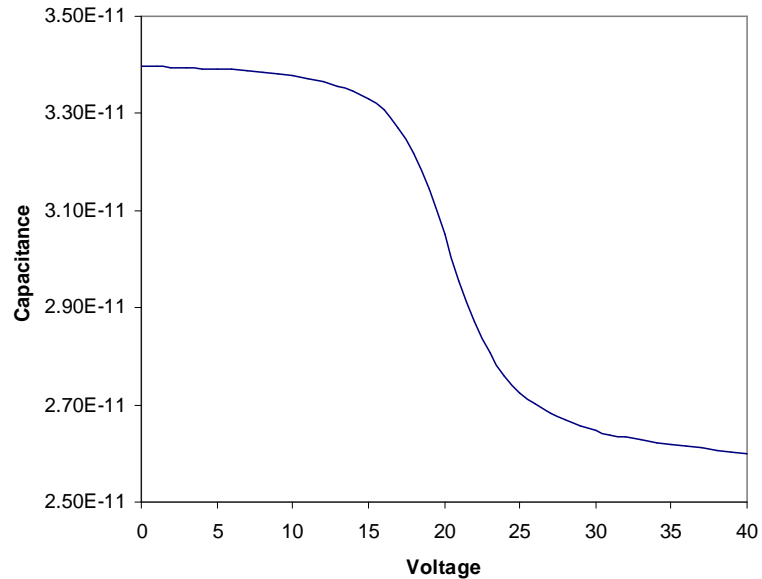


Isolated Si-OH

Plasma ashed film

MTCS sealed pore

SEM Images



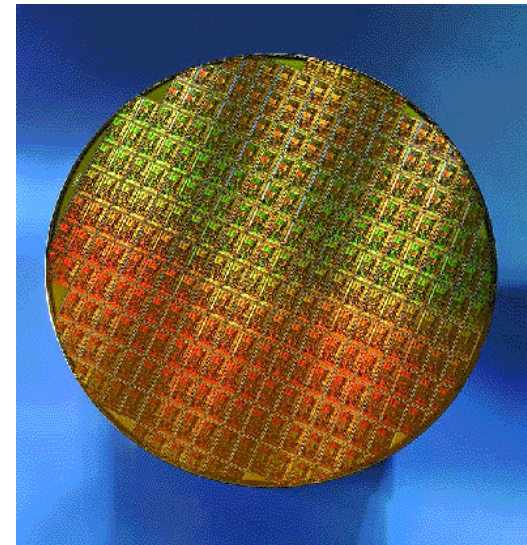
SEM image of processed sample

Conclusions

- Demonstrated that MTCS followed by TMCS restored the contact angle and sealed pores in p-MSQ
- Controlled repair thickness by controlling process T and P in solubility cell

Future Plans

- Pore Sizes
- Patterned/CVD low- k samples
- Other low- k films



Industrial Collaboration/ Technology Transfer

- Sematech
 - Steve Burnett (ESH Program Manager)
 - Eric Busch (Interconnect Division, AMD Assignee)
 - Frank Weber (Interconnect Division, Infineon Assignee)
 - Sharath Hosali
 - Sitaram Arkalgud
- NSF/SRC/Sematech EBSM Engineering Research Center (EEC-9528813/2001-MC-425)
- Texas Instruments
 - Phil Matz
- University of Arizona
 - Bo Xie, Adam Thorsness,
Gerardo Montano, Eduardo Vyhmeister



Low-Energy Hybrid (LEH) Water Purification Technology

**A Novel Method for Water Purification/Recycling
and Solid-Waste Minimization**

Co-sponsors: ERC and the University of Arizona TRIF Program

Kai Chen, Mike Schmotzer, Farhang Shadman

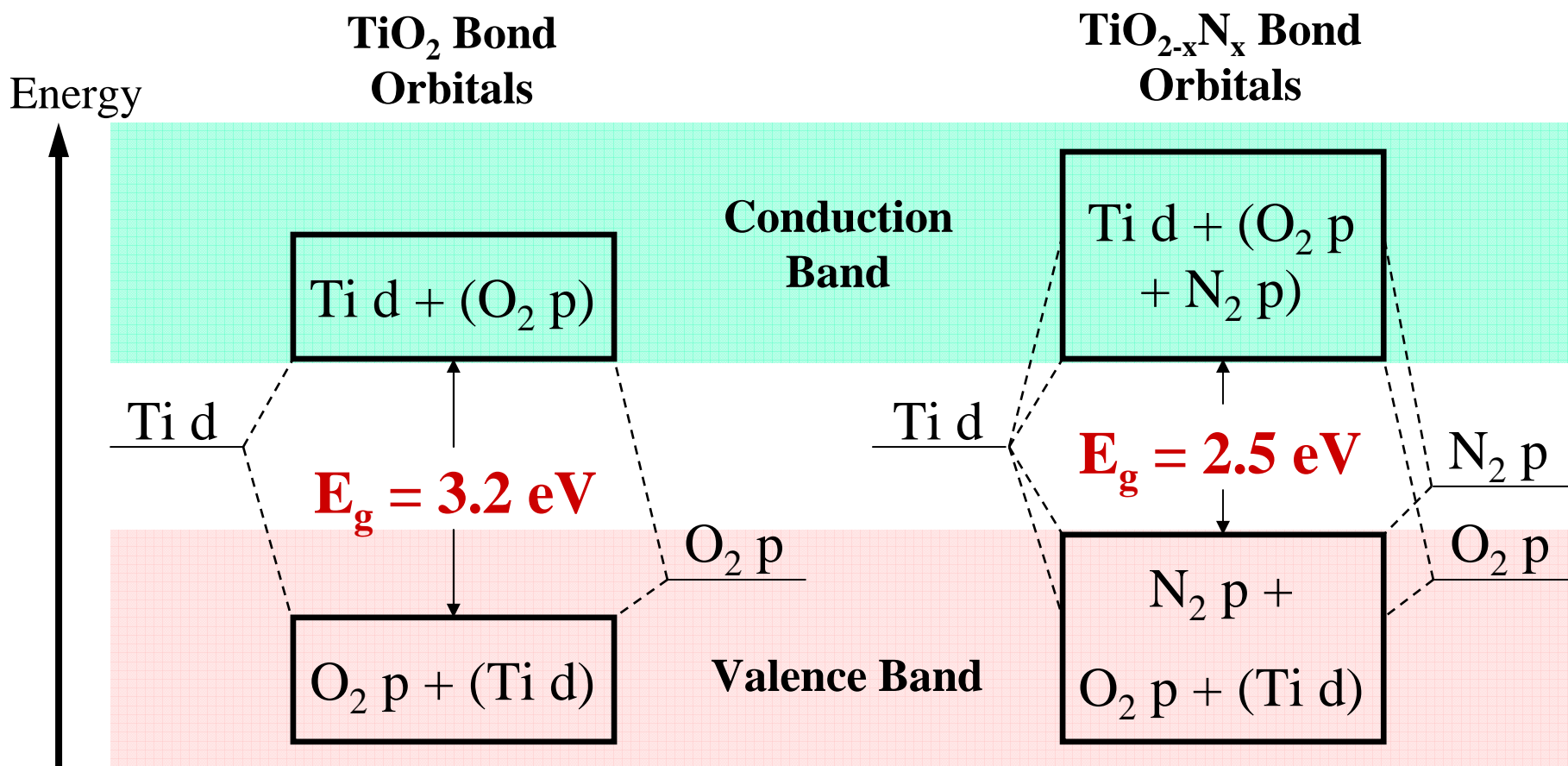
**Chemical and Environmental Engineering
University of Arizona**

SRC/Sematech Engineering Research Center for Environmentally Benign Semiconductor Manufacturing

Objectives

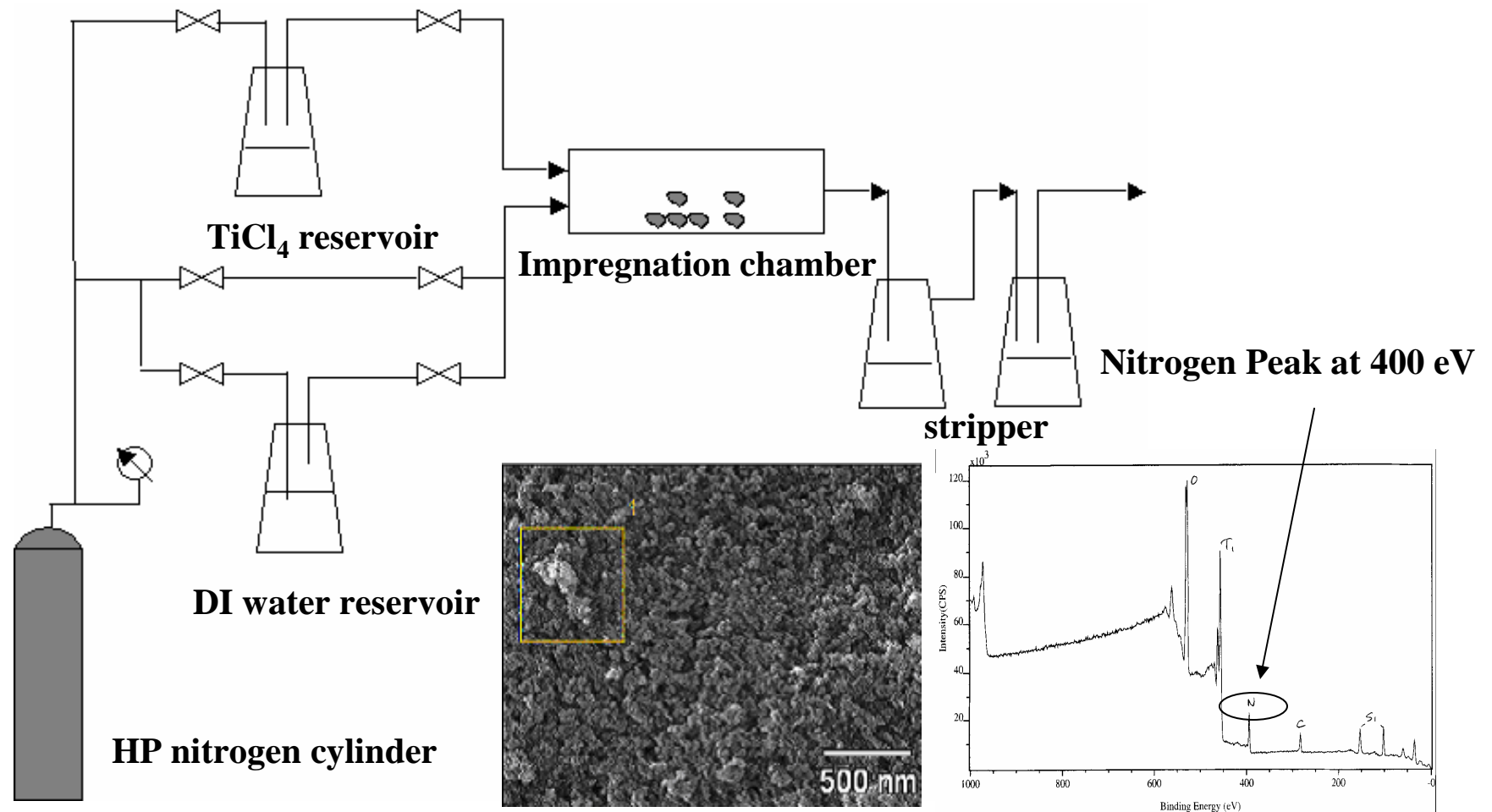
- **Develop a novel low-energy hybrid (LEH) purification technique for removal of recalcitrant organic impurities**
- **Combine the following desirable advantages:**
 - Lower energy use through enhanced catalytic oxidation
 - Low chemical use through extended ion-exchange life
 - Reduce waste through self-cleaning activated carbon
- **Integrate the new technology with typical fab UPW plant process flow to:**
 - Promote synergy and efficiency
 - Reduce energy usage and waste generation
- **Resolve long-term technology obstacles against true UPW recycling**

Effects of Nitrogen Doping in TiO_2



- Addition of nitrogen increases size of bond orbitals, thus **decreasing** the energy band gap.

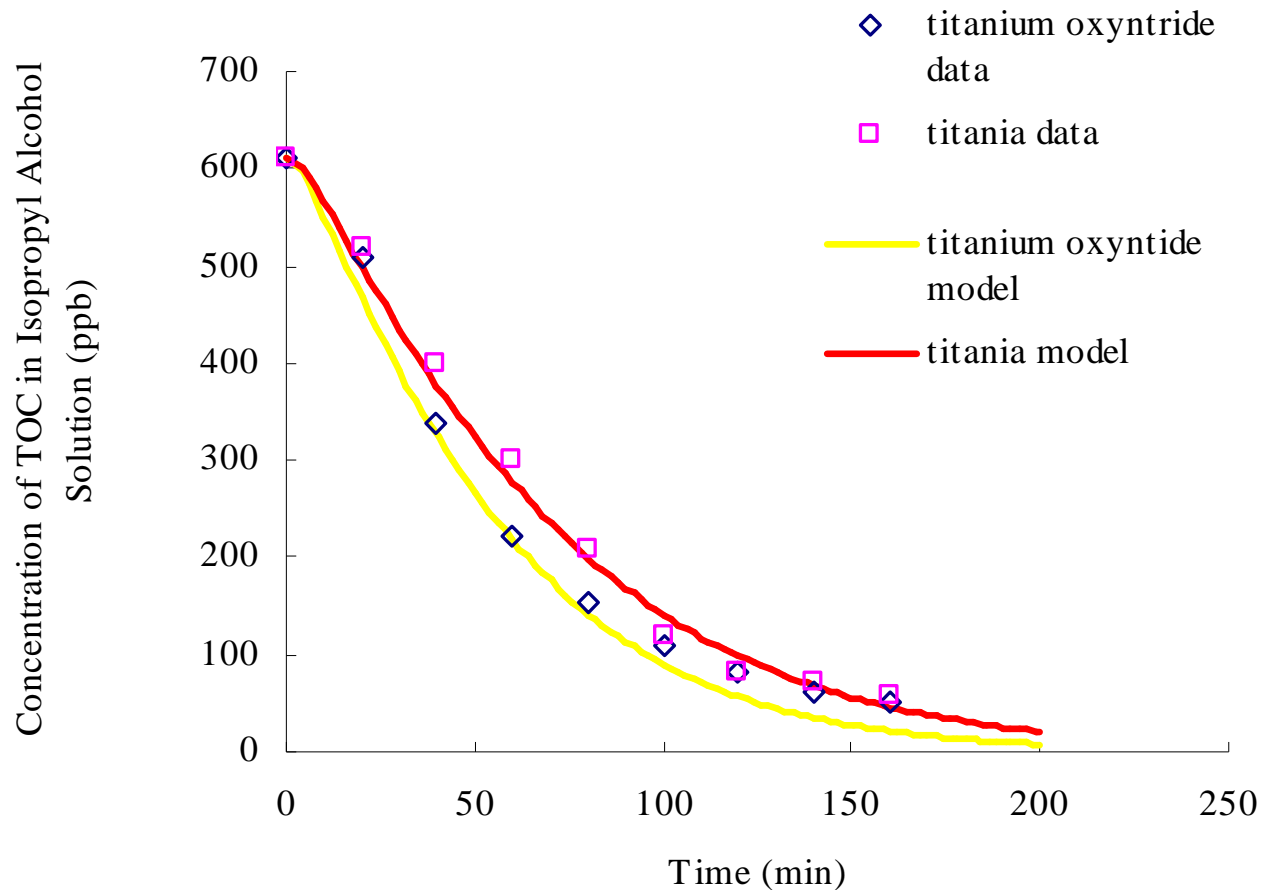
Preparation of Supported Catalyst by Chemical Vapor Deposition (CVD): Experimental Setup



SEM photograph of N-doped TiO_2 film on quartz particles

XPS spectra of the N-doped TiO_2 film on quartz particles

Photocatalytic Oxidation of Isopropyl Alcohol UV 185nm Illumination



Mechanism for Photocatalytic Reaction

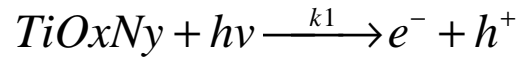
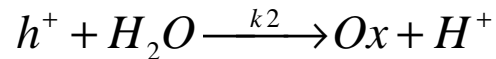
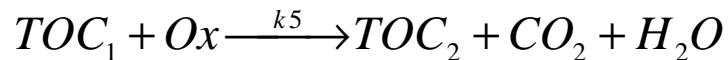
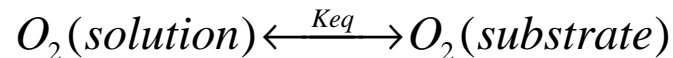
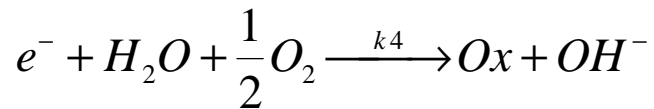
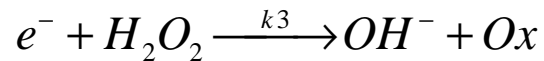


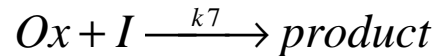
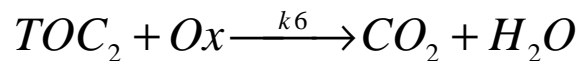
Photo-Generation of Electron/Hole Pair



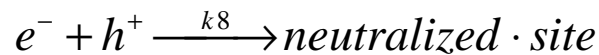
Radical Formation



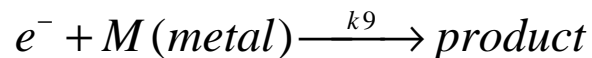
Two-Step Oxidation Process



Quenching Reaction



Recombination of Electron/Hole Pair



Noble Metal, M, Attracts Free Electron Slows Recombination, And Promotes Radical Generation

Comparison of Different Factors Influence Photocatalytical Reaction Efficiency

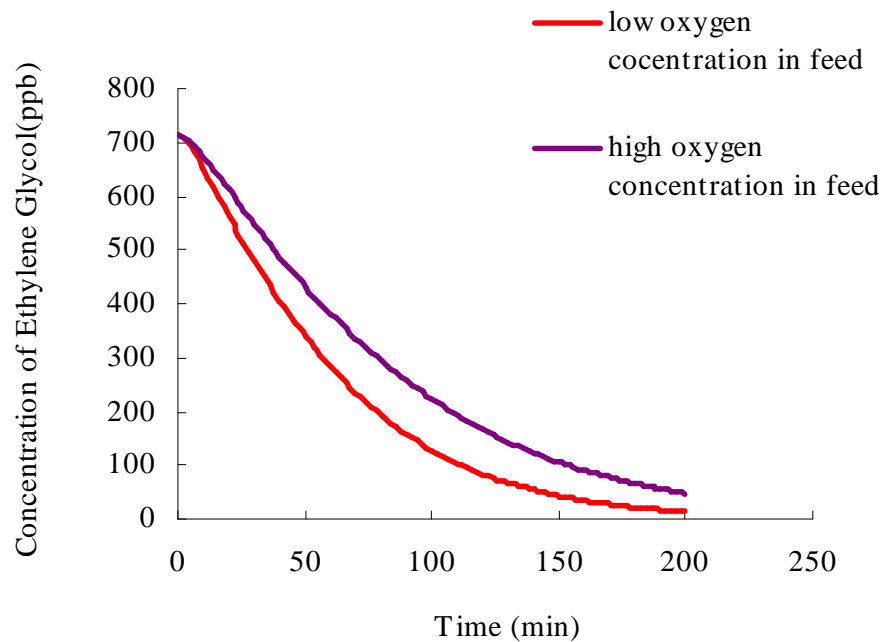


Fig model comparison the influence of oxygen solubility in the solution for batch reactor photocatalytic reaction: UV-185 irradiation with titanium oxynitride, model compound ethylene glycol, initial concentration 712 ppb

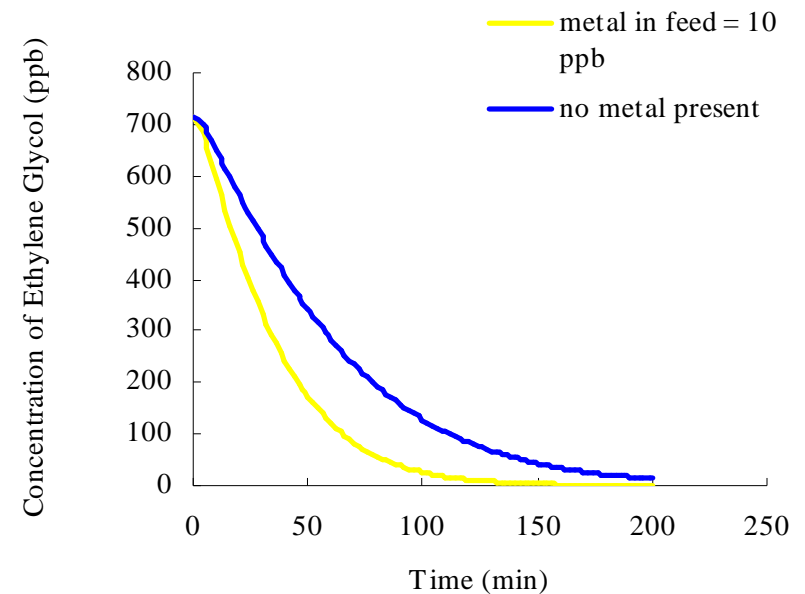
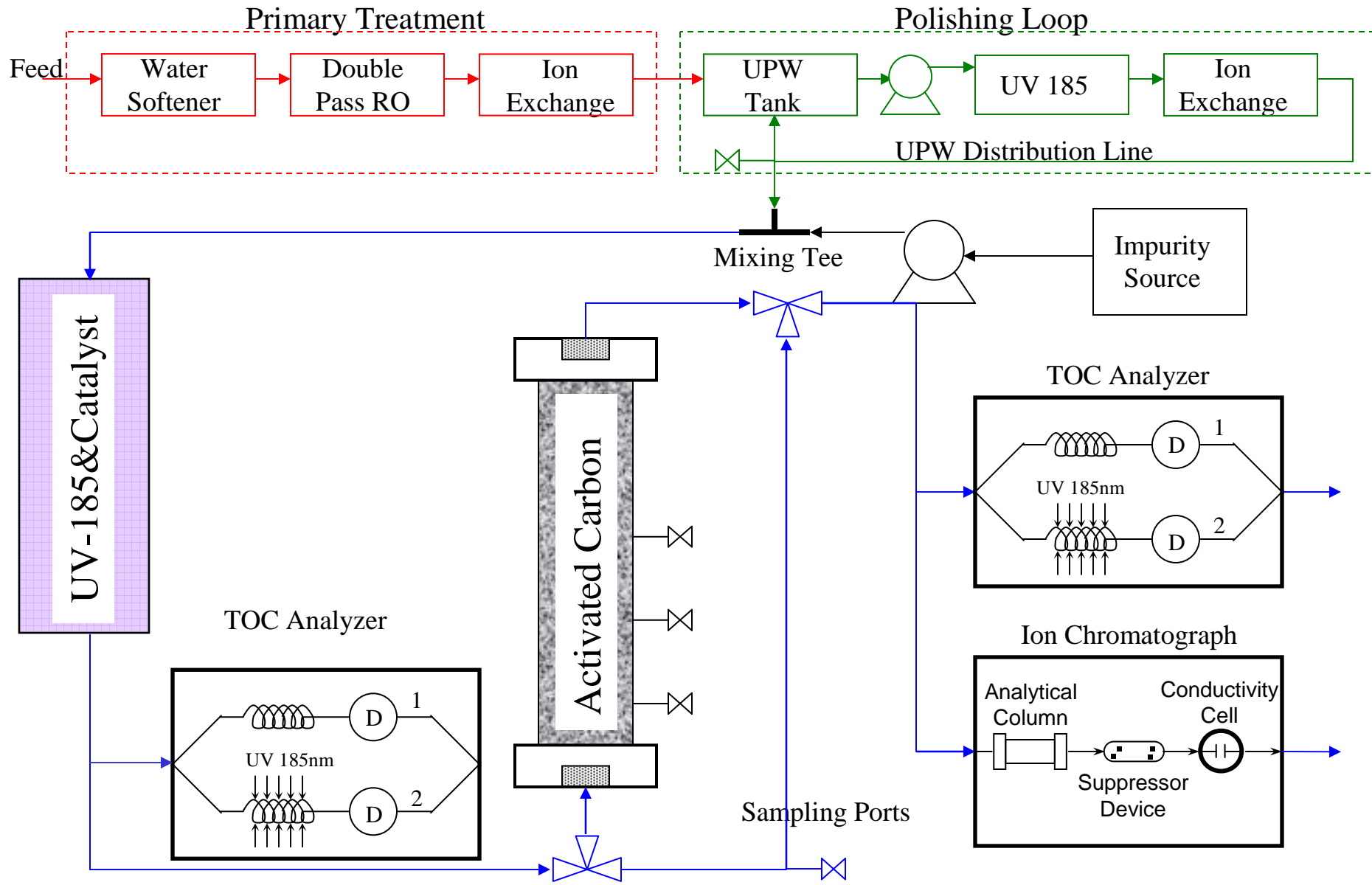


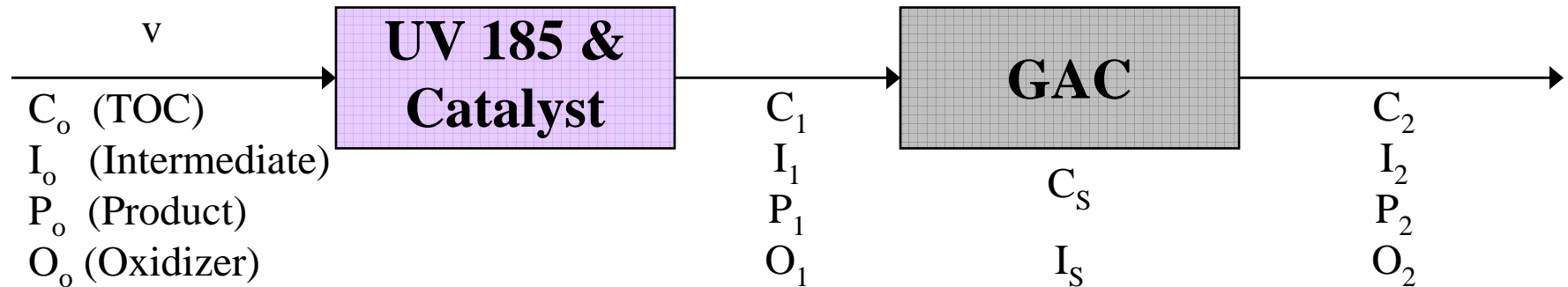
Fig model comparison the influence of present of metal in the contaminant solution for batch reactor photocatalytic reaction: UV-185 irradiation with titanium oxynitride, model compound ethylene glycol, initial concentration 712ppb

Experimental Setup for Adsorption Study



SRC/Sematech Engineering Research Center for Environmentally Benign Semiconductor Manufacturing

Process Model Development for UV Assisted TOC Removal by Activated Carbon



• Primary UV 185 processes

- Convection
- Oxidation reactions

• Characteristic equation

$$\frac{\partial C}{\partial t} + U1 \frac{\partial C}{\partial z} = D1 \frac{\partial^2 C}{\partial z^2} + R$$

$$R_c = -k_2 * C_c - k_3 * C_c * C_o$$

$$R_i = k_2 * C_c + k_3 * C_c * C_o - k_4 * C_i * C_o$$

$$R_o = k_1 - k_3 * C_c * C_o - k_4 * C_i * C_o$$

• Primary GAC processes :

- Convection & Dispersion
- Adsorption/desorption & Oxidation

• Characteristic equation

$$\frac{\partial C}{\partial t} + U2 \frac{\partial C}{\partial z} = D2 \frac{\partial^2 C}{\partial z^2} + R$$

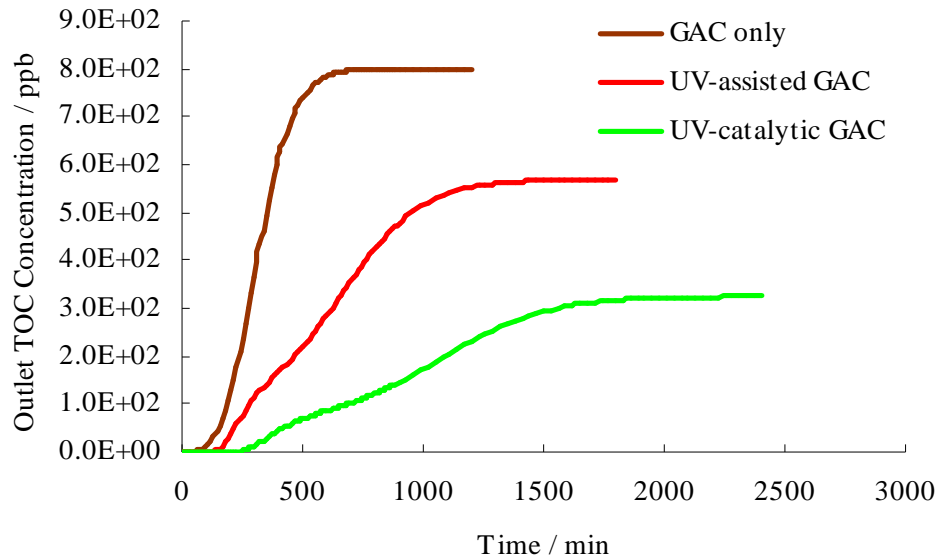
$$R_c = -\frac{(1-\epsilon)}{\epsilon} * K_{ac} * C_c * S + \frac{(1-\epsilon)}{\epsilon} * K_{dc} * C_{cs} - k_3 * C_c * C_o$$

$$R_i = -\frac{(1-\epsilon)}{\epsilon} * K_{ai} * C_i * S + \frac{(1-\epsilon)}{\epsilon} * K_{di} * C_{is} + k_3 * C_c * C_o - k_4 * C_i * C_o$$

$$R_o = -\frac{(1-\epsilon)}{\epsilon} * k_5 * C_{cs} * C_o - \frac{(1-\epsilon)}{\epsilon} * k_6 * C_{is} * C_o - k_3 * C_c * C_o$$

$$-k_4 * C_i * C_o - k_9 * C_o$$

Benefits of UV-Assisted Catalytic Adsorption



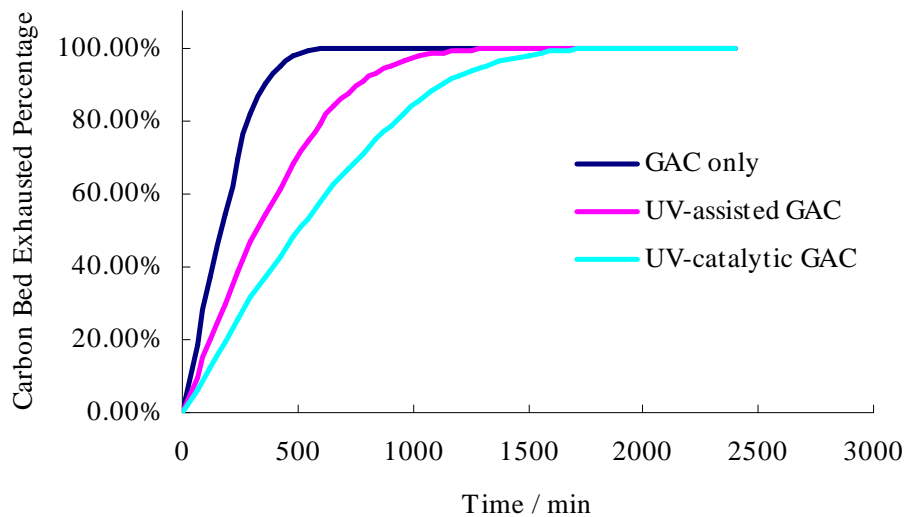
- **UV-assisted catalytic adsorption greatly improves the efficiency of GAC**

- **Takes advantage of both partial and total oxidation.**

- **More efficient oxidation due to:**

- **Capture of TOC**

- **Concentration of TOC**



- **The lifetime of GAC bed is prolonged significantly because of the formation of more absorbable intermediate organic compounds**

- **Combined effect promotes removal of “hard-to-remove” organic compounds, eg. IPA.**

Conclusions and Highlights:

- **The new integrated, hybrid oxidation/adsorption is an effective technique for the removal of recalcitrant organic compounds**
- **The proposed process reduces waste and chemical usage through prolonging the life of ion exchanges and activated carbon units**
- **The novel catalyst shows higher activity and reduces the energy requirement for oxidation.**

Future Plans:

- **Test the newly developed Ti oxi-nitride catalyst and the new deposition and nitridation methods with higher wavelength (lower-energy) UV sources.**
- **Test with other recalcitrant compounds such as fluorinated surfactants and simulated CMP rinse water.**
- **Industrial interactions:**
 - **John De Genova (TI); Kon-Tsu Kin (ITRI and TSMC)**

ESH Metrics and Impact

I) Basis of Comparison:

Current best technology: Water supply to Ultrapure Water (UPW) treatment facility completely from natural/municipal resource. Spent rinsewaters from wafer fab processes discharged to industrial wastewater system, treated, and sent to the municipal sewer, for sanitary treatment.

II) Manufacturing Metrics

The recycling of previously purified water has been proven to improve the water quality at the point of use and will lower the cost of purification. It also provides for an improved consistency of UPW quality as less maintenance and longer run times between regenerations are necessary. Cost savings are dependent on the region with varying costs of both water supply and wastewater discharge.

An impact on wafer yield has not been determined.

III) ESH Metrics

Goals / Possibilities	Usage Reduction			Emission Reduction			
	Energy	Water	Chemicals	PFCs	VOCs	HAPs	Other Hazardous Wastes
50% of spent UPW rinsewaters recycled to UPW plant.	Factor of 2	40 % reduction in municipal feed water	50% reduction in regeneration chemicals	N/A	N/A	Some reduction in acid vapors	50% reduction in regeneration waste/ and wastewater
90% of spent UPW rinsewaters recycled to UPW plant.	Factor of 3	70% reduction in municipal feedwater	75% reduction of regeneration chemicals	N/A	N/A	Some reduction in acid vapors	> 80% reduction in regeneration waste/ and wastewater



Evaluation of Radical- and Ion-Induced Damage on Low- k Films

Thrust A, Task 3

Mark Goldman and David Graves

UC Berkeley

Victor Vartanian, Brian Goolsby, Peter Ventzek, Da Zhang,
Shahid Rauf, and Laurie Beu

Motorola APRDL

Bing Ji

Air Products

SRC/Sematech Engineering Research Center for Environmentally Benign Semiconductor Manufacturing



Project Objectives

Goal: Understanding the mechanism of low- k film damage during processing

- Understood that plasma processing degrades the properties of low- k films: how?
- In a beam system, ion and radical sources are independent, allowing for study of each separately:
 - What is the role of ions? Is ion mass important? Ion energy?
 - What is the role of radicals? How is chemistry important?
 - How do they work together?
- In future device generations, it may be necessary to further process the films in order to restore k : can we avoid damaging it in the first place?



ESH Impact

- ESH Issues
 - Some possible photoresist strip chemistries include toxic gases
 - Impurities in etching chamber can form toxic byproducts
 - Any reduction in the number of steps will decrease the environmental impact



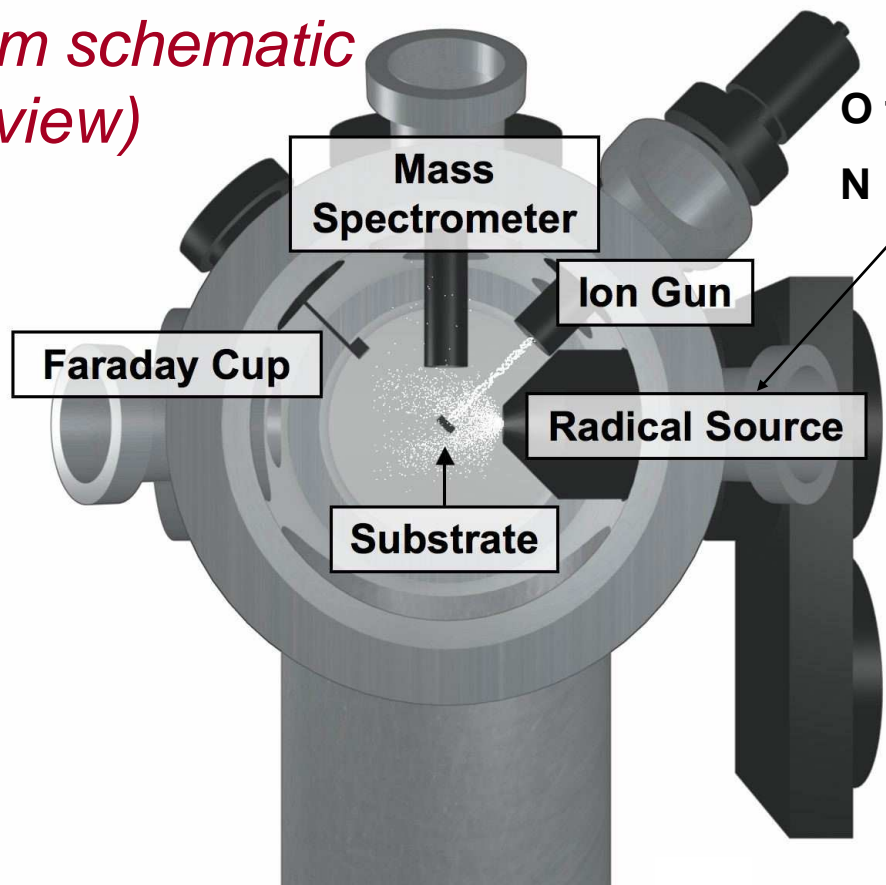
ESH Metrics

	Usage Reduction			Emission Reduction			
Goals / Possibilities	Energy	Water	Chemical	PFCs	VOCs	HAPs	Other Hazardous Wastes
Devise efficient, nontoxic PR strip processes	Efficient processing parameters could reduce power needs	N/A	N/A	N/A	Some by-products may be VOCs	Some by-products may be HAPs	N/A
Identify and reduce toxic etch byproducts	N/A	N/A	N/A	N/A	Reduce VOC emission	Presence of impurities in chamber can cause formation of HAPs	N/A



Experimental Setup

*System schematic
(side view)*



O fluence $\sim 3 \times 10^{13} \text{ cm}^{-2} \text{ s}^{-1}$

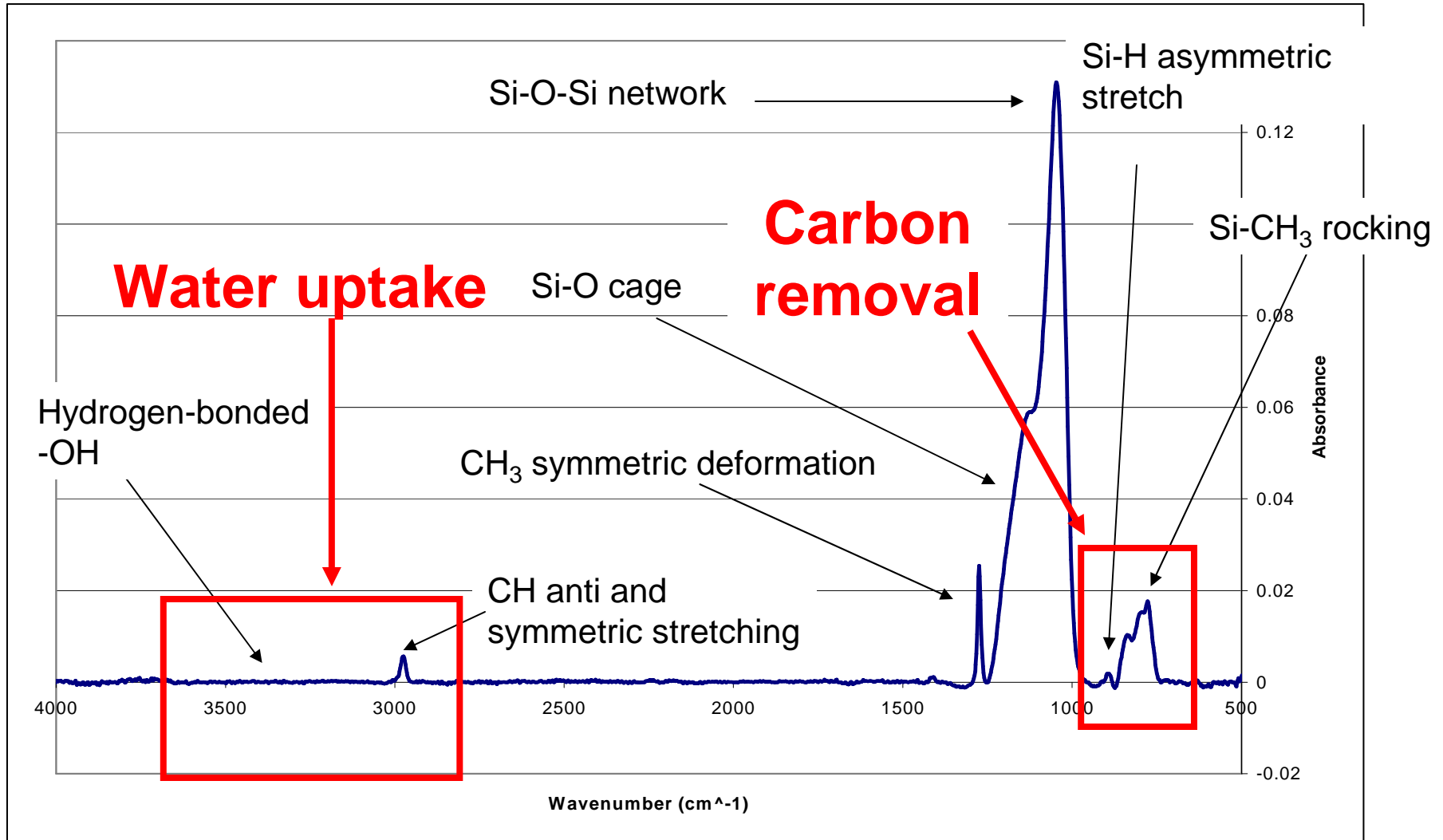
N fluence $\sim 1.5 \times 10^{13} \text{ cm}^{-2} \text{ s}^{-1}$

Films are methyl-doped,
nanoporous, -Si-O-
backboned ultra low-k
films

- Characterization done by ex-situ FTIR, AFM, contact angle, SEM



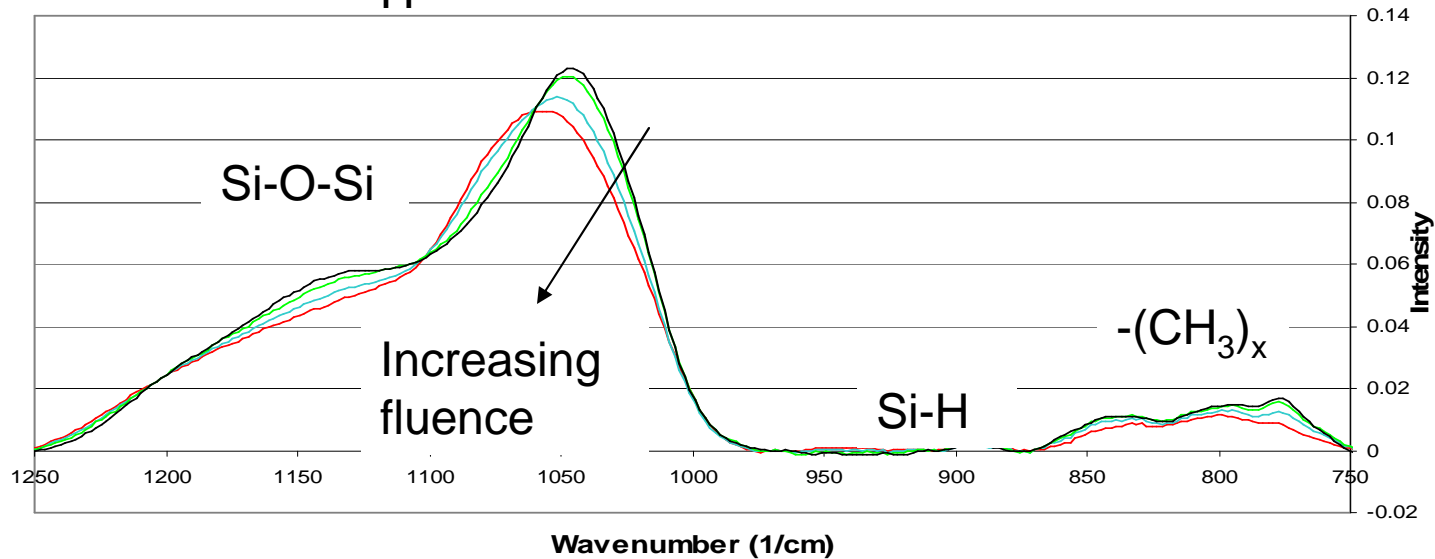
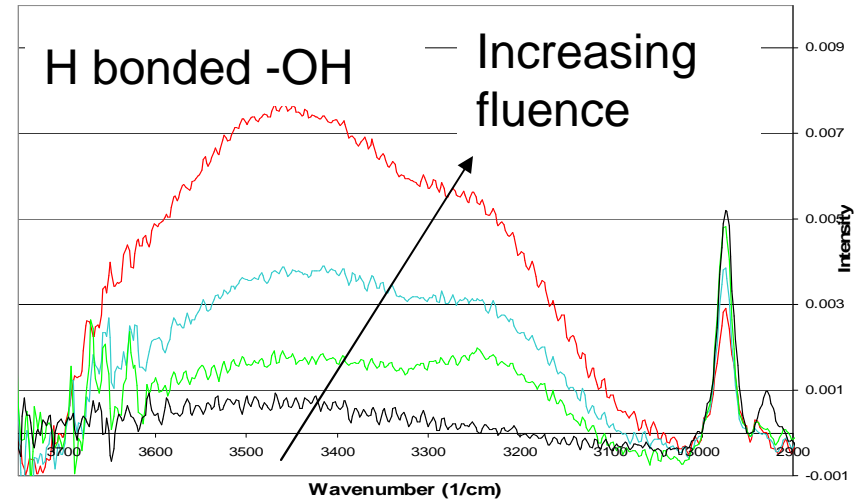
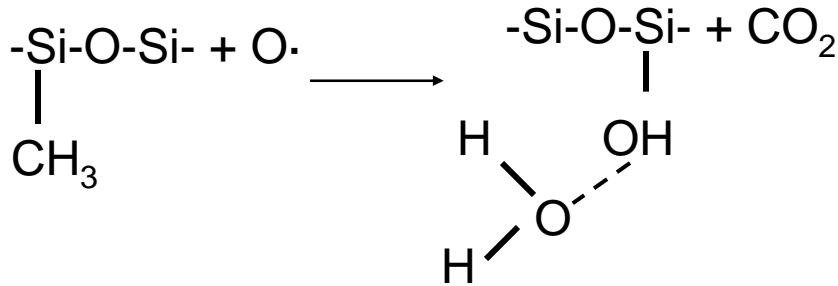
Unprocessed Film Spectrum





Oxygen Radical Damage

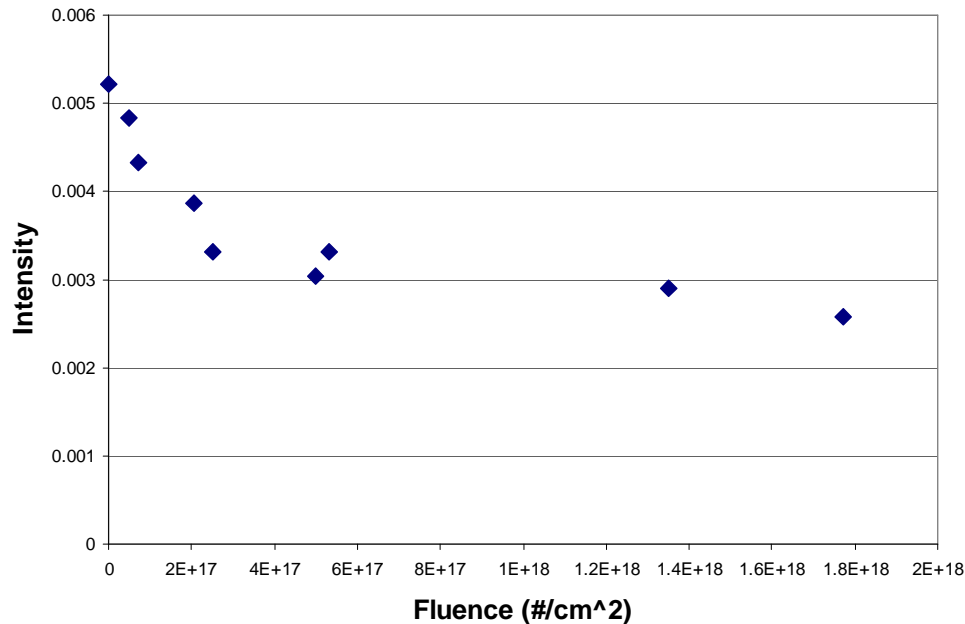
- Oxygen radicals increase H₂O uptake and remove carbon
- Peak shift of Si-O-Si due to change in surrounding bonds





Quantifying Oxygen Radical Damage

Peak intensity (~3000 cm⁻¹) vs. fluence



- Normalized carbon peak intensity can be used to determine penetration of oxygen → intensity is approx. **linear vs. time^{1/2}**
 - Deal-Grove type analysis yields diffusivity of oxygen radicals in nanoporous film

Find that $D_{\text{eff}} \sim 6 \times 10^{-5} \text{ cm}^2/\text{s}$

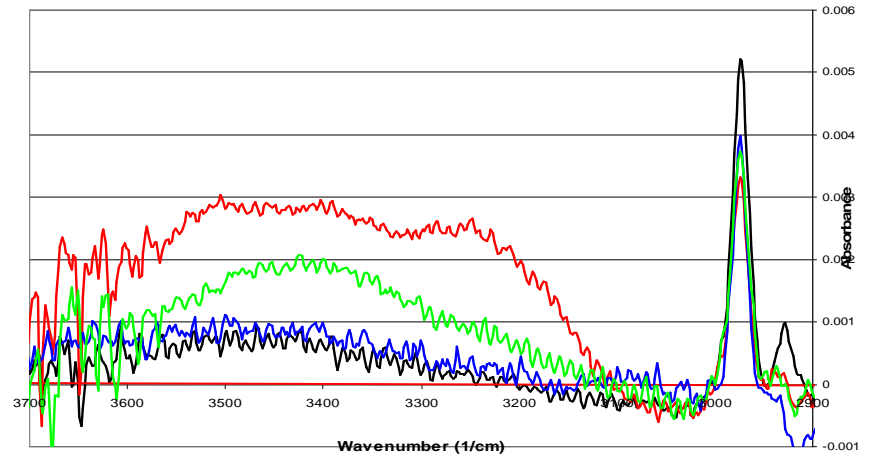


Effects of Radical Chemistry on Film Degradation

- At approximately equal fluences, damage trend is

$O > NO \text{ w/N} > N$

- **NO** forms from oxygen impurities in the presence of N

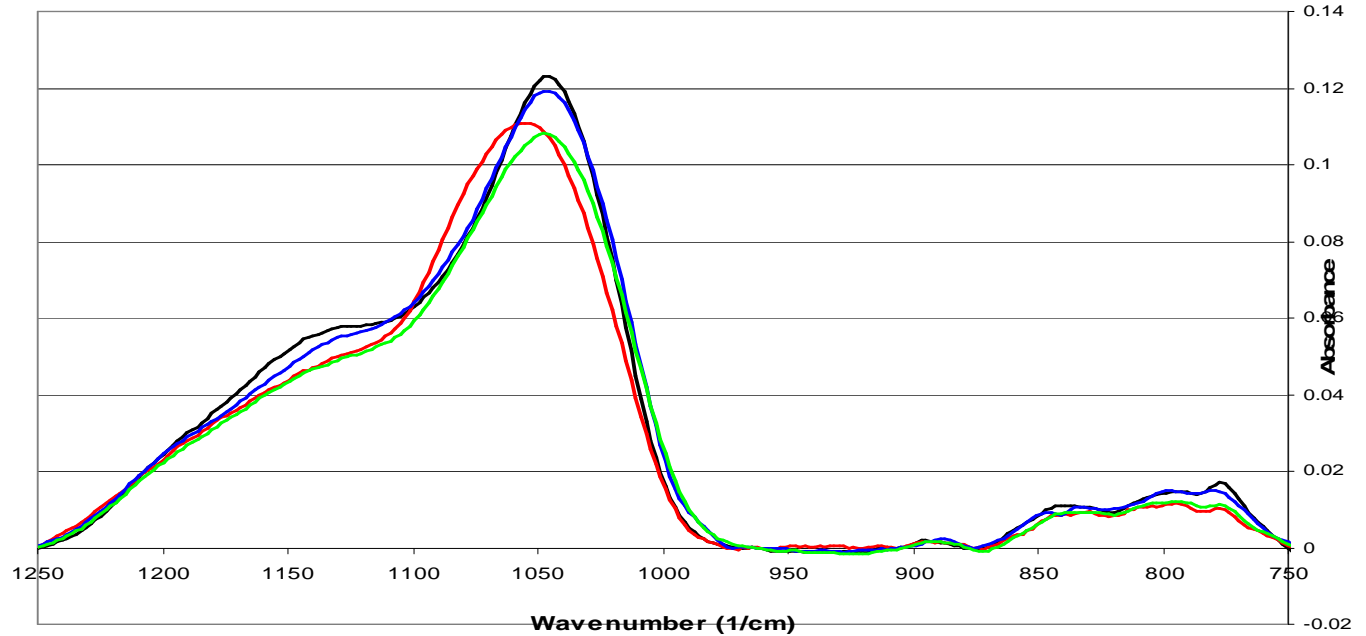


Unprocessed Film

Nitrogen
($3.18 \times 10^{17}/\text{cm}^2$)

NO w/N
($3.2 \times 10^{17}/\text{cm}^2$)

Oxygen
($2.5 \times 10^{17}/\text{cm}^2$)

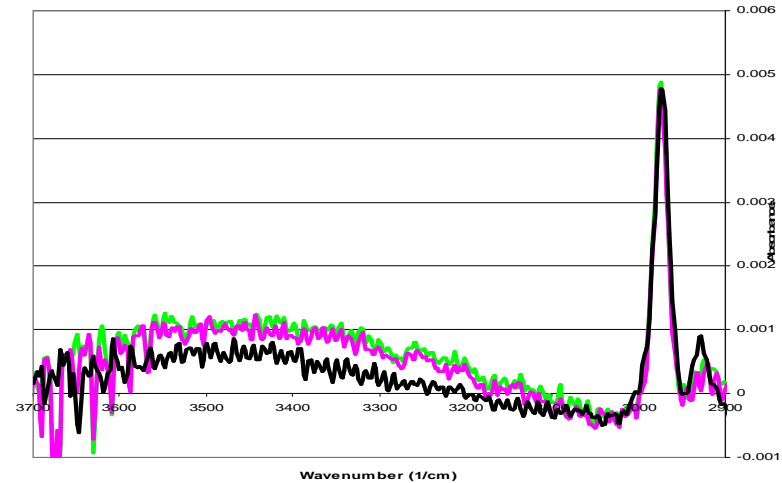


SRC/Sematech Engineering Research Center for Environmentally Benign Semiconductor Manufacturing

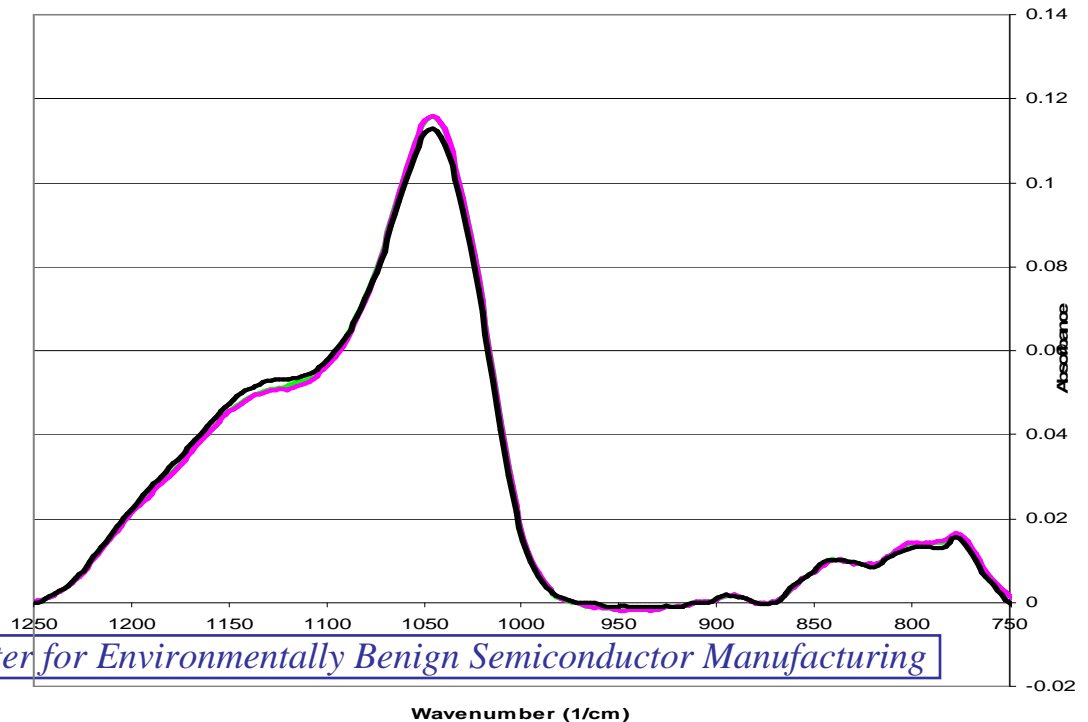


Effects of 500eV Ions

- Ions have an insignificant effect on the bulk film, but cause a **water contact angle increase**



— Unprocessed Film
— Xe+ $2.55 \times 10^{17}/\text{cm}^2$
— Ar+ $2.34 \times 10^{17}/\text{cm}^2$





Future Plans

- Add separate source of NO to beam system; test effects of NO with and without N from radical source (in progress)
- Study synergistic effects of simultaneous and sequential radical and ion beams (in progress)
- Use NH₃ in radical source. Characterize beam and measure damage. (in progress)
- Explore spin-on low k films for use on quartz crystal microbalance: QCM powerful tool in beam system. (proposed)
- Explore post-damage processing to test reversibility of damage (proposed)



Industrial Collaboration/Technology Transfer

- All materials obtained from industrial collaborators (Frank Greer) at Novellus
- Bi-annual meetings with collaborators to follow the progress of the project and obtain input/guidance

Conclusions

- Damage of low-k films by oxygen radicals is diffusion-limited
- Impurities in the processing chamber can significantly affect damage and cause toxic byproducts
- Rare gas ions damage the film surface, but do not penetrate and damage the film bulk



Treatment of Copper from Cu-CMP Waste Streams using Polyethyleneimine (PEI)

Subtask (C-1-2)



Worawan Kay Maketon and Kimberly Ogden
Chemical & Environmental Engineering, The University of Arizona

Objectives

- Develop a system for the treatment of semiconductor waste streams that contain copper using PEI.
- Determine the behavior of a single packed bed column, containing PEI-agarose gel, in treatment process for surrogate Cu-CMP wastes containing copper (II) ions.
- Compare the performance of ion exchange resin to chelator PEI. Cu^{2+} binding capacity of ion exchange resin is 0.07 g Cu^{2+} /g dry resin and 0.11 g Cu^{2+} /g dry adsorbent for PEI.
- Investigate the feasibility of chelator binding directly to the CMP-pad.

Cu-CMP Waste Compounds

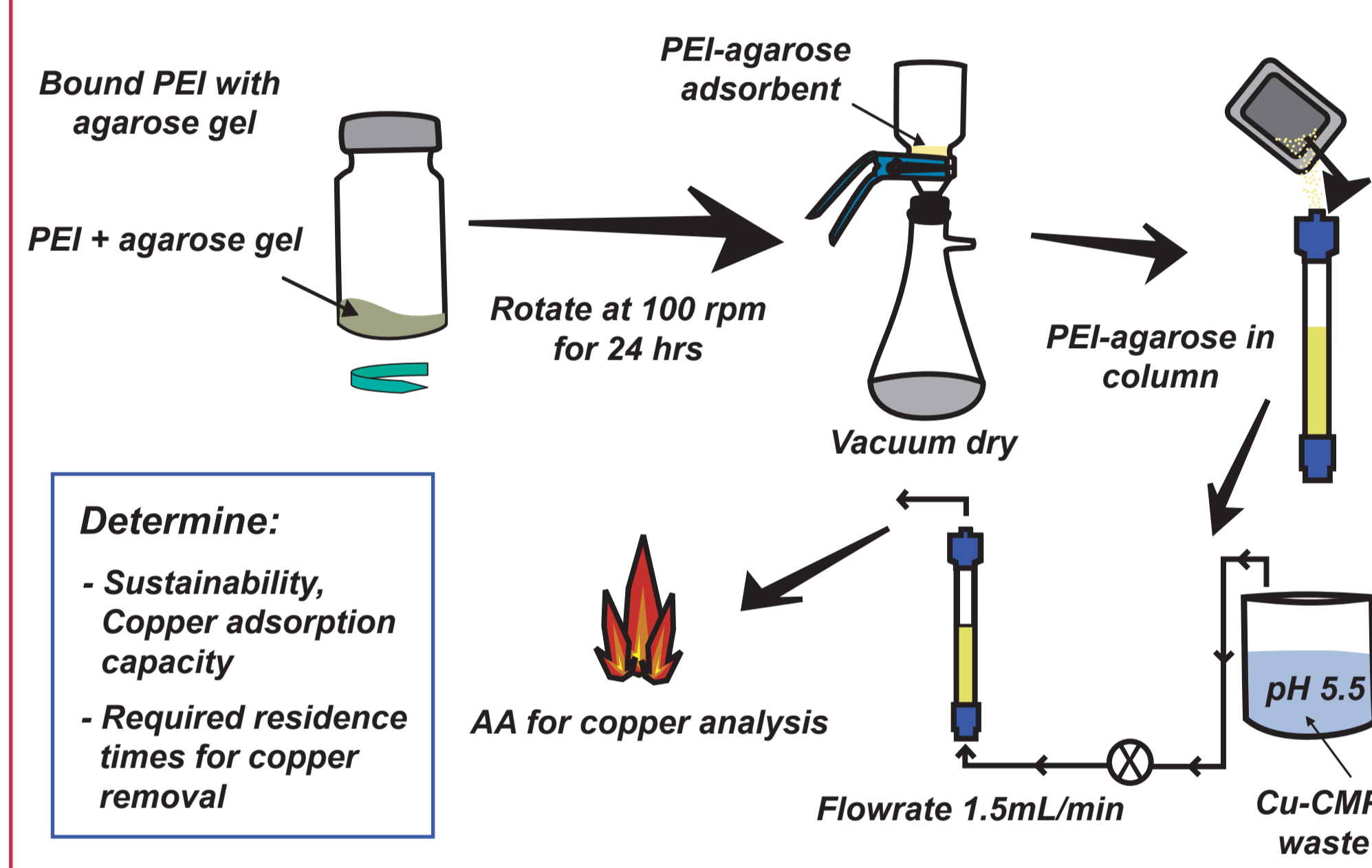
Type of Compound	Additives
Metal	Copper Nitrate
Surfactants	Triton, Sodium dodecyl sulfate
Inhibitors	Benzotriazole (BTA)
Abrasive Particles	Silica, Alumina, Ceria
Complexing Agent	EDTA, Citric Acid
Microemulsion	Isopropyl Alcohol
Amino Acid	Glycine
Oxidizing agent	Hydrogen peroxide

ESH Metrics for Task C-1-2: Novel Water Purification Technology

- I) **Basis of Comparison:**
Current best technology. Treatment of organic and copper containing effluent by a combination of Carbon Bed, UV, precipitation, membrane filtration, and Ion Exchange.
- II) **Manufacturing Metrics:**
This new treatment method will decrease the water usage by allowing for recycle of contaminated streams. This will improve the quality of water at point of use. However, the precise effect on the manufacturing metrics cannot be assessed at this stage of research.
- III) **ESH Metrics:**

Goals / Possibilities	Usage Reduction			Emission Reduction			
	Energy	Water	Chemical	PFCs	VOCs	HAPs	Other Hazardous Wastes
Copper removal from Cu-CMP	~50%	N/A	Combining ion exchange /precipitation	N/A	N/A	N/A	N/A

Method of Approach



Theory and Model

One dimensional Adsorption-Dispersion-Reaction equation [Hatzikioseyan et al., 2001]

$$\frac{\partial C}{\partial t} = D_z \frac{\partial^2 C}{\partial z^2} - u_z \frac{\partial C}{\partial z} - \frac{\rho_s(1-\epsilon)}{\epsilon} \left(\frac{\partial q}{\partial t} \right)$$

C – Copper concentration (mol/m³)
 D_z – Dispersion coefficient (m²/s)
 z – Length of column (m)
 u_z – Interstitial fluid velocity (m/s)
 ρ_s – Solid density (kg/m³)
 ϵ – Bed void volume

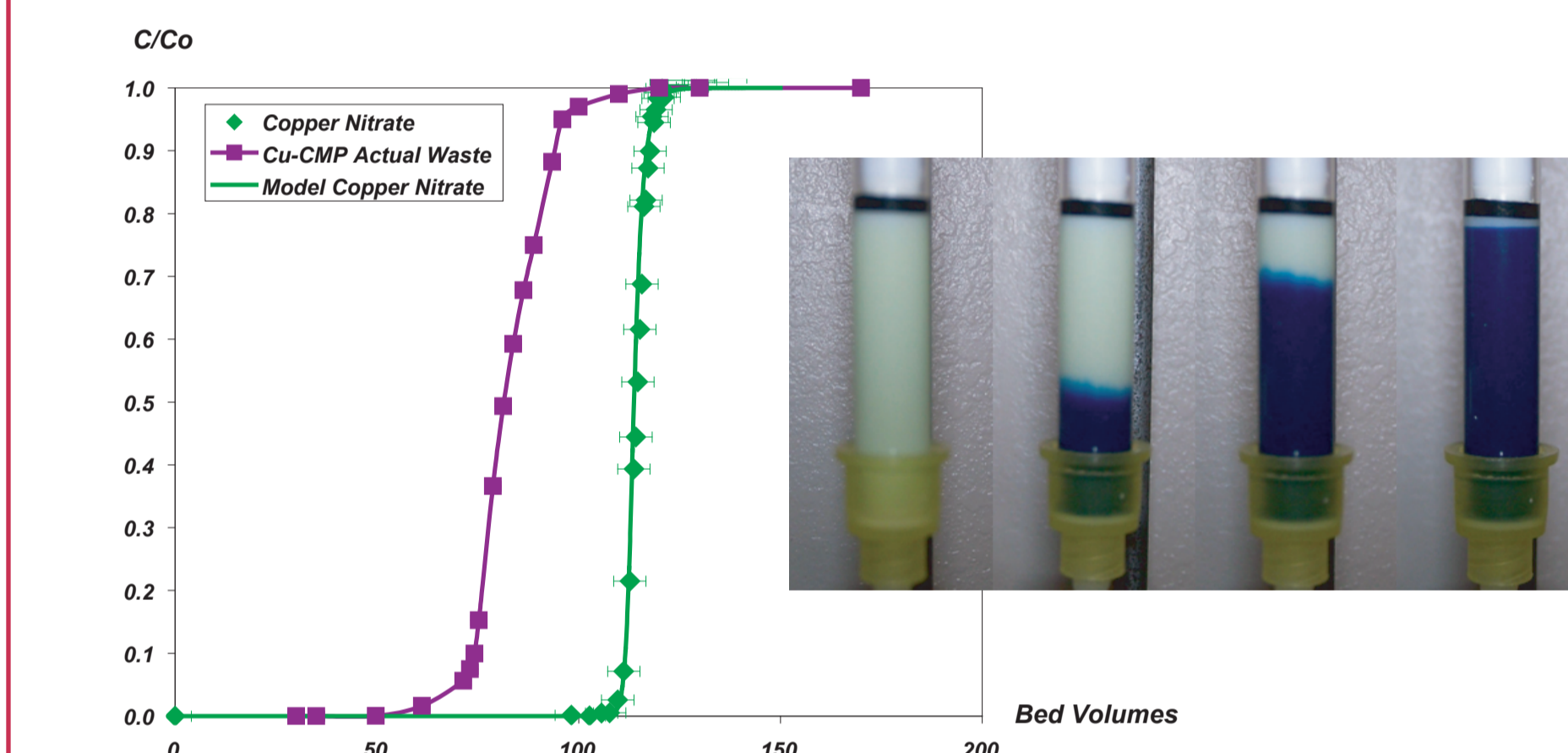
q is a function of Langmuir Isotherm model: $q = Q^a \frac{bC}{1+bC}$
 q – Amount copper adsorbed onto adsorbent (mol/kg)
 Q^a – Maximum Copper binding capacity (mol Cu^{2+} /kg adsorbent)
 b – Langmuir constant (m³/mol)

Final PDF model equation: $\left[1 + \frac{\rho_s(1-\epsilon)}{\epsilon} \frac{Q^a b}{(1+bC)^2} \right] \frac{\partial C}{\partial t} = D_z \frac{\partial^2 C}{\partial z^2} - u_z \frac{\partial C}{\partial z}$

Copper Breakthrough

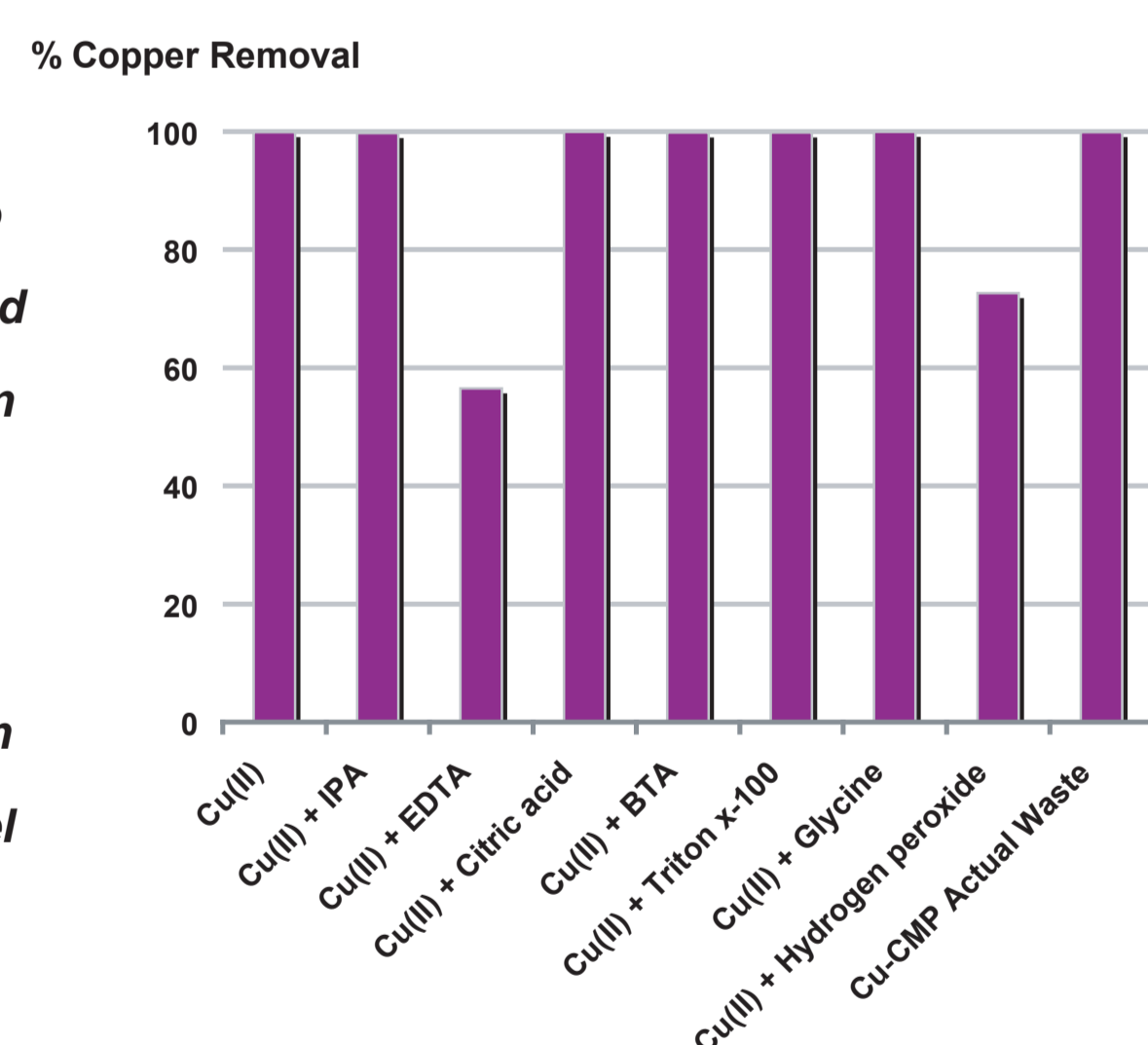
Copper binding capacity in a packed column

- Cu-CMP actual waste 21 ± 1 mg Cu^{2+} /mL adsorbent
- Waste solution contain copper nitrate 25 ± 0.9 mg Cu^{2+} /mL adsorbent



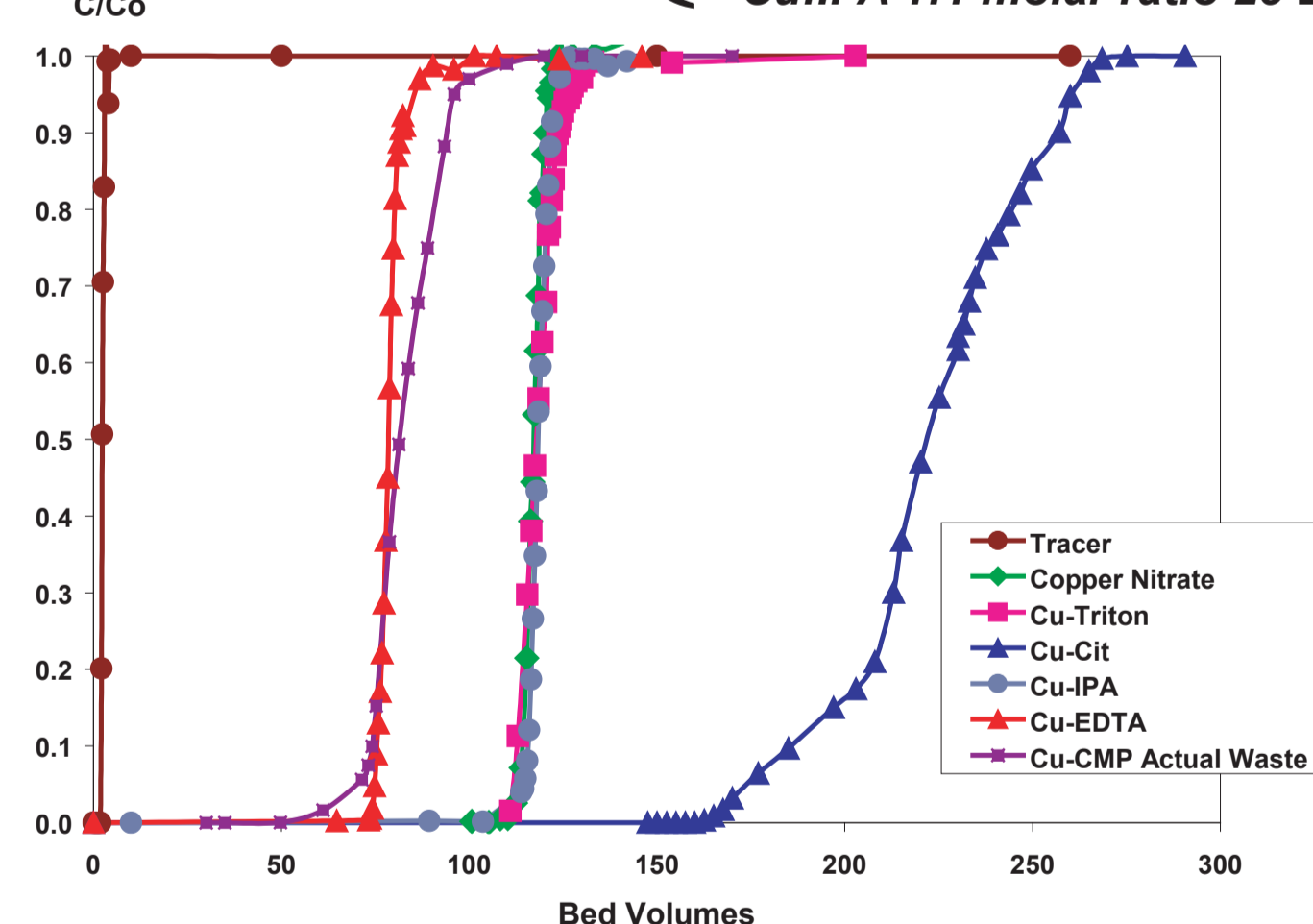
Removal of copper when other complexing agents present

- EDTA has a higher affinity to bind copper ions than PEI and forms complex with copper in the solution.
- Hydrogen peroxide 400ppm destroyed the bonds between PEI and the beads and the gel itself.



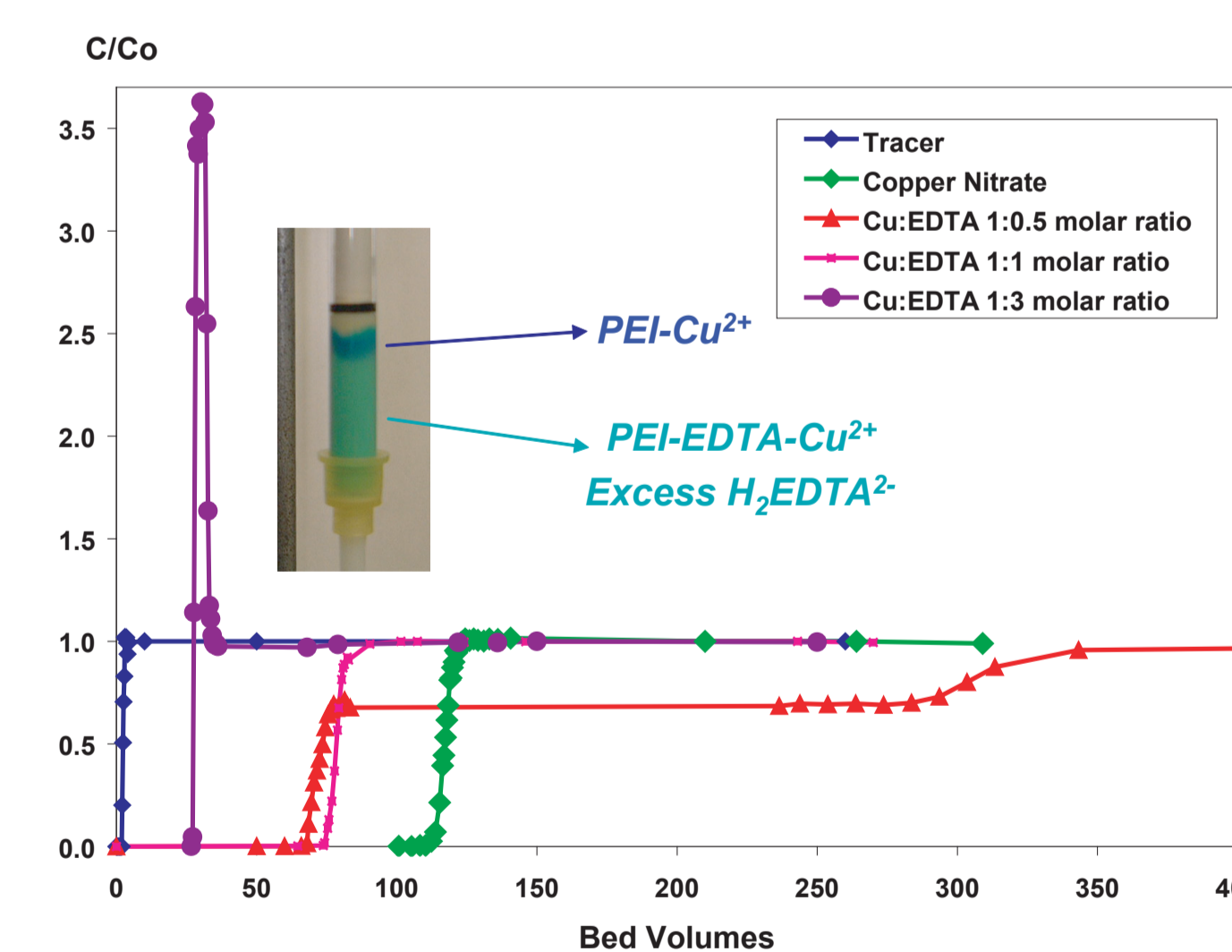
Copper binding capacity in a packed column (mg Cu^{2+} /mL adsorbent)

- Cu-CMP surrogate waste contain
 - Cu:Citric Acid 1:1 molar ratio 56 ± 0.2
 - Cu:EDTA 1:1 molar ratio 17 ± 1
 - Cu:Triton x-100 1:1 molar ratio 25 ± 0.5
 - Cu:IPA 1:1 molar ratio 25 ± 0.6

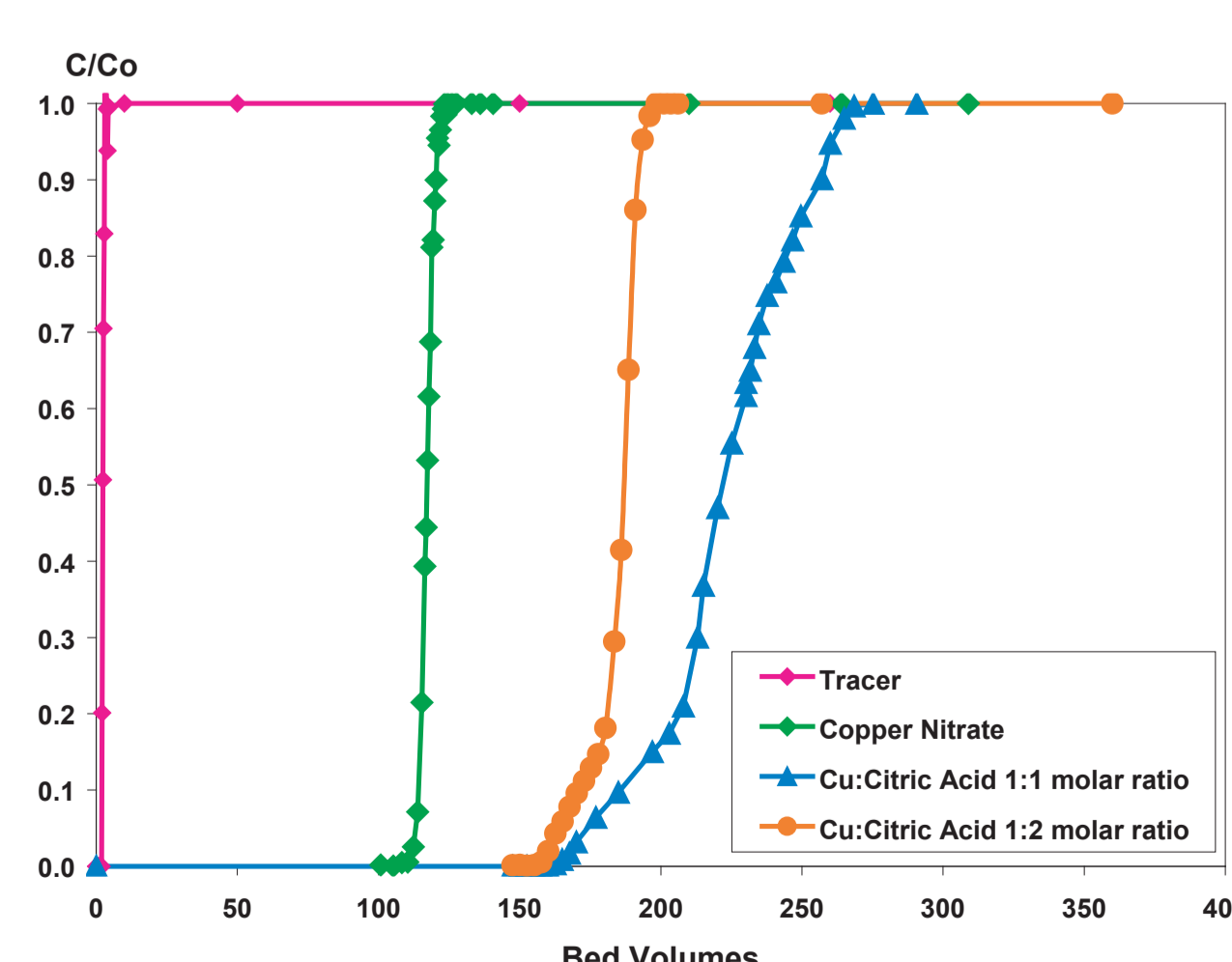


Copper Breakthrough of Cu-EDTA solutions

Excess EDTA can interfere with Cu-EDTA molecule that was already bound with PEI. As a result, some of copper ions could be released from the complexes to the solution and re-bind with EDTA or free PEI, causing an increase in the copper concentration.



Copper Breakthrough of Cu-Citric acid solutions



Excess citrate ions may help the binding of Cu-Citric acid molecule to PEI, results in higher copper binding in the column as the molar ratio to copper increases.

Conclusions

- PEI-agarose showed great affinity of binding copper in batch and continuous systems. The performance and reproducibility did not change even after several regenerations
- PEI-agarose is not only a complexing agent, but also an anion exchanger due to the protonation of its amino groups
- Large volumes of copper contaminated solutions from Cu-CMP wastes can be concentrated down to much smaller volumes for metal recovery
- Behavior of a packed bed column, containing PEI-agarose gel, can be expressed by ADR equation coupled with Langmuir isotherm

Future Plans

- Explore the PEI adsorption mechanisms
- Investigate the use of chelators directly added to CMP pads

Theory of chelators added to CMP pad

